Random Directional Nearest-Neighbour Graphs

Qasem Tawhari

A Thesis presented for the degree of
Doctor of Philosophy

Statistics and Probability
Department of Mathematical Sciences
University of Durham
England

November 2023

Dedicated to

My parents

for all their love, encouragements, and prayers

My wife and My kids

Munirah, Tamim, and Nadim who make my life convivial

My siblings

for their believes and wishes

Random Directional Nearest-Neighbour Graphs

Qasem Mohammed Tawhari

Submitted for the degree of Doctor of Philosophy
November 2023

Abstract

We look at a class of random spatial graphs constructed on random points (points of a Poisson process) in Euclidean space with edges defined by a geometrical rule based on proximity. Specifically, each point is joined by an edge to its nearest neighbour in a given direction specified by a cone. The unrestricted case is the ordinary nearest-neighbour graph; the restricted case is a version of the minimal directed spanning forest (MDSF) introduced by Bhatt & Roy. These graphs have been widely used for modelling networks with spatial content, such as in the communications sector, social networks, and transportation networks. The large-sample asymptotic behaviour of the total edge length of these graphs is our main interest. For the ordinary nearest-neighbour graph, the appropriate central limit theorem is due to Avram & Bertsimas. For the MDSF, the limit theory is known (Penrose & Wade) in two special cases, namely the 'south' and 'south-west' versions: here the limit is not normal, due to the presence of long edges near to the boundary. In this thesis, we will extend the limit theory to the case of general cones; depending on the parameters, the limit distribution may be normal, or the convolution of a normal distribution with a non-normal element due to boundary effects whose distribution can be characterized by a fixed-point equation.

Declaration

The work in this thesis is based on research carried out in the Department of Mathematical Sciences at Durham University. No part of this thesis has been submitted elsewhere for any degree or qualification, and it is all my own work unless referenced to the contrary in the text.

Acknowledgements

Alhamdulillah, all praise and thanks be to Allah, the Lord of all the worlds, for blessing me to complete this PhD research. From the depths of my heart, I express my utmost gratitude to the one who created us, sustains us, and guides us through every step of my short journey from birth to this PhD journey.

First and foremost, I would like to express my sincere gratitude to my great supervisors, Dr. Nicholas Georgiou and Professor Andrew Wade, for their valuable time, proper guidance, and patience during my PhD journey. Their support in keeping me on the right track and their vast knowledge and brilliant advice were indispensable. Their excellent guidance in research and teaching will always be a perfect example for me; they have supported and encouraged me over the last four years. I truly appreciate all their timely advice and proper guidance during my PhD journey. I am sincerely indebted to them for their invaluable mentorship, which has significantly contributed to the successful progression of my doctoral endeavours.

My kind gratitude goes to everybody in the Probability and Statistics groups at Durham University, particularly Muhammad Hasan and Clare Wallace, for creating an enjoyable working environment. I am grateful to all staff and postgraduate students in the Department of Mathematical Sciences for making it a friendly place to conduct research. I also extend my sincere appreciation to my examiners, Dr. Fraser Daly (Heriot-Watt University) and Dr. Mustazee Rahman (Durham University), for their invaluable comments and suggestions. Their guidance played a crucial role in the success of my endeavour.

I gratefully acknowledge the support of the Cultural Bureau, Embassy of Saudi Arabia (SACB) in London, and Jazan University (KSA), who funded my PhD not only by providing funding for this research but also by allowing me to attend conferences and meet so many interesting people. I also acknowledge the Department of Mathematical Sciences, Durham University, for covering all the expenses of participating in different conferences and workshops, which have added tremendous value to my short research journey.

Lastly, I am incredibly grateful to my beloved wife, Munirah, for sacrificing her potential career to accompany me in the United States and the United Kingdom while I studied abroad. Also, I would like to thank all of my family members (with a special mention to my beloved Mum, who passed away on 18 December 2020; may her soul rest in peace) for their moral support and for making this possible. Without your belief in me, I never would have made it.

Contents

List of Figures

Chapter 1

Introduction

1.1 Overview

This thesis explores the asymptotic behaviour of the total edge length of a family of random spatial graphs called the minimal directed spanning forest (MDSF) constructed on random points in Euclidean space. These graphs are constructed using randomly distributed points in the unit square, and edges are added based on a geometrical rule determined by proximity and a directional relation specified by a cone in the plane. There are several cases of directional relations. The first two cases (south & south-west versions) were studied by Penrose and Wade [31], who proved their limit theory. In this work, we consider five new cases (general cones) associated with unit square (see Section 4.3 for more details) singly-aligned cones and unaligned cone. We extend the limit theory for the south-west version to the case of general cones whose distribution depends well on the parameters. The primary objective of this thesis is to establish limit theorems for the total edge length of these graphs as the number of points tends to infinity, with a particular focus on convergence in distribution results. Additionally, we aim to illustrate the distinct behaviour of these models concerning the orientation of cones when compared to previous models.

1.2 Background on Random Spatial Graphs

This section covers background knowledge of classical results related to random spatial graphs and introduces some new insights. The probabilistic limit theory for such random spatial graphs began with the seminal paper by Beardwood, Halton, and Hammersley [5]. In their work, they established the proof of the law of large numbers for the travelling salesman problem (TSP), a famous problem in combinatorial optimization [5]. Graphs with spatial content are of significant interest and serve as desirable models for real-world networks. To gain a comprehensive understanding of the theory of Erdős-Rényi random graphs, see, e.g., [13]. In the Erdős-Rényi model, a random graph on the vertex set V is constructed by including each pair of vertices as an edge independently with some probability p. A graph has no spatial structure to the graph; an edge between two vertices is equally likely [13, 44].

There has been a recent interest in graphs constructed using random points in Euclidean space. In this construction, points are independently and uniformly distributed within a unit square, and their edges are defined based on a geometrical rule that considers proximity. Examples of such graphs include the nearest-neighbour graph, the Euclidean minimal spanning tree, and various other geometric graphs. These types of graphs, collectively known as spatial graphs, hold significant importance in applied probability research and find extensive applications in modelling social networks and statistical procedures.

One object we are interested in studying in this thesis is the total edge length of the graph (our random variable). This random variable can be obtained by considering the points in a space. Edges, which form segments aligned in various directions, have real lengths. These lengths are summed to create a random variable representing the total edge length of the graph. Studying simple models of random spatial graphs is a natural choice for inference or prediction due to our main interest in understanding their typical behaviours. Several types of graphs can be constructed using these random points, including the nearest-neighbour graph, the minimal spanning tree (MST), and graphs associated with the Voronoi diagram and

Delaunay triangulation.

The nearest-neighbour graph (NNG) is a directed graph that connects each point to its nearest neighbour. In the nearest-neighbour graph, it is important to note that the contributions to the total edge length from points are not independent due to the finite-range dependence. This dependence exhibits a form of local dependency, meaning that only nearby points can influence each other. Consequently, the total edge length of these graphs satisfies law of large numbers and central limit theorem as the number of points tends to infinity. Notable examples of laws of large numbers can be found in the works (Beardwood, Halton, and Hammersley) [5].

While the idea of central limit theorems (CLTs) has been around for some time, significant progress was made in the 1980s, by Ramey [37] and Bickel and Breiman [10]. Regarding Ramey's approach, Avram and Bertsimas [3, p.1034] note that "his approach, although very interesting, did not succeed because he needed some unproven, but plausible, lemmas from continuous percolation". Bickel and Breiman successfully proved the first CLT for the NNG making use of intricate fourth moment estimates. Later, a more robust approach was provided by work of Avram and Bertsimas [3], using the technique of the dependency graph introduced by Baldi and Rinott [4].

A variation on the ordinary nearest-neighbour graph is to place a restriction on the possible directions of edges. A model of this type, called the minimal directed spanning forest (MDSF), was introduced by Bhatt and Roy [8]. For the MDSF, the limit theory for the total edge length of the graph defined on random points has been established by Penrose and Wade [31] in two special cases of directional restrictions: the 'south' and 'south-west' versions. In these cases, the limiting distribution is given by the sum of a normal component in bulk and a contribution caused by the boundary effects due to the appearance of long edges near boundary of the unit square.

In the unrestricted case, Avram and Bertsimas [3] provided the proof of central limit theorems (CLTs) and the rate of convergence for various quantities defined in

terms of graphs constructed on random points (these points generated by the Poisson process within the unit square) in geometrical probability. This technique is particularly adept at handling sums of weakly-dependent random variables, quantified through dependency graphs introduced by Baldi and Rinott [4].

Moving from an unrestricted to a restricted case involves introducing generalizations that constrain the direction of a cone within the unit square. This restriction is the primary focus of the minimal directed spanning forest (MDSF). In MDSF, a set of points within $[0,1]^2$ allows edges only in specific relative directions, which can be achieved through a cone or, equivalently, in terms of a partial order in $\mathbb{R}^2$. In Bhatt and Roy [8] explored the 'south-west' model, so each vertex is joined by an edge to its nearest neighbour in the south-west direction. Bhatt and Roy [8] considered not the total edge length, but the length of edges joined to an additional vertex inserted at the origin. Penrose and Wade [32] considered the same quantity, and the length of the longest edge; the limiting distributions of these quantities are expressed in the form of certain Dickman-type distributions, which are derived from the Poisson-Dirichlet distribution.

The term 'MDSF' is derived from its corresponding formulation for a global optimization problem, such as the ordinary minimal spanning tree, but with a directional constraint. In general, the directional constraint is expressed using a partial order. Previous work on ordinary nearest-neighbour graphs respected directional constraints developed by Smith [41], and a closely related model to the 'south' version is associated with Manna [23].

Recalling the concept introduced by Bhatt and Roy [8], in the 'south-west' version, edges are exclusively connected in the relative 'south-west' direction, with some constraints (in a sense) for a directed edge from every vertex to a minimal element when defined in terms of a tree. In the 'south' version, each point is connected by an edge to its nearest-neighbour at a lower vertical coordinate. The limit distribution of the total edge length for both 'south' and 'south-west' versions is characterized by the sum of a normal component within the bulk, along with a contribution due

to boundary effects. These boundary contributions can be described in terms of the On-line nearest-neighbour graph (ONG), whose distribution can be characterized by a fixed-point equation. Boundary effects are significant and can be used to describe the minimal directed spanning tree (MDST) using the simplest form of a one-dimensional structure known as a directed linear tree (DLT), which is sequentially generated. In the DLT model, points in an interval arrive one by one, and each point in the sequence is an independent and uniformly random point connected by an edge to its nearest predecessor based on Euclidean distance. Examples associated with DLT include network modelling and molecular fragmentation, as seen in [6, 7], and among others. Other recent work on the minimal directed spanning tree and On-line nearest-neighbour graph or related models includes [9, 43].

In the present work, we apply the limit theory concepts used in calculating the total edge length of minimal directed spanning forest Penrose and Wade [31] to our models, which exhibit more interesting behaviour. In our new cases mentioned earlier, we initially divide the unit square into three regions with perfectly chosen sizes with respect to the Poisson point process. These regions include bulk, intermediate, and bottom boundary regions within $[0,1]^2$ (see Chapter 4 in more details). Our results for the bulk for both singly-aligned cones match with Penrose and Wade [31] result (in a sense) converging to a normal distribution as the number of points tends to infinity. Similarly, our results for the bottom boundary for both singly-aligned cones correspond to Penrose and Wade [31]. In this case, the central limit theory deviates from a normal distribution because the boundary effects disturb the nature of central limit theory. Moreover, the distribution of boundary effects can be characterized by a fixed-point equation. Finally, choosing the intermediate region associated with both singly-aligned cones is deliberate to ensure that (in the limit) the bulk and bottom boundary contributions do not influence each other. Moreover, the contribution to the total edge length from points in this intermediate region has a variance converging to zero as the number of points becomes sufficiently large. These limits for regions bulk, intermediate, and boundary can then be combined to give the limit theory for the total edge length of MDSF on the whole unit square. The last case is referred to as an unaligned cone, where none of the edges of a cone

are aligned with a coordinate axis. In this case, the limit distribution follows a normal distribution as there is no boundary contribution occurs.

This thesis presents convergence results for the unrestricted and restricted versions of the minimal directed spanning forest as the number of points becomes very large, as we will introduce in Chapters 3 and 4. The study of such random spatial graphs has been motivated by various fields. These graphs have found extensive applications in modelling networks with spatial content, including communication networks, social networks, and transportation platforms.

1.3 Organization of the Chapters

This thesis contains eight chapters, including the introduction. Our thesis focuses on limit theorems for various nearest-neighbour graphs respecting the unit square. Most of the results in this thesis are concerned with large sample asymptotic behaviour for the total edge length of these graphs. Our results consist of the laws of large numbers, convergence in distribution, and central limit theorems. These results are fundamental to the field of probability theory and have considerable applications in various areas of science and engineering. We will also demonstrate these results as the number of points tends to infinity. Chapter 8 contains concluding remarks, further research and research achievements from Chapter 3 to 7.

The overview of this thesis goes as follows. Chapters 1 – 3 introduce nearest-neighbour graphs and the minimal directed spanning forest (MDSF) that we will consider for the remainder of the thesis. We will provide historical background, motivation, and further references related to these topics. Minimal directed spanning forest (MDSF) is a particular graph that recently received significant attention, first explored by Bhatt and Roy [8], as a potential model for telecommunications and drainage networks. We present our main Theorem 3.3.2 for this thesis in Chapter 3, which will cover all types of general cones with respect to the unit square. Chapter 3 concludes by describing the distribution of the non-normal limit random variable that appears in Theorem 3.3.2 and arises from the boundary effects for the

singly-aligned cones. This distribution is the unique solution to a fixed point equation studied previously in Penrose and Wade [31]. Some of the material in these Chapters 1 – 3 is adapted from [3, 32, 45].

Chapter 4 discusses the process of partitioning the unit square. Initially, we partition the unit square into three segments: bulk, intermediate, and bottom boundary within $[0,1]^2$. To define and identify various cone geometries, we use terms like 'companions', 'boundary', and 'bulk'. We also examine the concept of local dependence and characterize the unit square in terms of its boundary and bulk. Finally, we explore the size of each region. By determining the size of each region, we can gain a better understanding of the distribution of points within the unit square.

In Chapter 5, we formally define the terminology of the dependency graph. We demonstrate that the dependency graphs with finite-range dependence provide a normal approximation as the number of points becomes sufficiently large. From a geometrical perspective, we divide the whole square into little squares, with side lengths chosen based on the Poisson point process. We also apply the local dependence approach introduced by Avram & Bertsimas [3] to both singly-aligned and unaligned cones, particularly focusing on bulk within $[0,1]^2$. Furthermore, we provide the proof of Theorem 5.1.1 (CLT for the bulk), and we discuss some general results related to geometric probability, particularly concerning stabilizing functionals (stabilization methodology), which we use to prove Theorem 5.1.2. This theorem states that as the number of points tends to infinity, the variance of the total edge length from the bulk of $[0,1]^2$ converges to a finite positive limit. Finally, we will provide the proof of part (iii) of our main result Theorem 3.3.2 for the unaligned cone.

Chapter 6 explores one-dimensional nearest-neighbour graphs using randomly generated points uniformly distributed within the interval $[0,1]$. These graphs are of particular interest and prove essential for analysing the boundary effects in the random minimal directed spanning forest with respect to $[0,1]^2$. Additionally, this chapter addresses the convergence in distribution to the total edge length of the

random MDSF within $[0,1]^2$. The limit distribution of total edge length involves two independent components: a normal element arising from points in the bulk (as discussed in Chapter 5) and a non-normal element resulting from boundary effects as given by (Theorem 6.1.1); this theorem will provide an important step in demonstrating the convergence behaviour to our main result Theorem 3.3.2 (ii) for both singly-aligned cones. To analyse these boundary effects, we shall use results from Chapter 3 and Chapter 5, where the stabilisation methodology deals with the normal element. Finally, we demonstrate how the directed linear forest (DLF) can be used to analyse the limiting behaviour of the contribution to the total edge length of the random minimal directed spanning forest near the boundary of the unit square.

Chapter 7 will offer two fundamental results associated with the interaction between bulk and boundary region of the unit square. First, we will show that as the number of points tends to infinity, the contribution to the total edge length from points in the intermediate region has variance converging to zero as given by (Theorem 7.2.1). Following that, we will show the asymptotic independence of the random variables corresponding to the contributions to the total edge length converging from the bulk and boundary regions. Finally, we will provide the proof of part (ii) of our main result Theorem 3.3.2 for both singly-aligned cones.

Chapter 8 contains concluding remarks, further research and research achievements from Chapters 3 to 7.

Chapter 2

Mathematical Prerequisites

2.1 Introduction

This chapter is designed to present mathematical introductions to several topics: random spatial graphs, the Poisson distribution, Poisson point processes, the convergence of random variables, and inequalities.

In Section 2.2, we outline the construction of random spatial graphs using the definition of the Euclidean norm. We will also offer an example of a random spatial graph, namely the nearest-neighbour graph, and introduce some fundamental definitions related to graph theory. Section 2.3 discusses the Poisson distribution with its properties and theorems, alongside an introduction to the Poisson point processes. Section 2.5 provides an exposition on the convergence of random variables. Section 2.6 highlights various inequalities, which we later rely on.

In the following section, we deliver one example of our spatial graphs and the rest of examples provided, for example, see Wade [44].

2.2 Random Spatial Graphs

Random spatial graph is one of the essential models in probability theory. It displays profound mathematical properties and has a wide and valuable range of applications in many scientific fields in modelling various networks with spatial content, such as communications networks, social networks, and transportation platforms. The random spatial graph is a stochastic process that can be constructed on randomly distributed points in the unit square, with edges added according to some geometrical rule based on proximity. In particular, these graphs in which each point joins by an edge to its nearest neighbour are locally determined in some sense. This topic has been extensively researched for a while, and notable examples include the Euclidean minimal spanning tree and the nearest-neighbour graph with its variants [31, 44].

Let $\|\cdot\|$ be the norm on space $\mathbb{R}^d$ for $\mathbf{X} = (x_1, \ldots, x_d) \in \mathbb{R}^d$. We write

$$\|\mathbf{X}\| := \sqrt{\sum_{i=1}^{d} |x_i|^2}.$$

Here, we provide a brief overview of fundamental graph theory concepts (see [14] for more details). In graph theory, a graph, denoted as G, is defined as an ordered pair $G = (V, E)$, where V represents a countable set of points or vertices, and E represents a set of unordered pairs of vertices selected from V. For the purposes of this thesis, we treat V as a random finite subset of Euclidean space, specifically $V = v_1, v_2, v_3, \ldots, v_n \subseteq \mathbb{R}^d$, usually $d = 2$. Every unordered pair of E denotes an edge between vertices $v, u \in V$. The graphical representation of the graph G is created by representing the points in V as nodes and connecting them with edges defined by the pairs in E.

2.2.1 The Nearest-Neighbour Graph (NNG)

In this section, we introduce the concept of the nearest-neighbour graph (NNG). Nearest-neighbour graphs (NNG) and nearest-neighbour distances (NND) can be defined in any metric space, and find extensive applications in various fields of applied science. These fields include the social sciences, geography, and ecology,

primarily focusing on proximity data analysis. For multivariate analysis, nearest-neighbour graphs and nearest-neighbour distances as well non-parametric statistics explored in many areas of research, such as classification, regression, goodness of fit, dimensionality, two and multiple sample problems, see e.g. [10, 15, 17, 18], and among others. Here is the definition; see for example, Wade [44].

Definition 2.2.1 (Nearest neighbour graph)**.** Let $\mathcal{X}$ be a finite set of points in $\mathbb{R}^2$. The nearest-neighbour graph on $\mathcal{X}$ is defined by joining a directed edge each point $\boldsymbol{x} \in \mathcal{X}$ to its nearest neighbour $\boldsymbol{y} \in \mathcal{X} \setminus \{\boldsymbol{x}\}$, whenever such a neighbour exists.

Figure 2.1 below shows the realization of the nearest-neighbour graph with 50 random points uniformly generated in the unit square.

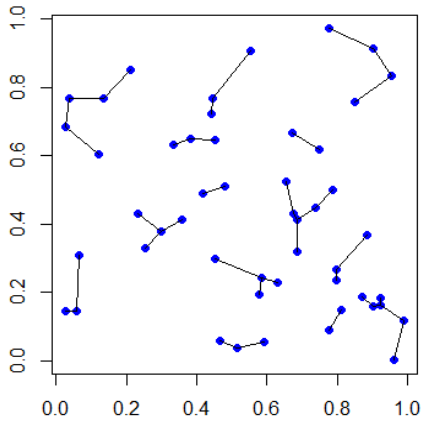

Figure 2.1: Realization of the NNG, with 50 random points uniformly generated in the unit square.

2.3 Poisson Distribution

In 1837, Simeon Denis Poisson introduced the Poisson distribution as part of his research on probability theory, which he documented in his work titled "Recherches sur la probabilité des jugements en matière criminelle et en matière civile" [42]. This research focused on addressing misconceptions related to the random probability associated with discrete events occurring at various time intervals, particularly in

the context of legal judgments. In 1860, Simon Newcomb extended the application of the Poisson distribution by modelling it to describe the number of stars observed in a given region of space [16]. Ladislaus Bortkiewicz made a significant contribution by further extending the Poisson distribution. In 1898, he applied this extension to assess and analyse the number of Prussian army soldiers killed by horse kicks. Ladislaus Bortkiewicz's work not only had implications in the field of mathematics but also found practical applications in engineering and related disciplines.

Poisson distribution is a discrete probability distribution and an aspect of probability theory and statistics. It is used to describe the probability of a given number of events occurring within a fixed period and/or space. For the rest of the intervals, for example, area, distance, or even volume, Poisson distribution is used and expressed for the number of events, see for example, [38]. An important feature of the Poisson distribution is its ability to estimate the count of events that occur independently and randomly [2]. This makes a valuable tool for analysing and predicting the occurrence of rare events or events with low probabilities.

Below we state the definition of Poisson distribution with parameter λ , see for example [12].

Definition 2.3.1. A discrete random variable X is said to have a Poisson distribution with non-negative parameter λ, if for $\ell \in \mathbb{Z}_+$, the probability mass function (pmf) of X is

$$\mathbf{P}(X = \ell) = \frac{\exp(-\lambda)\lambda^{\ell}}{\ell!}. \tag{2.3.1}$$

If (2.3.1) holds, we write $X \sim \mathbf{Po}(\lambda)$.

The following result is the "additivity property" of the Poisson distribution. It states that the sum of two independent Poisson random variables is also Poisson [12].

Theorem 2.3.2. *If* $X \sim \mathbf{Po}(\mu)$ *and* $Y \sim \mathbf{Po}(\lambda)$ *are independent, then* $X + Y \sim \mathbf{Po}(\mu + \lambda)$.

Proof. To find the probability mass function of the sum of two independent Poisson random variables $X + Y$, then we apply the partition theorem to obtain

$$\begin{aligned}
\mathbf{P}(X+Y=n) &= \sum_{\ell=0}^{n} \mathbf{P}(X+Y=n|X=\ell)\mathbf{P}(X=\ell) \\
&= \sum_{\ell=0}^{n} \mathbf{P}(Y=n-\ell|X=\ell)\mathbf{P}(X=\ell) \\
&= \sum_{\ell=0}^{n} \mathbf{P}(Y=n-\ell)\mathbf{P}(X=\ell) = \sum_{\ell=0}^{n} \frac{\exp(-\lambda)\lambda^{n-\ell}}{(n-\ell)!}\frac{\exp(-\mu)\mu^{\ell}}{\ell!} \\
&= \sum_{\ell=0}^{n} \frac{\exp(-\lambda)(\exp(-\mu))}{\ell!}\binom{n}{\ell}\mu^{\ell}\lambda^{n-\ell} \\
&= \frac{\exp(-(\mu+\lambda))}{n!}\sum_{\ell=0}^{n}\binom{n}{\ell}\mu^{\ell}\lambda^{n-\ell} = \frac{\exp(-(\lambda+\mu))(\lambda+\mu)^{n}}{n!}.
\end{aligned}$$

The last part of this equality is used the binomial theorem. The last expression is the probability mass function of a $\mathbf{Po}(\mu+\lambda)$ distribution, i.e. $X+Y \sim \mathbf{Po}(\mu+\lambda)$. □

2.4 Poisson Point Processes

Poisson point process stands as one of the most commonly employed counting processes. It is typically used in situations where it is necessary to count specific events that occur at a certain rate but in a completely random manner, devoid of any discernible structure. Poisson point process is considered a fundamental technique in geometrical probability. Here is a formal definition of the Poisson process. Consider a Poisson point process denoted as $\mathcal{P}_\lambda$, which is a random countable subset of the unit square. The key characteristic of this process is the randomness in the placement of points within the square, and the parameter λ governs the intensity or rate of point occurrences (see Kingman's book [21] for more details about the general definition and theory of Poisson processes).

In this thesis, we use $|\cdot|$ to denote both the cardinality (i.e., number of elements) for a finite set, and to denote the area (two-dimensional Lebesgue measure) for a subset of $\mathbb{R}^2$. Next we provide the definition of the Poisson point process with intensity λ.

Definition 2.4.1. For $\lambda > 0$, the random countable set $\mathcal{P}_\lambda \subset \mathbb{R}^2$ is said to be a homogeneous Poisson point process on $[0,1]^2$ with intensity λ, if the following two properties are satisfied by the collection of counting random variables $N(A) = |A \cap \mathcal{P}_\lambda|$ (the number of points in set $A \subseteq [0,1]^2$). The properties are given as follows.

- For every $n \in \mathbb{N}$, and all pairwise disjoint $A_1, \ldots, A_n \subseteq [0,1]^2$, the random variables $N(A_1), \ldots, N(A_n)$ are independent.
- The random variable $N(A) \sim \mathbf{Po}(\lambda|A|)$, where $|A|$ is the area of $A \subset \mathbb{R}^2$.

Alternative description in terms of randomized binomial process is given as follows. Assume that $X_1, X_2, X_3, \ldots$ be a sequence of random variables on $\mathbb{R}^d$, independently identically distributed with the uniform density on $[0,1]^2$. So for $n \in \mathbb{N}$, we can write

$$\mathcal{X}_n := \{X_1, X_2, \ldots, X_n\}.$$

Here, $\mathcal{X}_n$ is a point process consisting of n independent identically distributed random variable on $\mathbb{R}^d$, for us we consider only $d = 2$. We can obtain a Poisson point process by considering a random number of the random variables $X_1, X_2, \ldots$ For $\lambda > 0$, let N_λ be a Poisson random variable independent of $\{X_1, X_2, \ldots\}$, then $\mathcal{X}_{N_\lambda} = \{X_1, X_2, \ldots, X_{N_\lambda}\}$ is a Poisson process with intensity λ.

2.5 Convergence of Random Variables

This section will discuss two important theorems in probability: the law of large numbers (LLN) and the central limit theorem (CLT). Specifically, we will focus on these theorems in this thesis.

The concept of convergence of random variables is fundamental in probability theory and statistics. It deals with the behaviour of random variable sequences as they grow. Understanding the convergence of random variables is essential for making statistical inferences and drawing conclusions from data. There are many types of convergence for random variables lasted below, each having its properties

and implications. We define these types of convergence as follows. Let $X_1, X_2, \ldots$ be a sequence of random variables, e.g., see A. Gut [20] for more details.

Definition 2.5.1. A sequence of random variables $X_1, X_2, X_3, \ldots$ converges in probability to the random variable X if for every $\epsilon > 0$, that

$$\lim_{n\to\infty} \mathbf{P}(|X_n - X| \geq \epsilon) = 0.$$

Definition 2.5.2. A sequence of random variables $X_1, X_2, X_3, \ldots$ converges almost surely (a.s.) to the random variable X, if

$$\mathbf{P}\left(\left\{\lim_{n\to\infty} X_n = X\right\}\right) = 1.$$

The law of large numbers used to play a central role in probability and statistics. The law of large numbers states that as the number of independent and identically distributed random variables becomes sufficiently large, the sample mean (average) of these variables converges in probability to the expected value of the distribution. For example, let $X_1, X_2, ..., X_n$ be a sequence of independent and identically distributed random variables, if $\mathbf{E}[X_i] = \mu$, then $\overline{X}_n \overset{a.s.}{\to} \mu$, where

$$\overline{X}_n = \frac{\sum_{i=1}^{n} X_i}{n}.$$

This is the classical strong law of large numbers.

Definition 2.5.3. Let $p \geq 1$. A sequence of random variables $X_1, X_2, X_3, \ldots$ converges in p^{th}-mean to the random variable X, if

$$\lim_{n\to\infty} \mathbf{E}(|X_n - X|^p) = 0.$$

For a random variable X, write F_X for the cumulative distribution function $F_X(x) := \mathbf{P}(X \leq x)$.

Definition 2.5.4. A sequence of random variables $X_1, X_2, X_3, \ldots$ converges in distribution to the random variable X, if

$$\lim_{n\to\infty} F_{X_n}(x) = F_X(x), \text{ for all } x \in C(F_X),$$

where $C(F_X) = \{x : F_X(x) \text{ is continuous at } x\}$ which is the set of continuity points of F_X.

The previous concept is illustrated by the famous central limit theorem (CLT). The CLT states that if certain conditions are met, then the sum of a large number of random variables will have an approximately normal distribution. For example, let $X_1, X_2, ..., X_n$ be a sequence of independent and identically-distributed random variables with mean $\mathbf{E}[X_i] = \mu$ and variance $\mathbf{Var}[X_i] = \sigma^2 < \infty$. Then, we define

$$Z_n = \frac{\overline{X} - \mu}{\sigma/\sqrt{n}} = \frac{\sum_{i=1}^{n} X_i - n\mu}{\sqrt{n\sigma^2}},$$

the central limit theorem states that, if $\Phi(x)$ is the standard normal cumulative distribution function

$$\lim_{n\to\infty} \mathbf{P}(Z_n \leq x) = \Phi(x), \qquad \text{for all } x \in \mathbb{R},$$

i.e., converges in distribution to standard normal random variable as $n \to \infty$.

Slutsky's Theorem is a fundamental result in probability and statistics that describes the limiting behaviour of sequences of random variables and their relationships as they approach their limits. This theorem offers valuable insights into how the convergence of random variables impacts the convergence of functions involving these variables. Slutsky's Theorem (e.g., see Theorems 11.3 and 11.4 in A. Gut [20]) given as follows.

Theorem 2.5.5. *Let $X_1, X_2, \ldots$ and $Y_1, Y_2, \ldots$ be sequences of random variables, such that X_n converges in distribution to X and Y_n converges in probability to a constant $c \in \mathbb{R}$. Then, as $n \to \infty$*

$$X_n + Y_n \xrightarrow{d} X + c,$$
$$X_n Y_n \xrightarrow{d} Xc,$$
$$\frac{X_n}{Y_n} \xrightarrow{d} \frac{X}{c},$$

the last statement requires that $c \neq 0$.

We present the argument for the addition only, since the result for the rest will follow the same process.

Proof. Let $\epsilon > 0$. For $x \in \mathbb{R}$,

$$\begin{aligned} F_{X_n+Y_n}(x) = \mathbf{P}(X_n + Y_n \leq x) &\leq \mathbf{P}(\{X_n + Y_n \leq x\} \cap \{|Y_n - c| < \epsilon\}) \\ &\quad + \mathbf{P}(|Y_n - c| \geq \epsilon) \\ &\leq \mathbf{P}(X_n \leq x - c + \epsilon) + \mathbf{P}(|Y_n - c| \geq \epsilon). \end{aligned} \tag{2.5.1}$$

Similarly,

$$F_{X_n+Y_n}(x) \geq \mathbf{P}(X_n \leq x - c + \epsilon). \tag{2.5.2}$$

Hence, if $x - c$, $x - c + \epsilon$, and $x - c - \epsilon$ are continuity points of F_X, then it follows from inequality (2.5.1), inequality (2.5.2), and convergence of $X_n + Y_n$, that

$$F_X(x - c - \epsilon) \leq \liminf_{n\to\infty} F_{X_n+Y_n}(x) \leq \limsup_{n\to\infty} F_{X_n+Y_n}(x) \leq F_X(x - c + \epsilon).$$

Finally, let $\epsilon \to 0$, and as $n \to \infty$,

$$F_{X_n+Y_n}(x) \to F_X(x - c),$$

which is the cumulative distribution function of $c + X$. □

2.6 Inequalities

In probability theory, inequalities are the mathematical relationships between different events on random variables. These inequalities are essential for analysing and bounding probabilities on certain events or random variables. Here are a few notable inequalities connected with probability (see, e.g., [20, 25] for more details).

Markov's Inequality

Markov's inequality provides an upper bound on the probability that a non-negative random variable is greater than or equal to a positive constant. Let X be any non-negative random variable, i.e., $\mathbf{P}[X \geq 0] = 1$, and λ is a positive constant, then we can write $\mathbf{P}[X \geq \lambda] \leq \frac{\mathbf{E}[X]}{\lambda}$, which is known by Markov's inequality.

Cauchy–Schwarz Inequality

The Cauchy-Schwarz inequality is a fundamental mathematical inequality. There are several equivalent ways to express this inequality, but one of the most common forms is given as follows. For any two random variables X and Y on the same sample space, then $\mathbf{E}[|XY|] \leq \mathbf{E}[X^2]^{\frac{1}{2}} \cdot \mathbf{E}[Y^2]^{\frac{1}{2}}$, where inequality holds if and only if $X = \alpha Y$, for some constant $\alpha \in \mathbb{R}$.

Minkowski's Inequality

Minkowski's inequality is a significant mathematical inequality. It states that, for any random variables X and Y, and $1 \leq p < \infty$, the following statement holds $\mathbf{E}[|X + Y|^p]^{1/p} \leq \mathbf{E}[|X|^p]^{1/p} + \mathbf{E}[|Y|^p]^{1/p}$.

Chapter 3

Minimal Directed Spanning Forest (MDSF)

In this chapter, we study the concept of the minimal directed spanning forest (MDSF) in the unit square. MDSF is a particular graph that recently received significant attention, first explored by Bhatt and Roy [8], as a potential model for telecommunications and drainage networks.

Section 3.1 defines the concept of rays and the classification of cones. Section 3.2 introduces the background of MDSF. The MDSF defines with parameters θ, ϕ on a locally finite set of points in the unit square. In Section 3.3, we presents our main Theorem 3.3.2 for this thesis, which will cover all types of general cones with respect to the unit square. Finally, in Section 3.4, we show that a non-normal contribution from near boundary of the unit square, its contribution to the total edge length of the graph can be characterized by a fixed-point equation.

3.1 Direction Cones and Partial Orders

This section defines our cone with parameters θ, ϕ in the unit square. The directional relation that specifies which edges are permitted is expressed through a cone $C_{\theta,\phi}(\boldsymbol{x})$, or, equivalently, via a partial order. Note that this thesis only considers the general

cone in the unit square, not a partial order. We give below the formal definitions of rays and the cone classification with parameters θ, ϕ. Figure 3.1 below shows the general cone with some cone constraints in $[0,1]^2$.

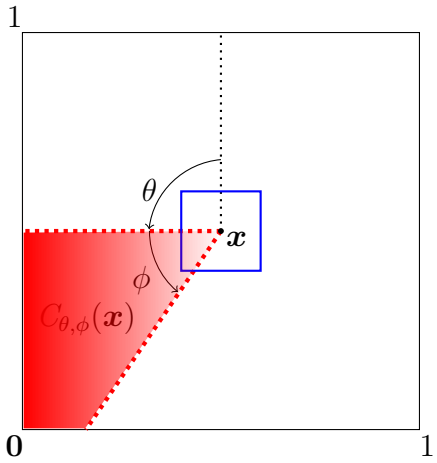

Figure 3.1: General cone in the unit square.

Definition 3.1.1. For $\boldsymbol{x} \in \mathbb{R}^2$ and any angle $\alpha \in [0, 2\pi)$ define the ray from $\boldsymbol{x}$ with angle α to be the half-line $\{\boldsymbol{x} + c\boldsymbol{e}_\alpha : c \in \mathbb{R}_+\}$ where $\boldsymbol{e}_\alpha = (-\sin\alpha, \cos\alpha)$ in standard basis of $\mathbb{R}^2$.

Call the 4 rays from $\boldsymbol{x}$ with angle $\alpha \in \{0, \frac{\pi}{2}, \pi, \frac{3\pi}{2}\}$ the coordinates axes from $\boldsymbol{x}$ (or axes for short). In our methodology, a general cone can be defined by two parameters $\theta \in [0, 2\pi)$ and $\phi \in (0, \pi]$, given by the following definition.

Definition 3.1.2. For $\theta \in [0, 2\pi)$, $\phi \in (0, \pi)$. Define $C_{\theta,\phi}(\boldsymbol{x})$ to be the cone with apex at $\boldsymbol{x}$ formed as a union of rays from $\boldsymbol{x}$ with angle $\alpha \in [\theta, \theta + \phi]$, measured anticlockwise from the vertical direction.

The cone $C_{\theta,\phi}(\boldsymbol{x})$ can also be used to define a partial order on $\mathbb{R}^2$. Recall that a partial order $\preccurlyeq$, (see e.g., [22]) in general, is a binary relationship between the elements of the set V, such that

(a) $\preccurlyeq$ is reflexive, meaning that $u \preccurlyeq u$, $\forall\ u \in V$;

(b) $\preccurlyeq$ is transitive, meaning that if $u \preccurlyeq v$, $v \preccurlyeq w$ then $u \preccurlyeq w$, $\forall\ u, v, w \in V$;

(c) $\preccurlyeq$ is anti-symmetric, meaning that if $u \preccurlyeq v$ and $v \preccurlyeq u$ then $u = v$, $\forall\, u, v \in V$.

The partial order satisfies the equivalence relations, so by setting $\boldsymbol{x}, \boldsymbol{y} \in \mathbb{R}^2$ (e.g., see Wade [45] for more details), the following equivalence relation holds.

$$\boldsymbol{x} \overset{\theta,\phi}{\preccurlyeq} \boldsymbol{y} \iff \boldsymbol{x} \in C_{\theta,\phi}(\boldsymbol{y}). \tag{3.1.1}$$

We use θ, ϕ to define a partial order $\overset{\theta,\phi}{\preccurlyeq}$ on $\mathbb{R}^2$ via (3.1.1). There are three types of general cones $\overset{\theta,\phi}{\preccurlyeq}$, we list them in the following definition.

Definition 3.1.3. (Cone classification): We classify the following categories $\overset{\theta,\phi}{\preccurlyeq}$, $\theta \in [0, 2\pi)$, and $\phi \in (0, \pi)$, as follows.

(a) The general cone is called doubly-aligned if both θ and $\theta + \phi$ are in $\frac{\pi}{2}\mathbb{Z}$.

(b) The general cone is called singly-aligned if exactly one of θ and $\theta + \phi$ belongs to $\frac{\pi}{2}\mathbb{Z}$.

(c) The general cone is called unaligned if neither θ nor $\theta + \phi$ belongs to $\frac{\pi}{2}\mathbb{Z}$.

The coordinate-wise partial order is a special case of a partial order, (for example see Figure 3.2 *Right panel*) denoted by '$\overset{\frac{\pi}{2},\frac{\pi}{2}}{\preceq}$' on $[0, 1]^2$. The coordinate-wise partial order satisfies the following property, for $\boldsymbol{x}_1 \leq \boldsymbol{x}_2$ and $\boldsymbol{y}_1 \leq \boldsymbol{y}_2$ if and only if $(\boldsymbol{x}_1, \boldsymbol{x}_2) \overset{\theta,\phi}{\preccurlyeq} (\boldsymbol{y}_1, \boldsymbol{y}_2)$.

3.2 MDSF: Definition, Background, Simulations

We define the the minimal directed spanning forest on a locally finite set $\mathcal{X}$ of points in $[0, 1]^2$ as follows, using the cones $C_{\theta,\phi}(\boldsymbol{x})$ defined in the previous section.

Definition 3.2.1 (Directed nearest-neighbours)**.** Fix $\theta \in [0, 2\pi)$, $\phi \in (0, \pi)$. Let $\mathcal{X} \subseteq \mathbb{R}^2$ be locally finite, non-empty with $\boldsymbol{x} \in \mathcal{X}$. Then,

- if $\mathcal{X} \cap C_{\theta,\phi}(\boldsymbol{x}) = \{\boldsymbol{x}\}$, set

$$\mathcal{D}_{\theta,\phi}(\boldsymbol{x}; \mathcal{X}) := 0$$

$$N_{\theta,\phi}(\boldsymbol{x}, \mathcal{X}) := \boldsymbol{x},$$

- if $|\mathcal{X} \cap C_{\theta,\phi}(\boldsymbol{x})| \geq 2$, set

$$\mathcal{D}_{\theta,\phi}(\boldsymbol{x};\mathcal{X}) := \inf\{\|\boldsymbol{y}-\boldsymbol{x}\| : \boldsymbol{y} \in C_{\theta,\phi}(\boldsymbol{x}) \setminus \{\boldsymbol{x}\}\}.$$

  By local finiteness $\mathcal{D}_{\theta,\phi}(\boldsymbol{x};\mathcal{X})$ is an attained by some $\boldsymbol{y} \in \mathcal{X} \cap C_{\theta,\phi}(\boldsymbol{x}) \setminus \{\boldsymbol{x}\}$, hence $(\mathcal{D}_{\theta,\phi}(\boldsymbol{x};\mathcal{X}) > 0)$. Choose arbitrary $N_{\theta,\phi}(\boldsymbol{x};\mathcal{X}) \in \mathcal{X} \cap C_{\theta,\phi}(\boldsymbol{x}) \setminus \{\boldsymbol{x}\}$, such that

$$\|\boldsymbol{x} - N_{\theta,\phi}(\boldsymbol{x};\mathcal{X})\| = \mathcal{D}_{\theta,\phi}(\boldsymbol{x};\mathcal{X}).$$

The $N_{\theta,\phi}(\boldsymbol{x};\mathcal{X})$, if different from $\boldsymbol{x}$, is the *directed nearest neighbour* of $\boldsymbol{x}$ in $\mathcal{X}$ (with respect to angles θ, ϕ), and $\mathcal{D}_{\theta,\phi}(\boldsymbol{x};\mathcal{X})$ is the corresponding nearest-neighbour distance.

Definition 3.2.2 (Minimal directed spanning forest)**.** For fixed cone parameters θ, ϕ, let $\mathcal{X}$ be a finite set of points in $\mathbb{R}^2$. The minimal directed spanning forest on $\mathcal{X}$ is defined by joining each point $\boldsymbol{x} \in \mathcal{X}$ by an edge to its directed nearest neighbour $N_{\theta,\phi}(\boldsymbol{x};\mathcal{X})$, provided this is different from $\boldsymbol{x}$, i.e., the closest point chosen from the set of points in $\mathcal{X} \setminus \{\boldsymbol{x}\}$ that lies inside the cone $C_{\theta,\phi}(\boldsymbol{x})$.

Bhatt and Roy [8] introduced the concept of the minimal directed spanning tree (MDST), and they illustrated that the MDST on random points in $[0,1]^2$ are similar to the standard minimal spanning tree and the nearest-neighbour graph for a set of points in the plane. The uniqueness of their method is to consider all edges aligned in the 'south-west' direction. The motivation behind exploring the concept of the MDST arises from its applications in communications and drainage networks [8, 32, 39]. One notable aspect that sets limit theory for the MDST apart from the ordinary nearest-neighbour graph (NNG) is the consideration of boundary effects. These boundary effects can introduce non-Gaussian contributions to the limit behaviour, making the study of MDSTs particularly relevant and distinct in scenarios where spatial distribution plays an essential role. Boundary effects in the context of minimal directed spanning trees are a consequence of the constraints placed on the direction of edges. These constraints arise due to the potential occurrence of long edges near the lower and left boundaries of $[0,1]^2$. Understanding the properties of minimal directed spanning trees when applied to random points within square,

especially as the number of points tends to infinity, is a topic of significant interest. It allows us to explore the behaviour of MDSTs under various conditions and gain insights into their limit behaviour, which can be important in various applications and studies involving spatial networks and distributions.

We also use the concept of minimal directed spanning forest, which is basically the minimal directed spanning tree when the edges are removed from the origin $\mathbf{0}$ (see for example, Figure 3.2 (*Right Panel*)). However, MDSF is more practical when the models assess the general partial order, e.g. see Wade [44]. The 'south-west' directional model can be extended to a large class of direction, defined in terms of cones parameterised by two angles θ, ϕ, as described in Section 3.1. Different cones within this parameterisation can influence the presence and behaviour of boundary effects, making a versatile framework for studying spatial networks under various directional constraints.

Figure 3.2 shows the difference between the south and south-west versions in the unit square. Figure 3.2 shows the minimal directed spanning forest with 50 uniform points generated randomly in the unit square. The *Left Panel* is the south version. The *Right Panel* is the 'south-west' version (also, is called a doubly-aligned cone since the long edges are aligned with the square $[0,1]^2$). The difference between the south and 'south-west' versions is that in the doubly-aligned cone, there are two boundary contributions from the bottom boundary and the most left boundary of the square. In the south case, there is only one boundary contribution from the lower vertical coordinate.

Figure 2.1 in Section 2.2 and Figure 3.2 (*Right Panel*) highlight the difference between the NNG and MDSF models. For the NNG model, each point is joined to its nearest neighbour (without any further condition). In the MDSF model, each point is joined to the nearest neighbour chosen from these points to the south-west direction. For NNG model, there is no boundary contribution associated with total edge length, as a result, the central limit theorem holds. On the other hand, in MDSF model, there are two boundary contributions from bottom boundary and

from most left boundary of the square. The limit distribution will follow two independent components: (i) a normal contribution from the bulk and (ii) a non-normal contribution from the near boundary of the unit square, whose distribution can be characterized by a fixed-point equation, for example, see Penrose and Wade [31] for more details.

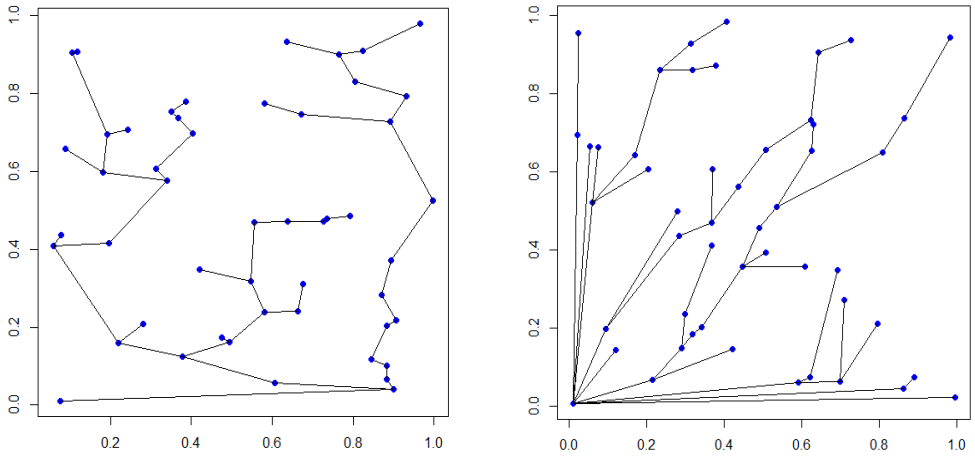

Figure 3.2: Realizations of the MDSF with 50 random points uniformly generated in the unit square. *Left Panel* south version with parameters: $\theta = \frac{\pi}{2}, \phi = \pi$; and south-west version with parameters: $\theta = \phi = \frac{\pi}{2}$.

Figures 3.3 – 3.5 below show the MDSF with 50 uniform points generated randomly in the unit square for both singly-aligned cones (obtuse and acute angles) and the unaligned cone. These diagrams show very long edges near the boundary of the unit square. The limit theory for the total edge length of these graphs does not follow a normal distribution, as the nature of the central limit theorem in this situation is disrupted due to long edges near the boundary. Both singly-aligned cones have one aligned ray along the side of the square. Moreover, it shows that asymptotically a non-normal limit due to boundary effects. The unaligned cone has no rays aligned with a square; as a result, it shows asymptotically a normal limit since no boundary effects are occurring.

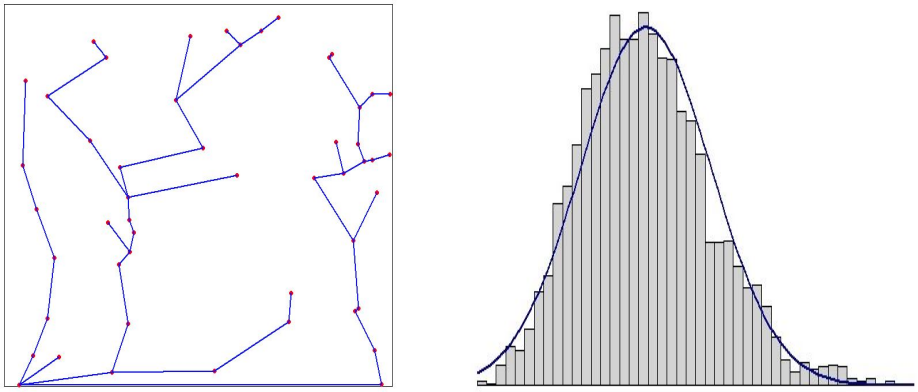

Figure 3.3: A realization of the MDSF, with 50 random points uniformly generated in the unit square with parameters: $\theta = \frac{\pi}{2}$, $\phi = \frac{3\pi}{4}$; and a histogram of simulated total edge lengths from a sample of 5×10^4 simulations. The histogram is overlaid with a plot of the normal density with mean and variance matching the sample mean and variance, illustrating an apparent non-normal distribution, due to boundary effects.

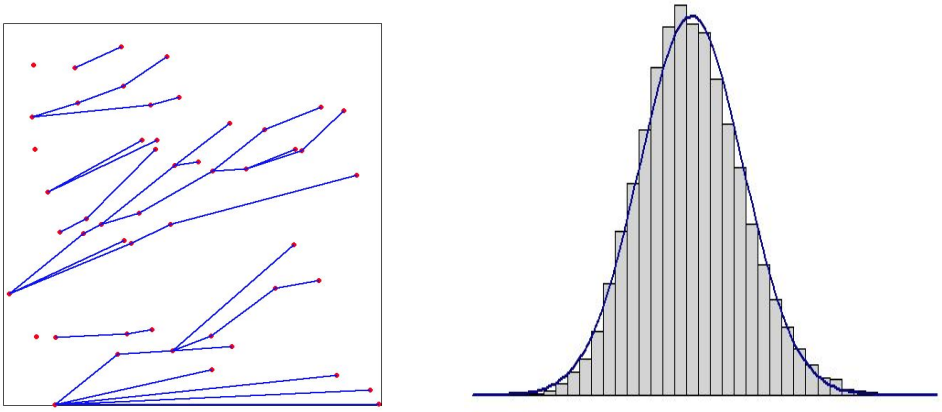

Figure 3.4: A realizations of the MDSF, with 50 random points uniformly generated in the unit square with parameters: $\theta = \frac{\pi}{2}$, $\phi = \frac{\pi}{4}$; and a histogram is overlaid with a plot of the normal density with mean and variance matching the sample mean and variance, illustrating an apparent non-normal distribution, due to boundary effects.

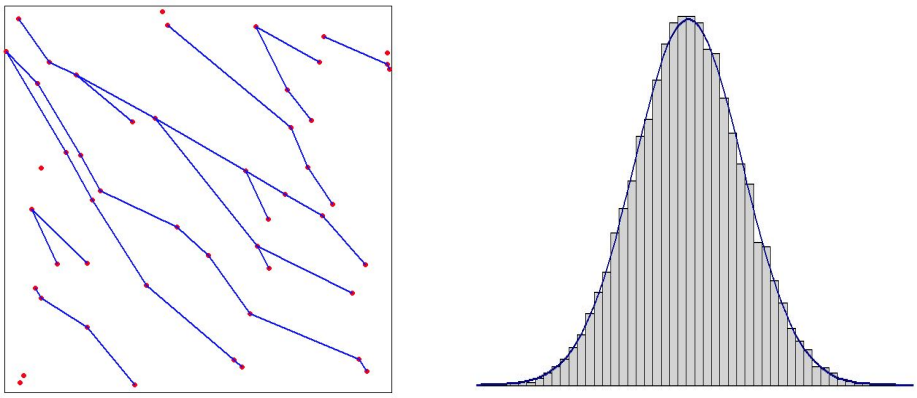

Figure 3.5: Realization of the MDSF, with 50 random points uniformly generated in the unit square with parameters: $\theta = \frac{\pi}{8}$, $\phi = \frac{\pi}{4}$; and a histogram is overlaid with a plot of the normal density with mean and variance matching the sample mean and variance, illustrating an apparent a normal distribution, due to absence of boundary effects.

3.3 Limit Theorem for Total Edge-Length

This section will state our main result for this thesis Theorem 3.3.2. Recall the definition of $N_{\theta,\phi}(\boldsymbol{x})$ and $\mathcal{D}_{\theta,\phi}(\boldsymbol{x};\mathcal{X})$ from Definition 3.2.1. In the case that $|\mathcal{X} \cap C_{\theta,\phi}(\boldsymbol{x})| \geq 2$, then $N_{\theta,\phi}(\boldsymbol{x},\mathcal{X})$ is a nearest neighbour of $\boldsymbol{x}$, and $\mathcal{D}_{\theta,\phi}(\boldsymbol{x};\mathcal{X})$ is the distance from $\boldsymbol{x}$ to this nearest neighbour.

Definition 3.3.1 (Total edge length of MDSF)**.** Let $\mathcal{L}(\mathcal{X})$ be the length of the minimal directed spanning forest on the locally finite set $\mathcal{X}$ in $[0,1]^2$ i.e.,

$$\mathcal{L}(\mathcal{X}) = \sum_{\boldsymbol{x}\in\mathcal{X}} \mathcal{D}_{\theta,\phi}(\boldsymbol{x};\mathcal{X}) = \sum_{\boldsymbol{x}\in\mathcal{X}} \|\boldsymbol{x} - N_{\theta,\phi}(\boldsymbol{x};\mathcal{X})\|.$$

Recall from the Definition 2.4.1 that $\mathcal{P}_\lambda$ is a homogeneous Poisson point process on $[0,1]^2$ of intensity λ. The main objective here is to study the centred total length of the minimal directed spanning forest. Let $\tilde{\mathcal{L}}_\lambda = \mathcal{L}(\mathcal{P}_\lambda) - \mathbf{E}[\mathcal{L}(\mathcal{P}_\lambda)]$ be the centred total length in $[0,1]^2$. The main result of this thesis is given below.

Theorem 3.3.2. *Let $\theta \in [0, 2\pi)$, $\phi \in (0, \pi)$. There exists a distribution $\mathcal{Q}$ on $\mathbb{R}$ and constants $s_\phi \in (0,\infty)$ such that if Q_1, Q_2, Z are mutually independent with*

$Q_1, Q_2 \sim \mathcal{Q}$ and $Z \sim \mathcal{N}(0,1)$, then the following limit theorems hold.

(i) If (θ, ϕ) is doubly-aligned, then, as $\lambda \to \infty$,

$$\tilde{\mathcal{L}_\lambda} \xrightarrow{d} s_\phi Z + Q_1 + Q_2. \tag{3.3.1}$$

(ii) If (θ, ϕ) is singly-aligned, then, as $\lambda \to \infty$,

$$\tilde{\mathcal{L}_\lambda} \xrightarrow{d} s_\phi Z + Q_1. \tag{3.3.2}$$

(iii) If (θ, ϕ) is unaligned, then, as $\lambda \to \infty$,

$$\tilde{\mathcal{L}_\lambda} \xrightarrow{d} s_\phi Z. \tag{3.3.3}$$

Remark 3.3.3. The normal random variable $s_\phi Z$ arises from the edges in bulk (see Section 5.3). The non-normal elements Q_1, Q_2 arise from the edges near boundary, where the minimal directed spanning forest is asymptotically close to the directed linear forest (see Section 6.2).

Remark 3.3.4. Part (i) of Theorem 3.3.2 was previously proved by [Penrose and Wade [31], Theorem 2.1.]. Parts (ii) & (iii) complete the classification for cones with parameters $\theta \in [0, 2\pi)$ and $\phi \in (0, \pi)$. The proof of part (iii) of Theorem 3.3.2 will be provided in Section 5.4, and the proof of part (ii) will be provided in Section 7.4.

The proof of Theorem 3.3.2 has the following plan. We shall show in Chapter 5 that the contribution to the total edge length of the MDSF from edges away from the boundary of the unit square converges in distribution to a normal random variable. Following that in Chapter 6, we will show that the contribution from edges close to the boundary converges in distribution to a non-normal random variable, whose distribution can be characterized by a fixed-point equation. Finally, in Chapter 7, we will show the asymptotic independence between these two contributions, and moreover, that the contribution to the total edge length of the MDSF from the intermediate region converges in probability to zero as the number of points becomes sufficiently large.

Note that the singly-aligned cones fall into two cases: either $\phi < \frac{\pi}{2}$ or $\phi > \frac{\pi}{2}$. By symmetry, the statement Theorem 3.3.2 (ii) only needs proving for the two specific cone types $\theta = \frac{\pi}{2},\ \phi < \frac{\pi}{2}$ (acute case) and $\theta = \frac{\pi}{2},\ \phi > \frac{\pi}{2}$ (obtuse case). In future sections, the names "acute" and "obtuse" refer to these specific cone types as shown in Figure 4.3 and Figure 4.4. Similarly, the only unaligned cones we need to consider for Theorem 3.3.2 (iii) are the three specific cases, as shown in Figures 4.5 – 4.7. Also, see Figures in Appendix B for the classification of general cones.

We give a description of the distribution $\mathcal{Q}$ in the next section via a distributional fixed-point equation.

3.4 Fixed-point Equation for Boundary Contribution

In this section, we shall see that in some cases, the non-normal contribution from near boundary of the unit sqaure. Those boundary contributions can be characterized by a fixed-point equation. The distribution of the random variables Q_1 and Q_2, that appear in Theorem 3.3.2 derived from points close to the bottom boundary of the unit square and is denoted by $\mathcal{Q}$, (see Penrose and Wade [31] for more details). We define below our limiting distribution $\mathcal{Q}$ in terms of a distributional fixed-point equation in (3.4.1). By $\stackrel{d}{=}$, we denote equality in distribution.

$$Q \stackrel{d}{=} U + UQ' + (1-U)Q'' + U\log U + (1-U)\log(1-U), \tag{3.4.1}$$

where $Q, Q', Q'' \sim \mathcal{Q}$, $U, (1-U) \sim \mathcal{U}(0,1)$ and U, Q', Q'' are independent. Theorem 3 of Rösler [40] states that there is a unique mean 0, finite-variance, distribution $\mathcal{Q}$ satisfies (3.4.1). The higher order moments of $\mathcal{Q}$ are obtained recursively from (3.4.1).

Lemma 3.4.1. *For $Q \sim \mathcal{Q}$, the unique mean-zero, finite variance solution to* (3.4.1)*, we have* $\mathbf{Var}[Q] = 2 - \frac{\pi^2}{6}$.

Proof. From equation (3.4.1), we let $f(U) = U + U\log U + (1-U)\log(1-U)$, where U and $(1-U)$ have the same distribution, i.e., $U, (1-U) \sim \mathcal{U}(0,1)$; where also

$Q', Q'' \sim \mathcal{Q}$, and Q', Q'' are independent random variables. We assume $\mathbf{E}[Q] = 0$ and $\mathbf{E}[Q^2] < \infty$.

Now we want to find the expectation and the variance of the random variable Q. To do this, we need to square equation (3.4.1) and apply the expectation. By Theorem 3 of Rösler [40], we see that $\mathbf{E}[Q] = 0$. Then,

$$Q^2 \stackrel{d}{=} U^2 Q'^2 + (1-U)^2 Q''^2 + f(U)^2 + 2UQ'(1-U)Q'' + 2f(U)UQ' + 2f(U)(1-U)Q'', \tag{3.4.2}$$

note that the stated terms $2UQ'(1-U)Q''$, $2f(U)UQ'$, and $2f(U)(1-U)Q''$ are equal zero in expectation.

Next we apply the expectation to (3.4.2), then

$$\mathbf{E}[Q^2] = \mathbf{E}[U^2]\mathbf{E}[Q'^2] + \mathbf{E}[(1-U)^2]\mathbf{E}[Q''^2] + \mathbf{E}[f(U)^2]. \tag{3.4.3}$$

Since U and $(1-U)$ have the same distribution, we have $\mathbf{E}[U^2] = \mathbf{E}[(1-U)^2] = \int_0^1 u^2\, du = \frac{1}{3}$. Now, we consider $\mathbf{E}[Q^2] = \frac{1}{3}(\mathbf{E}[Q^2] + \mathbf{E}[Q^2] + \mathbf{E}[f(U)^2])$ implies $\frac{1}{3}\mathbf{E}[Q^2] = \mathbf{E}[f(U)^2]$, which implies $\mathbf{E}[Q^2] = 3\mathbf{E}[f(U)^2]$ since $\mathbf{E}[Q^2] = \mathbf{E}[Q'^2] = \mathbf{E}[Q''^2]$.

Now we want to find $f(U)^2$, and apply the expectation

$$\begin{aligned} f(U)^2 = U^2 + U^2\log^2 U + (1-U)^2\log^2(1-U) + 2U^2\log U \\ + 2U(1-U)\log(1-U) \\ + 2U(1-U)\log U\log(1-U). \end{aligned} \tag{3.4.4}$$

hence (3.4.4), yields

$$\begin{aligned} \mathbf{E}[f(U)^2] = \mathbf{E}[U^2] + \mathbf{E}[U^2\log^2 U] + \mathbf{E}[(1-U)^2\log^2(1-U)] \\ + 2\mathbf{E}[U^2\log U] \\ + 2\mathbf{E}[U(1-U)\log(1-U)] \\ + 2\mathbf{E}[U(1-U)\log U\log(1-U)]. \end{aligned} \tag{3.4.5}$$

From $\mathbf{E}[f(U)^2]$, we know $\mathbf{E}[U^2] = 1/3$, and using integration by part to find

$$\begin{aligned}\mathbf{E}[U^2 \log^2 U] = \int_0^1 u^2 \log^2 u \, du &= 0 - \int_0^1 \frac{1}{3} u^3 \frac{1}{u} \log u \, du \\ &= -\frac{2}{3} \int_0^1 u^2 \log u \, du \\ &= -\left(-\frac{2}{3}\right) \int_0^1 \frac{1}{3} u^3 \frac{1}{u} \, du \\ &= \left(-\frac{2}{3}\right)\left(-\frac{1}{3}\right) \int_0^1 u^2 \, du = \frac{2}{27}. \end{aligned} \tag{3.4.6}$$

Note since U and $(1-U)$ have the same distribution, that $\mathbf{E}[(1-U)^2 \log^2(1-U)] = \mathbf{E}[U^2 \log^2 U] = \frac{2}{27}$.

Next we have $\mathbf{E}[2U^2 \log U]$ which will follow the same calculation as in (3.4.6), hence

$$\mathbf{E}[2U^2 \log U] = 2 \int_0^1 u^2 \log u \, du = \frac{-2}{9}. \tag{3.4.7}$$

Now we need to find $\mathbf{E}[2U \log U(1-U) \log(1-U)]$. Then we can write it, as follows

$$\begin{aligned}\mathbf{E}[2U \log U(1-U) \log(1-U)] = &\int_0^1 2u \log u \log(1-u) \, du \\ &+ \int_0^1 -2u^2 \log u \log(1-u) \, du. \end{aligned} \tag{3.4.8}$$

We examine (3.4.8) separately. To do this, we need first to find the Taylor series of $\log(1-U)$. Let $y = \log(1-U)$ for $|U| < 1$ implies $y' = -\frac{1}{1-U} = -\sum_{n=0}^{\infty} U^n$, then

$$\log(1-U) = -\sum_{n=0}^{\infty} \frac{U^{n+1}}{n+1} = -\sum_{n=1}^{\infty} \frac{U^n}{n}, \tag{3.4.9}$$

this is the power series, and it is converged since $|U| < 1$. Hence (3.4.9), yields

$$\begin{aligned}\mathbf{E}[2U \log U(1-U) \log(1-U)] &= 2 \int_0^1 u \log u \log(1-u) \, du \\ &= -\int_0^1 2 \sum_{n=1}^{\infty} \frac{u^{n+1}}{n} \log u \, du \\ &= -\sum_{n=1}^{\infty} \frac{2}{n} \int_0^1 u^{n+1} \log u \, du \\ &= \sum_{n=1}^{\infty} \frac{2}{n} \left(\frac{1}{(n+2)^2}\right). \end{aligned} \tag{3.4.10}$$

We calculate the second part of (3.4.8), as follows

$$\int_0^1 -2u^2 \log u \log(1-u)\, du = \sum_{n=1}^{\infty} \frac{2}{n} \int_0^1 u^{n+2} \log u \, du = -\sum_{n=1}^{\infty} \frac{2}{n} \left(\frac{1}{(n+3)^2} \right). \tag{3.4.11}$$

Combining (3.4.10) and (3.4.11), equation (3.4.8), yields

$$\mathbf{E}[2U \log U(1-U) \log(1-U)] = \sum_{n=1}^{\infty} \left(\frac{2}{n} \left(\frac{1}{(n+2)^2} - \frac{1}{(n+3)^2} \right) \right). \tag{3.4.12}$$

Next, we want to calculate $\mathbf{E}[2U(1-U)\log(1-U)]$, so since U and $(1-U)$ have the same distribution, we can write $\mathbf{E}[2U(1-U)\log(1-U)]$ as follows

$$\mathbf{E}[2U(1-U)\log(1-U)] = \mathbf{E}[2U \log U] - \mathbf{E}[2U^2 \log U] = -\frac{1}{2} - \left(-\frac{2}{9} \right) = -\frac{5}{18}. \tag{3.4.13}$$

Finally, combining (3.4.6), (3.4.7), (3.4.12), and (3.4.13), which yields (3.4.5) to be

$$\begin{aligned}
3\mathbf{E}[f(U)^2] &= 3 \left(\frac{1}{3} + \frac{4}{27} - \frac{2}{9} - \frac{5}{18} + \sum_{n=1}^{\infty} \frac{2}{n} \left(\frac{1}{(n+2)^2} - \frac{1}{(n+3)^2} \right) \right) \\
&= 3 \left(-\frac{1}{54} + \sum_{n=1}^{\infty} \left(\frac{2}{n(n+2)^2} - \frac{2}{(n+1)(n+3)^2} + \frac{2}{(n+3)^2} \left(\frac{1}{n+1} - \frac{1}{n} \right) \right) \right) \\
&= 3 \left(-\frac{1}{54} + \frac{2}{9} - \sum_{n=1}^{\infty} \left(\frac{2}{n(n+1)(n+3)^2} \right) \right) \\
&= 3 \left(-\frac{1}{54} + \frac{2}{9} - \sum_{n=1}^{\infty} \left(\frac{2/9}{n} - \frac{1/2}{n+1} \right) \right), \text{ by telescoping series} \\
&= 3 \left(-\frac{1}{54} + \frac{2}{9} - \sum_{n=1}^{\infty} \left(\frac{2/9}{n} - \frac{1/2}{n+1} + \frac{(1/2 - 2/9)}{n+3} + \frac{1/3}{(n+3)^2} \right) \right) \\
&= 3 \left(-\frac{1}{54} + \frac{2}{9} - \sum_{n=1}^{\infty} \left(\frac{2}{9} \left(\frac{1}{n} - \frac{1}{n+3} \right) - \frac{1}{2} \left(\frac{1}{n+1} - \frac{1}{n+3} \right) + \frac{1/3}{(n+3)^2} \right) \right) \\
&= 3 \left(-\frac{1}{54} + \frac{5}{18}\frac{5}{6} - \frac{1}{3} \left(\sum_{n=1}^{\infty} \frac{1}{n^2} - 1 - \frac{1}{4} - \frac{1}{9} \right) \right) = 3 \left(\frac{23}{108} + \frac{49}{108} - \frac{1}{3}\frac{\pi^2}{6} \right) \\
&= 3 \left(\frac{72}{108} - \frac{\pi^2}{18} \right) = 2 - \frac{\pi^2}{6}.
\end{aligned}$$

□

Chapter 4

Partitions of the Unit Square: Companions, Boundary, and Bulk

4.1 Introduction

This chapter aims to highlight the concept of partitioning the unit square, taking into consideration companions, boundaries, and the bulk region. We will use the tiles and companions as essential tools for analysing the properties of square.

In Section 4.2, we illustrate how $\mathbb{R}^2$ can be divided into squares labelled by $\mathbb{Z}^2$, each having a side length denoted as S. We explain the concept of local dependence in terms of these squares and the scale parameter S. Moving into Section 4.3, we will identify some 'good' choices of companions for the different cone geometries. In Section 4.4, we will go through the concept of bulk and boundary, providing a general understanding of these regions. Additionally, we discuss local dependence, which is an essential aspect of our analysis, particularly when studying bulk region. Finally, Section 4.5 demonstrates the size of different regions within the square, a key component of our analysis.

4.2 Tiles and Companions

In this section, our focus shifts towards the examination of tiles and companions. The intuitive idea here is to divide the whole of $\mathbb{R}^2$ into a grid of boxes, which we call 'tiles'. Then we will introduce the concept of companion. Our definitions of tiles and companions provide a way to describe the the local dependence of the random variables appearing in the collection of edge lengths in the minimal directed spanning forest originating from points in the bulk, which will be made precise later, in Section 5.2.2, once we have introduced the concept of dependency graph. The details will depend on the geometry of the cones and corresponding choice of companion (we see this in Section 4.3). First we give the formal definition of tile.

Fix a scale parameter S, which will always be the reciprocal of a positive integer. For every $p = (p_1, p_2) \in \mathbb{Z}^2$ we define an associated tile $T(p)$ which is the square whose top right corner is the point $(p_1 S, p_2 S)$, the bottom left corner is the point $((p_1 - 1)S, (p_2 - 1)S)$. More generally, we have the following definition.

Definition 4.2.1. For any $V \subseteq \mathbb{Z}^2$ define $T(V) \subseteq \mathbb{R}^2$ by

$$T(V) := \cup_{q=(q_1,q_2)\in V}[(q_1 - 1)S, q_1 S] \times [(q_2 - 1)S, q_2 S],$$

and write $T(q)$ for $T(\{q\})$.

The next two definitions give a distance function and a ball for the index set $\mathbb{Z}^2$ of tiles.

Definition 4.2.2. For $p = (p_1, p_2) \in \mathbb{Z}^2$ and $q = (q_1, q_2) \in \mathbb{Z}^2$, we define

$$d(p, q) = \max(|p_1 - q_1|, |p_2 - q_2|).$$

Definition 4.2.3. Let $\mathcal{S}_{p,R}$ be the ball of radius R such that $\mathcal{S}_{p,R} = \{q \in \mathbb{Z}^2 : d(p, q) \leq R\}$.

Lemma 4.2.4. *Suppose $z \in T(p)$, $z' \in T(q)$ satisfy $\|z - z'\| \leq CS$ for $C > 0$, then $d(p, q) \leq \lfloor C \rfloor + 1$.*

Proof. Let x be the horizontal (Euclidean) distance between z and z', and y be the vertical (Euclidean) distance between z and z'. Then by triangle inequality we have $\|z - z'\| = \sqrt{x^2 + y^2} \leq CS$, this means $x \leq CS$ and $y \leq CS$ where $x \leq \sqrt{x^2 + y^2} = \|z - z'\| \leq CS$ and similarly for $y \leq \sqrt{x^2 + y^2} = \|z - z'\| \leq CS$. Suppose for a contradiction that $|p_1 - q_1| \geq \lfloor C \rfloor + 2$. This implies that there must be a vertical strip of at least $\lfloor C \rfloor + 1$ squares wide separating p and q, which means the horizontal distance x is least $(\lfloor C \rfloor + 1)S$. But $\lfloor C \rfloor + 1 > C$, which contradicts our assumption $x \leq CS$. Similarly, $y \leq CS$ implies $|q_2 - p_2| \leq \lfloor C \rfloor + 1$. Hence, $d(p, q) = \max\{|p_1 - q_1|, |p_2 - q_2|\} \leq \lfloor C \rfloor + 1$, as indicated in Figure 4.1.

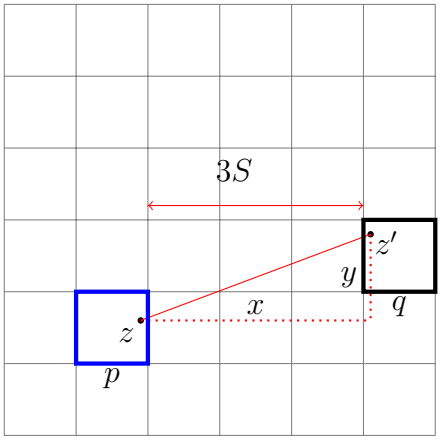

Figure 4.1: Squares $p = (p_1, p_2)$ and $q = (q_1, q_2)$, satisfy $|p_1 - q_1| = 4$ so $x \geq 3S$ for all $z \in p$ and $z' \in q$.

□

Now, we define the concept of companion and determine conditions that will allow us to find R explicitly, which appears in the Definition 4.2.3. Recall by the Definition 3.1.2 that $C_{\theta,\phi}(\boldsymbol{x})$ is a cone has apex at $\boldsymbol{x}$ formed as a union of rays from $\boldsymbol{x}$ with angle $\alpha \in [\theta, \theta + \phi]$, measured anticlockwise from a vertically upward direction.

Definition 4.2.5. For $\theta \in [0, 2\pi)$ and $\phi \in (0, \pi)$, for each $p \in \mathbb{Z}^2$, call $q \in \mathbb{Z}^2$ a companion of p if for all $\boldsymbol{x} \in T(p)$, it holds that $T(q) \subseteq C_{\theta,\phi}(\boldsymbol{x})$.

Note that, q is a companion of p if and only if $q - p$ is a companion of $\underline{\mathbf{0}} = (0, 0)$.

Definition 4.2.6. For squares $p = (p_1, p_2)$, $r = (r_1, r_2)$ with r a companion of $\underline{\mathbf{0}}$, define $\rho(r) := |r_1| + |r_2| + 2$. Then, we call

$$\mathcal{S}_{p,\rho(r)} = \{q \in \mathbb{Z}^2 : d(q, p) \leq |r_1| + |r_2| + 2\},$$

the ball of stabilization associated with p and r. Note that, $\mathcal{S}_{p,\rho(r)} = p + \mathcal{S}_{\underline{\mathbf{0}},\rho(r)}$.

The next result shows how companions lead to local dependence. Recall by Definition 3.2.1 that $N_{\theta,\phi}(\boldsymbol{x}, \mathcal{X})$ is a nearest neighbour of $\boldsymbol{x}$ on the locally finite set $\mathcal{X}$.

Theorem 4.2.7. *Suppose $r \in \mathbb{Z}^2$ is a companion of $\underline{\mathbf{0}}$. Then for any locally finite set $\mathcal{X} \subseteq \mathbb{R}^2$, $p \in \mathbb{Z}^2$, and $\boldsymbol{x}, \boldsymbol{y} \in \mathcal{X}$ with $\boldsymbol{x} \in T(p)$, $\boldsymbol{y} \in T(p + r)$, we have $N_{\theta,\phi}(\boldsymbol{x}; \mathcal{X}) \in T(\mathcal{S}_{p,\rho(r)})$.*

Proof. Take $\underline{\mathbf{0}}$ with companion r. Suppose $\boldsymbol{x}, \boldsymbol{y} \in \mathcal{X}$ with $\boldsymbol{x} \in T(p)$, $\boldsymbol{y} \in T(p + r)$. By Definition 4.2.5, it holds that $T(p+r) \subseteq C_{\theta,\phi}(\boldsymbol{x})$ and hence $\boldsymbol{y} \in C_{\theta,\phi}(\boldsymbol{x})$, so $\boldsymbol{y}$ is a candidate nearest-neighbour of $\boldsymbol{x}$. Moreover, $\|\boldsymbol{y} - \boldsymbol{x}\| \leq S\sqrt{(|r_1| + 1)^2 + (|r_2| + 1)^2}$, since

$$\begin{aligned}(|r_1| + |r_2| + 3/2)^2 &= r_1^2 + 3|r_1| + 9/8 \\ &\quad + r_2^2 + 3|r_2| + 9/8 + 2|r_1||r_2| \\ &> (|r_1| + 1)^2 + (|r_2| + 1)^2,\end{aligned}$$

then $\|\boldsymbol{y} - \boldsymbol{x}\| \leq (|r_1| + |r_2| + 3/2)S$, see Figure 4.2. Since $\boldsymbol{x}$ has at least one candidate nearest-neighbour (namely $\boldsymbol{y}$), by Definition 3.2.1, we have

$$\mathcal{D}_{\theta,\phi}(\boldsymbol{x}; \mathcal{X}) = \|\boldsymbol{x} - N_{\theta,\phi}(\boldsymbol{x}; \mathcal{X})\| \leq \|\boldsymbol{x} - \boldsymbol{y}\| \leq (|p_1| + |p_2| + 3/2)S.$$

Finally, let $q \in \mathbb{Z}^2$ be such that $N_{\theta,\phi}(\boldsymbol{x}; \mathcal{X}) \in T(q)$. Then Lemma 4.2.4 implies $d(p, q) \leq |r_1| + |r_2| + 2$, hence we verify that $q \in \mathcal{S}_{p,\rho(r)}$ (see Definition 4.2.6), and so $N_{\theta,\phi}(\boldsymbol{x}; \mathcal{X}) \in T(q) \subseteq T(\mathcal{S}_{p,\rho(r)})$.

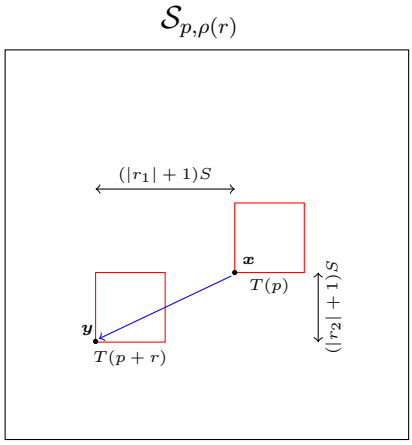

Figure 4.2: Here $r \in \mathbb{Z}^2$ is a companion of p in the ball $\mathcal{S}_{p,\rho(r)}$ with vertical distance $(|r_2|+1)S$ and horizontal distance $(|r_1|+1)S$.

□

The next result follows directly from Theorem 4.2.7.

Corollary 4.2.8. *Suppose $r \in \mathbb{Z}^2$ is a companion of $\underline{\mathbf{0}}$. Let $\mathcal{X}$ be a locally finite set, and $\boldsymbol{x}, \boldsymbol{y} \in \mathcal{X}$ satisfy $\boldsymbol{x} \in T(p)$ and $\boldsymbol{y} \in T(p+r)$ for some $p \in \mathbb{Z}^2$. Then, for any locally finite $\mathcal{Y} \subseteq \mathbb{R}^2 \setminus T(\mathcal{S}_{p,\rho(r)})$*

$$\mathcal{D}_{\theta,\phi}(\boldsymbol{x};\mathcal{X}) = \mathcal{D}_{\theta,\phi}(\boldsymbol{x};\mathcal{X} \cap T(\mathcal{S}_{p,\rho(r)})) = \mathcal{D}_{\theta,\phi}(\boldsymbol{x};\mathcal{X} \cap T(\mathcal{S}_{p,\rho(r)}) \cup \mathcal{Y}).$$

Proof. Theorem 4.2.7 implies that $N_{\theta,\phi}(\boldsymbol{x};\mathcal{X} \cap T(\mathcal{S}_{p,\rho(r)}) \cup \mathcal{Y})$ can not be in $\mathcal{Y}$ since $T(\mathcal{S}_{p,\rho(r)}) \cap \mathcal{Y} = \emptyset$, so $N_{\theta,\phi}(\boldsymbol{x};\mathcal{X} \cap T(\mathcal{S}_{p,\rho(r)}) \cup \mathcal{Y}) = N_{\theta,\phi}(\boldsymbol{x};\mathcal{X} \cap T(\mathcal{S}_{p,\rho(r)})$ for any $\mathcal{Y} \subseteq \mathbb{R}^2 \setminus T(\mathcal{S}_{p,\rho(r)})$. Moreover, the identity $N_{\theta,\phi}(\boldsymbol{x};\mathcal{X}) = N_{\theta,\phi}(\boldsymbol{x};\mathcal{X} \cap T(\mathcal{S}_{p,\rho(r)})$ is just the special case of $\mathcal{Y} = \mathcal{X} \setminus T(\mathcal{S}_{p,\rho(r)})$. The statement follows from the definition of $\mathcal{D}_{\theta,\phi}(\boldsymbol{x},\mathcal{X})$. □

Remark 4.2.9. In other words, given the conditions of Corollary 4.2.8, $\mathcal{D}_{\theta,\phi}(\boldsymbol{x};\mathcal{X})$ is not affected by any changes to $\mathcal{X}$ outside of $T(\mathcal{S}_{p,\rho(r)})$.

4.3 Identifying Companions for Different Cone Geometries

In this section, we study different types of cone geometries in the unit square. As mentioned in the discussion after the statement of Theorem 3.3.2 we consider five types of cone:

(a) singly-aligned, obtuse case,

(b) singly-aligned, acute case,

(c) unaligned, contains no axes,

(d) unaligned, contains one axis,

(e) unaligned, contains two axes.

Proposition 4.3.1 below, identifies companion in each case. The above categories are illustrated in Figures 4.3 (case (a)), 4.4 (case (b)), 4.5 (case (c)), 4.6 (case (d)), and Figure 4.7 (case (e)), helping us to understand the various geometric of the configurations.

Proposition 4.3.1.

(a) *(*Obtuse*): Let* $\theta = \pi/2$, $\phi > \pi/2$. *Set* $h = \cot(\phi - \frac{\pi}{2})$. *Then* $(0, -(\lfloor h \rfloor + 2))$ *is a companion of* $\underline{\mathbf{0}}$.

(b) *(*Acute*): Let* $\theta = \pi/2$, $\phi < \pi/2$. *Set* $h = 2\cot(\phi)$. *Then* $(-(\lfloor h \rfloor + 2), -1)$ *is a companion of* $\underline{\mathbf{0}}$.

(c) *(*Unaligned case *I): Let* $0 < \theta < \frac{\pi}{2}$ *and* $\theta + \phi < \frac{\pi}{2}$. *Then there exists a companion* r *of* $\underline{\mathbf{0}}$ *with* $d(\underline{\mathbf{0}}, r) \leq \left\lfloor \frac{3}{\sqrt{2}}(1 + \csc(\phi/2)) \right\rfloor + 1$.

(d) *(*Unaligned case *II): Let* $0 < \theta < \frac{\pi}{2}$ *and* $\frac{\pi}{2} < \theta + \phi < \pi$. *Set* $h_0 = \max(\cot(\frac{\pi}{2} - \theta), \cot(\theta + \phi - \frac{\pi}{2}))$. *Then,* $(-(\lfloor h_0 \rfloor + 2), 0)$ *is companion of* $\underline{\mathbf{0}}$.

(e) *(*Unaligned case *III): Let* $0 < \theta < \frac{\pi}{2}$, $\theta + \phi > \pi$, *where* $\phi < \pi$. *Set* $h_1 =$

$\cot(\frac{\pi}{2}-\theta)$ *and* $h_2 = \cot(\theta+\phi-\pi)$. *Then* $(-(\lfloor h_1 \rfloor+2),0)$ *and* $(0,-(\lfloor h_2 \rfloor+2))$ *are both companions of* $\underline{\mathbf{0}}$.

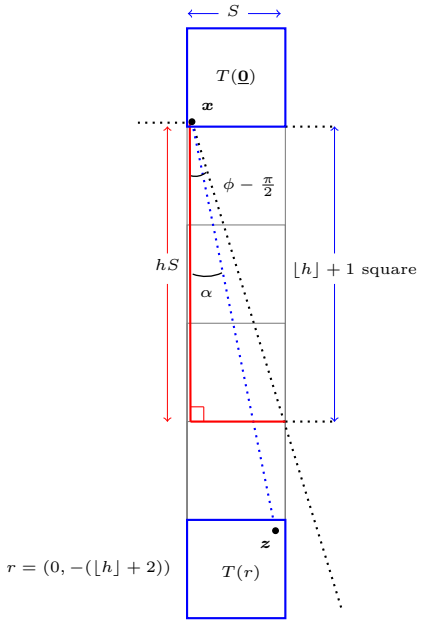

Figure 4.3: Case (a): obtuse angle with $\theta = \frac{\pi}{2}$ and $\phi \in (\frac{\pi}{2}, \pi)$ with $h = \cot(\theta - \frac{\pi}{2})$. Square $r = (0, -(\lfloor h \rfloor + 2))$ is a companion of $\underline{\mathbf{0}}$.

Proof of Proposition 4.3.1 (a).

Let $r = (0, -(\lfloor h \rfloor + 2))$. We need to show that r is a companion of $\underline{\mathbf{0}}$. It is enough to show that for every $\boldsymbol{x} \in T(\underline{\mathbf{0}})$ and every $\boldsymbol{z} \in T(r)$, $\boldsymbol{z} \in C_{\theta,\phi}(\boldsymbol{x})$. Take $\boldsymbol{z} \in T(r)$, then $|x_1 - z_1| \leq S$ and $|x_2 - z_2| > (\lfloor h \rfloor + 1)S$. Let α be the angle of ray from $\boldsymbol{x}$ to $\boldsymbol{z}$ measured anticlockwise relative to the downward vertical. Then,

$$|\tan\alpha| \leq \frac{|x_1 - z_1|}{|x_2 - z_2|} \leq \frac{1}{\lfloor h \rfloor + 1} < \tan\left(\phi - \frac{\pi}{2}\right),$$

since $\frac{1}{\lfloor h \rfloor + 1} < \frac{1}{h} = \tan(\phi - \frac{\pi}{2})$. So angle α is contained in $(-\frac{\pi}{2}, \phi - \frac{\pi}{2})$, which implies that $\boldsymbol{z} \in C_{\theta,\phi}(\boldsymbol{x})$. □

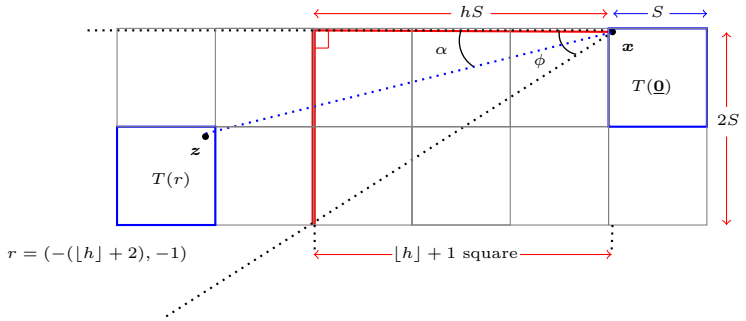

Figure 4.4: Case (b): acute angle θ, ϕ with $h = 2\cot(\phi)$ and $r = (-(\lfloor h \rfloor + 2), -1)$ is companion of $\underline{\mathbf{0}}$.

Proof of Proposition 4.3.1 (b).

Let $r = (-(\lfloor h \rfloor + 2), -1)$. We need to show that r is a companion of $\underline{\mathbf{0}}$. It is enough to show that for every $\boldsymbol{x} \in T(\underline{\mathbf{0}})$ and every $\boldsymbol{z} \in T(r)$, $\boldsymbol{z} \in C_{\theta,\phi}(\boldsymbol{x})$. Take $\boldsymbol{z} \in T(r)$, then $|x_1 - z_1| \geq (\lfloor h \rfloor + 1)S$ and $|x_2 - z_2| \leq 2S$. Let α be the angle of ray from $\boldsymbol{x}$ to $\boldsymbol{z}$ measured anticlockwise relative to the leftward horizontal. Then,

$$|\tan\alpha| \leq \frac{|x_2 - z_2|}{|x_1 - z_1|} \leq \frac{2}{\lfloor h \rfloor + 1} < \frac{2}{h} = \tan(\phi),$$

by the definition of $h = 2\cot(\phi)$. Then $|\alpha| < \phi$, which implies $\boldsymbol{z} \in C_{\theta,\phi}(\boldsymbol{x})$. □

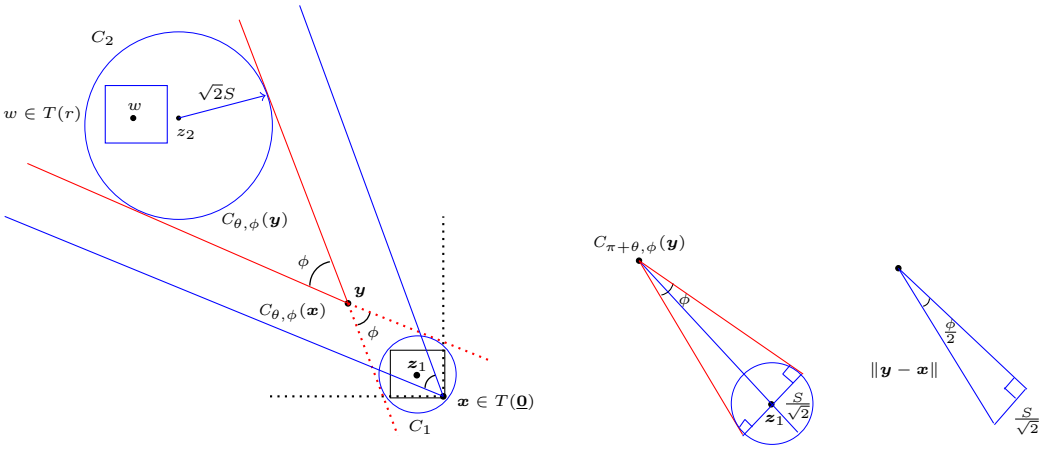

Figure 4.5: Case (c): unaligned cone with $0 < \theta < \frac{\pi}{2}$ and $\theta + \phi < \frac{\pi}{2}$, and containing no axes, with r is a companion of $\underline{\mathbf{0}}$.

Proof of Proposition 4.3.1 (c).

We make use of the fact that if $\boldsymbol{y} \in C_{\theta,\phi}(\boldsymbol{x})$, then $\boldsymbol{x} \in C_{\pi+\theta,\phi}(\boldsymbol{y})$, where $C_{\pi+\theta,\phi}(\boldsymbol{y})$ is a rotation by π of the cone $C_{\theta,\phi}(\boldsymbol{y})$, see Figure 4.5.

Consider tile $T(\underline{\mathbf{0}})$ and the circle C_1 of radius $\frac{S}{\sqrt{2}}$ that contains $T(\underline{\mathbf{0}})$. Let $\boldsymbol{y} \in \mathbb{R}^2$ be a point such that $C_{\pi+\theta,\phi}(\boldsymbol{y})$ contains C_1, and hence all points in $T(\underline{\mathbf{0}})$. We can choose $\boldsymbol{y}$ so that $\sup_{\boldsymbol{x}\in T(\underline{\mathbf{0}})} \|\boldsymbol{x}-\boldsymbol{y}\| \leq \ell = \frac{S}{\sqrt{2}}(1+\csc(\phi/2))$ since $\|\boldsymbol{x}-\boldsymbol{y}\| \leq \|\boldsymbol{x}-\boldsymbol{z}_1\| + \|\boldsymbol{z}_1-\boldsymbol{y}\|$ where $\boldsymbol{z}_1$ is the center of the C_1, and $\boldsymbol{y}$ can be chosen so that $\|\boldsymbol{z}_1-\boldsymbol{y}\| = \frac{S}{\sqrt{2}}\csc(\phi/2)$. By the first statement, this means that $\boldsymbol{y} \in C_{\theta,\phi}(\boldsymbol{x})$ for all $\boldsymbol{x} \in T(\underline{\mathbf{0}})$, and hence $C_{\theta,\phi}(\boldsymbol{y}) \subseteq \cap_{\boldsymbol{x}\in T(\underline{\mathbf{0}})} C_{\theta,\phi}(\boldsymbol{x})$. Hence $\underline{r}$ is a companion of $\underline{\mathbf{0}}$ if $T(r) \subseteq C_{\theta,\phi}(\boldsymbol{y})$. Let C_2 be a circle inside $C_{\theta,\phi}(\boldsymbol{y})$ large enough to guarantee that it contains some tile $T(r)$. The circle of radius $\sqrt{2}S$ centred at $\boldsymbol{z}_2$ with distance $\|\boldsymbol{z}_2-\boldsymbol{y}\| = \sqrt{2}S\csc(\phi/2)$ will achieve this, see Figure 4.5. Then for any $w \in T(r)$ and $\boldsymbol{x} \in T(\underline{\mathbf{0}})$, we have

$$\begin{aligned}\|w-\boldsymbol{x}\| &= \|w-\boldsymbol{z}_2\| + \|\boldsymbol{z}_2-\boldsymbol{y}\| + \|\boldsymbol{y}-\boldsymbol{x}\| \\ &\leq \frac{3}{\sqrt{2}}S(1+\csc(\phi/2)).\end{aligned}$$

Hence by Lemma 4.2.4, we obtain

$$d(\underline{\mathbf{0}}, r) \leq \left\lfloor \frac{3}{\sqrt{2}}(1+\csc(\phi/2)) \right\rfloor + 1.$$

□

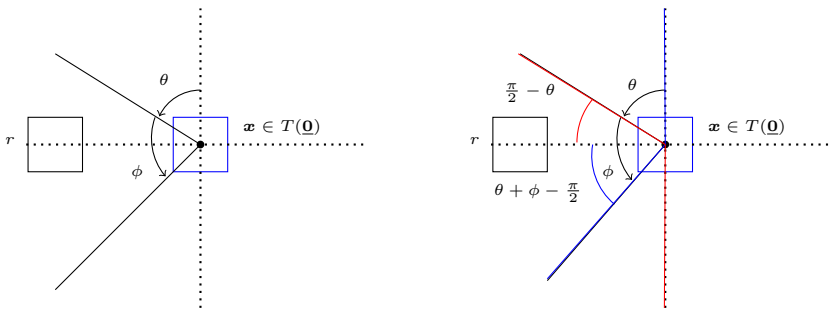

Figure 4.6: Case (d): unaligned cone with $0 < \theta < \frac{\pi}{2}$ and $\frac{\pi}{2} < \theta+\phi < \pi$, and it contains one axes, and $r = (-(\lfloor h_0 \rfloor + 2), 0)$ is a companion of $\underline{\mathbf{0}}$.

Proof of Proposition 4.3.1 (d).

We use the fact that $C_{\theta,\phi}(\boldsymbol{x}) = C_{0,\theta+\phi}(\boldsymbol{x}) \cap C_{\theta,\pi-\theta}(\boldsymbol{x})$ where both $C_{0,\theta+\phi}(\boldsymbol{x})$ and $C_{\theta,\pi-\theta}(\boldsymbol{x})$ are singly-aligned cones with obtuse angles at $\boldsymbol{x}$. Hence we can deduce using part (a) that for $C_{0,\theta+\phi}(\boldsymbol{x})$, any square $(-r_1, 0)$ is a companion of $\underline{\mathbf{0}}$ when

$r_1 \geq \lfloor \cot(\theta + \phi - \frac{\pi}{2}) \rfloor + 2$, and for $C_{\theta,\pi-\theta}(\boldsymbol{x})$, any square $(-r_1, 0)$ is a companion of $\underline{\mathbf{0}}$ when $r_1 \geq \lfloor \cot(\frac{\pi}{2} - \theta) \rfloor + 2$. Therefore $r = (-(\lfloor h_0 \rfloor + 2), 0)$ is a companion of $\underline{\mathbf{0}}$ for both cones, and hence is a companion of $\underline{\mathbf{0}}$ for their intersection. □

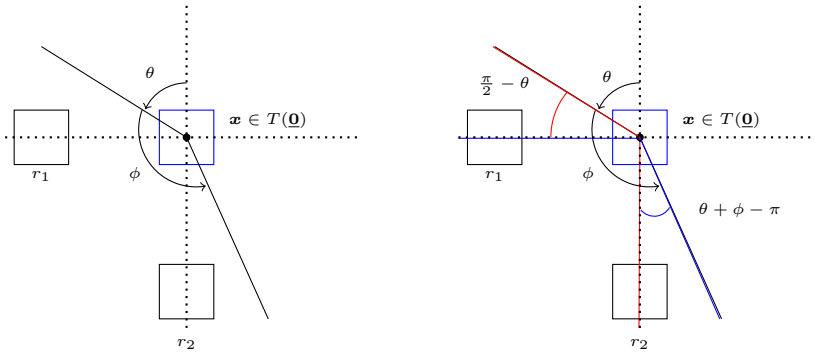

Figure 4.7: Case (e): unaligned cone with $0 < \theta < \frac{\pi}{2}$ and $\theta + \phi > \pi$, and it contains two axes, and companions $r_1 = (-(\lfloor \cot(\frac{\pi}{2} - \theta) \rfloor + 2), 0)$ and $r_2 = (0, -(\lfloor \cot(\theta + \phi - \pi) \rfloor + 2))$ of $\underline{\mathbf{0}}$.

Proof of Proposition 4.3.1(e).
We use the fact that $C_{\theta,\phi}(\boldsymbol{x}) = C_{\frac{\pi}{2},\theta+\phi-\frac{\pi}{2}}(\boldsymbol{x}) \cup C_{\theta,\pi-\theta}(\boldsymbol{x})$ where both $C_{\frac{\pi}{2},\theta+\phi-\frac{\pi}{2}}(\boldsymbol{x})$ and $C_{\theta,\pi-\theta}(\boldsymbol{x})$ are singly-aligned cones with obtuse angle at $\boldsymbol{x}$. Then from part (a) we know that

$$r_2 = \left(0, -(\left\lfloor \cot(\theta + \phi - \frac{\pi}{2} - \frac{\pi}{2}) \right\rfloor + 2)\right) = (0, -(\lfloor \cot(\theta + \phi - \pi) \rfloor + 2)),$$

is a companion of $\underline{\mathbf{0}}$ for $C_{\frac{\pi}{2},\theta+\phi-\frac{\pi}{2}}(\boldsymbol{x})$, and therefore a companion of $\underline{\mathbf{0}}$ for $C_{\theta,\phi}(\boldsymbol{x})$. Similarly, we know $r_1 = (-(\lfloor \cot(\frac{\pi}{2} - \theta) \rfloor + 2), 0)$ is a companion of $\underline{\mathbf{0}}$ for $C_{\theta,\pi-\theta}(\boldsymbol{x})$, and therefore a companion of $\underline{\mathbf{0}}$ for $C_{\theta,\phi}(\boldsymbol{x})$. □

4.4 Boundary and Composition of the Unit Square

In this section, we focus our attention on locally finite sets $\mathcal{X}$ in the unit square $[0, 1]^2$. Recall by Definition 3.3.1 that $\mathcal{L}(\mathcal{X})$ is the total length of MDSF on $\mathcal{X} \subseteq [0, 1]^2$. We define two regions of $[0, 1]^2$, $\mathcal{R}^3_\lambda$ (where long edges may appear) and $\mathcal{R}^1_\lambda$ (where a local dependence property holds, as we explain more in Chapter 5). In order to

discuss the contribution to $\mathcal{L}(\mathcal{X})$ coming from different regions of $[0,1]^2$, we define the following notation.

Definition 4.4.1. For $\mathcal{R} \subseteq \mathbb{R}^2$, define

$$\mathcal{L}(\mathcal{X}; \mathcal{R}) = \sum_{\boldsymbol{x} \in \mathcal{X} \cap \mathcal{R}} \mathcal{D}_{\theta,\phi}(\boldsymbol{x}; \mathcal{X}).$$

For the unaligned cone, we may take $\mathcal{R}_\lambda^3$ to be empty; for the singly-aligned cones $\mathcal{R}_\lambda^3$ will be a narrow strip $[0,1] \times [0, \lambda^{-\sigma}]$ along the bottom boundary of $[0,1]^2$. Once $\mathcal{R}_\lambda^3$ is chosen, the bulk $\mathcal{R}_\lambda^1$ is chosen to satisfy two conditions:

1. that the terms $\mathcal{D}_{\theta,\phi}(\boldsymbol{x}; \mathcal{X})$ contributing to $\mathcal{L}(\mathcal{X}; \mathcal{R}_\lambda^1)$ exhibit local dependence, and

2. that the nearest-neighbour $N_{\theta,\phi}(\boldsymbol{x}; \mathcal{X})$ of any point $\boldsymbol{x} \in \mathcal{X} \cap \mathcal{R}_\lambda^1$ is not in $\mathcal{R}_\lambda^3$.

For the random sets $\mathcal{P}_\lambda$ that we will consider, condition 1) will allow us to prove a CLT for $\mathcal{L}(\mathcal{P}_\lambda; \mathcal{R}_\lambda^1)$ and condition 2) will ensure an asymptotic independence of $\mathcal{L}(\mathcal{P}_\lambda; \mathcal{R}_\lambda^1)$ and $\mathcal{L}(\mathcal{P}_\lambda; \mathcal{R}_\lambda^3)$ (see Section 4.5 for more details). This motivates the definition of compatible bulk given below in Definition 4.4.5. Concerning condition 1), for $\boldsymbol{x} \in \mathcal{X} \subseteq [0,1]^2$, local dependence of $\mathcal{D}_{\theta,\phi}(\boldsymbol{x}; \mathcal{X})$ can be achieved in two ways. Either, we find a companion $p + r$ of p, where p satisfies $\boldsymbol{x} \in T(p)$, to apply Theorem 4.2.7 which requires that $T(p + r) \cap [0,1]^2 \neq \emptyset$; alternatively, $N_{\theta,\phi}(\boldsymbol{x}; \mathcal{X}) \in T(\mathcal{S}_{p(\boldsymbol{x}),R})$ may hold simply because all candidate nearest-neighbours are within a bounded distance of $\boldsymbol{x}$, for example because $\boldsymbol{x}$ is close to the boundary of $[0,1]^2$, and $C_{\theta,\phi}(\boldsymbol{x}) \cap [0,1]^2$ has small diameter. We quantify this second case as follows.

Definition 4.4.2. For $S > 0$ and $p \in \mathbb{Z}^2$, define

$$\nu(p) := \sup\{\|\boldsymbol{x} - \boldsymbol{y}\| : \boldsymbol{x} \in T(p), \boldsymbol{y} \in C_{\theta,\phi}(\boldsymbol{x}) \cap [0,1]^2\}.$$

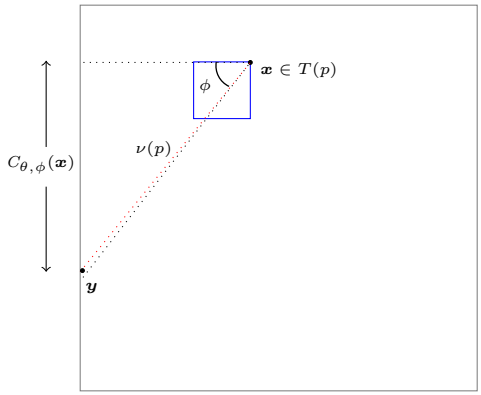

Figure 4.8: Furthest Euclidean distance between $\boldsymbol{x} \in T(p)$ and $\boldsymbol{y} \in C_{\theta,\phi}(\boldsymbol{x})$ is given by $\nu(p)$.

Lemma 4.4.3. *Fix θ, ϕ. Let $\mathcal{X} \subseteq [0,1]^2$ be a locally finite set. Suppose $\nu(p) \leq \delta S$ for some $\delta > 0$. For all $\boldsymbol{x} \in \mathcal{X} \cap T(p)$, we have $N_{\theta,\phi}(\boldsymbol{x}; \mathcal{X}) \in T(\mathcal{S}_{p,\lfloor\delta\rfloor+1}) \cap [0,1]^2$.*

Proof. Suppose $\boldsymbol{x} \in \mathcal{X} \cap T(p)$ and consider $N_{\theta,\phi}(\boldsymbol{x}; \mathcal{X})$ which by definition is a point in $C_{\theta,\phi}(\boldsymbol{x}) \cap \mathcal{X} \subseteq C_{\theta,\phi}(\boldsymbol{x}) \cap [0,1]^2$. Therefore,

$$\|\boldsymbol{x} - N_{\theta,\phi}(\boldsymbol{x}; \mathcal{X})\| \leq \nu(p) \leq \delta S.$$

Let q be such that $N_{\theta,\phi}(\boldsymbol{x}; \mathcal{X}) \in T(q)$. By Lemma 4.2.4, $d(p,q) \leq \lfloor\delta\rfloor + 1$, in other words, $q \in \mathcal{S}_{p,\lfloor\delta\rfloor+1}$. □

Definition 4.4.4. Let $\mathbb{T}_S$ be the set of all tiles in $[0,1]^2$, given by

$$\mathbb{T}_S = \{p \in \mathbb{Z}^2 : T(p) \subseteq [0,1]^2\}.$$

Note that, for a particular scale S being the reciprocal of a positive integer, $\mathbb{T}_S$ consist of all $p = (p_1, p_2) \in \mathbb{Z}^2$ satisfying ($1 \leq p_1 \leq \frac{1}{S}$ and $1 \leq p_2 \leq \frac{1}{S}$).

We now give the definition of compatible bulk. In Definition 4.4.5 below, $\mathcal{R}^3_\lambda$ is an arbitrary region of $[0,1]^2$ that we will later set to be a boundary region of $[0,1]^2$ where we expect to see long edges. The conditions (A) & $(B_1)/(B_2)$ ensure the conditions 1) & 2) described above are satisfied for $\mathcal{R}^1_\lambda$ and $\mathcal{R}^3_\lambda$. For now, think of λ as an arbitrary parameter that determines the region $\mathcal{R}^3_\lambda$ and S as an arbitrary

scale. In fact, we will see in Chapter 5 that λ will be the intensity of our Poisson process and S will be chosen as a function of λ, with $S \sim \sqrt{\frac{c \log \lambda}{\lambda}}$.

Definition 4.4.5. Fix θ, ϕ, S. Let $C_0 \subseteq \mathbb{Z}^2$ be a finite (non-empty) set of companions of $\underline{\mathbf{0}}$. Let $\mathcal{R}^3_\lambda \subseteq [0,1]^2$ and let $\delta \geq 0$. Define the following three properties of $p \in \mathbb{T}_S$ satisfying:

(A) : $p + r \in \mathbb{T}_S$ and $T(\mathcal{S}_{p,\rho(r)}) \cap \mathcal{R}^3_\lambda = \emptyset$ for some $r \in C_0$.

(B_1) : $\nu(p) \leq \delta S$ and

(B_2) : $(\cup_{\boldsymbol{x} \in T(p)} C_{\theta,\phi}(\boldsymbol{x})) \cap \mathcal{R}^3_\lambda = \emptyset$.

Let $\boldsymbol{B} \subseteq \mathbb{T}_S$ be any set of squares each satisfying either (A) or both (B_1) & (B_2). Let $\mathcal{R}^1_\lambda = T(\boldsymbol{B}) \subseteq [0,1]^2$. We call $\mathcal{R}^1_\lambda$ is a compatible bulk (for θ, ϕ, C_0, $\mathcal{R}^3_\lambda$, δ and S).

Now we specify the "boundary" region for each cone. We will start with singly-aligned cones (obtuse and acute angles) and unaligned cone in the unit square. Note in the statement of Lemma 4.4.6 (below) that h is the same as that defined in Proposition 4.3.1 (a), and in the statement of Lemma 4.4.7 (below) that h is the same as that defined in Proposition 4.3.1 (b).

Lemma 4.4.6. *(*Obtuse*) Set $\theta = \frac{\pi}{2}$ and $\phi \in (\frac{\pi}{2}, \pi)$. Let $C_0 = \{r\} = \{(0, -(\lfloor h \rfloor + 2))\}$, $\mathcal{R}^3_\lambda = [0,1] \times [0, \lambda^{-\sigma}]$ for $\sigma \in (\frac{1}{2}, \frac{2}{3})$, $\delta = 0$, $R = \lfloor h \rfloor + 5$, and $R + 1 \leq \frac{1}{S} < \lambda^\sigma$. Then, $\mathcal{R}^1_\lambda = [0,1] \times [RS, 1]$ is a compatible bulk.*

Proof. Let $\bar{\mathbf{B}}$ be all squares in $\mathbb{T}_S$ satisfying property (A), so that by definition $T(\boldsymbol{B})$ is a compatible bulk. We need to show that $T(\boldsymbol{B}) = [0,1] \times [RS, 1]$. By Definition 4.2.6, we have

$$\mathcal{S}_{p,\rho(r)} = \{q \in \mathbb{Z}^2 : d(q,p) \leq |r_1| + |r_2| + 2\},$$

so for this companion $\mathcal{S}_{p,\rho(r)} = \mathcal{S}_{p,\lfloor h \rfloor + 4}$, (see Figure 4.9). Now for $p = (p_1, p_2) \in \mathbb{T}_S$ to satisfy (A), we need $T(\mathcal{S}_{p,\lfloor h \rfloor + 4}) \cap \mathcal{R}^3_\lambda = \emptyset$ which holds if $p_2 - \lfloor h \rfloor - 4 \geq 2$ (i.e., $p_2 \geq \lfloor h \rfloor + 6$) since this guarantees that p is not in the bottom row of tiles in $\mathbb{T}_S$

(which necessarily contains $\mathcal{R}^3_\lambda$ since $S > \lambda^{-\sigma}$). We also need $p + r \in \mathbb{T}_S$ which requires $1 \le p_1 \le \frac{1}{S}$ and $p_2 - \lfloor h \rfloor - 2 \ge 1$. Hence,

$$\boldsymbol{B} = \left\{ p \in \mathbb{Z}^2 : 1 \le p_1 \le \frac{1}{S}, \lfloor h \rfloor + 6 \le p_2 \le \frac{1}{S} \right\},$$

and then, recalling Definition 4.2.1, we have $T(\boldsymbol{B}) = [0,1] \times [(\lfloor h \rfloor + 5)S, 1]$, see Figure 4.3.

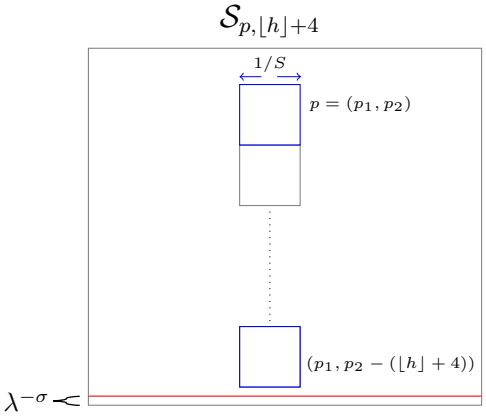

Figure 4.9: This ball is centred at p with radius $\lfloor h \rfloor + 4$.

□

Lemma 4.4.7. *(*Acute*) Set $\theta = \frac{\pi}{2}$ and $\phi \in (0, \pi/2)$. Let $C_0 = \{r\} = \{(-(\lfloor h \rfloor + 2), -1)\}$ and $\mathcal{R}^3_\lambda = [0,1] \times [0, \lambda^{-\sigma}]$. Set $\delta = (\lfloor h \rfloor + 2)\sec\phi$, $R = \max(\lfloor h \rfloor + 6, \lfloor (\lfloor h \rfloor + 2)\tan\phi \rfloor + 2)$, and $R + 1 \le \frac{1}{S} < \lambda^\sigma$. Then, $\mathcal{R}^1_\lambda = [0,1] \times [RS, 1]$ is a compatible bulk.*

Proof. Define $\boldsymbol{B} = \{p \in \mathbb{T}_S : p_2 > R\}$. We will show that all $p \in \boldsymbol{B}$ either satisfy (A) or both (B_1) and (B_2), which implies that $T(\boldsymbol{B}) = \mathcal{R}^1_\lambda$ is a compatible bulk.

Suppose $p \in \boldsymbol{B}$ has $p_1 > \lfloor h \rfloor + 2$, then $p + r \in \mathbb{T}_S$ since $p_1 + r_1 > 0$ (and $p_2 + r_2 > R - 1 > 0$). Also, since $\rho(r) = \lfloor h \rfloor + 5$ and $p_2 > R \ge \lfloor h \rfloor + 6$, we have $T(\mathcal{S}_{p,\lfloor h \rfloor + 5}) \cap \mathcal{R}^3_\lambda = \emptyset$ (because $p_2 - \lfloor h \rfloor - 5 > 1$). Therefore p satisfies (A).

Otherwise, suppose $p \in \boldsymbol{B}$ has $p_1 \le \lfloor h \rfloor + 2$, then Definition 4.4.2 implies that $\nu(p) \le (\lfloor h \rfloor + 2)S\sec\phi = \delta S$ by choice of δ, so p satisfies (B_1). To prove that p

satisfies (B_2), it is enough to show that for any $\boldsymbol{x} \in T(p)$ any $\boldsymbol{y} \in C_{\theta,\phi}(\boldsymbol{x}) \cap [0,1]^2$ has $y_2 > \lambda^{-\sigma}$ (this forces $\boldsymbol{y} \notin \mathcal{R}^3_\lambda$). But this follows, since $p_2 > R \geq \lfloor (\lfloor h \rfloor + 2) \tan\phi \rfloor + 2$, i.e., $p_2 \geq \lfloor (\lfloor h \rfloor + 2) \tan\phi \rfloor + 3$, and $\boldsymbol{x} \in T(p)$ means $x_2 \geq (p_2 - 1)S \geq (\lfloor (\lfloor h \rfloor + 2) \tan\phi \rfloor + 2)S$ and $x_2 - y_2 \leq (\lfloor h \rfloor + 2)S \tan\phi \leq (\lfloor (\lfloor h \rfloor + 2) \tan\phi \rfloor + 1)S$. So that $y_2 \geq S > \lambda^{-\sigma}$ so $\boldsymbol{y} \notin \mathcal{R}^3_\lambda$, and therefore p satisfies (B_2), see Figure 4.10. Hence $T(\boldsymbol{B}) = [0,1] \times [RS, 1] = \mathcal{R}^1_\lambda$ is a compatible bulk, see Figure 4.4.

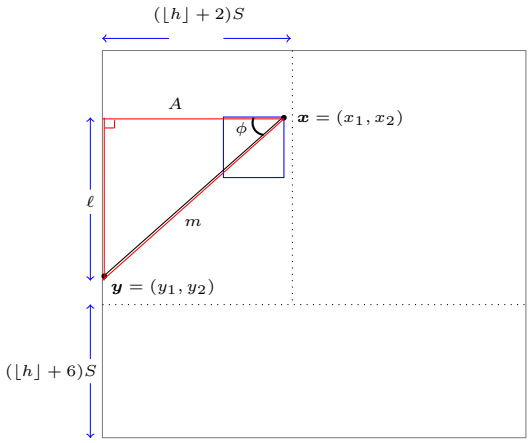

Figure 4.10: For acute case, we have $\tan\phi = \ell/A$ implies $\ell = A\tan\phi$ where $A \leq (\lfloor h \rfloor + 2)S$.

□

Lemma 4.4.8. *(*Unaligned*) Set $0 < \theta < \frac{\pi}{2}$ and $\phi < \pi$ with $\theta + \phi \notin \{\frac{\pi}{2}, \pi\}$. Let $\mathcal{R}^3_\lambda = \emptyset$ (no boundary) and let $\mathcal{R}^1_\lambda = [0,1]^2$. There exists a finite set C_0 of companions of $\underline{\mathbf{0}}$, large enough δ and small enough S such that $\mathcal{R}^1_\lambda$ is a compatible bulk.*

Since $\mathcal{R}^3_\lambda = \emptyset$, condition (A) reduces to $p + r \in \mathbb{T}_S$ for some $r \in C_0$ and (B_1) is trivially satisfied. Hence, we just need to show for all $p \in \mathbb{T}_S$ that either $p + r \in \mathbb{T}_S$ for some $r \in C_0$, or $\nu(p) \leq \delta S$. The argument for the 3 types of unaligned cone are very similar but rely on different parts of Proposition 4.3.1, so we prove the 3 cases separately.

Proof. Case (I) (Proposition 4.3.1 (c)):

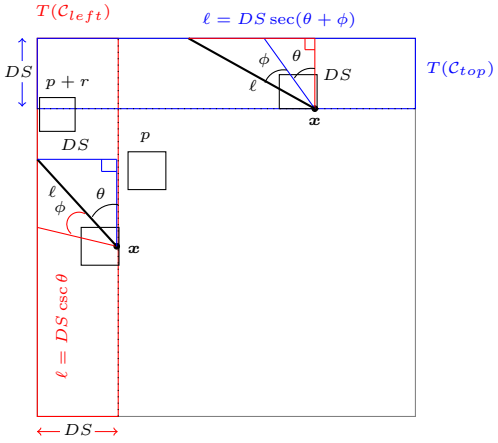

Figure 4.11: Case (I) for the unaligned cone.

Set $D = \left\lfloor \frac{3}{\sqrt{2}}(1+\csc(\phi/2)) \right\rfloor + 1$, and let r be a companion satisfying $d(\underline{\mathbf{0}}, \underline{r}) \leq D$, which exists by Proposition 4.3.1 (c). Let $C_0 = \{r\}$, let $\frac{1}{S} \geq D$ and define $\mathcal{C}_{left} = \{p = (p_1, p_2) \in \mathbb{Z}^2 : 1 \leq p_1 \leq D, 1 \leq p_2 \leq \frac{1}{S}\}$ and $\mathcal{C}_{top} = \{p = (p_1, p_2) \in \mathbb{Z}^2 : 1 \leq p_1 \leq \frac{1}{S}, \frac{1}{S} - D + 1 \leq p_2 \leq \frac{1}{S}\}$. If $p \in \mathbb{T}_S \setminus (\mathcal{C}_{left} \cup \mathcal{C}_{top})$, then $p + r \in \mathbb{T}_S$ because $p + r \in \mathcal{S}_{p,D}$ and $p + r$ is a square above and to the left of p (see Figure 4.11).

If $p \in \mathcal{C}_{left}$, then $\nu(p) \leq DS\csc\theta$ and if $p \in \mathcal{C}_{top}$, then $\nu(p) \leq DS\sec(\theta+\phi)$ (see Figure 4.11). Hence taking $\delta = \max(D\csc\theta, D\sec(\theta+\phi))$, we have $\nu(p) \leq \delta S$ for all $p \in \mathcal{C}_{left} \cup \mathcal{C}_{top}$. □

Proof. Case (II) (Proposition 4.3.1 (d)):

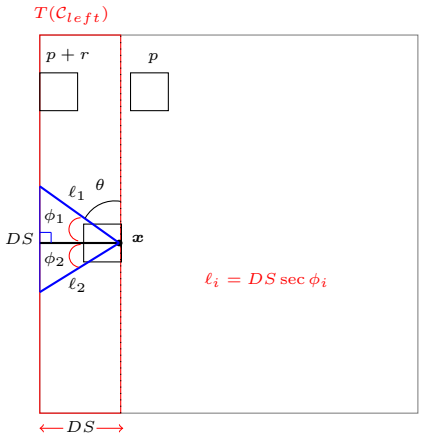

Figure 4.12: Case (II) for the unaligned cone.

Set $D = \lfloor h_0 \rfloor + 2$, where h_0 is as defined in Proposition 4.3.1 (d). Then $r = (-D, 0)$ is a companion of $\underline{\mathbf{0}}$. Set $C_0 = \{r\}$, let $\frac{1}{S} \geq D$ and define $\mathcal{C}_{left} = \{p = (p_1, p_2) \in \mathbb{Z}^2 : 1 \leq p_1 \leq D, 1 \leq p_2 \leq \frac{1}{S}\}$ as before. If $p \in \mathbb{T}_S \setminus \mathcal{C}_{left}$, then $p + r \in \mathbb{T}_S$ (see Figure 4.12).

If $p \in \mathcal{C}_{left}$ then $\nu(p) = \max(\nu_1(p), \nu_2(p))$ where $\nu_1(p) = \sup\{\|\boldsymbol{x} - \boldsymbol{y}\| : \boldsymbol{x} \in T(p), \boldsymbol{y} \in C_{\theta,\phi}(\boldsymbol{x}) \cap [0,1]^2, y_2 \geq x_2\}$ and $\nu_2(p) = \sup\{\|\boldsymbol{x} - \boldsymbol{y}\| : \boldsymbol{x} \in T(p), \boldsymbol{y} \in C_{\theta,\phi}(\boldsymbol{x}) \cap [0,1]^2, y_2 \leq x_2\}$ and $\nu_i(p) \leq DS \sec \phi_i$ for each $i = 1, 2$, where ϕ_1, ϕ_2 are angles satisfying $0 < \phi_i < \frac{\pi}{2}$ and $\phi = \phi_1 + \phi_2$ (see Figure 4.12). Hence taking $\delta = \max(D \sec \phi_1, D \sec \phi_2)$, we have $\nu(p) \leq \delta S$ for all $p \in \mathcal{C}_{left}$. □

Proof. Case (III) (Proposition 4.3.1 (e)):

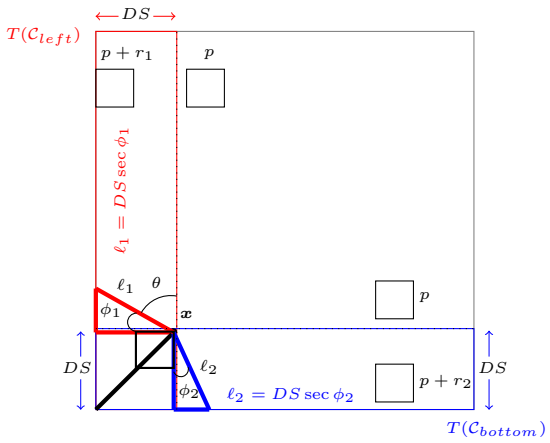

Figure 4.13: Case (III) for the unaligned cone.

Set $D = \max(\lfloor h_1 \rfloor + 2, \lfloor h_2 \rfloor + 2)$, where h_1 and h_2 are as defined in Proposition 4.3.1 (e). The squares $r_1 = (-(\lfloor h_1 \rfloor + 2), 0)$ and $r_2 = (0, -(\lfloor h_2 \rfloor + 2))$ are both companions of $\underline{\mathbf{0}}$. Set $C_0 = \{r_1, r_2\}$, let $\frac{1}{S} \geq D$ and define $\mathcal{C}_{left}$ as before. Let $\mathcal{C}_{bottom} = \{p = (p_1, p_2) \in \mathbb{Z}^2 : 1 \leq p_1 \leq \frac{1}{S}, 1 \leq p_2 \leq D\}$. If $p \in \mathbb{T}_S \setminus \mathcal{C}_{left}$, then $p + r_1 \in \mathbb{T}_S$ and if $p \in \mathbb{T}_S \setminus \mathcal{C}_{bottom}$, then $p + r_2 \in \mathbb{T}_S$ (see Figure 4.13). Hence for all $p \in \mathbb{T}_S \setminus (\mathcal{C}_{left} \cap \mathcal{C}_{bottom})$, then is an $r \in C_0$ with $p + r \in \mathbb{T}_S$.

If $p \in \mathcal{C}_{left} \cap \mathcal{C}_{bottom}$, then $\nu(p) = \max(\nu_1(p), \nu_2(p), \nu_3(p))$ where $\nu_1(p) = \sup\{\|\boldsymbol{x} - \boldsymbol{y}\| : \boldsymbol{x} \in T(p), \boldsymbol{y} \in C_{\theta,\phi}(\boldsymbol{x}) \cap [0,1]^2, y_2 \geq x_2\}$, $\nu_2(p) = \sup\{\|\boldsymbol{x} - \boldsymbol{y}\| : \boldsymbol{x} \in T(p), \boldsymbol{y} \in$

$C_{\theta,\phi}(\boldsymbol{x}) \cap [0,1]^2, y_1 \geq x_1\}$, and $\nu_3(p) = \sup\{\|\boldsymbol{x} - \boldsymbol{y}\| : \boldsymbol{x} \in T(p), \boldsymbol{y} \in C_{\theta,\phi}(\boldsymbol{x}) \cap [0,1]^2, y_1 \leq x_1, y_2 \leq x_2\}$, and $\nu_i(p) \leq DS \sec\phi_i$ for each $i = 1, 2$, where ϕ_1, ϕ_2 are angles satisfying $0 < \phi_i < \frac{\pi}{2}$ and $\phi = \phi_1 + \phi_2 + \frac{\pi}{2}$. Also $\nu_3(p) \leq \sqrt{2}DS$ (see Figure 4.13). Hence taking $\delta = \max(D\sec\phi_1, D\sec\phi_2, \sqrt{2}D)$, then $\nu(p) \leq \delta S$ for all $p \in \mathcal{C}_{left} \cap \mathcal{C}_{bottom}$. □

4.5 Regions in the Unit Square

In this section, we aim to study the regions in the unit square. These regions are often used as a framework for spatial analysis and are fundamental when studying point processes and random graphs within the unit square. Understanding the interplay between boundary and bulk regions is essential for effectively modelling and analysing spatial graphs. We will explore the region of the unit square for both singly-aligned cones (obtuse and acute angles). The other type of cone geometry is such an unaligned cone that the entire square falls under the bulk region in $[0,1]^2$, as shown below in Figure 4.14.

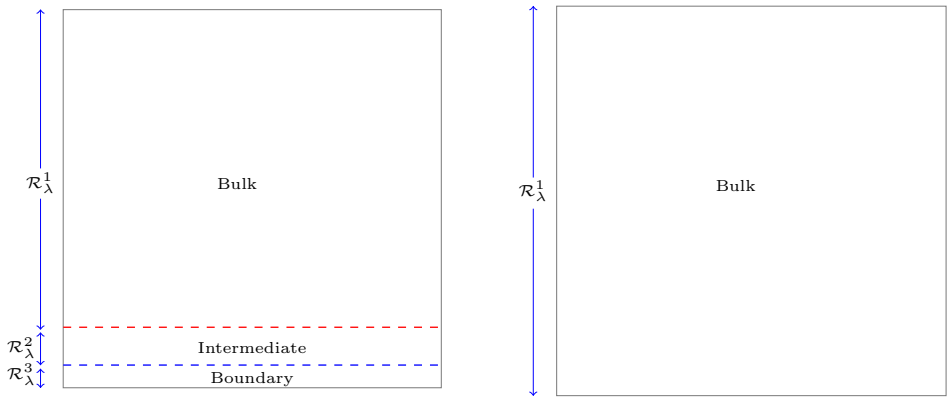

Figure 4.14: Region of the unit square (bulk, intermediate and boundary) for both singly-aligned and unaligned cones.

We consider the following regions in the unit square: region $\mathcal{R}_\lambda^1$ covers the bulk of $[0,1]^2$, region $\mathcal{R}_\lambda^3$ covers the bottom boundary, and $\mathcal{R}_\lambda^2$ covers the intermediate region. In the case of an unaligned cone, the entire unit square is considered part of the bulk region, denoted as $\mathcal{R}_\lambda^1 \equiv [0,1]^2$. This simplification arises from the fact

that no boundary effects are associated with an unaligned cone.

In the following definition we assume that λ is sufficiently large and S chosen so that the conditions of the relevant Lemma 4.4.6 – 4.4.8 hold.

Definition 4.5.1. Let (θ, ϕ) be singly-aligned. Let $S > \lambda^{-\sigma}$, and $\sigma \in (\frac{1}{2}, \frac{2}{3})$,

$$\mathcal{R}_\lambda^1 := [0,1] \times [RS, 1]; \tag{4.5.1}$$

$$\mathcal{R}_\lambda^2 := [0,1] \times \left[\lambda^{-\sigma}, RS\right]; \tag{4.5.2}$$

$$\mathcal{R}_\lambda^3 := [0,1] \times \left[0, \lambda^{-\sigma}\right], \tag{4.5.3}$$

where R is such that $\mathcal{R}_\lambda^1$ is compatible bulk specified by Lemmas 4.4.6, 4.4.7, with $R = R(\theta, \phi)$ as given in those statements. Moreover, if (θ, ϕ) is unaligned, we take $\mathcal{R}_\lambda^1 = [0,1]^2$ and $\mathcal{R}_\lambda^2 = \mathcal{R}_\lambda^3 = \emptyset$, so that $\mathcal{R}_\lambda^1$ is a compatible bulk according to Lemma 4.4.8.

Recall from the Definition 2.4.1 that $\mathcal{P}_\lambda$ is a homogeneous Poisson point process on $[0,1]^2$ with intensity λ. The next definition is to define the total length for all regions in $[0,1]^2$.

Definition 4.5.2. For $i = 1, 2, 3$, define

$$\mathcal{L}_\lambda^i = \mathcal{L}(\mathcal{P}_\lambda; \mathcal{R}_\lambda^i),$$

and define $\tilde{\mathcal{L}_\lambda^i} = \mathcal{L}_\lambda^i - \mathbf{E}[\mathcal{L}_\lambda^i]$ the centered random variable.

Here, we explore the size of the unit square. Initially, we partition the unit square into three segments, each with its choice size, as shown in Figure 4.14, the three segments: bulk, intermediate and bottom boundary. The reason for partitioning the unit square into these specific regions is to ensure that the central limit theorem (CLTs) holds due to local dependence in the $\mathcal{R}_\lambda^1$ bulk region. The $\mathcal{R}_\lambda^3$ bottom boundary which causes an approximation process to one-dimensional distance due to boundary effects. Finally, the intermediate region $\mathcal{R}_\lambda^2$ exhibits asymptotic independence between the bulk and bottom boundary of the unit square.

Chapters 5 – 7 progressively involved the foundational concepts established in

Chapters 3 and 4, each introducing more spatial relationships and their consequential implications. Chapter 5 focuses on local dependence, demonstrating how components within a finite range exhibit interdependence owing to compatible bulk. The chapter substantiates this by offering proof of the central limit theorem (Theorem 5.1.1). Chapter 6 explores boundary effects, particularly emphasizing the impact of one-dimensional distance and employing linear directed forest as an analytical tool to demonstrate the proof of Theorem 6.1.1. In what follows, Chapter 7 extends these ideas, exploring the concept of intermediate region and emphasizing the interaction between bulk and bottom boundary arising from the compatible bulk in the unit square. The chapter offers proof of Theorem 7.2.1, continuing to leverage the foundational ideas from Chapter 4 to explain the complex relationships between different spatial components in more significant detail.

We will start in the next chapter with our study of the bulk region $\mathcal{R}_\lambda^1$ in the unit square.

Chapter 5

Local Dependence and Central Limit Theorems

5.1 Introduction

This chapter explores several key topics. We will discuss the concept of the local dependence and central limit theorems, little squares and typical configurations, Poisson point process associated with squares, dependency graphs, and their connection to normal approximation. Finally, deliver the proofs of central limit theorem (Theorem 5.1.1) and convergence of variance (Theorem 5.1.2), which are our main results in this chapter.

The main result in Section 5.2 is on the normal approximation for a sum of weakly dependent variables by the dependence graph approach. Our methodology for proving the central limit theorems concerning geometrical probability relies heavily on dependency graphs. Avram and Bertsimas [3] have employed the dependence graph method to establish the proof of the central limit theorems for nearest-neighbour graphs and various other random geometric structures. Also, Section 5.2 presents probabilistic and geometric insights of the unit square. Section 5.3 discusses the analysis for the homogeneously stabilizing and some certain moments conditions for the random variable ξ.

In this section, we will use the dependency graph and method of moments. Regarding ease of use in applications, both the dependency graph method and method of moments require checking tail bounds for the radius of stabilization, where, in most cases, this process is generally straightforward whenever possible. However, the method of moments requires a more complicated version of the bounded moments condition as given in Lemma 5.3.9. On the other hand, the dependency graph method requires separate computations of variances if one explicitly intends to determine the resulting normal variable's variance.

The main quantity we are interested in here is the total edge length of the graph $\mathcal{L}_\lambda^1$. Recall from Definition 4.5.2 that $\mathcal{L}_\lambda^1 = \sum_{\boldsymbol{x}\in\mathcal{P}_\lambda\cap\mathcal{R}_\lambda^1} \mathcal{D}_{\theta,\phi}(\boldsymbol{x};\mathcal{P}_\lambda)$, where $\mathcal{D}_{\theta,\phi}(\boldsymbol{x};\mathcal{P}_\lambda)$ is the distance from point $\boldsymbol{x}$ to its nearest neighbour in $\mathcal{P}_\lambda \cap C_{\theta,\phi}(\boldsymbol{x})$ and $\mathcal{P}_\lambda$ is a homogeneous Poisson point process on $[0,1]^2$ with intensity λ. Recall by Definition 4.5.1 that $\mathcal{R}_\lambda^1 = [0,1]\times[RS,1]$, for the constant R given in Lemmas 4.4.6, 4.4.7, and 4.4.8. Previously, S was an arbitrary scale parameter that we will now fix. Note that our choice $S \sim \sqrt{\frac{c\log\lambda}{\lambda}}$ for some c sufficiently large, means that S satisfies the conditions of Lemmas 4.4.6 – 4.4.8. Define $b(c,\lambda) := \sqrt{\frac{c\log\lambda}{\lambda}}$, and we let $a_\lambda := \min(\frac{1}{2}, b(c,\max(3,\lambda)))$. For λ large enough (i.e., $\lambda \geq \lambda(c)$ depending on c), we have $a_\lambda = b(c,\lambda)$. We divide the unit square $[0,1]^2$ into k_λ^2 little squares, where $k_\lambda := \left\lfloor \frac{1}{a_\lambda} \right\rfloor$ is the number of squares along each side of the unit square, each having side length $S = 1/k_\lambda$. Below we state the main results of this chapter.

Theorem 5.1.1. *For all θ,ϕ, there exists $c_0 > 0$ such that for any S as defined above using $c > c_0$ the following statement holds. Let $\mathcal{R}_\lambda^1$ be the compatible bulk for θ,ϕ specified in Lemmas 4.4.6 – 4.4.8, i.e., $\mathcal{R}_\lambda^1 = [0,1]\times[RS,1]$, where $R = 0$ (unaligned) or $R = R(\theta,\phi) \in (0,\infty)$ (singly-aligned). Then, for every $y \in \mathbb{R}$, we have*

$$\lim_{\lambda\to\infty} \mathbf{P}\left\{ \frac{\mathcal{L}_\lambda^1 - \mathbf{E}[\mathcal{L}_\lambda^1]}{\sqrt{\mathbf{Var}[\mathcal{L}_\lambda^1]}} \leq y \right\} = \Phi(y),$$

where $\Phi(y)$ is the cumulative distribution function (cdf) of $\mathcal{N}(0,1)$.

Theorem 5.1.2. *For all θ,ϕ, there exists $c_0 > 0$ such that for any S as defined above using $c > c_0$ the following statement holds. Suppose $\phi \in (0,\pi)$. Let $\mathcal{R}_\lambda^1$ be the*

compatible bulk for θ, ϕ specified in Lemmas 4.4.6 – 4.4.8, i.e., $\mathcal{R}_\lambda^1 = [0,1] \times [RS, 1]$, where $R = 0$ (unaligned) or $R = R(\theta, \phi) \in (0, \infty)$ (singly-aligned). There exists $s_\phi \in (0, \infty)$ such that the following statement holds.

$$\lim_{\lambda \to \infty} \mathbf{Var}(\mathcal{L}_\lambda^1) = s_\phi^2.$$

We give the proof of the central limit theorem (CLTs) for the ordinary nearest neighbour graphs in Sections 5.2 using the technique of dependence graph. The proof of convergence of variance is given in Section 5.3 using the stabilization methodology.

5.2 Convergence to Normal Distribution

This section discusses the probabilistic technique useful in studying random geometric graphs. This technique mainly focuses on the Poisson process and normal approximations as the number of points tends to infinity.

Avram and Bertsimas [3] give the proof of central limit theorems of convergence for the nearest-neighbour graph using a dependency graph technique of Baldi and Rinott [4]. The fundamental concept here is that the graph's structure, in a sense, is locally determined. Consequently, with high probability, the dependency structure of graph exhibits a finite range dependence. We will use the dependence structure for all our problems associated with bulk to show convergence to a normal random variable as the number of points becomes very large. These points are generated by a Poisson process within the square $[0, 1]^2$.

The Poisson distribution is commonly used to approximate the sum of many independent Bernoulli random variables with small means. Conversely, if these means are bounded away from 0 and 1, the sum is approximated by a normal distribution. Our specific interest lies in scenarios where most, but not all, pairs of variables are independent. In such cases, the notation and concepts associated with dependency graphs offer a valuable means of characterizing this notion of near-independence, see for example [26].

5.2.1 Dependency Graph

We apply the results of dependency graphs with a finite-range dependence to the minimal directed spanning forest. We shall show the results where we have generalized the local dependence approach of Avram and Bertsimas [3] to the bulk of $[0,1]^2$. The main result of this section is on the normal approximation for a sum of weakly dependent variables by the dependency graph method. This result states that the dependency graphs with a finite-range dependence give a normal approximation as the intensity λ tends to infinity.

Definition 5.2.1 (Dependency graph)**.** Let $\mathcal{V}$ be a finite, non-empty set. Suppose that $\{Z_p : p \in \mathcal{V}\}$ is a collection of random variables. Then $\mathcal{G} = (\mathcal{V}, \mathcal{E})$ is said to be a dependency graph for $\{Z_p\}_{p\in\mathcal{V}}$ if it has the following property: for every $C_1, C_2 \subseteq \mathcal{V}$ with $C_1 \cap C_2 = \emptyset$ such that there is no edge in $\mathcal{E}$ that has one end in C_1 and the other in C_2, the collections of random variables $\{Z_p : p \in C_1\}$ and $\{Z_q : q \in C_2\}$ are independent.

Theorem 5.2.2 (Baldi and Rinott [4])**.** *Let $(\mathcal{V}_\lambda)_{\lambda>0}$ be a sequence of finite sets, and $\{Z_{\lambda,p}\}_{p\in\mathcal{V}_\lambda}$ accompanying collections of random variables admitting dependency graphs $\mathcal{G}_\lambda = (\mathcal{V}_\lambda, \mathcal{E}_\lambda)$ for all $\lambda > 0$. Define $\mathcal{J}_\lambda$ to be the sum $\mathcal{J}_\lambda = \sum_{p\in\mathcal{V}_\lambda} Z_{\lambda,p}$. Let $\mathcal{D}_\lambda$ be the maximum degree of the dependency graph $\mathcal{G}_\lambda$. Let $|Z_{\lambda,p}| \le \mathcal{A}_\lambda$, where $\mathcal{A}_\lambda$ is constant, i.e., $\mathbf{P}(|Z_{\lambda,p}| \le \mathcal{A}_\lambda) = 1$ for all $p \in \mathcal{V}_\lambda$ and all λ. Define $\sigma_\lambda^2 = Var(\mathcal{J}_\lambda)$. Then,*

$$\sup_{y\in\mathbb{R}} \left| \mathbf{P}\left\{ \frac{\mathcal{J}_\lambda - \mathbf{E}[\mathcal{J}_\lambda]}{\sigma_\lambda} \le y \right\} - \Phi(y) \right| \le 32(1+\sqrt{6}) \left(\frac{|\mathcal{V}_\lambda| \mathcal{D}_\lambda^2 \mathcal{A}_\lambda^3}{\sigma_\lambda^3} \right)^{\frac{1}{2}}. \tag{5.2.1}$$

Thus, if the right hand side of the inequality (5.2.1) tends to 0 as $\lambda \to \infty$, then the left hand side of the inequality implies convergence in distribution to standard normal distribution, i.e.,

$$\text{if} \quad \left(\frac{|\mathcal{V}_\lambda| \mathcal{D}_\lambda^2 \mathcal{A}_\lambda^3}{\sigma_\lambda^3} \right)^{\frac{1}{2}} \to 0 \quad \text{as} \quad \lambda \to \infty, \quad \text{then} \quad \frac{\mathcal{J}_\lambda - \mathbf{E}[\mathcal{J}_\lambda]}{\sigma_\lambda} \xrightarrow{d} \mathcal{N}(0,1) \quad \text{as} \quad \lambda \to \infty.$$

5.2.2 Local Dependence in MDSF Bulk

We split the unit square $[0,1]^2$ into little squares whose size is chosen so that with high probability, the Poisson process will have a point in every little square. Moreover, such 'typical configurations' of points exhibit a finite-range dependence, as the nearest neighbour of each point is only determined by the points in nearby little squares. Then, we represent $\mathcal{L}_\lambda^1$ as a sum of a collection of random variables associated with the little squares. To apply Theorem 5.2.2, we need to determine the appropriate values of $|\mathcal{V}_\lambda|$, $\mathcal{D}_\lambda$, $\mathcal{A}_\lambda$, and σ_λ, to ensure that $\frac{|\mathcal{V}_\lambda|\mathcal{D}_\lambda^2\mathcal{A}_\lambda^3}{\sigma_\lambda^3} \to 0 \quad \text{as} \quad \lambda \to \infty$. The choice of size of the little square gives natural bounds on $|\mathcal{V}_\lambda|$ and $\mathcal{D}_\lambda$; we need to also bound $\mathcal{A}_\lambda$ from above and σ_λ from below. First, we show that the event we require for finite-range dependence has a high probability of occurring (i.e., with probability tending to 1 as $\lambda \to \infty$).

Here, we briefly define and recall the relevant terminology. The square $[0,1]^2 \subseteq \mathbb{R}^2$ is tiled by tiles $T(p)$, where $p = (p_1, p_2)$, with p_1, p_2 integers satisfying $1 \le p_i \le k_\lambda$ for each $i = 1, 2$. Recall that from Definition 2.4.1 of $\mathcal{P}_\lambda$ is a homogeneous Poisson point process on $[0,1]^2$ with intensity λ, i.e., $\mathcal{P}_\lambda := \{Y_i \in [0,1]^2 : 1 \le i \le N_\lambda\}$, where $N_\lambda \sim \mathbf{Po}(\lambda)$. Let $N_{\lambda,p}$ be the number of points from the Poisson process $\mathcal{P}_\lambda$ in each little square p, in other words, $N_{\lambda,p} = |\mathcal{P}_\lambda \cap T(p)|$. By the definition of the Poisson process, the random variable $N_{\lambda,p} \sim \mathbf{Po}(\mu)$ is Poisson distributed with parameter $\mu = \lambda|T(p)| = \lambda S^2 = \frac{\lambda}{k_\lambda^2}$. Inequalities $\frac{1}{a_\lambda} - 1 < k_\lambda = \left\lfloor \frac{1}{a_\lambda} \right\rfloor \le \frac{1}{a_\lambda}$ imply

$$\lambda a_\lambda^2 \le \frac{\lambda}{k_\lambda^2} \le \lambda \left(\frac{1}{a_\lambda} - 1 \right)^{-2} = \lambda a_\lambda^2 (1 - a_\lambda)^{-2} \le 4\lambda a_\lambda^2,$$

thus we have μ is bounded by $\lambda a_\lambda^2 \le \mu \le 4\lambda a_\lambda^2$. Note that, in the last inequality we use that $a_\lambda \le \frac{1}{2}$ by definition.

Recall we have by Definition 4.4.4 that $\mathbb{T}_S$ is the set of all tiles in $[0,1]^2$, in other words, $\mathbb{T}_S = \{p \in \mathbb{Z}^2 : T(p) \subseteq [0,1]^2\}$. Define $\mathcal{B}_\lambda$ be the event such that $\mathcal{B}_\lambda = \cap_{p \in \mathbb{T}_S} \{1 \le N_{\lambda,p} \le 12\, c \log \lambda\}$. Then, since $\mu \le 4c \log \lambda$ the probability $\mathbf{P}(\mathcal{B}_\lambda)$ is bounded from below by $\mathbf{P}\left(\cap_{p \in \mathbb{T}_S} \{1 \le N_{\lambda,p} \le 3\mu\}\right)$. We make use of a standard fact that the Poisson random variable is concentrated around its mean. For example,

Lemma 1.2 from [26], states that if $X \sim \mathbf{Po}(\mu)$, then

$$\mathbf{P}[X \geq 3\mu] \leq \exp\left(-\mu H(3)\right), \tag{5.2.2}$$

where H satisfies $H(c) = 1 - c \ + c\log c$, so that $H(3) \approx 1.295837 \geq 1$.

The next result gives a probability of the event $\mathcal{B}_\lambda$, as $\lambda \to \infty$.

Lemma 5.2.3. *Suppose $c > 11$. We have $\mathbf{P}(\mathcal{B}_\lambda) \geq 1 - \lambda^{-10}$. In particular,*

$$\mathbf{P}(\mathcal{B}_\lambda) \to 1, \quad \textit{as} \quad \lambda \to \infty.$$

Proof. By independence property of the Poisson point Process, we have

$$\mathbf{P}(\mathcal{B}_\lambda) = \Pi_{p\in\mathbb{T}_S}\mathbf{P}(1 \leq N_{\lambda,p} \leq 12\ c\log\lambda) \geq \Pi_{p\in\mathbb{T}_S}\mathbf{P}(1 \leq N_{\lambda,p} \leq 3\mu).$$

Then $\mathbf{P}(N_{\lambda,p} = 0) = e^{-\mu}$ by definition, and from inequality (5.2.2), we have $\mathbf{P}(N_{\lambda,p} \geq 3\mu) \leq \exp\left(-\mu\ H(3)\right) \leq e^{-\mu}$. Hence,

$$\mathbf{P}(1 \leq N_{\lambda,p} \leq 3\mu) \geq 1 - \mathbf{P}(N_{\lambda,p} = 0) - \mathbf{P}(N_{\lambda,p} \geq 3\mu) \geq 1 - 2e^{-\mu}.$$

Using $k_\lambda^2 = \frac{\lambda}{\mu}$ then,

$$\begin{aligned}\mathbf{P}(\mathcal{B}_\lambda) = \Pi_{p\in\mathbb{T}_S}\mathbf{P}(1 \leq N_{\lambda,p} \leq 3\mu) &\geq (1 - 2e^{-\mu})^{k_\lambda^2} \\ &= \exp\left\{k_\lambda^2 \log(1 - 2e^{-\mu})\right\} \\ &= \exp\left\{\frac{\lambda}{\mu}\log(1 - 2e^{-\mu})\right\}.\end{aligned}$$

The expression $\exp\left\{\frac{\lambda}{\mu}\log(1 - 2e^{-\mu})\right\}$ is increasing in μ for $\mu > 0$. To see this, note that:

1. $\frac{\lambda}{\mu}$ is decreasing in μ;

2. $\log(1 - 2e^{-\mu})$ is negative and increasing in μ.

Hence, the product $\frac{\lambda}{\mu}\log(1 - 2e^{-\mu})$ is increasing in μ. Therefore,

$$\mathbf{P}(\mathcal{B}_\lambda) \geq \exp\left\{\frac{\lambda}{\mu}\log(1 - 2e^{-\mu})\right\} \geq \exp\left\{\frac{\lambda}{c\log\lambda}\log(1 - 2e^{-c\log\lambda})\right\}.$$

Using the inequality $\log(1-y) \geq -2y$ which holds for $0 \leq y \leq \frac{1}{2}$, and the fact that $2e^{-c\log\lambda} \leq \frac{1}{2}$ for λ large enough, then

$$\mathbf{P}(\mathcal{B}_\lambda) \geq \exp\left\{\frac{-2\lambda}{c\log\lambda}\cdot 2e^{-c\log\lambda}\right\} = \exp\left\{\frac{-4\lambda^{1-c}}{c\log\lambda}\right\} \geq 1 - \frac{4\lambda^{1-c}}{c\log\lambda}.$$

Taking c large enough say $c > 11$, hence

$$\mathbf{P}(\mathcal{B}_\lambda) \geq 1 - \lambda^{-10}, \quad \text{and therefore} \quad \mathbf{P}(\mathcal{B}_\lambda) \to 1 \quad \text{as} \quad \lambda \to \infty.$$

□

The next result is the heart of our development of the bulk with respect to the unit square, and it works for all types of general cones, i.e., singly-aligned and unaligned cones. Also, it proves the finite range dependence for squares in the bulk of $[0,1]^2$. Recall by Definition 4.5.1 that $\mathcal{R}_\lambda^1 = [0,1] \times [RS, 1]$, where R is constant given in Lemmas 4.4.6 – 4.4.8. Call $p \in \mathbb{Z}^2$ a square in the bulk if $T(p) \subseteq \mathcal{R}_\lambda^1$.

Definition 5.2.4. Let $\mathcal{L}_{\lambda,p}$ be the sum of edge lengths for all edges started in square p, then

$$\mathcal{L}_{\lambda,p} = \sum_{\boldsymbol{x}\in\mathcal{P}_\lambda\cap T(p)} \mathcal{D}_{\theta,\phi}(\boldsymbol{x}, \mathcal{P}_\lambda).$$

The following property encapsulates the finite-range dependence of the variables $\mathcal{L}_{\lambda,p}$ for squares p in the bulk.

Proposition 5.2.5. *Let δ and C_0 be the parameter appearing in Lemmas 4.4.6 – 4.4.8 for which $\mathcal{R}_\lambda^1$ is a compatible bulk. Define $\rho = \max(\lfloor\delta\rfloor+1, \max\{\rho(r) : r \in C_0\})$ where $\rho(r) = |r_1| + |r_2| + 2$ for $r = (r_1, r_2) \in C_0$. Given $\mathcal{B}_\lambda$ occurs, then*

1. *The nearest neighbour of any point $\boldsymbol{x} \in \mathcal{P}_\lambda \cap T(p)$ is in $T(\mathcal{S}_{p,\rho})$ for all p in the bulk.*

2. *If p and q are squares in the bulk and $d(p,q) > 2\rho$ then the lengths $\mathcal{L}_{\lambda,p}$ and $\mathcal{L}_{\lambda,q}$ are independent. More generally, if $\mathcal{C}_1$, $\mathcal{C}_2$ are collections of squares in the bulk such that $d(p,q) > 2\rho$ for all $p \in \mathcal{C}_1$, $q \in \mathcal{C}_2$, then the random variables $\{\mathcal{L}_{\lambda,p} : p \in \mathcal{C}_1\}$ and $\{\mathcal{L}_{\lambda,q} : q \in \mathcal{C}_2\}$ are independent.*

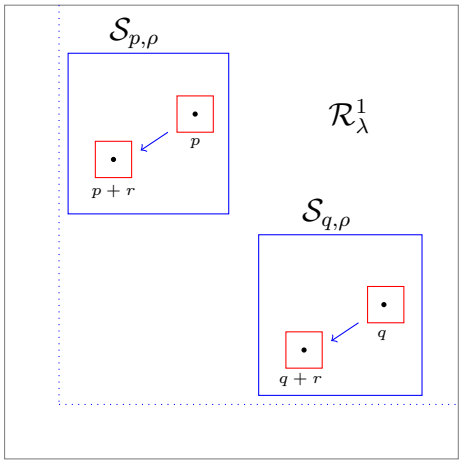

Figure 5.1: Example of two balls in the $[0,1]^2$, and they are not overlapped each other.

Proof. Since $\mathcal{R}^1_\lambda$ is a compatible bulk, any $p \in \mathbb{T}_S$ with $T(p) \subseteq \mathcal{R}^1_\lambda$ either satisfies condition (A) or (B_1) (see Definition 4.4.5). If (A) holds, then $T(p+r) \subseteq [0,1]^2$ for some $r \in C_0$. Given $\mathcal{B}_\lambda$ occurs, we have $\mathcal{P}_\lambda \cap T(p+r) \neq \emptyset$, so we can apply Theorem 4.2.7 to the square p, which proves that $N_{\theta,\phi}(\boldsymbol{x}; \mathcal{P}_\lambda) \in T(\mathcal{S}_{p,\rho(r)}) \subseteq T(\mathcal{S}_{p,\rho})$ for any point $\boldsymbol{x} \in \mathcal{P}_\lambda \cap T(p)$. Otherwise, if (B_1) holds, then $\nu(p) \leq \delta S$, so we can apply Lemma 4.4.3 to the square p, which proves that $N_{\theta,\phi}(\boldsymbol{x}; \mathcal{P}_\lambda) \in T(\mathcal{S}_{p,\lfloor\delta\rfloor+1}) \subseteq T(\mathcal{S}_{p,\rho})$ for any point $\boldsymbol{x} \in \mathcal{P}_\lambda \cap T(p)$. Hence property 1 holds as claimed.

Property 1) implies 2): The length contributing to $\mathcal{L}_{\lambda,p}$ is coming from points in square p and their nearest-neighbours. By property 1, these points are all contained in $T(\mathcal{S}_{p,\rho})$, and therefore $\mathcal{L}_{\lambda,p}$ is only determined by the Poisson point process restricted to $T(\mathcal{S}_{p,\rho})$. Since $d(p,q) > 2\rho$, the balls $T(\mathcal{S}_{p,\rho})$ and $T(\mathcal{S}_{q,\rho})$ are disjoint, and therefore the lengths $\mathcal{L}_{\lambda,p}$ and $\mathcal{L}_{\lambda,q}$ are determined by the Poisson process in non-overlapping regions (e.g. see Figure 5.1). This implies the independence of $\mathcal{L}_{\lambda,p}$ and $\mathcal{L}_{\lambda,q}$ by the independence property of Poisson process. Note that conditioning on the event $\mathcal{B}_\lambda$ is equivalent to conditioning separately on the numbers of points in each square so conditioning on $\mathcal{B}_\lambda$ preserves the independence property of the Poisson process. □

Remark 5.2.6. In all cases (singly aligned or unaligned cone), property 2 of Proposi-

tion 5.2.5 will allow us to define a dependency graph on all the set of squares in the bulk, that has an edge between p and q having a distance $d(p,q) \leq 2\rho$. Importantly, this gives a maximum degree of $(1+4\rho)^2$ that is independent of λ (see Section 5.2.3).

We now turn to upper bound for $\mathcal{A}_\lambda$ to apply Theorem 5.2.2. We shall show the upper bound on the length of $\mathcal{L}_{\lambda,p}$. Recall by Definition 5.2.4 that $\mathcal{L}_{\lambda,p} = \sum_{\boldsymbol{x}\in\mathcal{P}_\lambda\cap T(p)} \mathcal{D}_{\theta,\phi}(\boldsymbol{x},\mathcal{P}_\lambda)$ is the sum of the lengths for all edges started in square p. Recall that $S = 1/k_\lambda$, where $k_\lambda = \left\lfloor \frac{1}{a_\lambda} \right\rfloor$ and $a_\lambda = \min(\frac{1}{2}, b(c, \max(3,\lambda)))$ with $b(c,\lambda) := \sqrt{\frac{c\log\lambda}{\lambda}}$. For any c, there is some $\lambda(c)$, so that $a_\lambda = b(c,\lambda)$ for $\lambda \geq \lambda(c)$. Also, the inequality holds $\frac{1}{a_\lambda} - 1 \leq k_\lambda \leq \frac{1}{a_\lambda}$, which implies $1 - a_\lambda \leq a_\lambda k_\lambda \leq 1$, and therefore, $a_\lambda k_\lambda \to 1$ as $\lambda \to \infty$ (using that $a_\lambda \to 0$ as $\lambda \to \infty$). Thus for large enough λ, we have $a_\lambda k_\lambda \geq 1/2$, in other words, $S = 1/k_\lambda \leq 2a_\lambda = 2\sqrt{\frac{c\log\lambda}{\lambda}}$. The upper bound on the length of $\mathcal{L}_{\lambda,p}$ is provided in the following proposition.

Proposition 5.2.7. *There is a constant m such that for large enough λ, given $\mathcal{B}_\lambda$ occurs, and for all p with $T(p) \subseteq \mathcal{R}^1_\lambda$, we have*

$$\mathcal{L}_{\lambda,p} \leq m\frac{(\log\lambda)^{\frac{3}{2}}}{\lambda^{\frac{1}{2}}},$$

holds almost surely.

Proof. To prove Proposition 5.2.7, we need to check two aspects, they are

1. The maximum possible length of an edge contributing to $\mathcal{L}_{\lambda,p}$ becomes sufficiently small as $\lambda \to \infty$.

2. The number of points in square p, $N_{\lambda,p}$, does not grow too large as $\lambda \to \infty$.

Both aspects will follow due to the conditioning on $\mathcal{B}_\lambda$.

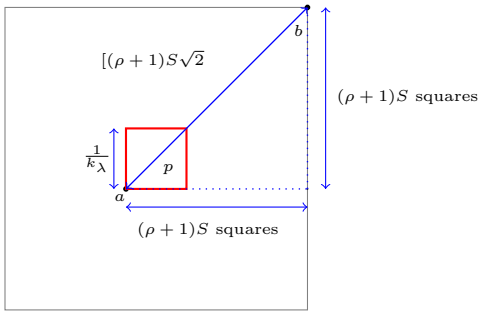

Figure 5.2: The longest distance between point a bottom-corner and b top-corner is $[(\rho+1)S]\sqrt{2}$ in $[0,1]^2$ with horizontal and vertical distances $\leq (\rho+1)S$.

Given $\mathcal{B}_\lambda$ occurs, by the Definition 5.2.4 and Proposition 5.2.5, we know that the nearest neighbour of any $\boldsymbol{x}$ in $\mathcal{P}_\lambda \cap T(p)$ must lie in $T(\mathcal{S}_{p,\rho})$, then

$$\begin{aligned}\mathcal{L}_{\lambda,p} = \sum_{\boldsymbol{x}\in\mathcal{P}_\lambda\cap T(p)} \mathcal{D}_{\theta,\phi}(\boldsymbol{x};\mathcal{P}_\lambda) &\leq N_{\lambda,p} \max_{a\in T(p),b\in T(\mathcal{S}_{p,\rho})} \|a-b\| \\ &= N_{\lambda,p} \max_{a,b} \left(\sqrt{(a_1-b_1)^2+(a_2-b_2)^2}\right) \\ &\leq N_{\lambda,p}\sqrt{((\rho+1)S)^2+((\rho+1)S)^2} = N_{\lambda,p}(\rho+1)S\sqrt{2}.\end{aligned}$$

By definition of $\mathcal{B}_\lambda$, we have $N_{\lambda,p} \leq 12\ c\log\lambda$, $S = 1/k_\lambda \leq 2a_\lambda = 2\sqrt{\frac{c\log\lambda}{\lambda}}$, and hence

$$\mathcal{L}_{\lambda,p} \leq N_{\lambda,p}(\rho+1)S\sqrt{2} \leq 12\sqrt{2}\ c\log\lambda\ (\rho+1)S \leq 24\sqrt{2}\ c^{\frac{3}{2}}(\rho+1)\frac{(\log\lambda)^{\frac{3}{2}}}{\lambda^{\frac{1}{2}}}.$$

Thus the upper bound on the length of $\mathcal{L}_{\lambda,p}$ has obtained, i.e., $\mathcal{L}_{\lambda,p} \leq m\frac{(\log\lambda)^{\frac{3}{2}}}{\lambda^{\frac{1}{2}}}$, where m is constant, in other words, $m = 24\sqrt{2}\ c^{\frac{3}{2}}(\rho+1)$. □

For the ingredient to Theorem 5.2.2, we want to show a lower bound on the variance of $\mathcal{L}_\lambda^1$. Recall from Definition 4.5.2, that $\mathcal{L}_\lambda^1 = \sum_{\boldsymbol{x}\in\mathcal{P}_\lambda\cap\mathcal{R}_\lambda^1} \mathcal{D}_{\theta,\phi}(\boldsymbol{x};\mathcal{P}_\lambda)$, where $\mathcal{D}_{\theta,\phi}(\boldsymbol{x};\mathcal{P}_\lambda)$ is the distance from point $\boldsymbol{x}$ to its nearest neighbour in $\mathcal{P}_\lambda \cap C_{\theta,\phi}(\boldsymbol{x})$. The lower bound on the variance of $\mathcal{L}_\lambda^1$ is provided in the following result.

Proposition 5.2.8. *There exists $\boldsymbol{q} > 0$ (depending on ϕ), such that, for all $\lambda > 1$,*

$$\mathbf{Var}[\mathcal{L}_\lambda^1] \geq \boldsymbol{q}.$$

We omit the proof of Proposition 5.2.8 here, as the proof follows similar lines to that of Proposition 5 in Avram and Bertsimas [3].

5.2.3 Proof of Central Limit Theorem

We give the proof of Theorem 5.1.1 in this subsection. The next lemma is a useful tool to establish the proof of CLT. The idea behind the lemma is to show the difference between the expectation and its conditional expectation, as well as the variance and its conditional variance.

Recall we have $\mathcal{B}_\lambda = \cap_{p\in\mathbb{T}_S}\{1 \le N_{\lambda,p} \le 12\ c\log\lambda\}$, where $N_{\lambda,p} = |\mathcal{P}_\lambda \cap T(p)|$ and $\mathbb{T}_S = \{p \in \mathbb{Z}^2 : T(p) \subseteq [0,1]^2\}$. Throughout this section, take $c > c_0 > 11$ so that the condition of Lemma 5.2.3 applies. Recall from Definition 4.5.2, that $\mathcal{L}^1_\lambda = \sum_{\boldsymbol{x}\in\mathcal{P}_\lambda\cap\mathcal{R}^1_\lambda} \mathcal{D}_{\theta,\phi}(\boldsymbol{x};\mathcal{P}_\lambda)$, where $\mathcal{D}_{\theta,\phi}(\boldsymbol{x};\mathcal{P}_\lambda)$ is the distance from point $\boldsymbol{x}$ to its nearest neighbour in $\mathcal{P}_\lambda \cap C_{\theta,\phi}(\boldsymbol{x})$.

Lemma 5.2.9. *For large enough λ, we have*

$$\left|\mathbf{E}[\mathcal{L}^1_\lambda] - \mathbf{E}[\mathcal{L}^1_\lambda|\mathcal{B}_\lambda]\right| \le 5\lambda^{-4},\ \textit{and}$$

$$\left|\mathbf{Var}(\mathcal{L}^1_\lambda\ |\mathcal{B}_\lambda) - \mathbf{Var}(\mathcal{L}^1_\lambda)\right| \le 30\lambda^{-3}.$$

Proof. Write $\mathcal{B}^{\complement}_\lambda$ for the complement of the event $\mathcal{B}_\lambda$. We want to show the difference $|\mathbf{E}[\mathcal{L}^1_\lambda] - \mathbf{E}[\mathcal{L}^1_\lambda|\mathcal{B}_\lambda]|$ is small. We write

$$\begin{aligned}
\left|\mathbf{E}[\mathcal{L}^1_\lambda] - \mathbf{E}[\mathcal{L}^1_\lambda|\mathcal{B}_\lambda]\right| &= \frac{1}{\mathbf{P}(\mathcal{B}_\lambda)}|\mathbf{E}[\mathcal{L}^1_\lambda]\mathbf{P}(\mathcal{B}_\lambda) - \mathbf{E}[\mathcal{L}^1_\lambda \mathbb{1}_{\mathcal{B}_\lambda}]| \\
&= \frac{1}{\mathbf{P}(\mathcal{B}_\lambda)}|\mathbf{E}[\mathcal{L}^1_\lambda]\mathbf{P}(\mathcal{B}_\lambda) - \mathbf{E}[\mathcal{L}^1_\lambda] + \mathbf{E}[\mathcal{L}^1_\lambda \mathbb{1}_{\mathcal{B}^{\complement}_\lambda}]| \\
&\le \frac{\mathbf{P}(\mathcal{B}^{\complement}_\lambda)}{\mathbf{P}(\mathcal{B}_\lambda)}\mathbf{E}[\mathcal{L}^1_\lambda] + \frac{1}{\mathbf{P}(\mathcal{B}_\lambda)}\mathbf{E}[\mathcal{L}^1_\lambda \mathbb{1}_{\mathcal{B}^{\complement}_\lambda}].
\end{aligned}$$

To bound $\mathbf{E}[\mathcal{L}^1_\lambda \mathbb{1}_{\mathcal{B}^{\complement}_\lambda}]$, we use the following aspects, they are,

1. The contribution to $\mathcal{L}^1_\lambda$ from each point in the Poisson point process is at most the diameter of $[0,1]^2$, which equals $\sqrt{2}$.

2. The number of points in the square $[0,1]^2$ is $N_\lambda \sim \mathbf{Po}(\lambda)$.

3. Using Cauchy-Schwarz inequality to bound $\mathbf{E}[N_\lambda \mathbb{1}_{\mathcal{B}_\lambda^{\complement}}] \leq \mathbf{E}\left[N_\lambda^2\right]^{\frac{1}{2}} \mathbf{P}\left(\mathcal{B}_\lambda^{\complement}\right)^{\frac{1}{2}}$.

Using the above aspects along with Lemma 5.2.3, which states that $\mathbf{P}(\mathcal{B}_\lambda^{\complement}) \leq \lambda^{-10}$, we find

$$\begin{aligned}\mathbf{E}[\mathcal{L}_\lambda^1 \mathbb{1}_{\mathcal{B}_\lambda^{\complement}}] &\leq \sqrt{2}\ \mathbf{E}\left[N_\lambda \mathbb{1}_{\mathcal{B}_\lambda^{\complement}}\right] \leq \sqrt{2}\ \mathbf{E}\left[N_\lambda^2\right]^{\frac{1}{2}} \mathbf{P}\left(\mathcal{B}_\lambda^{\complement}\right)^{\frac{1}{2}} \\ &\leq \sqrt{2}\left(\mathbf{Var}(N_\lambda) + \mathbf{E}[N_\lambda]^2\right)^{\frac{1}{2}} \mathbf{P}\left(\mathcal{B}_\lambda^{\complement}\right)^{\frac{1}{2}}, \quad \text{where } N_\lambda \sim \mathbf{Po}(\lambda) \\ &\leq \sqrt{2}\ \left(\lambda + \lambda^2\right)^{\frac{1}{2}} \left(\lambda^{-10}\right)^{\frac{1}{2}} \leq 2\lambda^{1-5} = 2\lambda^{-4}. \end{aligned} \tag{5.2.3}$$

Note that, we use the fact that $\mathbf{Var}(N_\lambda) = \mathbf{E}[N_\lambda^2] - [\mathbf{E}(N_\lambda)]^2$ implies $\mathbf{E}[N_\lambda^2] = \mathbf{Var}(N_\lambda) + [\mathbf{E}(N_\lambda)]^2$, where $\mathbf{E}[N_\lambda] = \lambda$ and $\mathbf{E}[N_\lambda^2] = \lambda + \lambda^2$. Therefore, $\mathbf{E}[\mathcal{L}_\lambda^1 \mathbb{1}_{\mathcal{B}_\lambda^{\complement}}] \leq 2\lambda^{-4}$.

Finally, by Lemma 5.2.3, we know that $\mathbf{P}(\mathcal{B}_\lambda) > \frac{1}{2}$ for sufficiently large enough λ, so we obtain the difference between the expectation and its conditional expectation, as follows

$$\left|\mathbf{E}[\mathcal{L}_\lambda^1] - \mathbf{E}[\mathcal{L}_\lambda^1 | \mathcal{B}_\lambda]\right| \leq 2\lambda^{-10} \cdot \lambda\sqrt{2} + 2 \cdot 2\lambda^{-4} \leq 5\lambda^{-4}. \tag{5.2.4}$$

The first term in (5.2.4) tends to 0 as $\lambda \to \infty$ much quicker compare the second term.

Next we will consider the conditional variance, given by

$$\mathbf{Var}(\mathcal{L}_\lambda^{\mathbf{1}} | \mathcal{B}_\lambda) = \mathbf{E}\left[(\mathcal{L}_\lambda^1 - \mathbf{E}[\mathcal{L}_\lambda^1 | \mathcal{B}_\lambda])^2 | \mathcal{B}_\lambda\right] = \mathbf{E}[(\mathcal{L}_\lambda^1)^2 | \mathcal{B}_\lambda] - (\mathbf{E}[\mathcal{L}_\lambda^1\ | \mathcal{B}_\lambda])^2.$$

Therefore,

$$\left|\mathbf{Var}(\mathcal{L}_\lambda^{\mathbf{1}}) - \mathbf{Var}(\mathcal{L}_\lambda^{\mathbf{1}} | \mathcal{B}_\lambda)\right| \leq |\mathbf{E}[(\mathcal{L}_\lambda^1)^2] - \mathbf{E}[(\mathcal{L}_\lambda^1)^2 | \mathcal{B}_\lambda]| + |\mathbf{E}(\mathcal{L}_\lambda^1)^2 - \mathbf{E}[\mathcal{L}_\lambda^1 | \mathcal{B}_\lambda]^2|.$$

Recall that $(\mathcal{L}_\lambda^1)^2 \leq (\sqrt{2}N_\lambda)^2$. We use fourth moment of the Poisson distribution ($\mathbf{E}[N_\lambda^4] \leq 2\lambda^4$ for sufficiently large enough λ) along with Cauchy-Schwarz inequality, hence

$$\begin{aligned}\mathbf{E}\left[(\mathcal{L}_\lambda^1)^2 \mathbb{1}_{\mathcal{B}_\lambda^{\complement}}\right] &\leq 2\mathbf{E}[N_\lambda^2 \mathbb{1}_{\mathcal{B}_\lambda^{\complement}}] \\ &\leq 2\mathbf{E}[N_\lambda^4]^{\frac{1}{2}} \mathbf{P}(\mathcal{B}_\lambda^{\complement})^{\frac{1}{2}} \leq 2\sqrt{2\lambda^4}\ (\lambda^{-10})^{\frac{1}{2}} \leq 2\lambda^2 \cdot \lambda^{-5}\sqrt{2} = 2\lambda^{-3}\sqrt{2}. \end{aligned} \tag{5.2.5}$$

Hence, by (5.2.5) along with Lemma 5.2.3, we get

$$\begin{aligned}\left|\mathbf{E}[(\mathcal{L}_\lambda^1)^2] - \mathbf{E}[(\mathcal{L}_\lambda^1)^2|\mathcal{B}_\lambda]\right| &= \frac{1}{\mathbf{P}(\mathcal{B}_\lambda)}|\mathbf{E}[(\mathcal{L}_\lambda^1)^2]\mathbf{P}(\mathcal{B}_\lambda) - \mathbf{E}[(\mathcal{L}_\lambda^1)^2\mathbb{1}_{\mathcal{B}_\lambda}]| \\ &= \frac{1}{\mathbf{P}(\mathcal{B}_\lambda)}|\mathbf{E}[(\mathcal{L}_\lambda^1)^2]\mathbf{P}(\mathcal{B}_\lambda) - \mathbf{E}[(\mathcal{L}_\lambda^1)^2] + \mathbf{E}[(\mathcal{L}_\lambda^1)^2\mathbb{1}_{\mathcal{B}_\lambda^\complement}]| \\ &\leq \frac{\mathbf{P}(\mathcal{B}_\lambda^\complement)}{\mathbf{P}(\mathcal{B}_\lambda)}\mathbf{E}[(\mathcal{L}_\lambda^1)^2] + \frac{1}{\mathbf{P}(\mathcal{B}_\lambda)}\mathbf{E}[(\mathcal{L}_\lambda^1)^2\mathbb{1}_{\mathcal{B}_\lambda^\complement}] \\ &\leq 2\lambda^{-10}\cdot 2(\lambda+\lambda^2) + 2\lambda^{-3}\cdot 2\sqrt{2} \leq 6\lambda^{-3}. \end{aligned} \tag{5.2.6}$$

Thus, $|\mathbf{E}[(\mathcal{L}_\lambda^1)^2] - \mathbf{E}[(\mathcal{L}_\lambda^1)^2|\mathcal{B}_\lambda]| \leq 6\lambda^{-3}$.

Now, we consider $|\mathbf{E}[\mathcal{L}_\lambda^1]^2 - \mathbf{E}[\mathcal{L}_\lambda^1|\mathcal{B}_\lambda]^2|$. Recall that, for λ sufficiently large enough, we have $\mathbf{P}(\mathcal{B}_\lambda) > \frac{1}{2}$, and by second moment of the Poisson distribution, that $\mathbf{E}[N_\lambda^2] = \lambda + \lambda^2$. Then, we obtain the difference between the squares, as follows

$$|\mathbf{E}[\mathcal{L}_\lambda^1]^2 - \mathbf{E}[\mathcal{L}_\lambda^1|\mathcal{B}_\lambda]^2| = |(\mathbf{E}[\mathcal{L}_\lambda^1] - \mathbf{E}[\mathcal{L}_\lambda^1|\mathcal{B}_\lambda])|(\mathbf{E}[\mathcal{L}_\lambda^1] + \mathbf{E}[\mathcal{L}_\lambda^1\ |\mathcal{B}_\lambda]). \tag{5.2.7}$$

The first term $|\mathbf{E}[\mathcal{L}_\lambda^1] - \mathbf{E}[\mathcal{L}_\lambda^1|\mathcal{B}_\lambda]|$ is bounded by (5.2.4). Next we have, $\mathbf{E}[\mathcal{L}_\lambda^1|\mathcal{B}_\lambda] = \frac{\mathbf{E}[\mathcal{L}_\lambda^1\mathbb{1}_{\mathcal{B}_\lambda}]}{\mathbf{P}(\mathcal{B}_\lambda)} \leq 2\mathbf{E}[\mathcal{L}_\lambda^1]$, so the second term of (5.2.7), becomes

$$\mathbf{E}[\mathcal{L}_\lambda^1] + \mathbf{E}[\mathcal{L}_\lambda^1|\mathcal{B}_\lambda] \leq 3\lambda\cdot\sqrt{2}, \tag{5.2.8}$$

hence (5.2.7), yields

$$|\mathbf{E}[\mathcal{L}_\lambda^1]^2 - \mathbf{E}[\mathcal{L}_\lambda^1|\mathcal{B}_\lambda]^2| \leq 5\lambda^{-4}\cdot 3\lambda\sqrt{2} = 15\sqrt{2}\lambda^{-3}. \tag{5.2.9}$$

Finally, combine (5.2.6) and (5.2.9), we obtain the second part of the Lemma 5.2.9

$$\left|\mathbf{Var}(\mathcal{L}_\lambda^1) - \mathbf{Var}(\mathcal{L}_\lambda^1\ |\mathcal{B}_\lambda))\right| \leq 6\lambda^{-3} + 15\sqrt{2}\lambda^{-3} \leq 30\lambda^{-3}.$$

□

Recall from Definition 4.5.2 that $\mathcal{L}_\lambda^1 = \sum_{\boldsymbol{x}\in\mathcal{P}_\lambda\cap\mathcal{R}_\lambda^1}\mathcal{D}_{\theta,\phi}(\boldsymbol{x};\mathcal{P}_\lambda)$, where $\mathcal{D}_{\theta,\phi}(\boldsymbol{x};\mathcal{P}_\lambda)$ is the distance from point $\boldsymbol{x}$ to its nearest neighbour in $\mathcal{P}_\lambda$ in $[0,1]^2$. Define $\tilde{\mathbf{U}}_\lambda := \frac{\mathcal{L}_\lambda^1 - \mathbf{E}[\mathcal{L}_\lambda^1|\mathcal{B}_\lambda]}{\sqrt{\mathbf{Var}[\mathcal{L}_\lambda^1|\mathcal{B}_\lambda]}}$. We now apply Theorem 5.2.2 to show that the conditional distribution of $\tilde{\mathbf{U}}_\lambda$ (given $\mathcal{B}_\lambda$) converges to a normal distribution.

Lemma 5.2.10. *Let $\Phi(y)$ be the cumulative distribution function of a standard normal distribution, i.e., $\mathcal{N}(0,1)$. Given $\mathcal{B}_\lambda$ occurs, we have*

$$\sup_{y\in\mathbb{R}}\left|\mathbf{P}(\tilde{\mathbf{U}}_\lambda \le y|\mathcal{B}_\lambda) - \Phi(y)\right| \to 0, \quad as \quad \lambda\to\infty. \tag{5.2.10}$$

Proof. We prove Lemma 5.2.10 using Theorem 5.2.2. Recall that μ is the expected number of points in each little square, where $\mu = \frac{\lambda}{k_\lambda^2}$ satisfies $c\log\lambda \le \mu \le 4c\log\lambda$ for large enough λ. Recall that, $|\mathcal{V}_\lambda|$ is the cardinality of the finite set $\mathcal{V}_\lambda$ of vertices defined by $\mathcal{V}_\lambda = \{p \in \mathbb{T}_S : T(p) \subseteq \mathcal{R}_\lambda^1 \subseteq \mathbb{T}_S\}$. So $|\mathcal{V}_\lambda| \le |\mathbb{T}_S| = k_\lambda^2$. The edges in the graph are determined by the finite-range dependence, in other words, $\mathcal{E}_\lambda = \{(p,q) \in \mathcal{V}_\lambda \times \mathcal{V}_\lambda$ such that $d(p,q) \le 2\rho\}$, as given in Proposition 5.2.5. The maximal degree of the dependence graph of $\mathcal{G}_\lambda = (\mathcal{V}_\lambda, \mathcal{E}_\lambda)$ satisfies $\mathcal{D}_\lambda \le (1+4\rho)^2$. Also, recall from Proposition 5.2.7, we get $\mathcal{L}_{\lambda,p} \le \mathcal{A}_\lambda = m\frac{(\log\lambda)^{\frac{3}{2}}}{\lambda^{\frac{1}{2}}} \le \frac{m}{c^{\frac{3}{2}}}\cdot\frac{\mu^{\frac{3}{2}}}{\lambda^{\frac{1}{2}}}$, where $m = 24\sqrt{2}\,c^{\frac{3}{2}}(\rho+1)$. From Proposition 5.2.8, we have that for large enough λ,

$$\begin{aligned}\sigma_\lambda^2 = \mathbf{Var}[\mathcal{L}_\lambda^1|\mathcal{B}_\lambda] &\overset{\text{Lemma 5.2.9}}{\ge} \mathbf{Var}[\mathcal{L}_\lambda^1] - 30\lambda^{-3} \\ &\overset{\text{Proposition 5.2.8}}{\ge} \boldsymbol{q} - 30\lambda^{-3} \ge \frac{\boldsymbol{q}}{2} > 0.\end{aligned} \tag{5.2.11}$$

Hence,

$$\begin{aligned}\left(\frac{|\mathcal{V}_\lambda|\mathcal{D}_\lambda^2\mathcal{A}_\lambda^3}{\mathbf{Var}[\mathcal{L}_\lambda^1|\mathcal{B}_\lambda]^3}\right)^{\frac{1}{2}} &= \left(\frac{k_\lambda^2\left[(1+4\rho)^2\right]^2\left[m\mu^{1+\frac{1}{2}}/c^{\frac{3}{2}}\lambda^{\frac{1}{2}}\right]^3}{(\boldsymbol{q}/2)^3}\right)^{\frac{1}{2}} = \left(\frac{\frac{\lambda}{\mu}[1+4\rho]^4\left[m^3\mu^{\frac{9}{2}}/\lambda^{\frac{3}{2}}\right]}{c^{\frac{9}{2}}(\boldsymbol{q}/2)^3}\right)^{\frac{1}{2}} \\ &= \left(\frac{\left(\frac{\lambda}{\mu}\right)^{\frac{1}{2}}[1+4\rho]^2\left[m^{\frac{3}{2}}\mu^{\frac{9}{4}}/\lambda^{\frac{3}{4}}\right]}{c^{\frac{9}{4}}(\boldsymbol{q}/2)^{\frac{3}{2}}}\right) = \frac{[1+4\rho]^2m^{\frac{3}{2}}}{c^{\frac{9}{4}}(\boldsymbol{q}/2)^{\frac{3}{2}}}\cdot\left[\left(\frac{\lambda}{\mu}\right)^{\frac{1}{2}}\frac{\mu^{\frac{9}{4}}}{\lambda^{\frac{3}{4}}}\right] \\ &\le w\cdot\left[\left(\frac{\lambda^{\frac{1}{2}}}{\lambda^{\frac{3}{4}}}\right)\frac{\mu^{\frac{9}{4}}}{\mu^{\frac{1}{2}}}\right] \le w\frac{\mu^{1+\frac{3}{4}}}{\lambda^{\frac{1}{4}}} \le w\frac{[4c\log\lambda]^{1+\frac{3}{4}}}{\lambda^{\frac{1}{4}}} \to 0, \quad \text{as} \quad \lambda\to\infty,\end{aligned}$$

where w is constant. Since, we have chosen $\mu < 4c\log\lambda$ for some $c > 11$, this obtains the last inequality which tends to 0 as $\lambda\to\infty$. Therefore, Theorem 5.2.2 implies that as $\lambda\to\infty$,

$$\frac{\mathcal{L}_\lambda^1 - \mathbf{E}[\mathcal{L}_\lambda^1|\mathcal{B}_\lambda]}{\sigma_\lambda^2} \xrightarrow{d} \mathcal{N}(0,1).$$

□

Now we show that the unconditional law of the random variable $\tilde{\mathbf{U}}_\lambda$ also converges to a normal distribution.

Lemma 5.2.11. *For every $y \in \mathbb{R}$, we have*

$$\sup_{y\in\mathbb{R}} \left| \mathbf{P}(\tilde{\mathbf{U}}_\lambda \leq y) - \Phi(y) \right| \to 0, \quad as \quad \lambda \to \infty, \tag{5.2.12}$$

where $\Phi(y)$ is a cumulative distribution function of $\mathcal{N}(0,1)$.

Proof. By the law of total probability, we have

$$\begin{aligned} |\mathbf{P}(\tilde{\mathbf{U}}_\lambda \leq y) - \Phi(y)| &= |\mathbf{P}(\mathcal{B}_\lambda)\mathbf{P}(\tilde{\mathbf{U}}_\lambda \leq y|\mathcal{B}_\lambda) \\ &\quad + \mathbf{P}(\mathcal{B}_\lambda^{\complement})\mathbf{P}(\tilde{\mathbf{U}}_\lambda \leq y|\mathcal{B}_\lambda^{\complement}) - \Phi(y)(\mathbf{P}(\mathcal{B}_\lambda) + \mathbf{P}(\mathcal{B}_\lambda^{\complement}))| \\ &\leq \mathbf{P}(\mathcal{B}_\lambda)|\mathbf{P}(\tilde{\mathbf{U}}_\lambda \leq y|\mathcal{B}_\lambda) - \Phi(y)| + \mathbf{P}(\mathcal{B}_\lambda^{\complement})|\mathbf{P}(\tilde{\mathbf{U}}_\lambda \leq y|\mathcal{B}_\lambda^{\complement}) - \Phi(y)|. \end{aligned}$$

Here $\mathbf{P}(\mathcal{B}_\lambda)$ and $\mathbf{P}(\mathcal{B}_\lambda^{\complement})$ are non-negative terms, so that

$$\begin{aligned} \sup_{y\in\mathbb{R}} |\mathbf{P}(\tilde{\mathbf{U}}_\lambda \leq y) - \Phi(y)| &\leq \sup_{y\in\mathbb{R}} \left[\mathbf{P}(\mathcal{B}_\lambda)|\mathbf{P}(\tilde{\mathbf{U}}_\lambda \leq y|\mathcal{B}_\lambda) - \Phi(y)| \right] \\ &\quad + \sup_{y\in\mathbb{R}} \left[\mathbf{P}(\mathcal{B}_\lambda^{\complement})|\mathbf{P}(\tilde{\mathbf{U}}_\lambda \leq y|\mathcal{B}_\lambda^{\complement}) - \Phi(y)| \right] \\ &\leq \sup_{y\in\mathbb{R}} |\mathbf{P}(\tilde{\mathbf{U}}_\lambda \leq y|\mathcal{B}_\lambda) - \Phi(y)| + \mathbf{P}(\mathcal{B}_\lambda^{\complement}), \end{aligned}$$

where the last inequality comes from the fact that $\mathbf{P}(\mathcal{B}_\lambda)$ and $|\mathbf{P}(\tilde{\mathbf{U}}_\lambda \leq y|\mathcal{B}_\lambda^{\complement}) - \Phi(y)|$ are both bounded above by 1. So, the first expression on the right-hand side tends to 0 by Lemma 5.2.10, and the second term tends to 0 as $\lambda \to \infty$ by Lemma 5.2.3. □

Finally, we need a lemma that shows $\mathbf{U}_\lambda := \frac{\mathcal{L}_\lambda^1 - \mathbf{E}[\mathcal{L}_\lambda^1]}{\sqrt{\mathbf{Var}[\mathcal{L}_\lambda^1]}}$, the centred and rescaled version of $\mathcal{L}_\lambda^1$ unconditional on $\mathcal{B}_\lambda$, is in fact close to $\tilde{\mathbf{U}}_\lambda$ for large enough λ.

Lemma 5.2.12. *The random variables $\mathbf{U}_\lambda$ and $\tilde{\mathbf{U}}_\lambda$ satisfy $\mathbf{U}_\lambda = (1 + u_\lambda)\ \tilde{\mathbf{U}}_\lambda + v_\lambda$, where*

$$u_\lambda := \frac{\sqrt{\mathbf{Var}[\mathcal{L}_\lambda^1|\mathcal{B}_\lambda]} - \sqrt{\mathbf{Var}[\mathcal{L}_\lambda^1]}}{\sqrt{\mathbf{Var}[\mathcal{L}_\lambda^1]}} = O\left(\lambda^{-3}\right),$$

and

$$v_\lambda := \frac{\mathbf{E}[\mathcal{L}_\lambda^1|\mathcal{B}_\lambda] - \mathbf{E}[\mathcal{L}_\lambda^1]}{\sqrt{\mathbf{Var}[\mathcal{L}_\lambda^1]}} = O\left(\lambda^{-4}\right).$$

Proof. We are going to write $\tilde{\mathbf{U}}_\lambda$ in terms of $\mathbf{U}_\lambda$. From Proposition 5.2.8, we have $\mathbf{Var}(\mathcal{L}_\lambda^{\mathbf{1}}) \geq \boldsymbol{q} > 0$, then

$$\begin{aligned}
\mathbf{U}_\lambda = \frac{\mathcal{L}_\lambda^1 - \mathbf{E}[\mathcal{L}_\lambda^1]}{\sqrt{\mathbf{Var}[\mathcal{L}_\lambda^1]}} &= \frac{\mathcal{L}_\lambda^1 - \mathbf{E}[\mathcal{L}_\lambda^1|\mathcal{B}_\lambda] + \mathbf{E}[\mathcal{L}_\lambda^1|\mathcal{B}_\lambda] - \mathbf{E}[\mathcal{L}_\lambda^1]}{\sqrt{\mathbf{Var}[\mathcal{L}_\lambda^1]}}, \quad \text{by Lemma 5.2.9} \\
&= \frac{\mathcal{L}_\lambda^1 - \mathbf{E}[\mathcal{L}_\lambda^1|\mathcal{B}_\lambda]}{\sqrt{\mathbf{Var}[\mathcal{L}_\lambda^1]}} + O\left(\lambda^{-4}\right) \\
&= \frac{\sqrt{\mathbf{Var}[\mathcal{L}_\lambda^1|\mathcal{B}_\lambda]}}{\sqrt{\mathbf{Var}[\mathcal{L}_\lambda^1]}} \left(\frac{\mathcal{L}_\lambda^1 - \mathbf{E}[\mathcal{L}_\lambda^1|\mathcal{B}_\lambda]}{\sqrt{\mathbf{Var}[\mathcal{L}_\lambda^1|\mathcal{B}_\lambda]}} \right) + O\left(\lambda^{-4}\right), \quad \text{by Lemma 5.2.10} \\
&= \left[\frac{\sqrt{\mathbf{Var}[\mathcal{L}_\lambda^1]} + \sqrt{\mathbf{Var}[\mathcal{L}_\lambda^1|\mathcal{B}_\lambda]} - \sqrt{\mathbf{Var}[\mathcal{L}_\lambda^1]}}{\sqrt{\mathbf{Var}[\mathcal{L}_\lambda^1]}} \right] \tilde{\mathbf{U}}_\lambda + O\left(\lambda^{-4}\right) \\
&= \left(1 + O(\lambda^{-3})\right) \tilde{\mathbf{U}}_\lambda + O\left(\lambda^{-4}\right), \quad \text{by Lemma 5.2.9.}
\end{aligned}$$

□

We can now deliver the proof of the central limit theorem (CLTs). Here we have all the ingredients to establish the proof of Theorem 5.1.1.

Proof of Theorem 5.1.1.

Proof. We only present the argument for $y > 0$ since the result for $y < 0$ will follow the same process. Now we use the monotonicity of the cumulative distribution function (cdf), for that we use $\mathbf{P}(\mathbf{U}_\lambda \leq y) = \mathbf{P}\left((1 + u_\lambda)\tilde{\mathbf{U}}_\lambda + v_\lambda \leq y\right)$. Let $\epsilon > 0$ be a small enough constant. Suppose we choose λ sufficiently large enough such that $|u_\lambda| < \epsilon$ and $|v_\lambda| < \epsilon$, which is possible, since u_λ and v_λ tend to 0, as $\lambda \to \infty$. For $y > 0$, and for all small enough ϵ, we have $\frac{1}{1-\epsilon} \leq 1 + 2\epsilon$, hence

$$\begin{aligned}
\mathbf{P}(\mathbf{U}_\lambda \leq y) &= \mathbf{P}\left((1 + u_\lambda)\ \tilde{\mathbf{U}}_\lambda + v_\lambda \leq y\right) \\
&= \mathbf{P}\left((1 + u_\lambda)\ \tilde{\mathbf{U}}_\lambda \leq y - v_\lambda\right) \\
&\leq \mathbf{P}\left((1 + u_\lambda)\ \tilde{\mathbf{U}}_\lambda \leq y + \epsilon\right) \\
&= \mathbf{P}\left(\tilde{\mathbf{U}}_\lambda \leq \frac{y + \epsilon}{1 + u_\lambda}\right) \leq \mathbf{P}\left(\tilde{\mathbf{U}}_\lambda \leq \frac{y + \epsilon}{1 - \epsilon}\right) \leq \mathbf{P}\left(\tilde{\mathbf{U}}_\lambda \leq (1 + 2\epsilon)(y + \epsilon)\right).
\end{aligned}$$

Then,

$$\limsup_{\lambda \to \infty} \mathbf{P}(\mathbf{U}_\lambda \leq y) \leq \lim_{\lambda \to \infty} \mathbf{P}\left(\tilde{\mathbf{U}}_\lambda \leq (1 + 2\epsilon)(y + \epsilon)\right) = \Phi\left((1 + 2\epsilon)(y + \epsilon)\right),$$

and by continuity normal cumulative distribution function, we have

$$\lim_{\epsilon \to 0} \Phi\left((1+2\epsilon)(y+\epsilon)\right) = \Phi(y).$$

Therefore, $\limsup_{\lambda\to\infty} \mathbf{P}(\mathbf{U}_\lambda \leq y) \leq \Phi(y)$.

Next, we do the other direction lim inf, so for $(y > 0)$, we have

$$\begin{aligned}\mathbf{P}(\mathbf{U}_\lambda \leq y) = \mathbf{P}\left((1+u_\lambda)\ \tilde{\mathbf{U}}_\lambda + v_\lambda \leq y\right) &\geq \mathbf{P}\left((1+u_\lambda)\ \tilde{\mathbf{U}}_\lambda \leq y-\epsilon\right) \\ &\geq \mathbf{P}\left(\tilde{\mathbf{U}}_\lambda \leq \frac{y-\epsilon}{1+\epsilon}\right) \\ &\geq \mathbf{P}\left(\tilde{\mathbf{U}}_\lambda \leq (1-2\epsilon)(y-\epsilon)\right),\end{aligned}$$

where here we use that $\frac{1}{1+\epsilon} \geq 1-2\epsilon$ and $y-\epsilon > 0$ for all small enough $\epsilon > 0$. Then,

$$\liminf_{\lambda\to\infty} \mathbf{P}(\mathbf{U}_\lambda \leq y) \geq \lim_{\lambda\to\infty} \mathbf{P}\left(\tilde{\mathbf{U}}_\lambda \leq (1-2\epsilon)(y-\epsilon)\right) = \Phi\left((1-2\epsilon)(y-\epsilon)\right),$$

and again by the continuity normal cdf, we have

$$\liminf_{\lambda\to\infty} \mathbf{P}(\mathbf{U}_\lambda \leq y) \geq \lim_{\epsilon\to 0} \Phi\left((1-2\epsilon)(y-\epsilon)\right) = \Phi(y).$$

Together, the bounds on the lim sup and lim inf yield

$$\Phi(y) \leq \liminf_{\lambda\to\infty} \mathbf{P}(\mathbf{U}_\lambda \leq y) \leq \limsup_{\lambda\to\infty} \mathbf{P}(\mathbf{U}_\lambda \leq y) \leq \Phi(y).$$

Thus, $\lim_{\lambda\to\infty} \mathbf{P}(\mathbf{U}_\lambda \leq y) = \Phi(y)$. □

5.3 Convergence of Variance

In this section, we will use the methodology of stabilization to prove the convergence of variance (Theorem 5.1.2), which we present in the following subsections.

5.3.1 Stabilization

The recent proof the concept of stabilizing functionals of point sets is playing a valuable role in constructing the fundamental methods for developing limit theorems for functionals of random point sets in $\mathbb{R}^2$. To be specific, the general results of central limit theorems and laws of large numbers for stabilizing functionals were provided

by Penrose and Yukich [33]. One could employ the results in reference [33] to derive the central limit theorem (as given earlier in this chapter) for edges in the bulk of the unit square for the minimal directed spanning forest (MDSF). Penrose and Yukich [27, 30, 33] conducted several works to enhance the stabilization technique to provide fundamental geometric probability results. Some considered laws of large numbers, see e.g., Penrose and Yukich [34] and central limit theorems [33, 36] that applied to a broad range of stabilizing functionals, including minimal spanning tree, nearest-neighbour graph, percolation, and Boolean models. The latest results on stabilization considered convergence of random measures in geometrical probability; see, for example, [28, 29, 35], and among others.

Here we state our notations and definitions to establish the proof of Theorem 5.1.2. We define Ω_λ, $\lambda > 0$, to be a family of subsets of $[0,1]^2$. There are two cases associated with Ω_λ such that:

1. (θ, ϕ) is unaligned, when we take $\Omega_\lambda \equiv [0,1]^2$ for all λ, and

2. (θ, ϕ) is singly-aligned, when we take $\Omega_\lambda = [0,1] \times [\alpha_\lambda, 1]$, where $\alpha_\lambda \in (0,1)$ is any sequence such that $\alpha_\lambda \sqrt{\lambda} \geq 2$ for all λ, and $\lim_{\lambda \to \infty} \alpha_\lambda = 0$ and $\alpha_\lambda > \sqrt{\frac{c \log \lambda}{\lambda}}$ for large enough λ, where $c > c_0$ is large enough.

The latter cone cases includes the sequence $\alpha_\lambda = RS$ and then $\Omega_\lambda = \mathcal{R}_\lambda^1$, because for $S = 1/k_\lambda$ with $k_\lambda = \left\lfloor \frac{1}{a_\lambda} \right\rfloor$, we have $Ra_\lambda \leq \alpha_\lambda = RS = \frac{R}{\left\lfloor \frac{1}{a_\lambda} \right\rfloor} \leq \frac{R}{\frac{1}{a_\lambda} - 1} = \frac{Ra_\lambda}{1 - a_\lambda} \leq 2Ra_\lambda$, meaning α_λ and a_λ exhibit the same asymptotic behaviour.

Recall that from Definition 3.2.1, we have $\mathcal{D}_{\theta,\phi}(\boldsymbol{x}; \mathcal{X})$ is the distance from point $\boldsymbol{x}$ to its nearest neighbour in $\mathcal{X} \cap C_{\theta,\phi}(\boldsymbol{x})$, where $\mathcal{X}$ is locally finite set of points. Recall by the Definition 3.1.2 that $C_{\theta,\phi}(\boldsymbol{x})$ is a cone with apex at $\boldsymbol{x}$ formed as a union of rays from $\boldsymbol{x}$ with angle $\alpha \in [\theta, \theta + \phi]$, measured anticlockwise from the vertical direction.

Definition 5.3.1. For $\boldsymbol{x} \in \mathbb{R}^2$ and $\mathcal{X} \subseteq \mathbb{R}^2$ a locally finite set, let $\xi(\boldsymbol{x}; \mathcal{X})$ be the distance from point $\boldsymbol{x}$ to its nearest neighbour in $\mathcal{X} \cap C_{\theta,\phi}(\boldsymbol{x})$, i.e.,

$$\xi(\boldsymbol{x}; \mathcal{X}) := \mathcal{D}_{\theta,\phi}(\boldsymbol{x}; \mathcal{X} \cup \{\boldsymbol{x}\}). \tag{5.3.1}$$

Note that ξ is *homogeneous*, meaning that

$$\xi(s\boldsymbol{x}; s\mathcal{X}) = s\xi(\boldsymbol{x}; \mathcal{X}), \quad \text{for all } s > 0;$$

this follows from the fact that the norm is homogeneous. Moreover, ξ is *translation-invariant*, meaning that

$$\xi(\boldsymbol{x}; \mathcal{X}) = \xi(\boldsymbol{y} + \boldsymbol{x}, \boldsymbol{y} + \mathcal{X}), \quad \text{for all } \boldsymbol{y} \in \mathbb{R}^2.$$

We define a re-scaled version of ξ as follows.

Definition 5.3.2. Let $\boldsymbol{x} \in \Omega_\lambda$, then for $\lambda > 0$, we define

$$\xi_\lambda(\boldsymbol{x}; \mathcal{X}) := \xi(\lambda^{\frac{1}{2}}\boldsymbol{x}; \lambda^{\frac{1}{2}}\mathcal{X})\mathbb{1}_{\Omega_\lambda}(\boldsymbol{x}) = \lambda^{\frac{1}{2}}\xi(\boldsymbol{x}; \mathcal{X})\mathbb{1}_{\Omega_\lambda}(\boldsymbol{x}) = \lambda^{\frac{1}{2}}\mathcal{D}_{\theta,\phi}(\boldsymbol{x}; \mathcal{X} \cup \{\boldsymbol{x}\})\mathbb{1}_{\Omega_\lambda}(\boldsymbol{x}),$$

where the first equality follows from the fact that $\xi(\boldsymbol{x}; \mathcal{X}) = \mathcal{D}_{\theta,\phi}(\boldsymbol{x}; \mathcal{X} \cup \{\boldsymbol{x}\})$ is homogeneous.

Remark 5.3.3. Note that, in both cases (unaligned, or singly-aligned for the appropriate choice of α_λ), we have

$$\mathcal{L}^1_\lambda = \sum_{\boldsymbol{x} \in \mathcal{P}_\lambda \cap \Omega_\lambda} \mathcal{D}_{\theta,\phi}(\boldsymbol{x}; \mathcal{P}_\lambda) = \lambda^{-\frac{1}{2}} \sum_{\boldsymbol{x} \in \mathcal{P}_\lambda} \xi_\lambda(\boldsymbol{x}; \mathcal{P}_\lambda).$$

5.3.2 Radius of Stabilization in MDSF

Now we introduce some notations and definitions of the radius of stabilization which some adapted from [29]. We employ the concept of stabilization with respect to ξ. Recall that $\|\cdot\|$ is the Euclidean norm on $\mathbb{R}^2$. For $r > 0$ and $\boldsymbol{x} \in \mathbb{R}^2$, let $B_r(\boldsymbol{x})$ denotes the Euclidean ball centered at $\boldsymbol{x}$ with radius r, in other words, $B_r(\boldsymbol{x}) = \{\boldsymbol{y} \in \mathbb{R}^2 : \|\boldsymbol{y} - \boldsymbol{x}\| \leq r\}$. Recall that we define $\mathcal{X}$ as a locally finite set of points in $\mathbb{R}^2$.

Definition 5.3.4. The radius of stabilization of ξ at $\boldsymbol{x} \in \mathbb{R}^2$ with respect to the point set $\mathcal{X} \subseteq \mathbb{R}^2$ and subset $A \subseteq \mathbb{R}^2$ is defined to be the smallest $r \in \mathbb{Z}_+$, such that

$$\xi(\boldsymbol{x}; \mathcal{X} \cap B_r(\boldsymbol{x})) = \xi(\boldsymbol{x}; (\mathcal{X} \cap B_r(\boldsymbol{x})) \cup \mathcal{Y}), \quad \text{for all finite} \quad \mathcal{Y} \subseteq A \setminus B_r(\boldsymbol{x}). \tag{5.3.2}$$

We write $R(\boldsymbol{x}; \mathcal{X}, A)$ for this smallest r; if no such r exists, set $R(\boldsymbol{x}; \mathcal{X}, A) = \infty$.

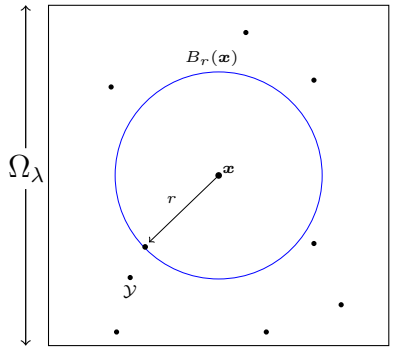

Figure 5.3: If one adds additional points farther away from the nearest-neighbour, that does not change the value of the function ξ, i.e., for all finite set $\mathcal{Y} \in \mathbb{R}^2$ that $\mathcal{Y} \subseteq \mathbb{R}^2 \setminus B_r(\boldsymbol{x})$.

Note that Definition 5.3.4 applies for any functional ξ, but we are exclusively concerned with $\xi(\boldsymbol{x}; \mathcal{X}) = \mathcal{D}_{\theta,\phi}(\boldsymbol{x}; \mathcal{X} \cup \{\boldsymbol{x}\})$. In what follows, $R(\boldsymbol{x}; \mathcal{X}, A)$ will always be the radius of stabilization of $\xi(\boldsymbol{x}; \mathcal{X}) = \mathcal{D}_{\theta,\phi}(\boldsymbol{x}; \mathcal{X} \cup \{\boldsymbol{x}\})$.

Definition 5.3.5. For $\boldsymbol{x} \in [0,1]^2$, we define the random variable $R_\lambda(\boldsymbol{x})$ by

$$R_\lambda(\boldsymbol{x}) = R(\lambda^{\frac{1}{2}}\boldsymbol{x}; \lambda^{\frac{1}{2}}\mathcal{P}_\lambda, \lambda^{\frac{1}{2}}[0,1]^2),$$

where $R(\boldsymbol{x}; \mathcal{X}, A)$ is the radius of stabilization for ξ at $\boldsymbol{x}$ with respect to $\mathcal{X}$, A (see Definition 5.3.4).

Definition 5.3.6. For all $\boldsymbol{x}, \boldsymbol{y} \in [0,1]^2$, we define

$$\nu_{\theta,\phi}(\boldsymbol{x}) := \sup\{\|\boldsymbol{x} - \boldsymbol{y}\| : \boldsymbol{y} \in C_{\theta,\phi}(\boldsymbol{x}) \cap [0,1]^2\}.$$

Note that $\xi(\boldsymbol{x}; \mathcal{X}) \leq \nu_{\theta,\phi}(\boldsymbol{x})$ for all $\boldsymbol{x} \in [0,1]^2$ and $\mathcal{X} \subseteq [0,1]^2$.

Definitions 5.3.4 – 5.3.6 immediately yield the following properties for $R(\boldsymbol{x}; \mathcal{X})$ and $R_\lambda(\boldsymbol{x})$.

Lemma 5.3.7. *For ξ the functional defined in Definition 5.3.1, and for all locally finite $\mathcal{X} \subseteq \mathbb{R}^2$ and all $\boldsymbol{x} \in \mathbb{R}^2$, the radius of stabilization for ξ is given by*

$$R(\boldsymbol{x};\mathcal{X}) = \begin{cases} \lceil \mathcal{D}_{\theta,\phi}(\boldsymbol{x};\mathcal{X}\cup\{\boldsymbol{x}\})\rceil & \text{if } \mathcal{D}_{\theta,\phi}(\boldsymbol{x};\mathcal{X}\cup\{\boldsymbol{x}\})>0, \\ \infty & \text{if } \mathcal{D}_{\theta,\phi}(\boldsymbol{x};\mathcal{X}\cup\{\boldsymbol{x}\})=0. \end{cases}$$

For all $\boldsymbol{x}\in[0,1]^2$, the random variable $R_\lambda(\boldsymbol{x})$ satisfies

$$R_\lambda(\boldsymbol{x}) \begin{cases} = \lceil \lambda^{\frac{1}{2}}\xi(\boldsymbol{x};\mathcal{P}_\lambda)\rceil & \text{if } \xi(\boldsymbol{x};\mathcal{P}_\lambda)>0, \\ \leq \lceil \lambda^{\frac{1}{2}}\nu_{\theta,\phi}(\boldsymbol{x})\rceil & \text{if } \xi(\boldsymbol{x};\mathcal{P}_\lambda)=0. \end{cases}$$

The following monotonicity property for R will be useful.

Lemma 5.3.8. *For all $A\subseteq\mathbb{R}^2$, all locally finite $\mathcal{X}\subseteq A$, and all $\boldsymbol{x},\boldsymbol{y}\in A$, the following inequality holds.*

$$R(\boldsymbol{x};\mathcal{X},A)\geq R(\boldsymbol{x};\mathcal{X}\cup\{\boldsymbol{y}\},A).$$

Proof. Fix $\boldsymbol{x},\boldsymbol{y}\in\mathbb{R}^2$ and $\mathcal{X}\subseteq\mathbb{R}^2$. We show that for each $r\geq 0$ if condition (5.3.2) (from Definition 5.3.4) holds for the set $\mathcal{X}$, then it also holds for the set $\mathcal{X}\cup\{\boldsymbol{y}\}$. Suppose (5.3.2) holds, $\mathcal{X}$ with $\xi(\boldsymbol{x};\mathcal{X}\cap B_r(\boldsymbol{x}))=0$. This requires that $((\mathcal{X}\cap B_r(\boldsymbol{x}))\cup\mathcal{Y})\cap C_{\theta,\phi}(\boldsymbol{x})=\emptyset$ for all $\mathcal{Y}\subseteq A\setminus B_r(\boldsymbol{x})$, then

$$\xi(\boldsymbol{x};((\mathcal{X}\cup\{\boldsymbol{y}\})\cap B_r(\boldsymbol{x}))\cup\mathcal{Y})=\xi(\boldsymbol{x};(\mathcal{X}\cup\{\boldsymbol{y}\})\cap B_r(\boldsymbol{x}))=\xi(\boldsymbol{x};(\mathcal{X}\cup\{\boldsymbol{y}\})\cap B_r(\boldsymbol{x})),$$

for all finite $\mathcal{Y}\subseteq A\setminus B_r(\boldsymbol{x})$.

Now, $\xi(\boldsymbol{x};\mathcal{X}\cap B_r(\boldsymbol{x}))>0$, so there is a nearest neighbour of $\boldsymbol{x}$ in $\boldsymbol{x}\cap B_r(\boldsymbol{x})$ of distance at most r, hence there also is a nearest neighbour of $\boldsymbol{x}$ in $(\mathcal{X}\cup\{\boldsymbol{y}\})\cap B_r(\boldsymbol{x})$ of distance at most r. Then for all $\mathcal{Y}\subseteq A\setminus B_r(\boldsymbol{x})$, the nearest neighbour of $\boldsymbol{x}$ is in $((\mathcal{X}\cup\{\boldsymbol{y}\})\cap B_r(\boldsymbol{x}))\cup\mathcal{Y}$ cannot be in $\mathcal{Y}$, so

$$\xi(\boldsymbol{x};(\mathcal{X}\cup\{\boldsymbol{y}\})\cap B_r(\boldsymbol{x}))\cup\mathcal{Y})=\xi(\boldsymbol{x};(\mathcal{X}\cup\{\boldsymbol{y}\})\cap B_r(\boldsymbol{x})),$$

in other words, (5.3.2) holds for $\mathcal{X}\cup\{\boldsymbol{y}\}$. Hence the infimum over r satisfying (5.3.2) for $\mathcal{X}\cup\{\boldsymbol{y}\}$ is less than or equal to infimum of r satisfying condition (5.3.2) for $\mathcal{X}$. □

The limit theorems associated with $\mathcal{L}^1_\lambda$ require some certain moments conditions on $\xi_\lambda(\boldsymbol{x};\mathcal{P}_\lambda)$. Recall by Definition 5.3.1 that $\xi(\boldsymbol{x};\mathcal{X})$ is the distance from point

$\boldsymbol{x}$ to its nearest neighbour in the locally finite set $\mathcal{X}$ in $[0,1]^2$. In the following lemma, we will show that the functional ξ satisfies the moment conditions for all types of general cones. First, we need to evaluate the moments of the functional $\xi_\lambda(\boldsymbol{x};\mathcal{P}_\lambda)$, as indicated in Lemma 5.3.9 (a) (below). Additionally, we analyse the moments of the functional ξ in case where it's possible to include points located further away from the nearest neighbour without changing the value of the function, i.e., $\xi_\lambda(\boldsymbol{x};\mathcal{P}_\lambda\cup\{\boldsymbol{y}\})$, as demonstrated in Lemma 5.3.9 (b), e.g., see Figure 5.3. Lastly, we need to verify the tail bound for $R_\lambda(\boldsymbol{x})$, as detailed in Lemma 5.3.12 for singly-aligned and Lemma 5.3.16 for the unaligned cone.

Lemma 5.3.9. *For all $\lambda \geq 1$, $c > 0$, let $p > 0$. Provided that $2c_\phi c > p$, ξ satisfies the moment conditions*

(*a*) $\sup_{\lambda\geq 1}\sup_{\boldsymbol{x}\in\Omega_\lambda}\mathbf{E}[\xi_\lambda^p(\boldsymbol{x};\mathcal{P}_\lambda)] < \infty$,

(*b*) $\sup_{\lambda\geq 1}\sup_{\boldsymbol{x},\boldsymbol{y}\in\Omega_\lambda}\mathbf{E}[\xi_\lambda^p(\boldsymbol{x};\mathcal{P}_\lambda\cup\{\boldsymbol{y}\})] < \infty$.

Note since $\xi_\lambda(\boldsymbol{x};\mathcal{P}_\lambda) \leq R_\lambda(\boldsymbol{x})$ any bounds we obtain on the tail probability or moments of R_λ immediately apply to those of ξ_λ too. Also, if $\xi_\lambda(\boldsymbol{x};\mathcal{P}_\lambda) > 0$ we have $R_\lambda(\boldsymbol{x}) \leq \xi_\lambda(\boldsymbol{x};\mathcal{P}_\lambda) + 1$.

Remark 5.3.10. Lemma 5.3.9 doesn't hold for all p^{th} moments simultaneously, but for any p, we can find a big enough value of c, for which $2c_\phi c > p$ will be true, but not for all values of p at the same time. For example, if we want to be held, say $p = 100$, we can do this by choosing c large enough, but it might not be held for $p = 1000$ for the same c and so on.

Remark 5.3.11. In the terminology of Penrose (Definition 2.3 [29]) ξ is homogeneously stabilizing. Most of the work in checking Penrose's condition amounts to estimate on tails of $R(\boldsymbol{x};\lambda^{\frac{1}{2}}\mathcal{P}_\lambda)$ or equivalently of $\mathcal{D}_{\theta,\phi}(\boldsymbol{x};\lambda^{\frac{1}{2}}\mathcal{P}_\lambda)$.

Before proving that our choice of ξ satisfies the moments condition for Lemma 5.3.9, we need to introduce geometrical definitions and lemmas. To prove Lemma 5.3.9, it suffices to demonstrate that $\xi_\lambda^p(\boldsymbol{x};\mathcal{P}_\lambda) \leq R_\lambda(\boldsymbol{x})$ and $\xi_\lambda^p(\boldsymbol{x};\mathcal{P}_\lambda\cup\{\boldsymbol{y}\}) \leq R_\lambda(\boldsymbol{x})$.

To do this, we need to identify an upper bound on the random variable $R_\lambda(\boldsymbol{x})$. First, we identify for each $s > 0$ a region $A_{\theta,\phi}(\boldsymbol{x}, s)$ of cone $C_{\theta,\phi}(\boldsymbol{x})$ that is suitably large, so that $R_\lambda(\boldsymbol{x})$ is only bigger than s if the region $A_{\theta,\phi}(\boldsymbol{x}, s)$ does not contain any points of $\mathcal{P}_\lambda$. Then the lower bound on the area $|A_{\theta,\phi}(\boldsymbol{x}, s)|$ will determine an upper bound for $\mathbf{P}(R_\lambda(\boldsymbol{x}) \geq r)$. Lemmas 5.3.14 and 5.3.15 will determine the lower bound on the region $|A_{\theta,\phi}(\boldsymbol{x}, s)|$ for both singly-aligned cones. Following that, we will provide the proof of the upper bound for $\mathbf{P}(R_\lambda(\boldsymbol{x}) \geq r)$ for both singly-aligned cones. Second (unaligned-cone), Lemma 5.3.16 will determine an upper bound for $\mathbf{P}(R_\lambda(\boldsymbol{x}) \geq r)$ using Lemma 5.3.17 to provide the appropriate lower bound on the region $|A_{\theta,\phi}(\boldsymbol{x}, s)|$ and Lemma 5.3.18 in which $A_{\theta,\phi}(\boldsymbol{x}, s) = A_{\theta,\phi}(\boldsymbol{x}, \nu(\boldsymbol{x}))$ contains a sector with angle apex at $\boldsymbol{x}$ bounded below by ϵ and radius of length at most $\epsilon\nu(\boldsymbol{x})$. Finally, on page 88 we provide the proof of Lemma 5.3.9 since the proof relies on several auxiliary lemmas and definitions (as mentioned above) to determine the appropriate bound on the random variable $\mathbf{P}(R_\lambda(\boldsymbol{x}) \geq r)$ for all cases of the general cones associated with the unit square.

Here we will start with a result that holds for both singly-aligned cones, in other words, obtuse and acute case. Recall that for singly-aligned cone, $\Omega_\lambda = [0, 1] \times [\alpha_\lambda, 1]$, where $\alpha_\lambda = RS$ and then $\Omega_\lambda = \mathcal{R}^1_\lambda$, because for $S = 1/k_\lambda$ with $k_\lambda = \left\lfloor \frac{1}{a_\lambda} \right\rfloor$ and $Ra_\lambda \leq \alpha_\lambda \leq 2Ra_\lambda$. We will prove the next lemma starting with the obtuse and then acute case respectively.

Lemma 5.3.12. *Suppose $\boldsymbol{x} \in \mathbb{R}^2$, and $\lambda > 0$, the tail probability of $R_\lambda(\boldsymbol{x})$ is bounded, as follows*

$$\tau_\lambda(r) := \sup_{\boldsymbol{x} \in \Omega_\lambda} \mathbf{P}(R_\lambda(\boldsymbol{x}) \geq r) \leq \begin{cases} \exp\{-c_\phi r^2\}, & \text{if } 2 \leq r \leq \alpha_\lambda\sqrt{\lambda} \\ \exp\{-\lambda c_\phi \alpha_\lambda^2\}, & \text{if } \alpha_\lambda\sqrt{\lambda} \leq r \leq \sqrt{2\lambda} + 1 \\ 0, & \text{if } r > \sqrt{2\lambda} + 1 \end{cases} \tag{5.3.3}$$

where c_ϕ is a constant.

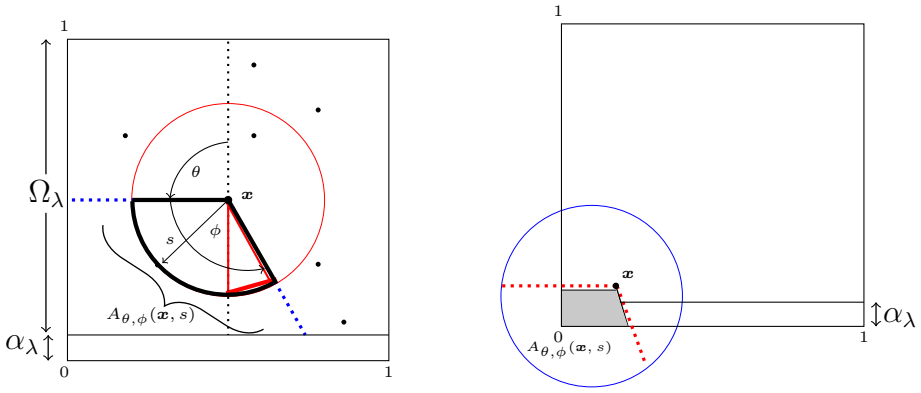

Figure 5.4: The set $A_{\theta,\phi}(\boldsymbol{x}, s)$ for different choices of $\boldsymbol{x}$ and s.

To prove Lemma 5.3.12, we give a geometrical definition and lemma, so that the lower bound on the area $|A_{\theta,\phi}(\boldsymbol{x}, s)|$ will determine an upper bound for $\mathbf{P}(R_\lambda(\boldsymbol{x}) \geq r)$. Recall $B_r(\boldsymbol{x})$ denotes the Euclidean ball centered at $\boldsymbol{x}$ with radius r, in other words, $B_r(\boldsymbol{x}) = \{\boldsymbol{y} \in \mathbb{R}^2 : \|\boldsymbol{y} - \boldsymbol{x}\| \leq r\}$. For any singly-aligned cone (obtuse or acute) the region $A_{\theta,\phi}(\boldsymbol{x}, s)$ is defined as follows.

Definition 5.3.13. Let $A_{\theta,\phi}(\boldsymbol{x}, s)$ be the region in $[0,1]^2$, such that

$$A_{\theta,\phi}(\boldsymbol{x}, s) = C_{\theta,\phi}(\boldsymbol{x}) \cap B_s(\boldsymbol{x}) \cap [0,1]^2.$$

For $\phi > \frac{\pi}{2}$, the lower bound on $|A_{\theta,\phi}(\boldsymbol{x}, s)|$ is uniform in $\boldsymbol{x} \in \Omega_\lambda$.

Lemma 5.3.14. *Suppose $\phi > \frac{\pi}{2}$. For all $\boldsymbol{x} \in \Omega_\lambda$ and for all $\lambda \geq 1$, there exists c_ϕ, such that*

$$\inf_{\boldsymbol{x} \in \Omega_\lambda} |A_{\theta,\phi}(\boldsymbol{x}, s)| \geq c_\phi (s \wedge \alpha_\lambda)^2, \quad \textit{for all} \quad s > 0.$$

Proof. We show $A_{\theta,\phi}(\boldsymbol{x}, s)$ always contains a sector with apex at $\boldsymbol{x}$, angle $\phi - \frac{\pi}{2}$, and radius $s \wedge \alpha_\lambda$.

- If $0 < s \leq \alpha_\lambda$, since $\boldsymbol{x} \in \Omega_\lambda$ we claim that the region $A_{\theta,\phi}(\boldsymbol{x}, s)$ will not cross the bottom boundary of $[0,1]^2$ (see Figure 5.4, *Left Panel*) and always we get at least a sector of radius s completely inside the unit square with angle $\phi - \frac{\pi}{2}$.

- If $s > \alpha_\lambda$, then $A_{\theta,\phi}(\boldsymbol{x}, s)$ contains $A_{\theta,\phi}(\boldsymbol{x}, \alpha_\lambda)$ and so the above argument shows that it contains the red sector of radius α_λ.

□

For $\phi < \frac{\pi}{2}$, we do not have a uniform lower bound, and instead we determine a bound in terms of the distance to the nearest boundary. For $\boldsymbol{x} = (x_1, x_2)$. Let $\ell(\boldsymbol{x}) = \min(x_1, x_2)$.

Lemma 5.3.15. *Suppose $\phi < \frac{\pi}{2}$. There exists c_ϕ, such that*

$$|A_{\theta,\phi}(\boldsymbol{x}, s)| \geq c_\phi (s \wedge \ell(\boldsymbol{x}))^2, \quad \textit{for all} \quad \boldsymbol{x} \in \Omega_\lambda.$$

Proof. If $s \leq \ell(\boldsymbol{x})$, $A_{\theta,\phi}(\boldsymbol{x}, s)$ equals the sector $C_{\theta,\phi}(\boldsymbol{x}) \cap B_s(\boldsymbol{x})$ which has area $c_\phi s^2$.

Otherwise, for $s > \ell(\boldsymbol{x})$, $A_{\theta,\phi}(\boldsymbol{x}, s)$ contains $A_{\theta,\phi}(\boldsymbol{x}, \ell(\boldsymbol{x}))$, so it has area $\geq c_\phi \ell(\boldsymbol{x})^2$. □

Now we can deliver the proof of Lemma 5.3.12 for first case of the singly-aligned cone, obtuse case.

Proof of Lemma 5.3.12 (Obtuse case)

Proof. Since $R_\lambda(\boldsymbol{x}) \leq \lceil \lambda^{\frac{1}{2}} \nu_{\theta,\phi}(\boldsymbol{x}) \rceil$ (by Lemma 5.3.7) and $\nu_{\theta,\phi}(\boldsymbol{x}) \leq \sqrt{2}$, we have $R_\lambda(\boldsymbol{x}) \leq \sqrt{2\lambda} + 1$. Therefore, $\mathbf{P}(R_\lambda(\boldsymbol{x}) \geq r) = 0$ for $r > \sqrt{2\lambda} + 1$.

For any $\boldsymbol{x} \in \Omega_\lambda$ and by the fact that (if $A \subseteq B$ then $\mathbf{P}(A) \leq \mathbf{P}(B)$), then

$$\mathbf{P}(R_\lambda(\boldsymbol{x}) \geq r) \leq \mathbf{P}(\mathcal{P}_\lambda \cap A_{\theta,\phi}(\boldsymbol{x}, \lambda^{-\frac{1}{2}} r) = \emptyset) = \exp\{-\lambda |A_{\theta,\phi}(\boldsymbol{x}, \lambda^{-\frac{1}{2}} r)|\}. \quad (5.3.4)$$

Using Lemma 5.3.14 and inequality (5.3.4) and taking a supremum over $\boldsymbol{x} \in \Omega_\lambda$, gives

$$\begin{aligned} \sup_{\boldsymbol{x} \in \Omega_\lambda} \mathbf{P}(R_\lambda(\boldsymbol{x}) \geq r) \leq \sup_{\boldsymbol{x} \in \Omega_\lambda} \exp\{-\lambda |A_{\theta,\phi}(\boldsymbol{x}, \lambda^{-\frac{1}{2}} r)|\} &= \exp\{-\lambda \inf_{\boldsymbol{x} \in \Omega_\lambda} |A_{\theta,\phi}(\boldsymbol{x}, \lambda^{-\frac{1}{2}} r)|\} \\ &\leq \exp\{-\lambda c_\phi (\lambda^{-\frac{1}{2}} r \wedge \alpha_\lambda)^2\}. \end{aligned}$$

This upper bound matches that claimed in the statement for the cases $r < \alpha_\lambda \sqrt{\lambda}$ and $r > \alpha_\lambda \sqrt{\lambda}$. □

Now we deliver the proof of Lemma 5.3.12 for the second case of singly-aligned cone, acute case.

Proof of Lemma 5.3.12 (Acute case)

Proof. The inequality (5.3.4) holds for the acute case as well. Here, we have by Lemma 5.3.15 that

$$\mathbf{P}(A_{\theta,\phi}(\boldsymbol{x}, \lambda^{-\frac{1}{2}}r) \cap \mathcal{P}_\lambda = \emptyset) = \exp\{-\lambda |A_{\theta,\phi}(\boldsymbol{x}, \lambda^{-\frac{1}{2}}r)|\} \leq \exp\{-\lambda c_\phi(\lambda^{-\frac{1}{2}}r \wedge \ell(\boldsymbol{x}))^2\}.$$

The statement $\mathbf{P}(R_\lambda(\boldsymbol{x}) \geq r) = 0$ if $r > \nu_{(\theta,\phi)}(\boldsymbol{x})\sqrt{\lambda} + 1$ holds since $R_\lambda(\boldsymbol{x}) \leq \lceil \lambda^{\frac{1}{2}} \nu_{\theta,\phi}(\boldsymbol{x}) \rceil$, by Lemma 5.3.7.

The left-hand side of the inequality (5.3.4), yields

$$\mathbf{P}(R_\lambda(\boldsymbol{x}) \geq r) \leq \begin{cases} \exp\{-\lambda c_\phi(\lambda^{-\frac{1}{2}}r \wedge \ell(\boldsymbol{x}))^2\}, & \text{if } r \leq \nu_{(\theta,\phi)}(\boldsymbol{x})\sqrt{\lambda} + 1 \\ 0, & \text{if } r > \nu_{(\theta,\phi)}(\boldsymbol{x})\sqrt{\lambda} + 1. \end{cases} \tag{5.3.5}$$

Now consider the supremum of the right hand side of (5.3.5) over all $\boldsymbol{x} \in \Omega_\lambda$. If $r > \sqrt{2\lambda} + 1$, then $r > \nu_{\theta,\phi}(\boldsymbol{x})\sqrt{\lambda} + 1$ for all $\boldsymbol{x} \in \Omega_\lambda$, so $\sup_{\boldsymbol{x}\in\Omega_\lambda} \mathbf{P}(R_\lambda(\boldsymbol{x}) \geq r) = 0$.

Otherwise, for $r \leq \sqrt{2\lambda} + 1$, if $\nu_{\theta,\phi}(\boldsymbol{x})\sqrt{\lambda} + 1 < r$, then $\mathbf{P}(R_\lambda(\boldsymbol{x}) \geq r) = 0$, so taking the supremum over $\boldsymbol{x} \in \Omega_\lambda$, gives

$$\sup_{\boldsymbol{x}\in\Omega_\lambda} \mathbf{P}(R_\lambda(\boldsymbol{x}) \geq r) \leq \exp\{-\lambda \inf_{\boldsymbol{x}\in\Omega_\lambda : \nu_{\theta,\phi}(\boldsymbol{x})\sqrt{\lambda} \geq r-1} c_\phi(\lambda^{-\frac{1}{2}}r \wedge \ell(\boldsymbol{x}))^2\}.$$

But for $\boldsymbol{x} \in \Omega_\lambda$, if $\ell(\boldsymbol{x}) \leq \alpha_\lambda$ then $x_1 \leq \alpha_\lambda$ (since $x_2 \geq \alpha_\lambda$ for all $\boldsymbol{x} \in \Omega_\lambda$) and $\nu_{\theta,\phi}(\boldsymbol{x}) \leq \sec\phi \cdot \ell(\boldsymbol{x})$, i.e., $\ell(\boldsymbol{x}) \geq \cos\phi \cdot \nu_{\theta,\phi}(\boldsymbol{x})$ see Figure 5.5. Therefore the minimum of $\ell(\boldsymbol{x})$ over $\{\boldsymbol{x} \in \Omega_\lambda : \nu_{\theta,\phi}(\boldsymbol{x})\sqrt{\lambda} \geq r-1\}$ is at least $\alpha_\lambda \wedge \cos\phi \cdot \lambda^{-\frac{1}{2}}(r-1)$. So taking a supremum over $\boldsymbol{x} \in \Omega_\lambda$, gives

$$\begin{aligned} \sup_{\boldsymbol{x}\in\Omega_\lambda} \mathbf{P}(R_\lambda(\boldsymbol{x}) \geq r) &\leq \exp\{-\lambda c_\phi(\alpha_\lambda \wedge \lambda^{-\frac{1}{2}}r \wedge \cos\phi\lambda^{-\frac{1}{2}}(r-1))^2\} \\ &\leq \exp\{-\lambda c_\phi(\alpha_\lambda \wedge \cos\phi\lambda^{-\frac{1}{2}}(r-1))^2\}. \end{aligned}$$

For $r \geq 2$, we have

$$\alpha_\lambda \wedge \cos\phi\lambda^{-\frac{1}{2}}(r-1) \geq \alpha_\lambda \wedge \frac{\cos\phi}{2}\lambda^{-\frac{1}{2}}r \geq \frac{\cos\phi}{2}(\alpha_\lambda \wedge \lambda^{-\frac{1}{2}}r),$$

because $\frac{\cos\phi}{2} < 1$, hence

$$\sup_{\boldsymbol{x}\in\Omega_\lambda} \mathbf{P}(R_\lambda(\boldsymbol{x}) \geq r) \leq \exp\{-c_\phi(\lambda\alpha_\lambda^2 \wedge r^2)\}.$$

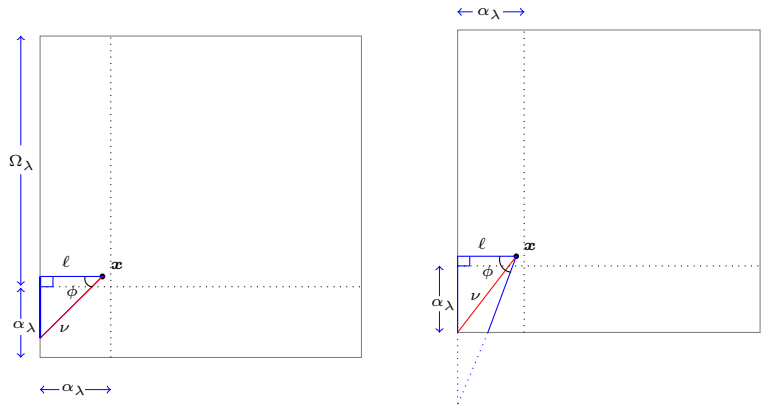

Figure 5.5: Acute angle in different regions in the square with considering the longest/shortest rays of the cone near the boundary.

□

Unaligned cone

Here we turn our attention to the unaligned cone where the cone has no rays aligned with a square. We will start by introducing the necessary notations and lemmas for our analysis. These notations and lemmas will be served for our subsequent discussions and proofs. Recall by Definition 5.3.13 that $A_{\theta,\phi}(\boldsymbol{x}, s)$ is a region in $[0,1]^2$, i.e., $A_{\theta,\phi}(\boldsymbol{x}, s) = C_{\theta,\phi}(\boldsymbol{x}) \cap B_s(\boldsymbol{x}) \cap [0,1]^2$, where $B_s(\boldsymbol{x})$ is the Euclidean ball centered at $\boldsymbol{x}$ with radius s. Recall by the Definition 5.3.6 that $\nu_{\theta,\phi}(\boldsymbol{x}) = \sup\{\|\boldsymbol{x}-\boldsymbol{y}\| : \boldsymbol{y} \in C_{\theta,\phi}(\boldsymbol{x}) \cap [0,1]^2\}$ for all $\boldsymbol{x}, \boldsymbol{y} \in [0,1]^2$. Recall from Lemma 5.3.7 we have, for all $\boldsymbol{x} \in \Omega_\lambda$ that $R_\lambda(\boldsymbol{x}) \leq \lceil \lambda^{\frac{1}{2}} \nu_{\theta,\phi}(\boldsymbol{x}) \rceil \leq \lambda^{\frac{1}{2}} \nu_{\theta,\phi}(\boldsymbol{x}) + 1$.

Lemma 5.3.16. *Let $\Omega_\lambda = [0,1]^2$. For all $\lambda > 0$, we have*

$$\tau_\lambda(r) := \sup_{\boldsymbol{x}\in\Omega_\lambda} \mathbf{P}(R_\lambda(\boldsymbol{x}) \geq r) \leq \begin{cases} \exp\{-c'_\phi r^2\}, & \text{if } 2 \leq r < \sqrt{2\lambda} + 1 \\ 0, & \text{if } r \geq \sqrt{2\lambda} + 1. \end{cases} \tag{5.3.6}$$

To prove 5.3.16, we require a lower bound for the region $A_{\theta,\phi}(\boldsymbol{x}, s)$, this lower bound will be provided in the following lemma.

Lemma 5.3.17. *(Unaligned case.) There exists $c_\phi > 0$, such that*

$$|A_{\theta,\phi}(\boldsymbol{x}, s)| \geq c_\phi (s \wedge \nu_{\theta,\phi}(\boldsymbol{x}))^2, \quad \textit{for all} \quad \boldsymbol{x} \in [0,1]^2$$

To prove this, we will need the following claim.

Lemma 5.3.18. *For θ, ϕ unaligned, $A_{\theta,\phi}(\boldsymbol{x}, \nu(\boldsymbol{x}))$ contains a sector with angle at $\boldsymbol{x}$ bounded below by ϵ and radius of length $\geq \epsilon\nu(\boldsymbol{x})$.*

Proof. Fix θ, ϕ (unaligned). Let $\boldsymbol{x} \in [0,1]^2$. By definition of $\nu_{\theta,\phi}(\boldsymbol{x})$ the ball $B_{\nu_{\theta,\phi}(\boldsymbol{x})}(\boldsymbol{x})$ contains $C_{\theta,\phi}(\boldsymbol{x}) \cap [0,1]^2$, so $A(\boldsymbol{x}) := A_{\theta,\phi}(\boldsymbol{x}, \nu_{\theta,\phi}(\boldsymbol{x})) = C_{\theta,\phi}(\boldsymbol{x}) \cap [0,1]^2$ and since $\boldsymbol{y} \mapsto \|\boldsymbol{x} - \boldsymbol{y}\|$ is convex, its maximum over $\boldsymbol{y} \in A(\boldsymbol{x})$ (equal to $\nu_{\theta,\phi}(\boldsymbol{x})$) is attained at an extreme point of the convex set $A(\boldsymbol{x})$, in other words either at a corner of $[0,1]^2$ or one of the two boundary points z_1, z_2 along the extreme rays of $C_{\theta,\phi}(\boldsymbol{x})$, (e.g., see [19] for maxima of convex functions).

For the unaligned case there are three situations we consider here, so either the cone contains one perpendicular ray, two perpendicular rays, or no perpendicular ray as detailed below.

In the case when cone contains one perpendicular ray the point $\boldsymbol{y} \in A(\boldsymbol{x})$ maximising $\|\boldsymbol{x} - \boldsymbol{y}\|$ is necessarily on the boundary orthogonal to and intersecting that ray. Hence the maximum $\nu_{\theta,\phi}(\boldsymbol{x})$ is attained at a point on H, the line containing this boundary and is therefore at most the maximum of the two distances $\|\boldsymbol{x} - v_1\|$ and $\|\boldsymbol{x} - v_2\|$ where v_1 & v_2 are the points of intersection between line H and the two extreme rays of $C_{\theta,\phi}(\boldsymbol{x})$. Write p_1 for the point of intersection of line H and the perpendicular ray in $C_{\theta,\phi}(\boldsymbol{x})$ and ϕ_1 and ϕ_2 for the two angles between extreme rays and the perpendicular ray (so that $\phi_1, \phi_2 > 0$ and $\phi = \phi_1 + \phi_2$). See Figures 5.6 – 5.8 for the possible cases (where $C_{\theta,\phi}(\boldsymbol{x})$ contains zero, one or two corners of $[0,1]^2$). For each $i = 1, 2$, we have $\|\boldsymbol{x} - p_1\| = \cos\phi_i \|\boldsymbol{x} - v_i\|$. So $\|\boldsymbol{x} - p_1\| \geq \epsilon \max\{\|\boldsymbol{x} - v_1\|, \|\boldsymbol{x} - v_2\|\}$, where $\epsilon = \min\{\cos\phi_1, \cos\phi_2\} > 0$ because

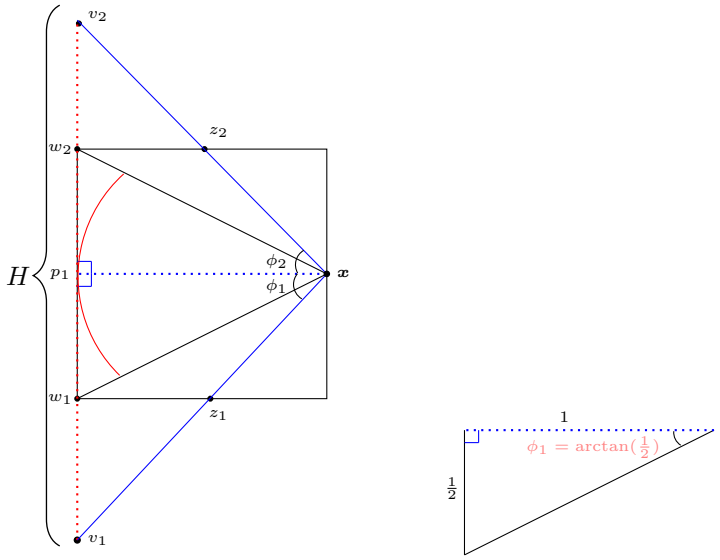

Figure 5.6: Cone contains one perpendicular ray, and the region $A(\boldsymbol{x})$ contains two corners in the square with angle $\geq 2\arctan(\frac{1}{2})$.

$\phi_i < \frac{\pi}{2}$ for each $i = 1, 2$. Since $\nu_{\theta,\phi}(\boldsymbol{x}) \leq \max\{\|\boldsymbol{x} - v_1\|, \|\boldsymbol{x} - v_2\|\}$ as argued earlier we have $\|\boldsymbol{x} - p_1\| \geq \epsilon\nu_{\theta,\phi}(\boldsymbol{x})$. Then $A(\boldsymbol{x})$ contains a sector with apex at $\boldsymbol{x}$ and angle at least the $\min\{\phi_1, \phi_2, 2\arctan(\frac{1}{2})\} > 0$, and radius at least $\epsilon\nu_{\theta,\phi}(\boldsymbol{x})$.

If cone contains two perpendicular rays. Then $\phi = \frac{\pi}{2} + \phi_1 + \phi_2$ for some positive ϕ_1, ϕ_2, e.g., see Figure 5.9. Now decompose $C_{\theta,\phi}(\boldsymbol{x})$ into $C_1(\boldsymbol{x}) \cup C_2(\boldsymbol{x})$ where $C_i(\boldsymbol{x})$ is a cone with angle $\frac{\pi}{4} + \phi_i$, (see Figure 5.9). Let $A(\boldsymbol{x}) = A_1(\boldsymbol{x}) \cup A_2(\boldsymbol{x})$ where $A_i(\boldsymbol{x}) = A(\boldsymbol{x}) \cap C_i(\boldsymbol{x})$ formed by bisecting $A(\boldsymbol{x})$ along the ray that bisects $C_{\theta,\phi}(\boldsymbol{x})$ into $C_1(\boldsymbol{x})$ and $C_2(\boldsymbol{x})$. Then $\nu_{\theta,\phi}(\boldsymbol{x}) = \max\{\nu_1(\boldsymbol{x}), \nu_2(\boldsymbol{x})\}$, where $\nu_i(\boldsymbol{x}) = \sup\{\|\boldsymbol{x} - \boldsymbol{y}\| : \boldsymbol{y} \in A_i(\boldsymbol{x})\}$. Now each cone $C_i(\boldsymbol{x})$ contains only one perpendicular ray, so repeating the previous argument shows that there are positive constants ϵ_1, ϵ_2 such that for each $i = 1, 2$, $A_i(\boldsymbol{x})$ contains a sector with apex at $\boldsymbol{x}$, angle at least ϵ_i and radius at least $\epsilon_i\nu_i(\boldsymbol{x})$. Therefore $A(\boldsymbol{x})$ contains sector with angle at least $\min\{\epsilon_1, \epsilon_2\}$ and radius at least $\min\{\epsilon_1, \epsilon_2\}\nu(\boldsymbol{x})$, e.g., see Figure 5.9.

Final case: if cone contains no perpendicular ray and $A(\boldsymbol{x})$ doesn't contain a corner of square, (see Figure 5.10) then $A(\boldsymbol{x})$ is a triangle. This triangle has angles ϕ, α, β where $0 < \phi < \frac{\pi}{2}$, $\frac{\pi}{2} < \alpha < \pi$, and $0 < \beta < \frac{\pi}{2}$, and the edges of the triangle incident to $\boldsymbol{x}$ have lengths $\nu(\boldsymbol{x})$ and $\ell(\boldsymbol{x}) = \frac{\sin\beta}{\sin\alpha}\nu(\boldsymbol{x})$. Since $\sin\alpha > \sin\beta > 0$, the

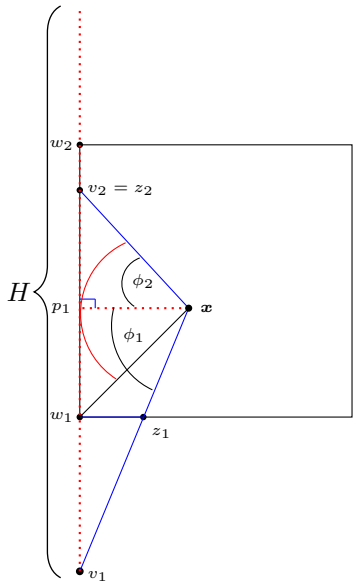

Figure 5.7: Cone contains one perpendicular ray and the region $A(\boldsymbol{x})$ contains a corner w of the square, and it has angles $\geq \min\{\phi_1, \phi_2\}$.

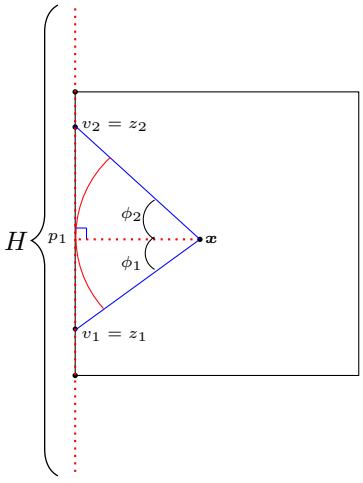

Figure 5.8: Cone contains one perpendicular ray and $A(\boldsymbol{x})$ contains no corner of the square, and it has angles $\phi_1 + \phi_2 \geq \min\{\phi_1, \phi_2\}$.

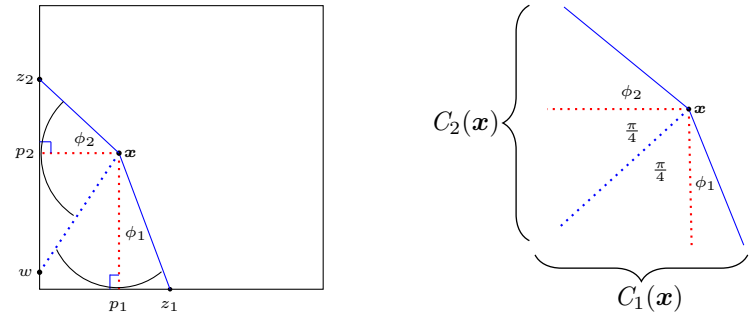

Figure 5.9: Cone contains two perpendicular rays and $A(\boldsymbol{x})$ does not contain any corner of the square.

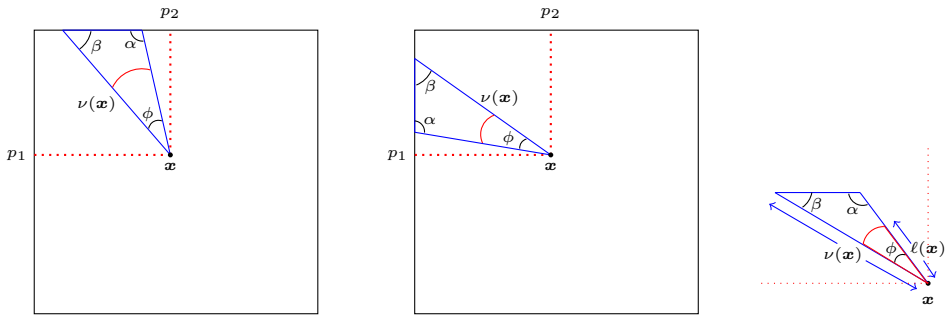

Figure 5.10: Cone does not contain any perpendicular rays and no corner in the square.

constant $\epsilon = \frac{\sin\beta}{\sin\alpha}$ satisfies $0 < \epsilon < 1$. Hence $A(\boldsymbol{x})$ contains a sector of angle $\phi > 0$ and radius at least $\epsilon\nu(\boldsymbol{x})$.

If $A(\boldsymbol{x})$ contains a corner of the square (see Figure 5.11) then $A(\boldsymbol{x})$ is the union $A_1(\boldsymbol{x}) \cup A_2(\boldsymbol{x})$ of two triangles each with a vertex at $\boldsymbol{x}$ and angle ϕ_i where $\phi_1 + \phi_2 = \phi$. Note that $\nu_i(\boldsymbol{x}) = \sup\{\|\boldsymbol{y} - \boldsymbol{x}\| : \boldsymbol{y} \in A_i(\boldsymbol{x})\}$ is equal to $\nu(\boldsymbol{x})$ for each $i = 1, 2$. Without loss of generality, suppose $\phi_1 \geq \phi_2$, so $\phi_1 \geq \frac{1}{2}\phi > 0$ and $\phi_1 \leq \phi < \frac{\pi}{2}$. Since $A_1(\boldsymbol{x})$ is a triangle, using the argument above shows that $A_1(\boldsymbol{x})$ contains a sector with apex at $\boldsymbol{x}$, angle $\geq \epsilon$, and radius $\geq \epsilon\nu_1(\boldsymbol{x}) = \epsilon\nu(\boldsymbol{x})$. □

Now we will apply Lemma 5.3.18 to establish the lower bound which we are interested in given by Lemma 5.3.17.

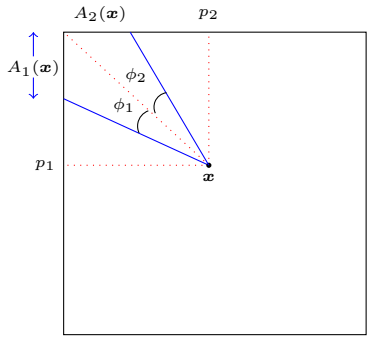

Figure 5.11: Cone doesn't include any perpendicular rays and $A(\boldsymbol{x})$ contains a corner in the square.

Proof of Lemma 5.3.17

Proof. By the claim $A_{\theta,\phi}(\boldsymbol{x}, \nu(\boldsymbol{x}))$ contains a sector with angle at least ϵ and radius of length $\geq \epsilon\nu(\boldsymbol{x})$.

If $s > \epsilon\nu(\boldsymbol{x})$, then $A_{\theta,\phi}(\boldsymbol{x}, s) = A_{\theta,\phi}(\boldsymbol{x}, \nu(\boldsymbol{x})) \cap B_s(\boldsymbol{x})$ (by definition of $\nu_{\theta,\phi}$ that $A_{\theta,\phi}(\boldsymbol{x}, \nu) = C_{\theta,\phi}(\boldsymbol{x}) \cap [0,1]^2$) contains a sector of angle at least ϵ and radius at least $\epsilon\nu(\boldsymbol{x})$, hence

$$|A_{\theta,\phi}(\boldsymbol{x}, s)| \geq \frac{1}{2}\epsilon(\epsilon\nu(\boldsymbol{x}))^2 \geq \frac{1}{2}\epsilon^3(s \wedge \nu(\boldsymbol{x}))^2.$$

Otherwise, if $s \leq \epsilon\nu(\boldsymbol{x})$, then $A_{\theta,\phi}(\boldsymbol{x}, s) = A_{\theta,\phi}(\boldsymbol{x}, \nu(\boldsymbol{x})) \cap B_s(\boldsymbol{x})$ contains a sector with angle $\geq \epsilon$ and radius $= s$, hence

$$|A_{\theta,\phi}(\boldsymbol{x}, s)| \geq \frac{1}{2}\epsilon s^2 \geq \frac{1}{2}\epsilon(s \wedge \nu(\boldsymbol{x}))^2.$$

Note that $B_s(\boldsymbol{x})$ contains a sector with angle $\geq \epsilon$ and radius s. □

Now we have all the ingredients to obtain the proof of Lemma 5.3.16 using the lemmas and claims mentioned earlier. Recall by Definition 5.3.13 that $A_{\theta,\phi}(\boldsymbol{x}, s)$ is a region in $[0,1]^2$, i.e., $A_{\theta,\phi}(\boldsymbol{x}, s) = C_{\theta,\phi}(\boldsymbol{x}) \cap B_s(\boldsymbol{x}) \cap [0,1]^2$ where $B_s(\boldsymbol{x})$ is the Euclidean ball centered at $\boldsymbol{x}$ with radius s, and recall by the Definition 3.1.2 that $C_{\theta,\phi}(\boldsymbol{x})$ is a cone with apex at $\boldsymbol{x}$ formed as a union of rays from $\boldsymbol{x}$ with angle $\alpha \in [\theta, \theta + \phi]$, measured anticlockwise from the vertical direction. Recall by the

Definition 5.3.6 that $\nu_{\theta,\phi}(\boldsymbol{x}) = \sup\{\|\boldsymbol{x}-\boldsymbol{y}\| : \boldsymbol{y} \in C_{\theta,\phi}(\boldsymbol{x}) \cap [0,1]^2\}$ for all $\boldsymbol{x}, \boldsymbol{y} \in [0,1]^2$.

Proof of Lemma 5.3.16

Proof. For all $\boldsymbol{x} \in \Omega_\lambda$ the inequality (5.3.4) for both singly-aligned cones holds for the unaligned cone. This implies,

$$\mathbf{P}(R_\lambda(\boldsymbol{x}) \geq r) \leq \begin{cases} \exp\{-\lambda|A_{\theta,\phi}(\boldsymbol{x}, \lambda^{-\frac{1}{2}}r)|\}, & \text{if } r \leq \lceil \lambda^{\frac{1}{2}}\nu(\boldsymbol{x})\rceil \\ 0, & \text{if } r > \lceil \lambda^{\frac{1}{2}}\nu(\boldsymbol{x})\rceil. \end{cases}$$

If $r > \sqrt{2\lambda}+1$, then $\lceil \lambda^{\frac{1}{2}}\nu(\boldsymbol{x})\rceil \leq \lceil\sqrt{2\lambda}\rceil < r$ for all $\boldsymbol{x} \in \Omega_\lambda$, so $\mathbf{P}(R_\lambda(\boldsymbol{x}) \geq r) = 0$ for all $\boldsymbol{x} \in \Omega_\lambda$. Therefore, $\sup_{\boldsymbol{x}\in\Omega_\lambda} \mathbf{P}(R_\lambda(\boldsymbol{x}) \geq r) = 0$.

Otherwise,

$$\begin{aligned} \sup_{\boldsymbol{x}\in\Omega_\lambda} \mathbf{P}(R_\lambda(\boldsymbol{x}) \geq r) &= \sup_{\boldsymbol{x}\in\Omega_\lambda : \lambda^{\frac{1}{2}}\nu(\boldsymbol{x}) \geq r-1} \mathbf{P}(R_\lambda(\boldsymbol{x}) \geq r) \\ &\overset{\text{by (5.3.4)}}{\leq} \sup_{\boldsymbol{x}\in\Omega_\lambda : \lambda^{\frac{1}{2}}\nu(\boldsymbol{x}) \geq r-1} \exp\{-\lambda c_\phi(\lambda^{-\frac{1}{2}}r \wedge \nu(\boldsymbol{x}))^2\}, \text{ by Lemma 5.3.17} \\ &\leq \exp\{-\lambda c_\phi(\lambda^{-\frac{1}{2}}(r-1))^2\} \leq \exp\{-c'_\phi r^2\}, \quad \text{for } r \geq 2. \end{aligned}$$

□

Now we use the above lemmas and definitions to state the proof of Lemma 5.3.9. Our aim is to show $2c_\phi c > p$ with ξ satisfies the moment conditions. Recall by the Definition 5.3.5 that $R_\lambda(\boldsymbol{x}) = R(\lambda^{\frac{1}{2}}\boldsymbol{x}; \lambda^{\frac{1}{2}}\mathcal{P}_\lambda, \lambda^{\frac{1}{2}}[0,1]^2)$ for $\boldsymbol{x} \in \mathbb{R}^2$, where $R(\boldsymbol{x}; \mathcal{X}, A)$ is a radius of stabilization for ξ at $\boldsymbol{x}$ with respect to $\mathcal{X}$ and A. Also, recall from Definition 5.3.1 that $\xi(\boldsymbol{x}; \mathcal{X})$ is the distance from point $\boldsymbol{x}$ to its nearest neighbour in $\mathcal{X} \cap C_{\theta,\phi}(\boldsymbol{x})$, such that $\xi(\boldsymbol{x}; \mathcal{X}) = \mathcal{D}_{\theta,\phi}(\boldsymbol{x}; \mathcal{X} \cup \{\boldsymbol{x}\})$.

Proof of Lemma 5.3.9

Proof. For all $\boldsymbol{x} \in \Omega_\lambda$ and for all $\lambda \geq 1$, we have

$$\xi_\lambda(\boldsymbol{x}; \mathcal{P}_\lambda\}) = \lambda^{\frac{1}{2}}\xi(\boldsymbol{x}; \mathcal{P}_\lambda) \leq \lceil \lambda^{\frac{1}{2}}\xi(\boldsymbol{x}; \mathcal{P}_\lambda)\rceil \leq R_\lambda(\boldsymbol{x}).$$

Also, we have for all $\boldsymbol{x} \in \Omega_\lambda$ and $\lambda \geq 1$, that

$$\begin{aligned}\xi_\lambda(\boldsymbol{x}; \mathcal{P}_\lambda \cup \{\boldsymbol{y}\}) \leq \lceil \lambda^{\frac{1}{2}} \xi(\boldsymbol{x}; \mathcal{P}_\lambda \cup \{\boldsymbol{y}\}) \rceil &\leq R(\lambda^{\frac{1}{2}}\boldsymbol{x}; \lambda^{\frac{1}{2}}(\mathcal{P}_\lambda \cup \{\boldsymbol{y}\}), [0, \lambda^{\frac{1}{2}}]^2) \\ &\leq R(\lambda^{\frac{1}{2}}\boldsymbol{x}; \lambda^{\frac{1}{2}}\mathcal{P}_\lambda, [0, \lambda^{\frac{1}{2}}]^2) = R_\lambda(\boldsymbol{x}).\end{aligned}$$

So to prove both statements (a) and (b) from Lemma 5.3.9, it suffices to prove that $\sup_{\lambda \geq 1} \sup_{\boldsymbol{x} \in \Omega_\lambda} \mathbf{E}[R_\lambda(\boldsymbol{x})^p] < \infty$.

For all $\boldsymbol{x} \in \Omega_\lambda$, the p^{th} moment of $R_\lambda(\boldsymbol{x})$ can be calculated using the tail-integral formula for expectation which is given, as follows

$$\mathbf{E}[R_\lambda(\boldsymbol{x})^p] = \int_0^\infty \mathbf{P}(R_\lambda(\boldsymbol{x})^p \geq s) ds \leq 2^p + \int_{2^p}^\infty \mathbf{P}(R_\lambda(\boldsymbol{x}) \geq s^{\frac{1}{p}}) ds. \tag{5.3.7}$$

We make change of variable in (5.3.7) by letting $\lambda^{\frac{1}{2}} r = s^{\frac{1}{p}}$, and $s = 2^p$ implies $r = 2\lambda^{-\frac{1}{2}}$. Use $\sqrt{2\lambda} + 1 < 3\sqrt{\lambda}$ for $\lambda \geq 1$, the right-hand-side of (5.3.7), becomes

$$\begin{aligned}\int_{2\lambda^{-\frac{1}{2}}}^\infty \mathbf{P}(R_\lambda(\boldsymbol{x}) \geq \lambda^{\frac{1}{2}} r) p\lambda^{\frac{p}{2}} r^{p-1} dr &\leq p\lambda^{\frac{p}{2}} \Big(\int_0^{\alpha_\lambda} \mathbf{P}(R_\lambda(\boldsymbol{x}) \geq \lambda^{\frac{1}{2}} r) r^{p-1} dr \\ &\quad + \int_{\alpha_\lambda}^3 \mathbf{P}(R_\lambda(\boldsymbol{x}) \geq \lambda^{\frac{1}{2}} r) r^{p-1} dr \\ &\quad + \int_3^\infty \mathbf{P}(R_\lambda(\boldsymbol{x}) \geq \lambda^{\frac{1}{2}} r) r^{p-1} dr \Big) \\ \leq p\lambda^{\frac{p}{2}} \left(\int_0^\infty \exp\{-\lambda c_\phi r^2\} r^{p-1} dr + \int_0^3 \exp\{-\lambda c_\phi \alpha_\lambda^2\} r^{p-1} dr \right) &+ 0, \text{ by Lemma 5.3.12.}\end{aligned} \tag{5.3.8}$$

We make another change of variable on this expression $\int_0^\infty \exp\{-\lambda c_\phi r^2\} r^{p-1} dr$, by setting $y = \lambda c_\phi r^2$ implies $dy = 2\lambda c_\phi r dr$ and $dr = \frac{dy}{2\lambda c_\phi r}$, where $r^2 = \frac{y}{\lambda c_\phi}$ implies that $r = (\frac{y}{\lambda c_\phi})^{\frac{1}{2}}$, then $r^{p-1} dr = \frac{r^{p-2} dy}{2\lambda c_\phi}$, which yields

$$p\lambda^{\frac{p}{2}} \int_0^\infty \exp\{-\lambda c_\phi r^2\} r^{p-1} dr = p\lambda^{\frac{p}{2}} \int_0^\infty \exp\{-y\} \left(\frac{y}{\lambda c_\phi} \right)^{\frac{p-2}{2}} \frac{1}{2\lambda c_\phi} dy = \frac{1}{2} p c_\phi^{-\frac{p}{2}} \Gamma\left(\frac{p}{2} \right),$$

by the integral definition $\int_0^\infty \exp\{-y\} y^{\frac{p}{2}-1} dy = \Gamma(\frac{p}{2})$.

Setting $C_p = \frac{1}{2} c_\phi^{-\frac{p}{2}} \Gamma(\frac{p}{2})$, the upper bound in (5.3.8), becomes

$$C_p + p\lambda^{\frac{p}{2}} \exp\{-\lambda c_\phi \alpha_\lambda^2\} \int_0^3 r^{p-1} dr = C_p + (9\lambda)^{\frac{p}{2}} \exp\{-\lambda c_\phi \alpha_\lambda^2\}. \tag{5.3.9}$$

Finally, we show that $(9\lambda)^{\frac{p}{2}} \exp\{-\lambda c_\phi \alpha_\lambda^2\} \to 0$ as $\lambda \to \infty$ for c big enough. To see this, observe that whatever value we choose for c, we have $\alpha_\lambda \to 0$, so $\alpha_\lambda < \frac{1}{2}$ for sufficiently large λ.

Hence,

$$\begin{aligned}(9\lambda)^{\frac{p}{2}} \exp\{-\lambda c_\phi \alpha_\lambda^2\} \leq (9\lambda)^{\frac{p}{2}} \exp\left\{-\lambda c_\phi \frac{c \log \lambda}{\lambda}\right\} &\leq (9\lambda)^{\frac{p}{2}} \exp\{-c_\phi c \log \lambda\} \\ &= (9\lambda)^{\frac{p}{2}} \exp\{\log \lambda^{-c_\phi c}\} \\ &= (9\lambda)^{\frac{p}{2}} \lambda^{-c_\phi c} \ \to 0 \text{ as } \lambda \to \infty,\end{aligned} \tag{5.3.10}$$

provided that $c_\phi c > \frac{p}{2}$, i.e., $c > \frac{p}{2c_\phi}$. Therefore,

$$\sup_{\lambda \geq 1} \sup_{\boldsymbol{x} \in \Omega_\lambda} \mathbf{E}[R_\lambda(\boldsymbol{x})^p] \leq C_p + \sup_{\lambda \geq 1}[(9\lambda)^{\frac{p}{2}} \exp\{-\lambda c_\phi \alpha_\lambda^2\}] < \infty.$$

as required. □

In the subsequent discussion, we focus on another condition known as the 'power-law stabilization' of the functional ξ at point $\boldsymbol{x}$. Instead of relying on moment conditions, we turn to tail-bounds. We introduce the following definition to elucidate the concept of the tail probability of the radius of stabilization.

Definition 5.3.19. For $s > 0$, and $\lambda \geq 1$, we have

$$\tau(s) := \sup_{\lambda \geq 1} \tau_\lambda(s),$$

where $\tau_\lambda(s) := \sup_{\boldsymbol{x} \in \Omega_\lambda} \mathbf{P}(R_\lambda(\boldsymbol{x}) \geq s)$.

Note that, in the singly-aligned cone, Lemma 5.3.12 gives the upper bound (5.3.3) for $\tau_\lambda(s)$. In the unaligned cone, Lemma 5.3.16 gives the upper bound (5.3.6) for $\tau_\lambda(s)$.

In the singly-aligned cone we prove the following condition on $\tau(s)$, which says that ξ is power-law stabilizing with power q.

Lemma 5.3.20. *(singly-aligned cone:) Let $q > 0$. If $2c_\phi c > q$, then*

$$\sup_{s \geq 1} s^q \tau(s) < \infty. \tag{5.3.11}$$

Proof. Take s fixed but sufficiently large so that for all λ satisfying $\sqrt{2\lambda}+1 \geq s$, we have $\alpha_\lambda > \sqrt{\frac{c\log\lambda}{\lambda}}$. The supremum of $\tau_\lambda(s)$ over $\lambda \geq 1$ is equal to the supremum over λ such that $\sqrt{2\lambda}+1 \geq s$ and for this range of λ, Lemma 5.3.12 gives

$$\begin{aligned}\tau_\lambda(s) \leq \exp(-c_\phi(s^2 \wedge \lambda\alpha_\lambda^2)) &\leq \exp(-c_\phi(s^2 \wedge c\log\lambda)) \\ &\leq \exp\left(-c_\phi\left(s^2 \wedge c\log\left(\frac{(s-1)^2}{2}\right)\right)\right).\end{aligned}$$

Hence, for large enough s,

$$\tau(s) = \sup_{\lambda\geq 1}\tau_\lambda(s) \leq \exp\left(-c_\phi \cdot c\log\left(\frac{(s-1)^2}{2}\right)\right) = 2^{c_\phi c}\cdot(s-1)^{-2c_\phi c} = o(s^{-q}), \tag{5.3.12}$$

implying $s^q\tau(s) \to 0$ as $s \to \infty$. □

Remark 5.3.21. In particular Lemma 5.3.20 shows that we may choose $c > c_0 > 0$ large enough such that (5.3.11) holds for $q = 304$, as will be required for verifying hypothesis of Theorem 5.3.23 below. Following [29], we say ξ is power-law of stabilizing of order $q = 304$.

Lemma 5.3.22. *(Unaligned cone:) For $s > 0$ and $\lambda \geq 1$, the following inequality holds.*

$$\tau(s) = \sup_{\lambda\geq 1}\tau_\lambda(s) \leq \exp\{-c'_\phi s^2\},$$

so $s^q\tau(s) \to 0$, for any $q > 0$.

We omit the proof of Lemma 5.3.22 which follows immediately from Lemma 5.3.16. Furthermore, it is established that Lemma 5.3.20 also holds for the unaligned cone.

5.3.3 Proof of Convergence of Variance

Now we have all the ingredients along with a combination of sufficient versions of Theorem 2.1 and Theorem 2.2 [29] to establish the proof of our main Theorem 5.1.2. Recall from Definition 4.5.2, that $\mathcal{L}^1_\lambda = \sum_{\boldsymbol{x}\in\mathcal{P}_\lambda\cap\mathcal{R}^1_\lambda}\mathcal{D}_{\theta,\phi}(\boldsymbol{x};\mathcal{P}_\lambda)$ where $\mathcal{D}_{\theta,\phi}(\boldsymbol{x};\mathcal{P}_\lambda)$ is the distance from point $\boldsymbol{x}$ to its nearest neighbour in $\mathcal{P}_\lambda$ and $\mathcal{P}_\lambda$ is homogeneous Poisson process with intensity λ. Recall from Definition 5.3.1 that $\xi(\boldsymbol{x};\mathcal{X})$ is the

distance from point $\boldsymbol{x}$ to its nearest neighbour in $\mathcal{X} \cap C_{\theta,\phi}(\boldsymbol{x})$. Also, recall $\tilde{\mathcal{L}}_\lambda^1 = \mathcal{L}_\lambda^1 - \mathbf{E}[\mathcal{L}_\lambda^1]$, ($\tilde{\mathcal{L}}_\lambda^1$ is centered random variable). Here we restate the Theorems 2.1 and 2.2 of [29] as follows.

Theorem 5.3.23. *Suppose $\xi(\boldsymbol{x}, \mathcal{X})$ is homogeneously stabilizing and translation-invariant. Suppose also that $\xi(\boldsymbol{x}, \mathcal{X})$ satisfies the moments conditions of Lemma 5.3.9 for $p = 4$, and is power-law stabilizing for order $q = 304$. Then there exists $s_\phi^2 < \infty$ such that $\lambda^{-1}\mathbf{Var}\sum_{\boldsymbol{x}\in\mathcal{P}_\lambda} \xi_\lambda(\boldsymbol{x}; \mathcal{P}_\lambda) \to s_\phi^2$, as $\lambda \to \infty$.*

Remark 5.3.24. The limit s_ϕ appearing in Theorem 5.3.23 can be expressed in terms of functionals of a homogeneous Poisson process on $\mathbb{R}^2$, which is rotationally invariant (see [29] for more details), and therefore depends only on ϕ and not θ.

Proof of Theorem 5.1.2.

Proof. We show that we may apply Theorem 5.3.23 with $\xi(\boldsymbol{x}, \mathcal{X}) = \mathcal{D}_{\theta,\phi}(\boldsymbol{x}, \mathcal{X})$. First, in the unaligned cone, Lemma 5.3.22 shows that ξ is q power-law stabilizing for any $q > 0$, and in particular for $q = 304$; similarly, ξ satisfies the $p = 4$ moments condition. Second, in the singly-aligned cone, Lemmas 5.3.9 and 5.3.20 show the same conditions are satisfied provided $c > c_0$ in the definition of S satisfies $2c_\phi c > 4$ and $2c_\phi c > 304$; taking $c_0 = \frac{152}{c_\phi}$ suffices for this. Hence Theorem 5.3.23 applies.

Therefore,

$$\begin{aligned}\lambda^{-1}\mathbf{Var}\left[\sum_{\boldsymbol{x}\in\mathcal{P}_\lambda} \xi_\lambda(\boldsymbol{x}; \mathcal{P}_\lambda)\right] &= \lambda^{-1}(\lambda^{\frac{1}{2}})^2\mathbf{Var}\left[\sum_{\boldsymbol{x}\in\mathcal{P}_\lambda\cap\mathcal{R}_\lambda^1} \xi(\boldsymbol{x}; \mathcal{P}_\lambda)\right] \\ &= \mathbf{Var}\left[\sum_{\boldsymbol{x}\in\mathcal{P}_\lambda\cap\mathcal{R}_\lambda^1} \xi(\boldsymbol{x}; \mathcal{P}_\lambda)\right],\end{aligned}$$

hence, $\mathbf{Var}(\mathcal{L}_\lambda^1) \equiv \mathbf{Var}(\tilde{\mathcal{L}}_\lambda^1) \to s_\phi^2$, as $\lambda \to \infty$ for some $s_\phi < \infty$. By Proposition 5.2.8, this limit s_ϕ^2 is greater than or equal to $\boldsymbol{q} > 0$, and therefore positive. □

5.4 Proof of Theorem 3.3.2 (iii)

In this section, we will provide the proof of our main result of this thesis specifically part (iii) of Theorem 3.3.2. This proves only holds for the unaligned cone since $\mathcal{R}_\lambda^1 = [0,1]^2$. In our proof, we will use the ingredients mentioned above along with the proof of Theorem 5.1.1 and Theorem 5.1.2.

For the unaligned cone, $\mathcal{R}_\lambda^1 = [0,1]^2$ so $\mathcal{L}_\lambda = \mathcal{L}_\lambda^1$. Then apply Slutsky (Theorem 2.5.5) to $\frac{\mathcal{L}_\lambda^1 - \mathbf{E}[\mathcal{L}_\lambda^1]}{\sqrt{\mathbf{Var}[\mathcal{L}_\lambda^1]}}$ and $\sqrt{\mathbf{Var}[\mathcal{L}_\lambda^1]}$, using Theorems 5.1.1 & 5.1.2 to give

$$\tilde{\mathcal{L}}_\lambda = \tilde{\mathcal{L}}_\lambda^1 = \frac{\mathcal{L}_\lambda^1 - \mathbf{E}[\mathcal{L}_\lambda^1]}{\sqrt{\mathbf{Var}[\mathcal{L}_\lambda^1]}} \cdot \sqrt{\mathbf{Var}[\mathcal{L}_\lambda^1]} \xrightarrow{d} s_\phi Z, \quad \text{as } \lambda \to \infty.$$

Chapter 6

Boundary Effects

6.1 Introduction

This chapter aims to provide an important ingredient for the proof of second part of the main result in this thesis (Theorem 3.3.2, (ii)) for both singly-aligned cones. Recall from Chapter 4 that for both the obtuse case (Lemma 4.4.6) and acute case (Lemma 4.4.7), we define a non-empty boundary region $\mathcal{R}_\lambda^3 = [0,1] \times [0, \lambda^{-\sigma}]$, for $\sigma \in (\frac{1}{2}, \frac{2}{3})$ where we expect to see long edges. Recall from Definition 4.5.2 that $\mathcal{L}_\lambda^3 = \mathcal{L}(\mathcal{P}_\lambda, \mathcal{R}_\lambda^3)$ is the contribution to the total length from points in $\mathcal{P}_\lambda \cap \mathcal{R}_\lambda^3$, where $\mathcal{P}_\lambda$ is the homogeneous Poisson process of intensity λ, and $\tilde{\mathcal{L}}_\lambda^3 = \mathcal{L}_\lambda^3 - \mathbf{E}[\mathcal{L}_\lambda^3]$ is centered random variable. We will show convergence in distribution of $\tilde{\mathcal{L}}_\lambda^3$ as the intensity λ tends to infinity. Recall $\xrightarrow{d}$ denotes convergence in distribution. The principal result of this chapter is Theorem 6.1.1.

Theorem 6.1.1. *If (θ, ϕ) is singly-aligned, then*

$$\tilde{\mathcal{L}}_\lambda^3 \xrightarrow{d} Q, \quad as \quad \lambda \to \infty, \tag{6.1.1}$$

where the distribution of Q is characterized by the fixed point equation (3.4.1).

The concept proof of the Theorem 6.1.1 is to show that the minimal directed spanning forests (MDSF) near the bottom boundary, which is close to a directed linear forest (DLF) system (definition given in Section 6.2) can be defined as a

sequence of random variables coupled to the points of the MDSF. To make this clear, we need to produce an explicit sequence of random variables such that DLF coupled to the Poisson point process $\mathcal{P}_\lambda$ with intensity λ on $(0,1]^2$, on which the MDSF can be constructed and we constructed the directed linear forest on the same process.

In Section 6.2, we introduce the directed linear forest in order to compare a asymptotic behaviour of the total edge length of $\tilde{\mathcal{L}}^3_\lambda$ with Theorem 6.3.2. In Section 6.3, we prove Theorem 6.3.2 for the obtuse cone, and in Section 6.4 we prove for the acute cone. Lastly, in Section 6.5, we derive the proof of Theorem 6.1.1 for both singly-aligned cones since the proof is identical for obtuse case and acute case.

6.2 Directed Linear Forest

In this section, we will present the results of our analysis of the directed linear forests, and we will provide proof for these results in the following sections. Our analysis persists, focusing on the minimal directed spanning forest constructed over randomly selected points within the unit square. Specifically, we focus on the lengths of edges in proximity to the boundaries of the unit square. The objective is to identify the limiting distribution for random MDSF concerning regions near the boundaries. The on-line nearest-neighbour graph serves as a characterisation tool, assisting in our understanding of these limiting distributions.

The directed linear forest is in studying random directed graphs and graph theory. It is primarily employed in analysing minimal directed spanning forests in various geometric settings respecting the unit square. In the context of DLF, the term 'linear' signifies that the edges of the forest follow a linear ordering, often from left to right or right to left. This ordering constraint distinguishes DLF from other graph structures and is essential in understanding its behaviour and applications.

The directed linear forest shares similarities with the on-line nearest neighbour process regarding one-dimensional distance, with the key distinction that the edges exclusively extend to the left of a newly added point in a sequence. In analysing

random minimal directed spanning forest within the unit square $(0,1)^2$ with respect to the general cone $\preccurlyeq$, the DLF plays an essential role, particularly concerning edges located near the boundaries. These boundary regions allow for the estimation of the MDSF using DLF principles. The objective of this section primary is to establish the essential properties and definitions of DLF. Subsequently, we will observe that the total edge length contributed by points near the boundaries converges in distribution to the limit of the total edge length of the DLF as a number of points tends to infinity.

To provide a better understanding, let us first define the directed linear forest (DLF) as DLF(n). The DLF(n) is a graph on the sequence of independent and uniformly distributed random variables on $(0,1)$, in other words, $(X_i, i = 1, 2, \ldots, n) \in (0,1)^n$ so that a directed edge joins X_i to closest X_j with $j < i$ and $X_j < X_i$, i.e., (earlier in the sequence and to the left). In the directed linear forest, every point in a sequence of independent uniform random points within an interval is connected to its closest left neighbour among the preceding points; for example, see Penrose and Wade [31] for further details.

Now we start with some notations and definitions that will be used throughout this chapter to prove the Theorem 6.1.1. By the property of Poisson process the region $\mathcal{R}_\lambda^3$ contains M_λ points, where $M_\lambda \sim \mathbf{Po}(\lambda^{1-\sigma})$. Recall that U denotes the uniform random variable on $[0,1]$, and $\stackrel{d}{=}$ denotes equality in distribution. Let $\mathcal{V}_\lambda := \mathcal{P}_\lambda \cap \mathcal{R}_\lambda^3$ and, as above, let $M_\lambda = \text{card}(\mathcal{V}_\lambda)$ be the cardinality (number of elements) of $\mathcal{V}_\lambda$. We order these points (i.e., $\mathcal{V}_\lambda$) by y-coordinate so that in two-dimensional space, we have the set of points $\mathcal{V}_\lambda := (Z_i = (X_i, Y_i), i = 1, 2, \ldots, M_\lambda)$, where $Y_1 < Y_2 < \cdots < Y_{M_\lambda}$. We couple the MDSF in two-dimensional space on these points $\mathcal{V}_\lambda$ with the directed linear forest defined on the x-coordinates $(X_i, i = 1, 2, \ldots, M_\lambda)$. This sequence is formally denoted as $\mathscr{U}_\lambda$.

Definition 6.2.1. Let $D(\mathscr{U}_\lambda)$ be the total length of the DLF on the sequence $\mathscr{U}_\lambda$ given by

$$\mathscr{U}_\lambda := (X_i, i = 1, 2, \ldots, M_\lambda),$$

where $M_\lambda \sim \mathbf{Po}(\lambda^{1-\sigma})$.

Define Q_n be the total length of the DLF(n). We recall Theorem 3.1 of Penrose and Wade [31] below for the total length of the directed linear forest DLF(n).

Theorem 6.2.2 (Penrose and Wade [31]). *As $n \to \infty$,*

$$Q_n - \mathbf{E}[Q_n] \xrightarrow{d} Q, \tag{6.2.1}$$

where $Q \sim \mathcal{Q}$ is characterized by the fixed point equation (3.4.1).

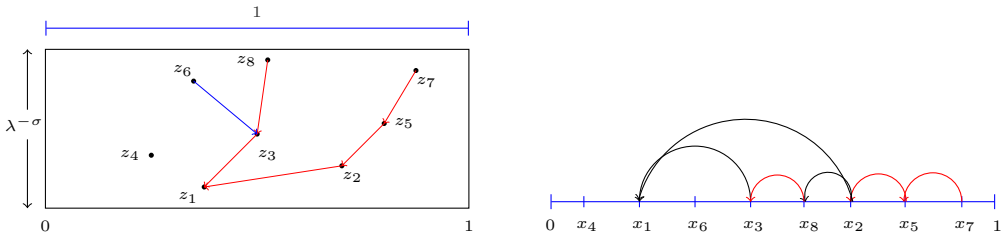

Figure 6.1: *Left Panel:* Realization of two dimensional distance with obtuse case, for example, z_6 can pick z_3 as a nearest neighbour in $d = 2$, but this can't be happened when $d = 1$,, where $z_i, i = 1, 2, \ldots$ and $x_i, i = 1, 2, \ldots$ are points of Poisson process in $[0, 1]^2$; *Right Panel:* transformation from two-dimensional distance to one-dimensional distance of the directed linear forest.

Recall that $\xrightarrow{L^p}$ denotes convergence in p^{th} mean, we consider $p = 1, 2$. To prove Theorem 6.1.1, we need to control the difference between the total edge lengths of the coupled MDSF and DLF provided in the following theorem.

Theorem 6.2.3. *If (θ, ϕ) is singly-aligned. Then,*

$$S_\lambda = \mathcal{L}^3_\lambda - D(\mathscr{U}_\lambda) \xrightarrow{L^2} 0, \quad as \quad \lambda \to \infty. \tag{6.2.2}$$

Before proving Theorem 6.2.3, we first write $\mathcal{L}^3_\lambda$ and $D(\mathscr{U}_\lambda)$ as sums of random variables associated with points in $\mathcal{V}_\lambda$. For this we require the following definitions.

Definition 6.2.4. Let $J(i)$ be the index of the nearest left neighbour of X_i such that $J(i) < i$, defined by

$$J(i) := \arg\max_j \{X_j : X_j < X_i, j < i\},$$

and set

$$J(i) := \infty \text{ if } \{X_j : X_j < X_i, j < i\} = \emptyset.$$

Definition 6.2.5. Let $K(i)$ be the index of the nearest neighbour in the cone $C_{\theta,\phi}(Z_i) \setminus \{Z_i\}$ of Z_i, defined by

$$K(i) := \text{argmin}_{\substack{1 \le k \le M_\lambda \\ k \neq i}} \{\|Z_k - Z_i\| : Z_k \in C_{\theta,\phi}(Z_i)\},$$

and set

$$K(i) := \infty \text{ if } C_{\theta,\phi}(Z_i) \setminus \{Z_i\} \text{ contains no points of } \mathcal{V}_\lambda.$$

Recall that M_λ is the number of points of the finite set $\mathcal{V}_\lambda$, i.e., $M_\lambda \sim \mathbf{Po}(\lambda^{1-\sigma})$. Using Definition 6.2.4, we can write $D(\mathscr{U}_\lambda)$ as

$$D(\mathscr{U}_\lambda) = \sum_{i=1}^{M_\lambda} |X_i - X_{J(i)}| \mathbb{1}_{\{J(i)<\infty\}}. \tag{6.2.3}$$

and using Definition 6.2.5, we can write $\mathcal{L}^3_\lambda$ as

$$\mathcal{L}^3_\lambda = \sum_{i=1}^{M_\lambda} \|Z_i - Z_{K(i)}\| \mathbb{1}_{\{K(i)<\infty\}}. \tag{6.2.4}$$

Hence $S_\lambda = \sum_{i=1}^{M_\lambda} \Delta_i$, where $\Delta_i = \|Z_i - Z_{K(i)}\| \mathbb{1}_{\{K(i)<\infty\}} - |X_i - X_{J(i)}| \mathbb{1}_{\{J(i)<\infty\}}$, and to prove Theorem 6.2.3 we need to show that S_λ converges in L^2 to 0 as $\lambda \to \infty$. The arguments required for this are slightly different for the two type of cones. Section 6.3 covers the obtuse cone and Section 6.4 covers the acute cone.

6.3 Coupling for Obtuse Cone

We begin by defining a region of $\mathcal{R}^3_\lambda$ for each point of $\mathcal{V}_\lambda$ which plays an important role in controlling the size of Δ_i.

Definition 6.3.1. For each $i = 1, 2, \ldots, M_\lambda$, define

$$E_i := \{(x, y) \in \mathcal{R}^3_\lambda : x > X_i, (x, y) \in C_{\theta,\phi}(Z_i)\}.$$

Note that E_i is always contained in a right-angled triangle with height $\lambda^{-\sigma}$ and width $\tan(\phi - \frac{\pi}{2})\lambda^{-\sigma}$.

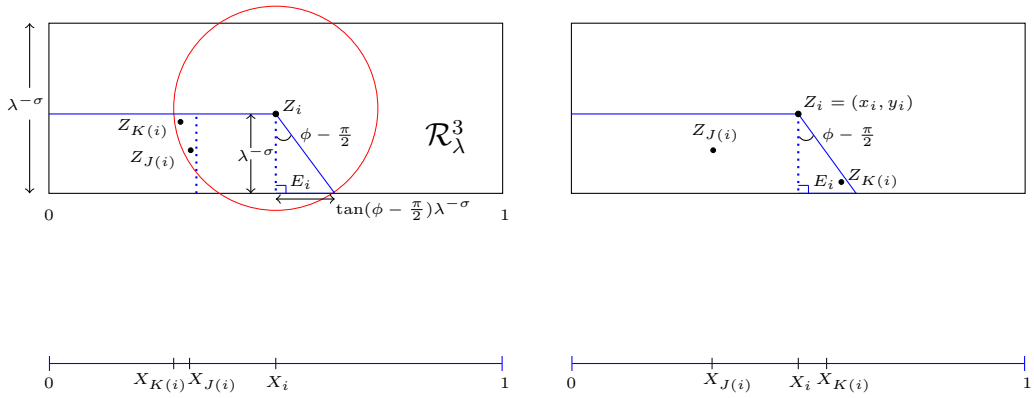

Figure 6.2: *Left Panel:* Realization of two-dimensional distance with obtuse case and error term is E_i i.e. the little triangle, the bottom picture is projected to one-dimensional distance in this case $\mathcal{P}_\lambda \cap E_i = \emptyset$; similarly for the *Right Panel:* if $K(i) < \infty$ and $Z_{K(i)} \in E_i$, then $J(i) \neq K(i)$.

Write E_i defined as above, we write $S_\lambda = \sum_{i=1}^{M_\lambda} \Delta_i$ as $S'_\lambda + S''_\lambda$ where $S'_\lambda = \sum_{i=1}^{M_\lambda} \Delta_i \mathbb{1}_{A_i^\complement}$, and $S''_\lambda = \sum_{i=1}^{M_\lambda} \Delta_i \mathbb{1}_{A_i}$, and $A_i = \{J(i) < \infty, K(i) < \infty, Z_{K(i)} \in E_i\}$. We examine these two sums S'_λ and S''_λ separately. First consider the sum for S'_λ which will be provided in Lemma 6.3.2 and S''_λ given in Lemma 6.3.4.

Lemma 6.3.2. *Suppose that $\sigma \in (\frac{1}{2}, \frac{2}{3})$. Let S'_λ be defined as above, then*

$$S'_\lambda \xrightarrow{L^2} 0, \quad \text{as} \quad \lambda \to \infty.$$

Proof. Given that $A_i^\complement$ occurs, exactly one of the events

(i) $\{K(i) = \infty\}$,

(ii) $\{J(i) = \infty, K(i) < \infty\}$,

(iii) $\{J(i) < \infty, K(i) < \infty, Z_{K(i)} \notin E_i\}$.

occurs.

Case (i): $K(i) = \infty$ means $C_{\theta,\phi}(Z_i)$ contains no other points of $\mathcal{V}_\lambda$, so $J(i) = \infty$

also. Then $\Delta_i = 0 - 0 = 0$.

Case (ii): $J(i) = \infty$ and $K(i) < \infty$, means $C_{\theta,\phi}(Z_i)$ contains $Z_{K(i)}$ the nearest-neighbour of Z_i (hence $K(i) < i$) but $X_{K(i)} > X_i$ (otherwise $J(i) < \infty$). Hence $Z_{K(i)} \in E_i$ and $\Delta_i = \|Z_i - Z_{K(i)}\|$ satisfies

$$0 \leq \|Z_i - Z_{K(i)}\| \leq \sec\left(\phi - \frac{\pi}{2}\right) \lambda^{-\sigma}, \tag{6.3.1}$$

since the length $\|Z_i - Z_{K(i)}\|$ is at most the length of the hypotenuse of E_i.

Case (iii): $J(i) < \infty$, $K(i) < \infty$, and $Z_{K(i)} \notin E_i$ means $K(i) < i$ and $X_{K(i)} < X_i$, hence $|X_{J(i)} - X_i| \leq |X_{K(i)} - X_i|$ by definition of $J(i)$. Also, $Z_{J(i)} \in C_{\theta,\phi}(Z_i)$ so $\|Z_{K(i)} - Z_i\| - \|Z_{J(i)} - Z_i\|$ by definition of $K(i)$. Then by the inequality the following inequalities hold

$$\begin{aligned} |X_{J(i)} - X_i| &\leq |X_{K(i)} - X_i| \leq \|Z_{K(i)} - Z_i\| \\ &\leq \|Z_{J(i)} - Z_i\| \leq |X_{J(i)} - X_i| + |Y_{J(i)} - Y_i| \\ &\leq |X_{J(i)} - X_i| + \lambda^{-\sigma}. \end{aligned}$$

Therefore, $\Delta_i = \|Z_{K(i)} - Z_i\| - |X_{J(i)} - X_i|$ satisfies $0 \leq \Delta_i \leq \lambda^{-\sigma}$.

Combining cases (i), (ii), and (iii), yields

$$0 \leq \Delta_i \mathbb{1}_{A_i^{\complement}} \leq \sec\left(\phi - \frac{\pi}{2}\right) \lambda^{-\sigma}. \tag{6.3.2}$$

Now apply the absolute value over S'_λ and use the right-hand side of (6.3.2), hence

$$|S'_\lambda| = |\sum_{i=1}^{M_\lambda} \Delta_i \mathbb{1}_{A_i^{\complement}}| \leq \sum_{i=1}^{M_\lambda} \sec\left(\phi - \frac{\pi}{2}\right) \lambda^{-\sigma} = M_\lambda \lambda^{-\sigma} \sec\left(\phi - \frac{\pi}{2}\right). \tag{6.3.3}$$

Squaring and applying the expectation over S'_λ and using the right-hand side of (6.3.3), yields

$$\mathbf{E}[(S'_\lambda)^2] \leq \mathbf{E}\left[\left(\lambda^{-\sigma} M_\lambda \sec\left(\phi - \frac{\pi}{2}\right)\right)^2\right] = \left(\lambda^{-\sigma} \sec\left(\phi - \frac{\pi}{2}\right)\right)^2 \mathbf{E}[(M_\lambda)^2].$$

By the second moment of Poisson distribution, we have $\mathbf{E}[(M_\lambda)^2] \leq 2(\lambda^{1-\sigma})^2$, since $M_\lambda \sim \mathbf{Po}(\lambda^{1-\sigma})$. Whence, since $\sigma \in (\frac{1}{2}, \frac{2}{3})$,

$$\mathbf{E}[(S'_\lambda)^2] \leq 2\lambda^{2-2\sigma} \cdot \lambda^{-2\sigma} \sec^2\left(\phi - \frac{\pi}{2}\right) \leq 2\lambda^{2-4\sigma} \sec^2\left(\phi - \frac{\pi}{2}\right) \to 0, \quad \text{as} \quad \lambda \to \infty. \tag{6.3.4}$$

Thus as $\lambda \to \infty$, $S'_\lambda \xrightarrow{L^2} 0$, we obtain the lemma. □

We turn our attention to the second sum S''_λ. We show in the following lemma that S''_λ converges in L^2 to 0 as the intensity λ tends to infinity. Recall by definition of $S''_\lambda = \sum_{i=1}^{M_\lambda} \Delta_i \mathbb{1}_{A_i}$, where $M_\lambda \sim \mathbf{Po}(\lambda^{1-\sigma})$, $A_i = \{J(i) < \infty, K(i) < \infty, Z_{K(i)} \in E_i\}$, and $\Delta_i = \|Z_i - Z_{K(i)}\| \mathbb{1}_{\{K(i)<\infty\}} - |X_i - X_{J(i)}| \mathbb{1}_{\{J(i)<\infty\}}$. In the proof we will relate the length $|X_{J(i)} - X_i| \mathbb{1}_{\{J(i)<\infty\}}$ to the spacings of the order statistics of $X_1, X_2, \ldots, X_i$ as given by the following definition.

Definition 6.3.3. Denote the (increasing) order statistics of the random variables $X_1, X_2, \ldots, X_i$ by $X_{(1)} < X_{(2)} < \cdots < X_{(i)}$ and set $X_{(0)} := 0, X_{(i+1)} := 1$. Define the corresponding spacings by $I_{i,j} := X_{(j)} - X_{(j-1)}$ for $j \in [1, i+1]$.

Note that, since $X_1, \ldots, X_i$ are independent identically distributed $\mathcal{U}(0,1)$ random variables, for each j, we have $I_{i,j} \sim \beta(1, i)$.

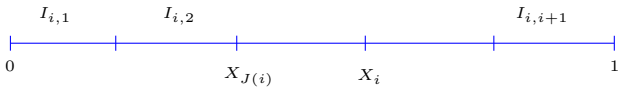

Figure 6.3: At arrival time of i^{th} points there are gaps of length $I_i = (I_{i,1}, I_{i,2}, \ldots, I_{i,i+1}) \sim \text{Dirichlet}(1, 1, \ldots, 1)$, where $\sum_{j=1}^{i+1} I_{i,j} = 1$ with initial $I_{i,1} \sim \beta(1, i)$ and $\sum_{j=1}^{k} I_j \sim \beta(k, i+1-k)$ with respect to $[1, i+1]$.

This definition is key in establishing the proof of Lemma 6.3.4, below, as it provides the necessary foundation for our argument, especially with regard to the spacings $I_{i,j}$ between order statistics of uniform random variables.

Lemma 6.3.4. *Suppose that $\sigma \in (\frac{1}{2}, \frac{2}{3})$. Then,*

$$S''_\lambda \xrightarrow{L^2} 0, \quad \text{as} \quad \lambda \to \infty.$$

Proof. We are going to partition on the size of M_λ, so either $M_\lambda > 3\lambda^{1-\sigma}$ or $M_\lambda \leq 3\lambda^{1-\sigma}$, in other words, $S''_\lambda = S''_\lambda \mathbb{1}_{\{M_\lambda \leq 3\lambda^{1-\sigma}\}} + S''_\lambda \mathbb{1}_{\{M_\lambda > 3\lambda^{1-\sigma}\}}$. We want show that, as $\lambda \to \infty$

$$\mathbf{E}[(S''_\lambda)^2] = \mathbf{E}[(S''_\lambda \mathbb{1}_{\{M_\lambda \leq 3\lambda^{1-\sigma}\}})^2] + \mathbf{E}[(S''_\lambda \mathbb{1}_{\{M_\lambda > 3\lambda^{1-\sigma}\}})^2] \to 0. \tag{6.3.5}$$

First observe that the absolute value of S''_λ is bounded by $M_\lambda\sqrt{2}$, since $|\Delta_i| \le \sqrt{2}$. Then by Cauchy–Schwarz inequality and the 4^{th} moments of Poisson distribution (i.e., if $X \sim \mathbf{Po}(\mu)$ then $\mathbf{E}[X^4] \le 15\mu^4$, for $\mu > 1$), we get

$$\begin{aligned}\mathbf{E}[(S''_\lambda \mathbb{1}_{\{M_\lambda > 3\lambda^{1-\sigma}\}})^2] &\le 2\mathbf{E}[M_\lambda^2 \mathbb{1}_{\{M_\lambda > 3\lambda^{1-\sigma}\}}] \\ &\le 2(\mathbf{E}[M_\lambda^4])^{\frac{1}{2}} \mathbf{P}(M_\lambda > 3\lambda^{1-\sigma})^{\frac{1}{2}} \\ &\le 2(16\lambda^{4-4\sigma})^{\frac{1}{2}} e^{-\frac{1}{2}\lambda^{1-\sigma}} \le 8\lambda^2 e^{-\frac{1}{2}\lambda^{1-\sigma}} \to 0, \quad \text{as} \quad \lambda \to \infty,\end{aligned} \tag{6.3.6}$$

by the inequality (5.2.2). Therefore, $\mathbf{E}[(S''_\lambda \mathbb{1}_{\{M_\lambda > 3\lambda^{1-\sigma}\}})^2] \to 0$, as $\lambda \to \infty$. Now we consider the term $S''_\lambda \mathbb{1}_{\{M_\lambda \le 3\lambda^{1-\sigma}\}}$. We write $\tilde{\Delta}_i = \Delta_i \mathbb{1}_{A_i}$ so that $\Delta_i \mathbb{1}_{A_i} \equiv \tilde{\Delta}_i \mathbb{1}_{A_i}$. Then,

$$|S''_\lambda \mathbb{1}_{\{M_\lambda \le 3\lambda^{1-\sigma}\}}| \le \sum_{i=1}^{\lfloor 3\lambda^{1-\sigma} \rfloor} |\Delta_i \mathbb{1}_{A_i}| \mathbb{1}_{\{M_\lambda \le 3\lambda^{1-\sigma}\}} \le \sum_{i=1}^{\lfloor 3\lambda^{1-\sigma} \rfloor} |\tilde{\Delta}_i| \mathbb{1}_{A_i}. \tag{6.3.7}$$

Squaring and applying the expectation over S''_λ given in (6.3.7), the right-hand side yields

$$\mathbf{E}[(S''_\lambda \mathbb{1}_{\{M_\lambda \le 3\lambda^{1-\sigma}\}})^2] \le \sum_{i,j=1}^{\lfloor 3\lambda^{1-\sigma} \rfloor} \mathbf{E}[|\tilde{\Delta}_i||\tilde{\Delta}_j| \mathbb{1}_{A_i \cap A_j}]. \tag{6.3.8}$$

We apply the Cauchy-Schwarz inequality (twice) to each term in the sum in (6.3.8), then

$$\mathbf{E}[|\tilde{\Delta}_i||\tilde{\Delta}_j| \mathbb{1}_{A_i \cap A_j}] \le \mathbf{E}[(\tilde{\Delta}_i \tilde{\Delta}_j)^2]^{\frac{1}{2}} \mathbf{P}(A_i \cap A_j)^{\frac{1}{2}} \le \mathbf{E}[\tilde{\Delta}_i^4]^{\frac{1}{4}} \mathbf{E}[\tilde{\Delta}_j^4]^{\frac{1}{4}} \mathbf{P}(A_i \cap A_j)^{\frac{1}{2}},$$

which yields

$$\mathbf{E}[(S''_\lambda \mathbb{1}_{\{M_\lambda \le 3\lambda^{1-\sigma}\}})^2] \le \sum_{i,j=1}^{\lfloor 3\lambda^{1-\sigma} \rfloor} \mathbf{E}[\tilde{\Delta}_i^4]^{\frac{1}{4}} \mathbf{E}[\tilde{\Delta}_j^4]^{\frac{1}{4}} \mathbf{P}(A_i \cap A_j)^{\frac{1}{2}}. \tag{6.3.9}$$

Here we want to find $\mathbf{P}(A_i \cap A_j)$ appears in (6.3.9). To do so, we let $\mathbf{P}(A_i \cap A_j) \le \mathbf{P}(W_\lambda > 0)$, where W_λ is the number of points of $\mathcal{P}_\lambda$ in $E_i \cup E_j$. Since $|E_i \cup E_j| \le c\lambda^{-2\sigma}$ (because $|E_i \cup E_j| \le |E_i| + |E_j|$ and each E is a triangle with area at most $c_\phi \lambda^{-2\sigma}$, for some constant $c_\phi > 0$). So W_λ is a Poisson random variable with

parameter less than or equal to $c_\phi \lambda^{1-2\sigma}$, then $\mathbf{E}[W_\lambda] \leq c\lambda^{1-2\sigma}$ for $\sigma > \frac{1}{2}$. Hence, by Markov's inequality

$$\mathbf{P}(A_i \cap A_j) \leq \mathbf{P}(W_\lambda \geq 1) \leq c\lambda^{1-2\sigma}, \text{ for } \sigma > \frac{1}{2}. \tag{6.3.10}$$

Finally, we bound $|\tilde{\Delta}_i| = |\Delta_i| \mathbb{1}_{A_i}$ which will lead to a bound on $\mathbf{E}[\tilde{\Delta}_i^4]$. Given A_i occurs, the point $Z_{K(i)}$ is in E_i, so we have by (6.3.1) that

$$0 \leq \|Z_{K(i)} - Z_i\| \leq \sec\left(\phi - \frac{\pi}{2}\right) \lambda^{-\sigma}. \tag{6.3.11}$$

Subtracting $|X_{J(i)} - X_i|$ from each side gives bound on Δ_i as

$$-|X_{J(i)} - X_i| \leq \Delta_i \leq -|X_{J(i)} - X_i| + \sec\left(\phi - \frac{\pi}{2}\right) \lambda^{-\sigma}. \tag{6.3.12}$$

Then we apply the absolute value over Δ_i, we write (6.3.12), as follows

$$|\Delta_i| \leq |X_{J(i)} - X_i| + \sec\left(\phi - \frac{\pi}{2}\right) \lambda^{-\sigma}.$$

In terms of $|\tilde{\Delta}_i| = \Delta_i \mathbb{1}_{A_i}$, we have

$$|\tilde{\Delta}_i| \leq |X_{J(i)} - X_i| \mathbb{1}_{\{J(i)<\infty\}} + \sec\left(\phi - \frac{\pi}{2}\right) \lambda^{-\sigma}.$$

From (6.3.9), we need to find the 4^{th} moment of $\tilde{\Delta}_i$. Using the fact that for $a, b > 0$, we have $(a+b)^4 \leq (2\max\{a,b\})^4 = 2^4 \max\{a^4, b^4\} \leq 2^4(a^4 + b^4)$, hence

$$\begin{aligned}\tilde{\Delta}_i^4 &\leq \left(|X_{J(i)} - X_i| \mathbb{1}_{\{J(i)<\infty\}} + \lambda^{-\sigma} \sec\left(\phi - \frac{\pi}{2}\right)\right)^4 \\ &\leq 2^4 \left(|X_{J(i)} - X_i|^4 \mathbb{1}_{\{J(i)<\infty\}} + \lambda^{-4\sigma} \sec^4\left(\phi - \frac{\pi}{2}\right)\right).\end{aligned} \tag{6.3.13}$$

Next we aim to find the expectation of $|X_{J(i)} - X_i|^4 \mathbb{1}_{\{J(i)<\infty\}}$. We relate the length $|X_{J(i)} - X_i|^4 \mathbb{1}_{\{J(i)<\infty\}}$ to the spacings $I_{i,j}$ between order statistics of uniform random variables (see Definition 6.3.3). We think of point in $Z_i = (X_i, Y_i) \in \mathcal{V}_\lambda$ as an arrival at time Y_i of a point at $X_i \in [0,1]$. By the Poisson property, each X_i is uniformly distributed on $[0,1]$, and the ordering of points in $\mathcal{V}_\lambda$ by y-coordinate means points arrive in order X_1 then X_2 then X_3 and so on. At the arrival time of i^{th} point X_i, the points $X_1, X_2, \ldots, X_i$ are placed in one of $i!$ possible orders: if $X_{(1)} < X_{(2)} \cdots < X_{(i)}$ are the order statistics of $X_1, X_2, \ldots, X_i$, then for any

permutation $\pi \in S_i$ the probability $\mathbf{P}(X_{(j)} = X_{\pi(j)}, \forall j = 1, \ldots, i) = \frac{1}{i!}$ Let G_j be the event $\{X_i = X_{(j)}\}$, which has probability $\mathbf{P}(G_j) = \frac{1}{i}$ for all $j = 1, \ldots, i$. If G_j occurs, and $j \neq 1$, the length $|X_{J(i)} - X_i|$ equals $I_{i,j}$ the gap between $X_{(j)}$ and $X_{(j-1)}$. Otherwise, if G_1 occurs then $J(i) = \infty$. So $|X_{J(i)} - X_i|^4 \mathbb{1}_{\{J(i)<\infty\}} = \sum_{j=2}^{i} (I_{i,j})^4 \mathbb{1}_{\{G_j\}}$, where $I_{i,j}$ and G_j are independent random variables. Then, we have

$$\begin{aligned}\mathbf{E}\left[|X_{J(i)} - X_i|^4 \mathbb{1}_{\{J(i)<\infty\}}\right] &= \mathbf{E}\left[\sum_{j=2}^{i} (I_{i,j})^4 \mathbb{1}_{\{G_j\}}\right] \\ &= \sum_{j=2}^{i} \mathbf{E}\left[(I_{i,j})^4\right] \mathbf{P}(G_j) = \frac{1}{i} \cdot \sum_{j=2}^{i} \mathbf{E}\left[(I_{i,j})^4\right]. \qquad (6.3.14)\end{aligned}$$

Let $I_{i,j} \sim \beta(1, i)$, where β is Beta distribution, then by its definition we derive $\mathbf{E}[(I_{i,j})^4]$, as follows

$$\begin{aligned}\mathbf{E}[(I_{i,j})^4] = \int_0^1 \frac{x^4(1-x)^{i-2}}{B(1, i-1)} dx = \frac{B(5, i-1)}{B(1, i-1)} &= \frac{\Gamma(5)\Gamma(i-1)}{\Gamma(5+i-1)} \cdot \frac{\Gamma(i)}{\Gamma(1)\Gamma(i-1)} \\ &= \frac{4!(i-1)!}{(i+3)!} = \frac{4!(i-1)!}{(i+3)(i+2)(i+1)i(i-1)!} \\ &= \frac{4!}{(i+3)(i+2)(i+1)i}. \qquad (6.3.15)\end{aligned}$$

Thus by (6.3.15), the right-hand side of (6.3.14), yields

$$\begin{aligned}\mathbf{E}\left[|X_{J(i)} - X_i|^4 \mathbb{1}_{\{J(i)<\infty\}}\right] &= \frac{1}{i} \cdot \sum_{j=2}^{i} \mathbf{E}\left[(I_{i,j})^4\right] \\ &= \frac{i-1}{i} \cdot \frac{4!}{(i+3)(i+2)(i+1)i} \leq \frac{4!}{i^4}. \qquad (6.3.16)\end{aligned}$$

Combining (6.3.13) and (6.3.16), yields

$$\mathbf{E}[\tilde{\Delta}_i^4] \leq \frac{2^4 \cdot 4!}{i^4} + 2^4 \cdot \lambda^{-4\sigma} \sec^4\left(\phi - \frac{\pi}{2}\right). \qquad (6.3.17)$$

Combining inequalities (6.3.9), (6.3.10), and (6.3.17) results

$$\begin{aligned}\mathbf{E}[(S''_\lambda \mathbb{1}_{\{M_\lambda \le 3\lambda^{1-\sigma}\}})^2] &\le \left(c\lambda^{1-2\sigma}\right)^{\frac{1}{2}} \left(\sum_{i=1}^{\lfloor 3\lambda^{1-\sigma}\rfloor} \mathbf{E}[\tilde{\Delta}_i^4]^{\frac{1}{4}}\right)^2 \\ &\le c'\lambda^{\frac{1}{2}-\sigma}\left(\sum_{i=1}^{\lfloor 3\lambda^{1-\sigma}\rfloor}\left(\frac{2^4\cdot 4!}{i^4} + 2^4\cdot\lambda^{-4\sigma}\sec^4\left(\phi-\frac{\pi}{2}\right)\right)^{\frac{1}{4}}\right)^2 \\ &\le c'\lambda^{\frac{1}{2}-\sigma}\left(\sum_{i=1}^{\lfloor 3\lambda^{1-\sigma}\rfloor}\left(\frac{2\cdot 4!^{\frac{1}{4}}}{i} + 2\cdot\lambda^{-\sigma}\sec\left(\phi-\frac{\pi}{2}\right)\right)\right)^2 \\ &\le c''\lambda^{\frac{1}{2}-\sigma}\left(\log(3\lambda^{1-\sigma}) + \lambda^{1-2\sigma}\right)^2 \to 0, \text{ as } \lambda\to\infty, \text{ for } \sigma > \frac{1}{2},\end{aligned} \tag{6.3.18}$$

where $\left(\sum_{i=1}^{\lfloor 3\lambda^{1-\sigma}\rfloor} \mathbf{E}[\tilde{\Delta}_i^4]^{\frac{1}{4}}\right)^2 = \sum_{i,j=1}^{\lfloor 3\lambda^{1-\sigma}\rfloor} \mathbf{E}[\tilde{\Delta}_i^4]^{\frac{1}{4}}\mathbf{E}[\tilde{\Delta}_j^4]^{\frac{1}{4}}$, and c, c', and c'' are constants. Since $\sigma > \frac{1}{2}$, the right-hand side of (6.3.18) tends to 0 as $\lambda\to\infty$, hence $S''_\lambda \mathbb{1}_{\{M_\lambda\le 3\lambda^{1-\sigma}\}} \xrightarrow{L^2} 0$, as $\lambda\to\infty$. Note that in line 2 of the above inequality, we use $(a+b)^{\frac{1}{4}} \le a^{\frac{1}{4}} + b^{\frac{1}{4}}$ for $a, b \ge 0$, also in line 4 we use $\sum_{i=1}^n \frac{1}{i} \le 1 + \log n \le 2\log n$ for all $n > e$.

Finally, we combine (6.3.6) and (6.3.18), with (6.3.5) which completes the proof.

□

Here we have all ingredients to deliver the proof of Theorem 6.2.3. Recall that $S_\lambda = \mathcal{L}_\lambda^3 - D(\mathscr{U}_\lambda) = \sum_{i=1}^{M_\lambda} \Delta_i$, where $\Delta_i = \|Z_i - Z_{K(i)}\|\mathbb{1}_{\{K(i)<\infty\}} - |X_i - X_{J(i)}|\mathbb{1}_{\{J(i)<\infty\}}$ and $M_\lambda \sim \mathbf{Po}(\lambda^{1-\sigma})$.

Proof of Theorem 6.2.3. (Obtuse case) Combining Lemma 6.3.2 and Lemma 6.3.4 and applying Minkowski's inequality to S'_λ and S''_λ. Hence, $S_\lambda = S'_\lambda + S''_\lambda \xrightarrow{L^2} 0$, as $\lambda\to\infty$. □

6.4 Coupling for Acute Cone

In this section, we will employ the same notations and definitions as in the obtuse case, specifically referencing Definition 6.2.4 for $J(i)$ and Definition 6.2.5 for $K(i)$.

It's worth noting that the set E_i differs from its use in the obtuse cone.

Before proving Theorem 6.2.3, recall that $S_\lambda = \mathcal{L}^3_\lambda - D(\mathscr{U}_\lambda)$ and we define $D(\mathscr{U}_\lambda)$ by (6.2.3) and $\mathcal{L}^3_\lambda$ by (6.2.4) as the sums of random variables associated with points in $\mathcal{V}_\lambda$. Let $S_\lambda = \sum_{i=1}^{M_\lambda} \Delta_i$, where $\Delta_i = \|Z_i - Z_{K(i)}\| \mathbb{1}_{\{K(i)<\infty\}} - |X_i - X_{J(i)}| \mathbb{1}_{\{J(i)<\infty\}}$, and to prove Theorem 6.2.3, we need to show that S_λ converges in L^2 to 0 as $\lambda \to \infty$. For this we require the following definitions. We begin by defining a region of $\mathcal{R}^3_\lambda$ for each point of $\mathcal{V}_\lambda$, which plays an important role in controlling the size of Δ_i.

Definition 6.4.1. For each $i = 1, 2, \ldots, M_\lambda$, define

$$E_i := \{(x, y) \in \mathcal{R}^3_\lambda : x < X_i, y < Y_i, (x, y) \notin C_{\theta,\phi}(Z_i)\}.$$

Note that E_i is always contained in a right-angled triangle with height $\lambda^{-\sigma}$ and width $\lambda^{-\sigma} \cot \phi$.

Definition 6.4.2. Let $\tilde{J}(i)$ be defined in terms of the X-process as the index of the nearest left neighbour of X_i at distance greater than $\lambda^{-\sigma} \cot \phi$ such that $\tilde{J}(i) < i$ (see Figure 6.5), defined by

$$\tilde{J}(i) := \arg\max_j \{X_j : X_j < X_i - \lambda^{-\sigma} \cot(\phi), j < i\},$$

and set

$$\tilde{J}(i) = \infty \quad \text{if} \quad \{X_j : X_j < X_i - \lambda^{-\sigma} \cot(\phi), j < i\} = \emptyset.$$

Definition 6.4.3. Let $I(i) \leq i$ be defined by

$$I(i) := \text{argmin}_j \{X_j : X_i - \lambda^{-\sigma} \cot \phi \leq X_j \leq X_i, j \leq i\}.$$

The definitions of E_i and $\tilde{J}(i)$ mean that if $\tilde{J}(i) < \infty$ then $Z_{\tilde{J}(i)} \notin E_i$. The definitions of $\tilde{J}(i)$ and $I(i)$ mean that if $\tilde{J}(i) < \infty$ then $X_{\tilde{J}(i)}$ and $X_{I(i)}$ are a consecutive pair of order statistics of the random variable $X_1, X_2, \ldots, X_i$.

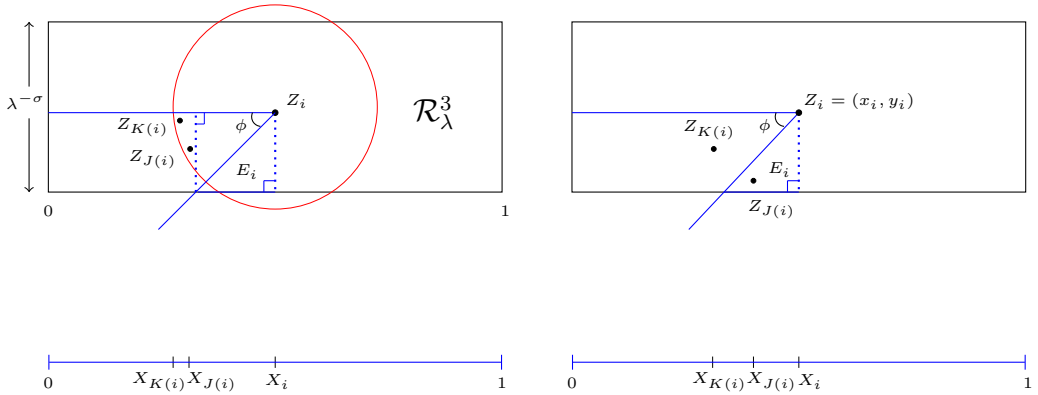

Figure 6.4: *Left Panel:* Realization of two-dimensional distance with acute case and error term is E_i i.e. the little triangle, the bottom picture is projected to one-dimensional distance in this case $\mathcal{P}_\lambda \cap E_i = \emptyset$; *Right Panel:* if $J(i) < \infty$ and $Z_{J(i)} \in E_i$, then $J(i) \neq K(i)$.

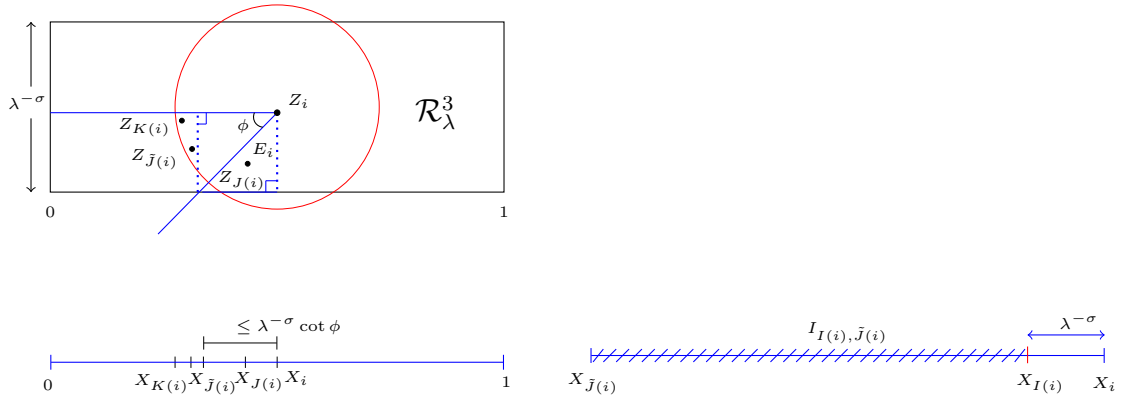

Figure 6.5: *Left Panel:* In the one-dimensional picture the interval of length $\leq \lambda^{-\sigma} \cot \phi$ contains the projection of any point in the little triangle E_i; the point $X_{\tilde{J}(i)}$ is the projection of a candidate nearest neighbour that cannot be in E_i; *Right Panel:* The distance between X_i & $X_{\tilde{J}(i)}$ is of the form $|X_{\tilde{J}(i)} - X_i| \leq |X_{\tilde{J}(i)} - X_{I(i)}| + \lambda^{-\sigma}$ where $I(i) \leq i$, and $\tilde{J}(i)$, $I(i)$ are consecutive order statistics.

Write E_i defined as above, we write $S_\lambda = \sum_{i=1}^{M_\lambda} \Delta_i$ as $S'_\lambda + S''_\lambda$, where $S'_\lambda = \sum_{i=1}^{M_\lambda} \Delta_i \mathbb{1}_{A_i^\complement}$ and $S''_\lambda = \sum_{i=1}^{M_\lambda} \Delta_i \mathbb{1}_{A_i}$, and $A_i = \{J(i) < \infty, K(i) < \infty, Z_{J(i)} \in E_i\}$. Notice here that the definition of A_i refers to the event $Z_{J(i)} \in E_i$, in contrast to the definition for the obtuse cone, which refers to event $Z_{K(i)} \in E_i$. We examine these two sums S'_λ and S''_λ separately. First consider the sum for S'_λ given in Lemma 6.4.4 and S''_λ given in Lemma 6.4.5.

Lemma 6.4.4. *Suppose that $\sigma \in (\frac{1}{2}, \frac{2}{3})$. Let S'_λ be defined as above, then*

$$S'_\lambda \xrightarrow{L^2} 0, \quad as \quad \lambda \to \infty.$$

Proof. Given that $A_i^{\complement}$ occurs, exactly one of the events

(a) $\{J(i) = \infty\}$,

(b) $\{J(i) < \infty, K(i) = \infty\}$,

(c) $\{J(i) < \infty, K(i) < \infty, Z_{J(i)} \notin E_i\}$.

occurs. Note that cases (a), (b), and (c) correspond to the cases (i), (ii), and (iii) appearing in proof of Lemma 6.3.2 but with the roles of $J(i)$ & $K(i)$ swapped.

Case (a): If $J(i) = \infty$ then $C_{\theta,\phi}(Z_i)$ contains no other points of $\mathcal{V}_\lambda$, so $K(i) = \infty$ also. Then $\Delta_i = 0 - 0 = 0$ as for the case (i) in Lemma 6.3.2.

Case (b): If $K(i) = \infty$ and $J(i) < \infty$, means $C_{\theta,\phi}(Z_i) \setminus \{Z_i\}$ is empty, but there is a candidate nearest neighbour with $X_{J(i)} < X_i$ and $J(i) < i$. Hence $Z_{J(i)}$ is in E_i and $|\Delta_i| = |X_{J(i)} - X_i|$, satisfies

$$0 \leq |X_{J(i)} - X_i| \leq \lambda^{-\sigma} \cot(\phi). \tag{6.4.1}$$

Since the length $|X_{J(i)} - X_i|$ is at most the width of triangle E_i.

Case (c): $J(i) < \infty$, $K(i) < \infty$ and $Z_{J(i)} \notin E_i$ means $Z_{J(i)} \in C_{\theta,\phi}(Z_i)$, hence by definition of $K(i)$, we have $\|Z_{K(i)} - Z_i\| \leq \|Z_{J(i)} - Z_i\|$. Also, $X_{K(i)} < X_i$ and $K(i) < i$, hence $|X_{J(i)} - X_i| \leq |X_{K(i)} - X_i|$ by definition of $J(i)$. Then, by triangle inequality the following inequalities hold

$$\begin{aligned} |X_{J(i)} - X_i| \leq |X_{K(i)} - X_i| \leq \|Z_{K(i)} - Z_i\| &\leq \|Z_{J(i)} - Z_i\| \\ &\leq |X_{J(i)} - X_i| + |Y_{J(i)} - Y_i| \\ &\leq |X_{J(i)} - X_i| + \lambda^{-\sigma}. \end{aligned}$$

Therefore $\Delta_i = \|Z_{K(i)} - Z_i\| - \|Z_{J(i)} - Z_i\|$ satisfies $0 \leq \Delta_i \leq \lambda^{-\sigma}$. So combining cases (a), (b), and (c) we see that $|\Delta_i| \mathbb{1}_{A_i^{\complement}} \leq \lambda^{-\sigma} \cot(\phi)$.

Apply the absolute value over S'_λ and use the bound on $|\Delta_i|\mathbb{1}_{A_i^\complement}$, to get

$$|S'_\lambda| = |\sum_{i=1}^{M_\lambda} \Delta_i \mathbb{1}_{A_i^\complement}| \leq \sum_{i=1}^{M_\lambda} \lambda^{-\sigma} \cot(\phi) = M_\lambda \lambda^{-\sigma} \cot(\phi). \tag{6.4.2}$$

Squaring and applying the expectation over S'_λ, hence

$$\mathbf{E}[(S'_\lambda)^2] \leq \mathbf{E}\left[(\lambda^{-\sigma} M_\lambda \cot(\phi))^2\right] = (\lambda^{-\sigma} \cot(\phi))^2 \mathbf{E}[(M_\lambda)^2].$$

By the second moment of Poisson distribution we have $\mathbf{E}[(M_\lambda)^2] \leq 2(\lambda^{1-\sigma})^2$, since $M_\lambda \sim \mathbf{Po}(\lambda^{1-\sigma})$. Whence, since $\sigma \in (\frac{1}{2}, \frac{2}{3})$,

$$\mathbf{E}[(S'_\lambda)^2] \leq 2\lambda^{2-2\sigma} \cdot \lambda^{-2\sigma} \cot^2(\phi) \leq 2\lambda^{2-4\sigma} \cot^2(\phi) \to 0, \quad \text{as} \quad \lambda \to \infty. \tag{6.4.3}$$

Thus, we obtain the lemma. □

We show in the following lemma that S''_λ converges in L^2 to 0 as the intensity λ tends to infinity. Let $A_i = \{J(i) < \infty, K(i) < \infty, Z_{J(i)} \in E_i\}$. We have by definition of S''_λ that $S''_\lambda = \sum_{i=1}^{M_\lambda} \Delta_i \mathbb{1}_{A_i}$, where $\Delta_i = \|Z_i - Z_{K(i)}\|\mathbb{1}_{\{K(i)<\infty\}} - |X_i - X_{J(i)}|\mathbb{1}_{\{J(i)<\infty\}}$, and $M_\lambda \sim \mathbf{Po}(\lambda^{1-\sigma})$.

Lemma 6.4.5. *Suppose that $\sigma \in (\frac{1}{2}, \frac{2}{3})$. Then,*

$$S''_\lambda \xrightarrow{L^2} 0, \quad \textit{as} \quad \lambda \to \infty.$$

Proof. We follow the proof of Lemma 6.3.4 where possible but making appropriate changes specific to the acute case where necessary. We are going to partition on the size of M_λ, so either $M_\lambda > 3\lambda^{1-\sigma}$ or $M_\lambda \leq 3\lambda^{1-\sigma}$, in other words, $S''_\lambda = S''_\lambda \mathbb{1}_{\{M_\lambda \leq 3\lambda^{1-\sigma}\}} + S''_\lambda \mathbb{1}_{\{M_\lambda > 3\lambda^{1-\sigma}\}}$. We want show that as $\lambda \to \infty$,

$$\mathbf{E}[(S''_\lambda)^2] = \mathbf{E}[(S''_\lambda \mathbb{1}_{\{M_\lambda \leq 3\lambda^{1-\sigma}\}})^2] + \mathbf{E}[(S''_\lambda \mathbb{1}_{\{M_\lambda > 3\lambda^{1-\sigma}\}})^2] \ \to 0. \tag{6.4.4}$$

First observe that the absolute value of S''_λ is bounded by $\sqrt{2}M_\lambda$, since $|\Delta_i| \leq \sqrt{2}$. Then by Cauchy–Schwarz inequality and the 4^{th} moments of Poisson distribution, we have

$$\begin{aligned}
\mathbf{E}[(S''_\lambda \mathbb{1}_{\{M_\lambda > 3\lambda^{1-\sigma}\}})^2] &\leq 2\mathbf{E}[M_\lambda^2 \mathbb{1}_{\{M_\lambda > 3\lambda^{1-\sigma}\}}] \\
&\leq 2(\mathbf{E}[M_\lambda^4])^{\frac{1}{2}} \mathbf{P}(M_\lambda > 3\lambda^{1-\sigma})^{\frac{1}{2}} \\
&\leq 2(16\lambda^{4-4\sigma})^{\frac{1}{2}} e^{-\frac{1}{2}\lambda^{1-\sigma}} \leq 8\lambda^2 e^{-\frac{1}{2}\lambda^{1-\sigma}} \ \to 0, \text{ as } \lambda \to \infty,
\end{aligned} \tag{6.4.5}$$

by the inequality (5.2.2). Therefore, $\mathbf{E}[(S''_\lambda \mathbb{1}_{\{M_\lambda > 3\lambda^{1-\sigma}\}})^2] \to 0$ as $\lambda \to \infty$.

Now we consider the term $S''_\lambda \mathbb{1}_{\{M_\lambda \leq 3\lambda^{1-\sigma}\}}$. We write $\tilde{\Delta}_i := \Delta_i \mathbb{1}_{A_i}$ so that $\Delta_i \mathbb{1}_{A_i} \equiv \tilde{\Delta}_i \mathbb{1}_{A_i}$. Then,

$$|S''_\lambda \mathbb{1}_{\{M_\lambda \leq 3\lambda^{1-\sigma}\}}| \leq \sum_{i=1}^{\lfloor 3\lambda^{1-\sigma} \rfloor} |\Delta_i \mathbb{1}_{A_i}| \mathbb{1}_{\{M_\lambda \leq 3\lambda^{1-\sigma}\}} \leq \sum_{i=1}^{\lfloor 3\lambda^{1-\sigma} \rfloor} |\tilde{\Delta}_i| \mathbb{1}_{A_i}. \tag{6.4.6}$$

Squaring and applying the expectation over S''_λ given in (6.4.6), hence the right hand side yields

$$\mathbf{E}[(S''_\lambda \mathbb{1}_{\{M_\lambda \leq 3\lambda^{1-\sigma}\}})^2] \leq \sum_{i,j=1}^{\lfloor 3\lambda^{1-\sigma} \rfloor} \mathbf{E}[|\tilde{\Delta}_i||\tilde{\Delta}_j| \mathbb{1}_{A_i \cap A_j}]. \tag{6.4.7}$$

We apply the Cauchy-Schwarz inequality (twice) to each term in the sum in (6.4.7), then

$$\mathbf{E}[|\tilde{\Delta}_i||\tilde{\Delta}_j| \mathbb{1}_{A_i \cap A_j}] \leq \mathbf{E}[(\tilde{\Delta}_i \tilde{\Delta}_j)^2]^{\frac{1}{2}} \mathbf{P}(A_i \cap A_j)^{\frac{1}{2}} \leq \mathbf{E}[\tilde{\Delta}_i^4]^{\frac{1}{4}} \mathbf{E}[\tilde{\Delta}_j^4]^{\frac{1}{4}} \mathbf{P}(A_i \cap A_j)^{\frac{1}{2}},$$

which yields

$$\mathbf{E}[(S''_\lambda \mathbb{1}_{\{M_\lambda \leq 3\lambda^{1-\sigma}\}})^2] \leq \sum_{i,j=1}^{\lfloor 3\lambda^{1-\sigma} \rfloor} \mathbf{E}[\tilde{\Delta}_i^4]^{\frac{1}{4}} \mathbf{E}[\tilde{\Delta}_j^4]^{\frac{1}{4}} \mathbf{P}(A_i \cap A_j)^{\frac{1}{2}}. \tag{6.4.8}$$

Here we want to find $\mathbf{P}(A_i \cap A_j)$ appears in (6.4.8). To do so, we let $\mathbf{P}(A_i \cap A_j) \leq \mathbf{P}(W_\lambda > 0)$, where W_λ is the number of points of $\mathcal{P}_\lambda$ in $E_i \cup E_j$. Since $|E_i \cup E_j| \leq c\lambda^{-2\sigma}$ (because $|E_i \cup E_j| \leq |E_i| + |E_j|$ and each E is a triangle with area at most $c_\phi \lambda^{-2\sigma}$, for some constant $c_\phi > 0$). So W_λ is a Poisson random variable with parameter less than or equal to $c_\phi \lambda^{1-2\sigma}$, then $\mathbf{E}[W_\lambda] \leq c\lambda^{1-2\sigma}$ for $\sigma > \frac{1}{2}$. Hence, by Markov's inequality

$$\mathbf{P}(A_i \cap A_j) \leq \mathbf{P}(W_\lambda \geq 1) \leq c\lambda^{1-2\sigma}, \text{ for } \sigma > \frac{1}{2}. \tag{6.4.9}$$

Now we need to find an upper bound for $\mathbf{E}[\tilde{\Delta}_i^4]$ that appears in (6.4.8). At this point the proof deviates from the one for the obtuse case. For the obtuse case we showed that the length Δ_i was close to the one-dimensional distance $|X_{J(i)} - X_i|$ (see inequality (6.3.12)). In the acute case, as we will see, the corresponding argument

only yields an upper bound on Δ_i in terms of two-dimensional distance $\|Z_{K(i)} - Z_i\|$ and we need an additional argument to bound Δ_i in terms of an appropriate one-dimensional distance. Given $J(i) < \infty$ and $K(i) < \infty$, by the definition of $J(i)$, we have $X_{K(i)} \leq X_{J(i)}$, so

$$|X_{J(i)} - X_i| \leq |X_{K(i)} - X_i| \leq \|Z_{K(i)} - Z_i\|. \tag{6.4.10}$$

Hence $0 \leq \Delta_i \leq \|Z_{K(i)} - Z_i\|$. Note that $\|Z_{K(i)} - Z_i\|$ is the long two-dimensional distance. So we need to work out to find the upper bound in terms of one-dimensional distance, and this is provided by the following two statements.

First, if $\tilde{J}(i) = \infty$, then set $\{X_j : X_j < X_i - \lambda^{-\sigma}\cot(\phi), j < i\}$ is empty. But $K(i) < i$ since $Z_{K(i)} \in C_{\theta,\phi}(Z_i)$ so the inequality $X_{K(i)} \geq X_i - \lambda^{-\sigma}\cot\phi$ must hold to avoid a contradiction. Then, by triangle inequality

$$\|Z_{K(i)} - Z_i\| \leq \lambda^{-\sigma} + |X_{K(i)} - X_i| \leq \lambda^{-\sigma} + \lambda^{-\sigma}\cot(\phi) \leq \lambda^{-\sigma}(1 + \cot(\phi)). \tag{6.4.11}$$

Second, if $\tilde{J}(i) < \infty$, we know $Z_{\tilde{J}(i)} \notin E_i$ and so $Z_{\tilde{J}(i)} \in C_{\theta,\phi}(Z_i)$. Then by definition 6.4.3 of $I(i)$ along with triangle inequality, we have

$$\begin{aligned}
\|Z_{K(i)} - Z_i\|\mathbb{1}_{\{\tilde{J}(i)<\infty\}} &\leq \|Z_{\tilde{J}(i)} - Z_i\|\mathbb{1}_{\{\tilde{J}(i)<\infty\}} \\
&\leq \left(|X_{\tilde{J}(i)} - X_i| + \lambda^{-\sigma}\right)\mathbb{1}_{\{\tilde{J}(i)<\infty\}} \\
&\leq \left(|X_{\tilde{J}(i)} - X_{I(i)}| + |X_{I(i)} - X_i| + \lambda^{-\sigma}\right)\mathbb{1}_{\{\tilde{J}(i)<\infty\}} \\
&\leq \left(|X_{\tilde{J}(i)} - X_{I(i)}| + \lambda^{-\sigma}(1 + \cot(\phi))\right)\mathbb{1}_{\{\tilde{J}(i)<\infty\}}.
\end{aligned}$$

In term of $\tilde{\Delta}_i = \Delta_i \mathbb{1}_{A_i}$, the upper bound of $\tilde{\Delta}_i$ is given by the following inequality

$$0 \leq \tilde{\Delta}_i \leq |X_{\tilde{J}(i)} - X_{I(i)}|\mathbb{1}_{\{\tilde{J}(i)<\infty\}} + \lambda^{-\sigma}(1 + \cot(\phi)) \leq \max_j I_{i,j} + \lambda^{-\sigma}(1 + \cot(\phi)). \tag{6.4.12}$$

For the final inequality, we used that $X_{\tilde{J}(i)}$, $X_{I(i)}$ are a consecutive pair of order statistics and therefore equal to $I_{i,j}$ for some $j \in \{1, \ldots, i+1\}$. From (6.4.12), we need to find the 4^{th} moments of $\tilde{\Delta}_i$, hence

$$\tilde{\Delta}_i^4 \leq 2^4 \cdot (\max_j I_{i,j}^4 + (\lambda^{-\sigma}(1 + \cot\phi))^4). \tag{6.4.13}$$

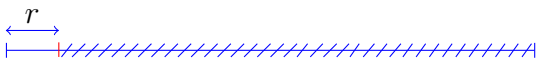

Figure 6.6: We look at the most left spacing, so the distance here is $\mathbf{P}(I_{i,j} > r) = \int_r^1 i(1-x)^{i-1}dx = (1-r)^i$, i.e., the probability of this event $I_{i,j} > r$ if and only if there is no points to the right.

To calculate the 4^{th} moments of $\tilde{\Delta}_i$, we first need to find the marginal probability density function (pdf) of the spacing. Let $I_{i,j} \sim \beta(1,i)$, where β is Beta distribution and i is number of points. The pdf is given as follows, $f_{I_{i,j}}(x) = i(1-x)^{i-1}$ (e.g. see Figure 6.6). The $\mathbf{P}(I_{i,j} > r) = (1-r)^i$ for all $j = 1, \ldots, i+1$. The probability of the maximum over all j given by

$$\mathbf{P}(\max_j I_{i,j} > r) = \mathbf{P}(\cup_{j=1}^{i+1}\{I_{i,j} > r\}) \leq (i+1)(1-r)^i \leq (i+1)e^{-ir},$$

which holds for all $r \geq 0$. Choosing $r = \frac{5\log i}{i}$, gives $\mathbf{P}\left(\max_j I_{i,j} > \frac{5\log i}{i}\right) \leq 2i^{-4}$. Since $I_{i,j} \leq 1$ for all j, we have

$$\max_j I_{i,j}^4 \leq \left(\frac{5\log i}{i}\right)^4 \mathbb{1}_{\max_j I_{i,j}^4 \leq \left(\frac{5\log i}{i}\right)^4} + \mathbb{1}_{\max_j I_{i,j}^4 > \left(\frac{5\log i}{i}\right)^4}. \tag{6.4.14}$$

Apply the expectation over $\max_j I_{i,j}^4$ appears in (6.4.14), hence

$$\begin{aligned}\mathbf{E}(\max_j I_{i,j}^4) &\leq \left(\frac{5\log i}{i}\right)^4 + \mathbf{P}\left(\max_j I_{i,j}^4 > \left(\frac{5\log i}{i}\right)^4\right) \\ &\leq \left(\frac{5\log i}{i}\right)^4 + \frac{2}{i^4} \leq \frac{627\log^4 i}{i^4}, \quad \text{for} \quad i \geq 3. \end{aligned} \tag{6.4.15}$$

Combining inequalities (6.4.13) and (6.4.15) yields

$$\mathbf{E}[\tilde{\Delta}_i^4] \leq \frac{2^4 C\log^4 i}{i^4} + 2^4\lambda^{-4\sigma}(1+\cot\phi)^4 = \frac{2^4 C\log^4 i}{i^4} + 2^4 c''\lambda^{-4\sigma}. \tag{6.4.16}$$

Combining (6.4.8), (6.4.9), and (6.4.16), results

$$\begin{aligned}
\mathbf{E}[(S''_\lambda \mathbb{1}_{\{M_\lambda \le 3\lambda^{1-\sigma}\}})^2] &\le \left(c\lambda^{1-2\sigma}\right)^{\frac{1}{2}} \left(\sum_{i=1}^{\lfloor 3\lambda^{1-\sigma} \rfloor} \mathbf{E}[\tilde{\Delta}_i^4]^{\frac{1}{4}} \right)^2 \\
&\le c'\lambda^{\frac{1}{2}-\sigma} \left(\sum_{i=1}^{\lfloor 3\lambda^{1-\sigma} \rfloor} \left(\frac{2^4 C \log^4 i}{i^4} + 2^4 c'' \lambda^{-4\sigma} \right)^{\frac{1}{4}} \right)^2 \\
&\le c'\lambda^{\frac{1}{2}-\sigma} \left(2C \sum_{i=1}^{\lfloor 3\lambda^{1-\sigma} \rfloor} \left(\frac{\log i}{i} + 2c''\lambda^{-\sigma} \right) \right)^2 \\
&\le c''\lambda^{\frac{1}{2}-\sigma} \left((\log(3\lambda^{1-\sigma}))^2 + \lambda^{1-2\sigma} \right)^2 \ \to 0, \text{ as } \lambda \to \infty, \text{ for } \sigma > \frac{1}{2},
\end{aligned} \tag{6.4.17}$$

where $\left(\sum_{i=1}^{\lfloor 3\lambda^{1-\sigma} \rfloor} \mathbf{E}[\tilde{\Delta}_i^4]^{\frac{1}{4}} \right)^2 = \sum_{i,j=1}^{\lfloor 3\lambda^{1-\sigma} \rfloor} \mathbf{E}[\tilde{\Delta}_i^4]^{\frac{1}{4}} \mathbf{E}[\tilde{\Delta}_j^4]^{\frac{1}{4}}$, and c, c', and c'' are constants. Since $\sigma > \frac{1}{2}$, the right hand-side of (6.4.17) tends to 0 as $\lambda \to \infty$, and hence $S''_\lambda \mathbb{1}_{\{M_\lambda \le 3\lambda^{1-\sigma}\}} \xrightarrow{L^2} 0$ as $\lambda \to \infty$. Note that in line 2 of the above inequality, we use $(a+b)^{\frac{1}{4}} \le a^{\frac{1}{4}} + b^{\frac{1}{4}}$ for $a, b \ge 0$, also in line 4 we use $\sum_{i=1}^{n} \frac{\log i}{i} \le 2\log^2 n$ for all $n > e$.

Finally, we combine (6.4.5) and (6.4.17) with (6.4.4), which completes the proof. □

The proof of Theorem 6.2.3 in the acute case now follows exactly as for the obtuse case.

Proof of Theorem 6.2.3. We combine Lemma 6.4.4 and Lemma 6.4.5 and apply Minkowski's inequality to S'_λ and S''_λ, which yields $S_\lambda = S'_\lambda + S''_\lambda \xrightarrow{L^2} 0$, as $\lambda \to \infty$. □

6.5 Convergence to Boundary Limit

In this section, we derive the proof of Theorem 6.1.1 for both singly-aligned cones since the proof is identical for both obtuse case and acute case. Theorem 6.1.1 plays a significant role in our analysis in which the approximation process to one-dimensional distance holds due to the boundary effect. These boundary effects can

be characterized by the fixed point equation given by (3.4.1). Recall that Theorem 6.1.1 states that the total edge length $\tilde{\mathcal{L}}_\lambda^3$ converges in distribution to Q, where the distribution of $Q \sim \mathcal{Q}$ given by the fixed point equation (3.4.1) as the number of points tends to infinity.

Proof of Theorem 6.1.1

Proof. Recall that, Q_n is the total length of the DLF(n). Define $q_n := \mathbf{E}[Q_n]$, then

$$q_n = \sum_{i=2}^{n} \frac{1}{i+1} = \log(n+1) + c + O\left(\frac{1}{n}\right), \text{where } c = \gamma - \frac{3}{2}, \tag{6.5.1}$$

for γ denotes Euler's constant, in other words, $\gamma = \lim_{n\to\infty}\left(\sum_{i=1}^{n} \frac{1}{i} - \log n\right)$, (see e.g. [1]).

By definition, $q_{M_\lambda} = \sum_{n=0}^{\infty} q_n \mathbb{1}_{\{M_\lambda = n\}} = \mathbf{E}[Q_{M_\lambda}|M_\lambda]$, where $M_\lambda \sim \mathbf{Po}(\lambda^{1-\sigma})$. By the strong law of large numbers, $M_\lambda \overset{a.s.}{\to} \infty$ as $\lambda \to \infty$.

By (6.5.1), there exists a random variable ϵ_λ and a constant $C < \infty$ such that

$$q_{M_\lambda} = \log(M_\lambda + 1) + c + \epsilon_\lambda, \tag{6.5.2}$$

where $|\epsilon_\lambda| \leq \frac{C}{M_\lambda+1}$ and hence $\epsilon_\lambda \to 0$ a.s. as $\lambda \to \infty$.

Now observe that, by the strong law of large numbers for the Poisson random variable M_λ and continuity of log, we have

$$\log(M_\lambda+1) - \log \lambda^{1-\sigma} = \log\left(\frac{M_\lambda+1}{\lambda^{1-\sigma}}\right) = \log\left(\frac{M_\lambda+1}{\mathbf{E}[M_\lambda]}\right) \overset{a.s.}{\to} 0, \text{ as } \lambda \to \infty. \tag{6.5.3}$$

Next, we apply the expectation over $\log(M_\lambda + 1)$ and we will show that, as $\lambda \to \infty$

$$|\mathbf{E}[\log(M_\lambda + 1)] - \log \lambda^{1-\sigma}| \to 0. \tag{6.5.4}$$

By triangle inequality and Cauchy-Schwarz inequality, we write (6.5.4), as follows

$$\begin{aligned}
|\mathbf{E}[\log(M_\lambda+1)] - \log\lambda^{1-\sigma}| &= |\mathbf{E}[\log(M_\lambda+1)\mathbb{1}_{\{|M_\lambda-\lambda^{1-\sigma}|\le\lambda^{\frac{3}{4}(1-\sigma)}\}}] \\
&\quad + \mathbf{E}[\log(M_\lambda+1)\mathbb{1}_{\{|M_\lambda-\lambda^{1-\sigma}|>\ \lambda^{\frac{3}{4}(1-\sigma)}\}}] - \log\lambda^{1-\sigma}| \\
&\le |\log(\lambda^{1-\sigma}(1+O(\lambda^{-\frac{1}{4}(1-\sigma)})))\mathbb{1}_{\{|M_\lambda-\lambda^{1-\sigma}|\le\lambda^{\frac{3}{4}(1-\sigma)}\}} - \log\lambda^{1-\sigma}| \\
&\quad + \Big(\mathbf{E}[(\log(M_\lambda+1))^2]\cdot\mathbf{P}[|M_\lambda-\lambda^{1-\sigma}|>\lambda^{\frac{3}{4}(1-\sigma)}]\Big)^{\frac{1}{2}} \\
&\le O(\lambda^{-\frac{1}{4}(1-\sigma)}) + \log\lambda^{1-\sigma}\cdot\mathbb{1}_{\{|M_\lambda-\lambda^{1-\sigma}|>\ \lambda^{\frac{3}{4}(1-\sigma)}\}} \\
&\quad + \Big(\mathbf{E}[(\log(M_\lambda+1))^2]\cdot\mathbf{P}[|M_\lambda-\lambda^{1-\sigma}|>\lambda^{\frac{3}{4}(1-\sigma)}]\Big)^{\frac{1}{2}}.
\end{aligned} \tag{6.5.5}$$

By Chernoff bounds on the tail probabilities of a Poisson distribution (e.g., see Corollary 4.6 [24]), that $(\mathbf{P}(|M_\lambda-\lambda^{1-\sigma}|>\lambda^{\frac{3}{4}(1-\sigma)}))^{\frac{1}{2}} \le \exp\{-\frac{1}{3}\lambda^{\frac{1}{2}(1-\sigma)}\}$, hence the inequality (6.5.5) can be written, as follows

$$|\mathbf{E}[\log(M_\lambda+1)] - \log\lambda^{1-\sigma}| \le O(\lambda^{-\frac{1}{4}(1-\sigma)}) + 2\lambda^{1-\sigma}\exp\left\{-\frac{1}{3}\lambda^{\frac{1}{2}(1-\sigma)}\right\} \to 0, \text{ as } \lambda\ \to\infty, \tag{6.5.6}$$

for $\sigma > \frac{1}{2}$, where in the inequality (6.5.5) line 3 we use $\log(1+x) \le x$ for all $x > 0$.

Next we want to show the difference between q_{M_λ} and its expectation is converging to 0 almost surely as $\lambda \to \infty$. To do so, by (6.5.2), (6.5.3), and triangle inequality, we have

$$\begin{aligned}
|q_{M_\lambda} - \mathbf{E}[q_{M_\lambda}]| &= |\log(M_\lambda+1) + c + \epsilon_\lambda - \mathbf{E}[\log(M_\lambda+1)] - c + o(1)| \\
&\le |\log(M_\lambda+1) - \log\lambda^{1-\sigma}| + |\mathbf{E}[\log(M_\lambda+1)] - \log\lambda^{1-\sigma}| + \epsilon_\lambda + o(1) \\
&\overset{a.s.}{\to} 0, \text{ as } \lambda\ \to\infty,
\end{aligned} \tag{6.5.7}$$

where we reserve $o(1)$ for non-random sequence.

It remains to compare $|q_{M_\lambda} - \mathbf{E}[Q_{M_\lambda}]|$ with inequality (6.5.7) using the fact that for all $n \in \mathbb{Z}_+$, we have from (6.5.1) that

$$|q_n - (\gamma - \frac{3}{2}) - \log(n+1)| \le \frac{c}{n+1}. \tag{6.5.8}$$

Here we replace the error term appears in (6.5.8), so by triangle inequality, we have

$$\begin{aligned}|q_{M_\lambda} - \mathbf{E}[Q_{M_\lambda}]| &\leq |q_{M_\lambda} - (\gamma - 3/2) - \log(M_\lambda + 1)| \\ &\quad + |-\mathbf{E}[q_{M_\lambda}] + (\gamma - 3/2) + \mathbf{E}[\log(M_\lambda + 1)]| \\ &\quad + |\log(M_\lambda + 1) - \mathbf{E}[\log(M_\lambda + 1)]| \\ &\leq \frac{c}{M_\lambda + 1} + \mathbf{E}\left[\frac{c}{M_\lambda + 1}\right] + |\log(M_\lambda + 1) - \mathbf{E}[\log(M_\lambda + 1)]|,\end{aligned}$$

since $M_\lambda \overset{a.s.}{\to} \infty \; as \; \lambda \to \infty$, the last term of the inequality almost surely convergence to 0, as $\lambda \to \infty$, also by (6.5.7). Where $\mathbf{E}\left[\frac{c}{M_\lambda+1}\right] = \frac{c}{\lambda^{1-\sigma}} \to 0$, as $\lambda \to \infty$, thus by Slutsky's theorem the right-hand side converges almost surely to 0 as $\lambda \to \infty$.

Finally, it remains to show that as $\lambda \to \infty$, $\tilde{\mathcal{L}}^3_\lambda \overset{d}{\to} Q$, where the distribution of $Q \sim \mathcal{Q}$ characterized by the fixed point equation (3.4.1). Recall that $\tilde{\mathcal{L}}^3_\lambda = \mathcal{L}^3_\lambda - \mathbf{E}[\mathcal{L}^3_\lambda]$. We use the above calculations to obtain the proof of Theorem 6.1.1. Hence,

$$\tilde{\mathcal{L}}^3_\lambda = (\mathcal{L}^3_\lambda - Q_{M_\lambda}) + (Q_{M_\lambda} - q_{M_\lambda}) + (q_{M_\lambda} - \mathbf{E}[q_{M_\lambda}]) + (\mathbf{E}[q_{M_\lambda}] - \mathbf{E}[\mathcal{L}^3_\lambda]). \quad (6.5.9)$$

The first bracket converges in L^2 and hence in $\mathbf{P}$ to 0, as $\lambda \to \infty$ by Theorem 6.2.3, note that Q_{M_λ} as defined here is the same as $D(\mathscr{U}_\lambda)$ appearing in Theorem 6.2.3. The second bracket converges in distribution to Q, as $\lambda \to \infty$ by Theorem 6.2.2, where Q given by equation (3.4.1), here we use that $M_\lambda \to \infty$, a.s. as $\lambda \to \infty$. The third bracket converges $a.s.$ to 0, as $\lambda \to \infty$ by inequality (6.5.7). The final bracket converges to 0, as $\lambda \to \infty$. To see this, note that $\mathbf{E}[q_{M_\lambda}] = \mathbf{E}[Q_{M_\lambda}]$ and Theorem 6.2.3 implies L^2 convergence of $Q_{M_\lambda} - \mathcal{L}^3_\lambda$ to 0, hence $\mathbf{E}[|Q_{M_\lambda} - \mathcal{L}^3_\lambda|] \to 0$, as $\lambda \to \infty$. Hence, by Slutsky's theorem we obtain the proof of Theorem 6.1.1. □

Chapter 7

Asymptotic Independence

7.1 Introduction

This chapter illustrates the analysis of the asymptotic independence between the bulk and bottom boundary of the unit square. In Section 7.2, we will introduce Theorem 7.2.1 shortly, which states that the contribution to the total edge lengths from points in of $\mathcal{R}_\lambda^2$ (intermediate region) has variance converging to zero as the intensity λ tends to infinity. This theorem holds for both singly-aligned cones (obtuse and acute angles) in the unit square. In Section 7.4 we prove part (ii) of our main Theorem 3.3.2 stated in Chapter 3 for both singly-aligned cones in the unit square.

7.2 Intermediate Region for both Singly-Aligned Cones

We turn our attention to the area of $\mathcal{R}_\lambda^2$ in the unit square. The purpose of introducing this the intermediate region will, asymptotically, contain enough points to ensure that the contribution of the bulk to the total edge length does not interfere with the contribution from bottom region, and vice versa, within the unit square. This provides the asymptotic independence. We will show shortly that the limiting distribution is given by the sum of a normal component in the bulk and a non-normal

component arising from edges near boundary of $[0,1]^2$, whose distribution can be characterized by a fixed-point equation (3.4.1) Recall that $\xrightarrow{d}$ denotes convergence in distribution.

Theorem 3.3.2 (ii). *If (θ,ϕ) is singly-aligned, then*

$$\tilde{\mathcal{L}_\lambda} \xrightarrow{d} s_\phi Z + Q_1, \quad as \quad \lambda \to \infty,$$

where Z & Q_1 are independent with $Z \sim \mathcal{N}(0,1)$ and $Q_1 \sim \mathcal{Q}$.

We will prove part (ii) of Theorem 3.3.2 for both singly-aligned cones.

Now we start defining the intermediate region with respect to the unit square. Recall by the Definition 4.5.1 for $\sigma \in (\frac{1}{2},\frac{2}{3})$ that $\mathcal{R}_\lambda^2 = [0,1]\times[\lambda^{-\sigma}, RS]$, for R given in Lemmas 4.4.6 and 4.4.7 for singly-aligned cones; also recall $\mathcal{R}_\lambda^3 = [0,1]\times[0,\lambda^{-\sigma}]$. Recall by the Definition 2.4.1 of $\mathcal{P}_\lambda$ is a homogeneous Poisson point process on $[0,1]^2$ with intensity λ. Recall by the Definition of 4.5.2 that $\mathcal{L}_\lambda^2 = \sum_{\boldsymbol{x}\in\mathcal{P}_\lambda\cap\mathcal{R}_\lambda^2} \mathcal{D}_{\theta,\phi}(\boldsymbol{x},\mathcal{P}_\lambda)$, where $\mathcal{D}_{\theta,\phi}(\boldsymbol{x},\mathcal{P}_\lambda)$ is the distance from point $\boldsymbol{x}$ to its nearest neighbour in $\mathcal{P}_\lambda \cap C_{\theta,\phi}(\boldsymbol{x})$, and $\tilde{\mathcal{L}_\lambda^2} = \mathcal{L}_\lambda^2 - \mathbf{E}[\mathcal{L}_\lambda^2]$ is centered random variable. The principal result of this section is the following theorem.

Theorem 7.2.1. *Let $\tilde{\mathcal{L}_\lambda^2}$ be defined as above. Then, as $\lambda\to\infty$,*

$$\tilde{\mathcal{L}_\lambda^2} \xrightarrow{\mathbf{P}} 0. \tag{7.2.1}$$

Before we start working on the proof of Theorem 7.2.1, we require certain preliminary results and notations. Recall $S = \frac{1}{k_\lambda}$. We partition $\mathcal{R}_\lambda^2$ region into $\ell_\lambda = \left\lfloor \frac{\lambda^{1-\sigma}}{c\log^2\lambda} \right\rfloor$ cells $\Gamma_i, i = 1,\dots,\ell_\lambda$ (from left to right) of height $RS - \lambda^{-\sigma}$ and width $\frac{1}{\ell_\lambda}$. Similarly, partition $\mathcal{R}_\lambda^3$ region into cells β_i, $i = 1,\dots,\ell_\lambda$ (also from left to right) of height $\lambda^{-\sigma}$ and width $\frac{1}{\ell_\lambda}$, see Figure 7.1. For each $i = 1,\dots,\ell_\lambda$ define $X_i := \sum_{\boldsymbol{x}\in\mathcal{P}_\lambda\cap\Gamma_i} \mathcal{D}_{\theta,\phi}(\boldsymbol{x},\mathcal{P}_\lambda)$ and define $\tau_i = \{|\mathcal{P}_\lambda \cap \beta_i| > 0\}$ as the event that β_i contains at least one point of Poisson process $\mathcal{P}_\lambda$. Recall that $a_\lambda = \sqrt{\frac{c\log\lambda}{\lambda}}$ for large enough λ, and also, recall $k_\lambda = \left\lfloor \frac{1}{a_\lambda} \right\rfloor$. The ratio of the height and width of the cells Γ_i given by

$$\frac{\text{height}(\Gamma_i)}{\text{width}(\Gamma_i)} = \left(\frac{R}{k_\lambda} - \lambda^{-\sigma}\right)\cdot\left\lfloor\frac{\lambda^{1-\sigma}}{c\log^2\lambda}\right\rfloor \sim \sqrt{\frac{\log\lambda}{\lambda}}\cdot\frac{\lambda^{1-\sigma}}{c\log^2\lambda} \to 0, \quad \text{as} \quad \lambda\to\infty.$$

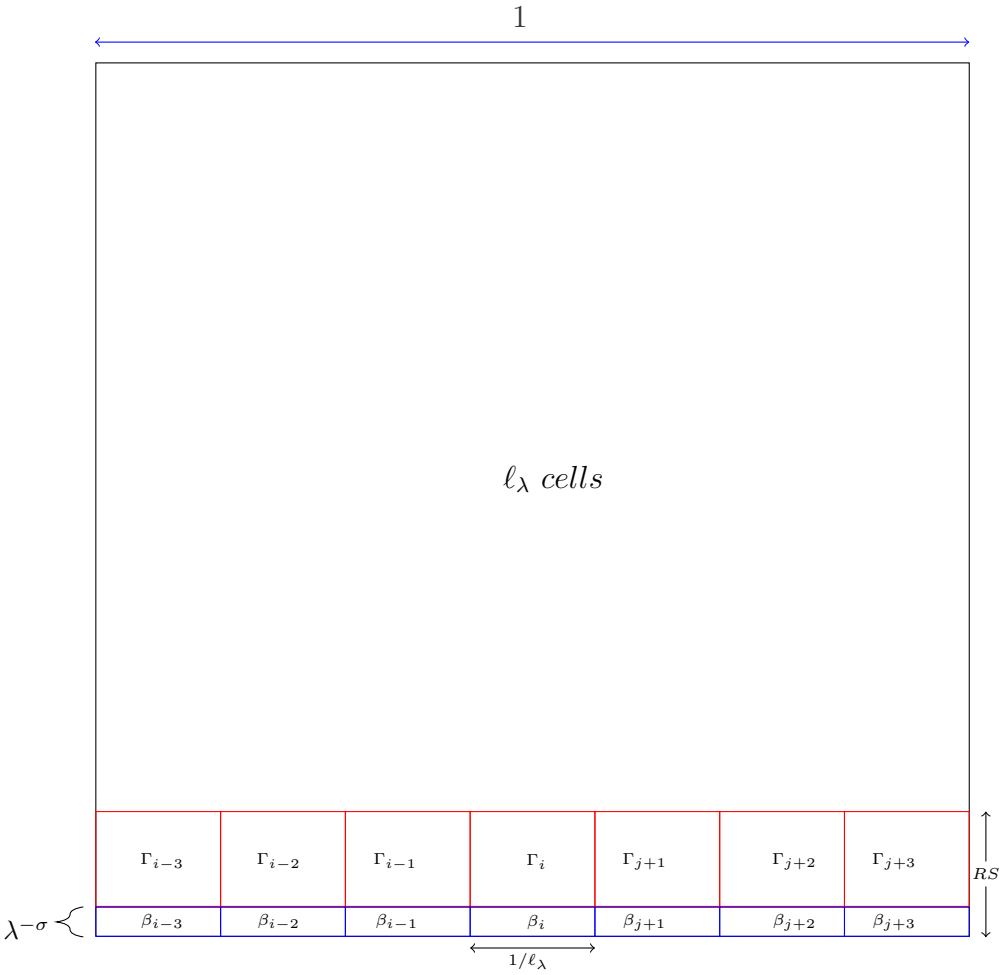

Figure 7.1: Partitioning the regions of $\mathcal{R}^2_\lambda$ and $\mathcal{R}^3_\lambda$ in $[0,1]^2$.

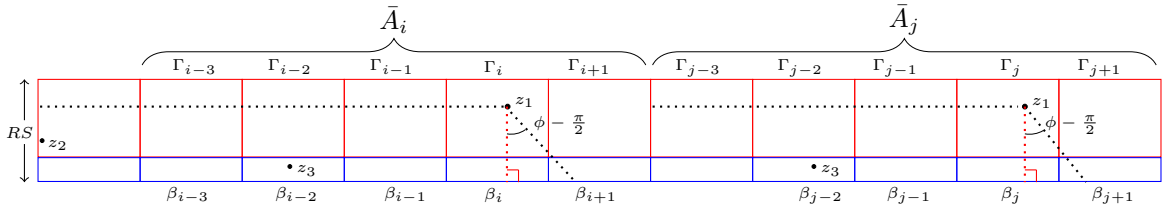

Figure 7.2: Obtuse angle; the regions of the unit square where $X_i \mathbb{1}_{\tau_{i-2}}$ depends only on $\mathcal{P}_\lambda \cap \bar{A}_i$ and $X_j \mathbb{1}_{\tau_{j-2}}$ depends only on $\mathcal{P}_\lambda \cap \bar{A}_j$.

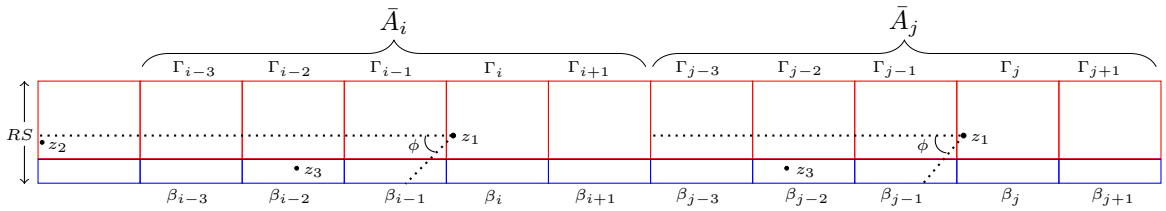

Figure 7.3: Acute angle; the regions of the unit square where $X_i \mathbb{1}_{\tau_{i-2}}$ depends only on $\mathcal{P}_\lambda \cap \bar{A}_i$ and $X_j \mathbb{1}_{\tau_{j-2}}$ depends only on $\mathcal{P}_\lambda \cap \bar{A}_j$.

Let $\bar{A}_i$ be the region in $\mathcal{R}^2_\lambda$ such that $\bar{A}_i = \bigcup_{i-3\le \ell \le i+1}(\Gamma_j \cup \beta_j)$. In the following lemma, we show for large enough λ, the random variable $\mathbb{1}_{\tau_{i-2}} X_i$ is determined by $\mathcal{P}_\lambda \cap \bar{A}_i$ because $\bar{A}_i$ and $\bar{A}_j$ are disjoint sets for $|i-j| > 4$, similarly for $\bar{A}_j$, see Figures 7.2 and 7.3.

Lemma 7.2.2. *For $i, j = 1, \dots, \ell_\lambda$ with $|i-j| > 4$. The random variables $\mathbb{1}_{\tau_{i-2}} X_i$ and $\mathbb{1}_{\tau_{j-2}} X_j$ are independent (with the convention that $\tau_{-1} = \tau_0 = \Omega$).*

Proof. First we show that given τ_{i-2}, the nearest-neighbour of any point in $\mathcal{P}_\lambda \cap \Gamma_i$ must lie in $\bar{A}_i$ (for sufficiently large λ). Let $z_1 \in \mathcal{P}_\lambda \cap \Gamma_i$. For all $i = 1, \dots, \ell_\lambda$, the nearest neighbour of z_1 can not be in $\bigcup_{j>i+1}(\Gamma_j \cup \beta_j)$. This is immediate for the acute cone, for the obtuse cone we need to check that for $z_2 \in C_{\theta,\phi}(z_1)$ with $x_2 > x_1$ then $z_2 \in \bar{A}_i$. Hence,

$$x_2 - x_1 < RS \tan\left(\phi - \frac{\pi}{2}\right) < \frac{1}{\ell_\lambda}, \tag{7.2.2}$$

which holds for large enough λ.

Hence for $i = 1, 2, 3, 4$, the nearest-neighbour of z_1 can only be found in $\bar{A}_i$. For $i \ge 5$, given that τ_{i-2} occurs, take $z_3 \in \mathcal{P}_\lambda \cap \beta_{i-2}$. Note that z_3 is in $C_{\theta,\phi}(z_1)$ for large enough λ, and hence a candidate nearest neighbour for z_1. This is true for all λ for the obtuse case (since $x_3 < x_1$ and $y_3 < y_1$), and for the acute case, we observe that

$$x_3 < x_1 - \frac{1}{\ell_\lambda} < x_1 - RS\cot\phi, \tag{7.2.3}$$

since $S = O(a_\lambda) = O\left(\sqrt{\frac{\log\lambda}{\lambda}}\right) = o(\frac{1}{\ell_\lambda})$ because $\frac{1}{\ell_\lambda} \ge \frac{\log^2\lambda}{\lambda^{1-\sigma}}$ and $\sigma > \frac{1}{2}$. Inequality (7.2.3) and $y_3 < y_1$ implies $z_3 \in C_{\theta,\phi}(z_1)$.

Now suppose $z_2 \in C_{\theta,\phi}(z_1)$ but not in $\bar{A}_i$ (see Figures 7.2 and 7.3). By the earlier reasoning we must have $x_2 < x_3 - \frac{1}{\ell_\lambda}$ since z_2 is to the left of cell Γ_{i-3}. We want to show that the Euclidean distance between points z_1 and $z_3 \in \beta_{i-2}$ is much smaller than the distance between $z_1 \in \Gamma_i$ and $z_2 \notin \bar{A}_i$. Since $S = o(\frac{1}{\ell_\lambda})$, for large enough λ, we have

$$\|z_2 - z_1\| \geq |x_2 - x_1| > |x_2 - x_1| - \frac{1}{\ell_\lambda} + RS \geq |x_3 - x_1| + |y_3 - y_1| \geq \|z_3 - z_1\|,$$

hence z_2 is not a nearest neighbour of z_1.

We deduce that the random variable $\mathbb{1}_{\tau_{i-2}} X_i$ is determined by $\mathcal{P}_\lambda \cap \bar{A}_i$. Indeed, either τ_{i-2} does not occur (not possible for $i = 1$ or 2) meaning β_{i-2} is empty and $\mathbb{1}_{\tau_{i-2}} X_i \equiv 0$; otherwise τ_{i-2} occurs and $X_i = \sum_{\boldsymbol{x} \in \mathcal{P}_\lambda \cap \Gamma_i} \mathcal{D}_{\theta,\phi}(\boldsymbol{x}, \mathcal{P}_\lambda)$ is the sum of nearest neighbour distances, where each distance $\mathcal{D}_{\theta,\phi}(\boldsymbol{x}, \mathcal{P}_\lambda)$ is determined by $\mathcal{P}_\lambda \cap \bar{A}_i$.

Finally, for $|i - j| > 4$, the region $\bar{A}_i$ and $\bar{A}_j$ are disjoint, so the random variables $\mathbb{1}_{\tau_{i-2}} X_i$ and $\mathbb{1}_{\tau_{j-2}} X_j$ depend on disjoint regions of Poisson process $\mathcal{P}_\lambda$, so are independent. □

To prove Theorem 7.2.1, it is enough to show that the variance of $\mathcal{L}_\lambda^2$ converges to 0 as the intensity λ tends to infinity, where this is provided in the following lemma.

Lemma 7.2.3. *As $\lambda \to \infty$,*

$$\mathbf{Var}[\mathcal{L}_\lambda^2] \to 0. \tag{7.2.4}$$

Proof. For simplicity of notation, we write $\mathcal{L}_\lambda^2 = \sum_{i=1}^{\ell_\lambda} X_i$, where $X_i = X_i \mathbb{1}_{\tau_{i-2}} + X_i \mathbb{1}_{\tau_{i-2}^{\complement}}$, for $i = 1, \ldots, \ell_\lambda$, then

$$\mathbf{Var}(\mathcal{L}_\lambda^2) = \mathbf{Var}\left(\sum_{i=1}^{\ell_\lambda} X_i\right) = \mathbf{Var}\left(\sum_{i=1}^{\ell_\lambda} X_i \mathbb{1}_{\tau_{i-2}} + \sum_{i=1}^{\ell_\lambda} X_i \mathbb{1}_{\tau_{i-2}^{\complement}}\right). \tag{7.2.5}$$

To show $\mathbf{Var}(\mathcal{L}_\lambda^2) \to 0$, it is enough to see that $\mathbf{Var}\left(\sum_{i=1}^{\ell_\lambda} X_i \mathbb{1}_{\tau_{i-2}}\right) \to 0$ and $\mathbf{Var}\left(\sum_{i=1}^{\ell_\lambda} X_i \mathbb{1}_{\tau_{i-2}^{\complement}}\right) \to 0$, as $\lambda \to \infty$. To see this, we make use of the fact that if Y

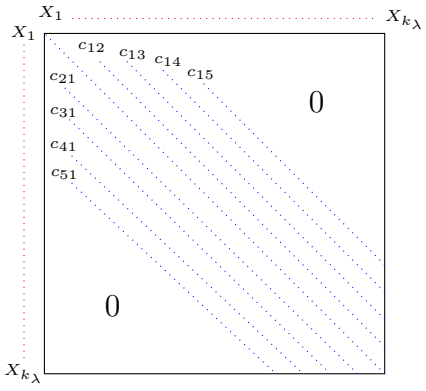

Figure 7.4: Here $c_{ij} = \mathbf{Cov}(X'_i, X'_j)$, which is 0 if $|i-j| > 4$ by Lemma 7.2.2. For fixed i, condition $|i-j| \leq 4$, means we get at most 9-choices of j. The number of non-zero covariances is most $9\ell_\lambda$.

and Z are random variables, then $\mathbf{Var}(Y+Z) = \mathbf{Var}(Y) + \mathbf{Var}(Z) + 2\mathbf{Cov}(Y,Z) \leq \mathbf{Var}(Y) + \mathbf{Var}(Z) + 2\sqrt{\mathbf{Var}(Y)\mathbf{Var}(Z)}$ by Cauchy-Schwarz inequality.

Here we set $X'_i = X_i \mathbb{1}_{\tau_{i-2}}$. Observe that $\mathbf{Cov}(X'_i, X'_j) = 0$, if $|i-j| > 4$ for large enough λ by Lemma 7.2.2. Therefore, (see Figure 7.4) that

$$\begin{aligned}\mathbf{Var}\left(\sum_{i=1}^{\ell_\lambda} X'_i\right) = \sum_{i,j=1}^{\ell_\lambda} \mathbf{Cov}(X'_i, X'_j) = \sum_{\substack{i,j=1 \\ |i-j|\leq 4}}^{\ell_\lambda} \mathbf{Cov}(X'_i, X'_j) &\leq 9\ell_\lambda \max_{i,j} \mathbf{Cov}(X'_i, X'_j) \\ &\leq 9\ell_\lambda \max_i \mathbf{Var}(X'_i),\end{aligned} \tag{7.2.6}$$

where the last inequality follows from Cauchy-Schwarz inequality.

Now, we want to find the $\max_i \mathbf{Var}(X'_i)$. Recall by definitions of $\ell_\lambda = \left\lfloor \frac{\lambda^{1-\sigma}}{c\log^2\lambda} \right\rfloor$ and $a_\lambda = \sqrt{\frac{c\log\lambda}{\lambda}}$ for large enough λ. We need first to find $|X'_i|$ using the fact that $\mathbf{Var}(X'_i) \leq \mathbf{E}[(X'_i)^2]$, then

$$|X'_i| \leq |\mathcal{P}_\lambda \cap \Gamma_i| \frac{5}{\ell_\lambda}, \tag{7.2.7}$$

since (see proof of Lemma 7.2.2) given τ_{i-2}, the nearest neighbour of any $\mathcal{P}_\lambda \cap \Gamma_i$ is in $\bar{A}_i$. Here $|\mathcal{P}_\lambda \cap \Gamma_i|$ is Poisson with

$$\max_i \mathbf{E}[|\mathcal{P}_\lambda \cap \Gamma_i|] \leq \frac{\lambda RS}{\ell_\lambda} = O\left(\lambda^{\sigma-\frac{1}{2}} \log^{\frac{5}{2}} \lambda\right).$$

Squaring $[|X_i'|^2]$ given in (7.2.7) and apply the expectation over $\mathbf{E}[|X_i'|^2]$, hence

$$|X_i'|^2 \leq |\mathcal{P}_\lambda \cap \Gamma_i|^2 \frac{25}{\ell_\lambda^2} \quad \text{and} \quad \mathbf{E}[|\mathcal{P}_\lambda \cap \Gamma_i|^2] = O\left(\left(\lambda^{\sigma-\frac{1}{2}} \log^{\frac{5}{2}} \lambda\right)^2\right). \tag{7.2.8}$$

By comparing (7.2.7) and (7.2.8), we get

$$\max_i \mathbf{Var}(X_i') = O\left(\lambda^{4\sigma-3} \log^9 \lambda\right). \tag{7.2.9}$$

By Cauchy-Schwarz inequality along with (7.2.9), we obtain

$$\begin{aligned} \ell_\lambda \max_i \mathbf{Var}(X_i') &= O\left(\ell_\lambda \lambda^{4\sigma-3} \log^9 \lambda\right) \\ &= O\left(\lambda^{3\sigma-2} \log^7 \lambda\right) \ \to 0, \text{ as } \lambda \ \to \infty, \text{ since } \sigma < \frac{2}{3}. \end{aligned}$$

Hence by (7.2.6), we obatin

$$\mathbf{Var}\left(\sum_{i=1}^{\ell_\lambda} X_i \mathbb{1}_{\tau_{i-2}}\right) \to 0, \quad \text{as} \quad \lambda \to \infty. \tag{7.2.10}$$

Consider $\mathbf{Var}\left(\sum_{i=1}^{\ell_\lambda} X_i \mathbb{1}_{\tau_{i-2}^{\complement}}\right) \leq \mathbf{E}\left(\left(\sum_{i=1}^{\ell_\lambda} X_i \mathbb{1}_{\tau_{i-2}^{\complement}}\right)^2\right)$ using $X_i' \leq \sqrt{2}|\mathcal{P}_\lambda \cap \mathcal{R}_\lambda^2|$, we have

$$\mathbf{E}\left(\left(\sum_{i=1}^{\ell_\lambda} X_i \mathbb{1}_{\tau_{i-2}^{\complement}}\right)^2\right) \leq 2\mathbf{E}\left(|\mathcal{P}_\lambda \cap \mathcal{R}_\lambda^2|^2 \left(\sum_{i=3}^{\ell_\lambda} \mathbb{1}_{\tau_{i-2}^{\complement}}\right)^2\right) \leq 2\mathbf{E}\left(|\mathcal{P}_\lambda \cap \mathcal{R}_\lambda^2|^2\right) \ell_\lambda^2 \cdot \mathbf{P}\left(\tau_1^{\complement}\right), \tag{7.2.11}$$

where the final inequality follows from independence $|\mathcal{P}_\lambda \cap \mathcal{R}_\lambda^2|$ and $\mathbb{1}_{\tau_{i-2}^{\complement}}$, and the Cauchy-Schwarz inequality applied to the identically distributed random variables $\mathbb{1}_{\tau_{i-2}^{\complement}}$, for $i = 1, \ldots, \ell_\lambda$. Then,

$$\mathbf{E}(|\mathcal{P}_\lambda \cap \mathcal{R}_\lambda^2|^2) \leq \mathbf{E}(|\mathcal{P}_\lambda|^2) \leq 2\lambda^2, \tag{7.2.12}$$

and

$$\mathbf{P}\left(\tau_1^{\complement}\right) \leq \exp\{-c \log^2 \lambda\} = O(\lambda^{-10}), \text{ for } \lambda \to \infty. \tag{7.2.13}$$

Combine inequalities (7.2.11), (7.2.12), and (7.2.13) we obtain

$$\mathbf{Var}\left(\sum_{i=1}^{\ell_\lambda} X_i \mathbb{1}_{\tau_{i-2}^{\complement}}\right) = O\left(\lambda^2 \ell_\lambda^2 \lambda^{-10}\right) = O\left(\lambda^{2+2-2\sigma-10}\right) \to 0, \text{ as } \lambda \to \infty. \tag{7.2.14}$$

Finally, by combining inequalities (7.2.10) and (7.2.14), we obtain

$$\mathbf{Var}\left(\sum_{i=1}^{\ell_\lambda} X_i \mathbb{1}_{\tau_{i-2}} + \sum_{i=1}^{\ell_\lambda} X_i \mathbb{1}_{\tau_{i-2}^{\complement}}\right) \to 0, \quad \text{as} \quad \lambda \to \infty.$$

Therefore, the above sums tend to 0 when $\frac{1}{2} < \sigma < \frac{2}{3}$. □

7.3 Asymptotic Independence Between Bulk and Bottom Boundary

In this section, we will demonstrate for both singly-aligned cones the independent relationship between the bulk and bottom boundary of the unit square $[0,1]^2$; specifically between the random variables $\tilde{\mathcal{L}}_\lambda^1$ and $\tilde{\mathcal{L}}_\lambda^3$.

Recall $S = \frac{1}{k_\lambda}$ and by the Definition 4.4.4 that $\mathbb{T}_S = \{p \in \mathbb{Z}^2 : T(p) \subseteq [0,1]^2\}$. Let $\mathcal{C} := \{p = (p_1, p_2) \in \mathbb{Z}^2 : 1 \le p_1, p_2 \le k_\lambda\}$, where $k_\lambda = \left\lfloor \frac{1}{a_\lambda} \right\rfloor$ 'little squares'. Recall by Definition of the regions 4.5.1 of the unit square $[0,1]^2$, specifically, for $\sigma \in (\frac{1}{2}, \frac{2}{3})$, we have

$$\begin{aligned}
\mathcal{R}_\lambda^1 &:= \{(x,y) : 0 \le x \le 1,\ RS \le y \le 1\};\\
\mathcal{R}_\lambda^2 &:= \{(x,y) : 0 \le x \le 1,\ \lambda^{-\sigma} \le y \le RS\};\\
\mathcal{R}_\lambda^3 &:= \{(x,y) : 0 \le x \le 1,\ 0 \le y \le \lambda^{-\sigma}\}.
\end{aligned}$$

Let $\mathcal{C}_1$ be the squares in $\mathbb{T}_S$ corresponding to $\mathcal{R}_\lambda^1$ (bulk region), in other words, $\mathcal{C}_1 = \{p = (p_1, p_2) \in \mathbb{Z}^2 : 1 \le p_1 \le k_\lambda, R+1 \le p_2 \le k_\lambda\}$, so $T(\mathcal{C}_1) = \mathcal{R}_\lambda^1$. Let $\mathcal{C}_2$ be the remaining squares in $\mathbb{T}_S$ excluding the bottom row, i.e., $\mathcal{C}_2 = \{p = (p_1, p_2) \in \mathbb{Z}^2 : 1 \le p_1 \le k_\lambda, 2 \le p_2 \le R\}$ and $\mathcal{C}_3$ be the bottom row, i.e., $\mathcal{C}_3 = \{p = (p_1, 1) \in \mathbb{Z}^2 : 1 \le p_1 \le k_\lambda\}$. Then $T(\mathcal{C}_2 \cup \mathcal{C}_3) = \mathcal{R}_\lambda^2 \cup \mathcal{R}_\lambda^3$ and $T(\mathcal{C}_2) \subseteq \mathcal{R}_\lambda^2$ and $T(\mathcal{C}_3) \subseteq \mathcal{R}_\lambda^3$. Note also that $T(\mathcal{C}_1 \cup \mathcal{C}_2) \subseteq \mathcal{R}_\lambda^1 \cup \mathcal{R}_\lambda^2$.

Let $\mathcal{B}'_\lambda$ be the event such that $\mathcal{B}'_\lambda = \{\mathcal{P}_\lambda \cap T(p) \neq \emptyset\ \forall\ p \in \mathcal{C}_1 \cup \mathcal{C}_2\}$ (meaning every square in $\mathcal{C}_1 \cup \mathcal{C}_2$ contains at least one point of Poisson process $\mathcal{P}_\lambda$). Since $\mathcal{B}_\lambda \subseteq \mathcal{B}'_\lambda$, we have by Lemma 5.2.3 that $\mathbf{P}(\mathcal{B}'_\lambda) \ge \mathbf{P}(\mathcal{B}_\lambda) \to 1$ as $\lambda \to \infty$, then $\mathbf{P}(\mathcal{B}'_\lambda) \to 1$, as $\lambda \to \infty$.

Use the above information and combine with next lemma which gives the asymptotic independence between the random variables $\tilde{\mathcal{L}}_\lambda^1$ and $\tilde{\mathcal{L}}_\lambda^3$. Recall from Definition 4.5.2 that $\mathcal{L}_\lambda^1 = \sum_{\boldsymbol{x}\in\mathcal{P}_\lambda\cap\mathcal{R}_\lambda^1} \mathcal{D}_{\theta,\phi}(\boldsymbol{x},\mathcal{P}_\lambda)$ where $\mathcal{D}_{\theta,\phi}(\boldsymbol{x},\mathcal{P}_\lambda)$ is the distance from point $\boldsymbol{x}$ to its nearest neighbour in $\mathcal{P}_\lambda$ and $\tilde{\mathcal{L}}_\lambda^1 = \mathcal{L}_\lambda^1 - \mathbf{E}[\mathcal{L}_\lambda^1]$ is centred random variable. Recall by the Definition 4.5.2 that $\mathcal{L}_\lambda^3 = \sum_{\boldsymbol{x}\in\mathcal{P}_\lambda\cap\mathcal{R}_\lambda^3} \mathcal{D}_{\theta,\phi}(\boldsymbol{x},\mathcal{P}_\lambda)$, and $\tilde{\mathcal{L}}_\lambda^3 = \mathcal{L}_\lambda^3 - \mathbf{E}[\mathcal{L}_\lambda^3]$ is centered random variable.

Lemma 7.3.1. *Suppose (θ,ϕ) is singly-aligned. The random variables $\tilde{\mathcal{L}}_\lambda^1\mathbb{1}_{\mathcal{B}'_\lambda}$ and $\tilde{\mathcal{L}}_\lambda^3$ are independent.*

Proof. We show $\tilde{\mathcal{L}}_\lambda^1\mathbb{1}_{\mathcal{B}'_\lambda}$ is determined by $\mathcal{P}_\lambda\cap(\mathcal{R}_\lambda^1\cup\mathcal{R}_\lambda^2)$, whereas $\tilde{\mathcal{L}}_\lambda^3$ is determined by $\mathcal{P}_\lambda\cap\mathcal{R}_\lambda^3$. Since $\mathcal{R}_\lambda^1\cup\mathcal{R}_\lambda^2$ and $\mathcal{R}_\lambda^3$ are disjoint, then the random variables $\tilde{\mathcal{L}}_\lambda^1\mathbb{1}_{\mathcal{B}'_\lambda}$ and $\tilde{\mathcal{L}}_\lambda^3$ are independent by the spatial independence property of the Poisson process $\mathcal{P}_\lambda$.

Suppose $\mathcal{B}'_\lambda$ occurs, where $\mathcal{B}'_\lambda$ is determined by $\mathcal{P}_\lambda\cap T(\mathcal{C}_1\cup\mathcal{C}_2)\subseteq\mathcal{P}_\lambda\cap(\mathcal{R}_\lambda^1\cup\mathcal{R}_\lambda^2)$. Lemma 4.4.6 in the obtuse case and Lemma 4.4.7 in the acute case imply that $\mathcal{R}_\lambda^1 = T(\mathcal{C}_1)$ is a compatible bulk, which means that for each $p\in\mathcal{C}_1$ either $p+r\in\mathbb{T}_S$ and $T(\mathcal{S}_{p,\rho(r)})\cap\mathcal{R}_\lambda^3=\emptyset$ for some $r\in C_0$ (Definition 4.4.5, (A)) or $(\cup_{\boldsymbol{x}\in T(p)}C_{\theta,\phi}(\boldsymbol{x}))\cap\mathcal{R}_\lambda^3 = \emptyset$ (Definition 4.4.5, (B_2)), where C_0 is given by Lemmas 4.4.6 & 4.4.7. Now let $\boldsymbol{x}$ be a point in $\mathcal{P}_\lambda\cap\mathcal{R}_\lambda^1$, set $p\in\mathcal{C}_1$ such that $\boldsymbol{x}\in T(p)$. If p satisfies (A), then (noting that $p+r\in\mathcal{S}_{p,\rho(r)}$ implies $T(p+r)\cap\mathcal{R}_\lambda^3=\emptyset$) $\mathcal{P}_\lambda\cap T(p+r)\neq\emptyset$, so we deduce by Theorem 4.2.7 that $N_{\theta,\phi}(\boldsymbol{x};\mathcal{P}_\lambda)\in T(\mathcal{S}_{p,\rho(r)})$, hence $N_{\theta,\phi}(\boldsymbol{x};\mathcal{P}_\lambda)\notin\mathcal{R}_\lambda^3$.

Otherwise, if p satisfies (B_2) then, because $N_{\theta,\phi}(\boldsymbol{x};\mathcal{P}_\lambda)$ is by definition in $C_{\theta,\phi}(\boldsymbol{x})$, we have $N_{\theta,\phi}(\boldsymbol{x};\mathcal{P}_\lambda)\notin\mathcal{R}_\lambda^3$. Hence $\mathcal{L}_\lambda^1 = \sum_{\boldsymbol{x}\in\mathcal{P}_\lambda\cap\mathcal{R}_\lambda^1}\mathcal{D}_{\theta,\phi}(\boldsymbol{x};\mathcal{P}_\lambda)$ is a sum of random variables determined by $\mathcal{P}_\lambda\cap(\mathcal{R}_\lambda^1\cup\mathcal{R}_\lambda^2)$, and therefore $\tilde{\mathcal{L}}_\lambda^1\mathbb{1}_{\mathcal{B}'_\lambda}$ is determined by $\mathcal{P}_\lambda\cap(\mathcal{R}_\lambda^1\cup\mathcal{R}_\lambda^2)$ as claimed.

Finally, it is clear from the geometry of the cone that $N_{\theta,\phi}(\boldsymbol{y};\mathcal{P}_\lambda)\in C_{\theta,\phi}(\boldsymbol{y})\subseteq\mathcal{R}_\lambda^3$ for all $\boldsymbol{y}\in\mathcal{P}_\lambda\cap\mathcal{R}_\lambda^3$, so $\tilde{\mathcal{L}}_\lambda^3$ is determined by $\mathcal{P}_\lambda\cap\mathcal{R}_\lambda^3$. □

7.4 Proof of Theorem 3.3.2 (ii)

In this section, we have all the ingredients to establish the proof of part (ii) of our main result Theorem 3.3.2, which will show the asymptotic independence of the random variable $\tilde{\mathcal{L}}_\lambda^i$ for $i = 1, 2, 3$.

Proof of Theorem 3.3.2 (ii). It is clear that $\tilde{\mathcal{L}}_\lambda^1 \xrightarrow{d} s_\phi Z$ as $\lambda \to \infty$ for some $s_\phi \in (0, \infty)$ using Theorems 5.1.1 & 5.1.2 (compare with proof of Theorem 3.3.2 (iii)). Also, $\tilde{\mathcal{L}}_\lambda^3 \xrightarrow{d} Q_1$ as $\lambda \to \infty$ by Theorem 6.1.1 and $\tilde{\mathcal{L}}_\lambda^2 \xrightarrow{\mathbf{P}} 0$ by Theorem 7.2.1. We show that $\tilde{\mathcal{L}}_\lambda^1 \mathbb{1}_{\mathcal{B}_\lambda'^{\complement}} \xrightarrow{P} 0$ as $\lambda \to \infty$. To see this, for all $\epsilon > 0$, we have

$$\mathbf{P}(|\tilde{\mathcal{L}}_\lambda^1 \mathbb{1}_{\mathcal{B}_\lambda'^{\complement}}| > \epsilon) \leq \mathbf{P}(\mathcal{B}_\lambda'^{\complement}) \leq \mathbf{P}(\mathcal{B}_\lambda^{\complement}) \to 0, \quad \text{as} \quad \lambda \to \infty. \tag{7.4.1}$$

By Slutsky theorem we have that as $\lambda \to \infty$, $\tilde{\mathcal{L}}_\lambda^1 \mathbb{1}_{\mathcal{B}_\lambda'} = \tilde{\mathcal{L}}_\lambda^1 - \tilde{\mathcal{L}}_\lambda^1 \mathbb{1}_{\mathcal{B}_\lambda'^{\complement}} \xrightarrow{d} s_\phi Z$. By the independence and proved in Lemma 7.3.1, we have

$$\tilde{\mathcal{L}}_\lambda^1 \mathbb{1}_{\mathcal{B}_\lambda'} + \tilde{\mathcal{L}}_\lambda^3 \xrightarrow{d} s_\phi Z + Q_1, \text{ as } \lambda \to \infty, \tag{7.4.2}$$

and the random variables Z and Q_1 are independent. Therefore, by (7.4.2) and Slutsky theorem, we obtain our main result

$$\tilde{\mathcal{L}}_\lambda = (\tilde{\mathcal{L}}_\lambda^1 \mathbb{1}_{\mathcal{B}_\lambda'} + \tilde{\mathcal{L}}_\lambda^3) + (\tilde{\mathcal{L}}_\lambda^1 \mathbb{1}_{\mathcal{B}_\lambda'^{\complement}} + \tilde{\mathcal{L}}_\lambda^2) \xrightarrow{d} s_\phi Z + Q_1.$$

Since the first bracket converges in distribution to the random variables $s_\phi Z + Q_1$ and the second bracket converges in probability to 0 as $\lambda \to \infty$ by (7.4.1) and Theorem 7.2.1. □

Chapter 8

Conclusions

8.1 Discussion

Our thesis focuses on analysing the total edge length of the minimal directed spanning forest (MDSF), which an interesting and relevant research topic in the field of graph theory and network analysis. The total edge length is the sum of the lengths of the edges.

We present three main cases: (i) double-aligned cone, (ii) singly-aligned cone, and (iii) unaligned cone. We extend the limit theory of the doubly aligned cone to the case of general cone; here, the limit distribution will depend on the parameters θ and ϕ. The limit distribution for the total edge length of the MDSF has at most two (independent) components namely (i) a normal contribution from the bulk and in some cases, (ii) a non-normal contribution from near the boundary of the unit square. The boundary contributions can be characterized by a fixed-point equation. The limit theory for the unaligned cone follows a normal distribution as there is no boundary contribution.

We have generalized the local dependence approach of Avram and Bertsimas [3], who proved CLTs for the ordinary nearest-neighbour graph using the technique of dependency graph of Baldi and Rinott [4]. We extend the theoretical approach of

Penrose and Wade [31] for the doubly-aligned cone to work for a general cone, giving limit results for the singly-aligned cone and unaligned cone in the unit square.

One direction for possible future work to investigate further and obtain weak convergence results for the total power-weighted edge lengths for the general dimension respecting the MDSF on $\mathcal{P}_\lambda$ in $(0,1)^d$ for $d \geq 3$, on the general cone. Even in the two-dimensional setting, some other cases are yet to be obtained, including general reflex cones ($\pi < \phi < 2\pi$) in the unit square, or cones in other polygonal domains.

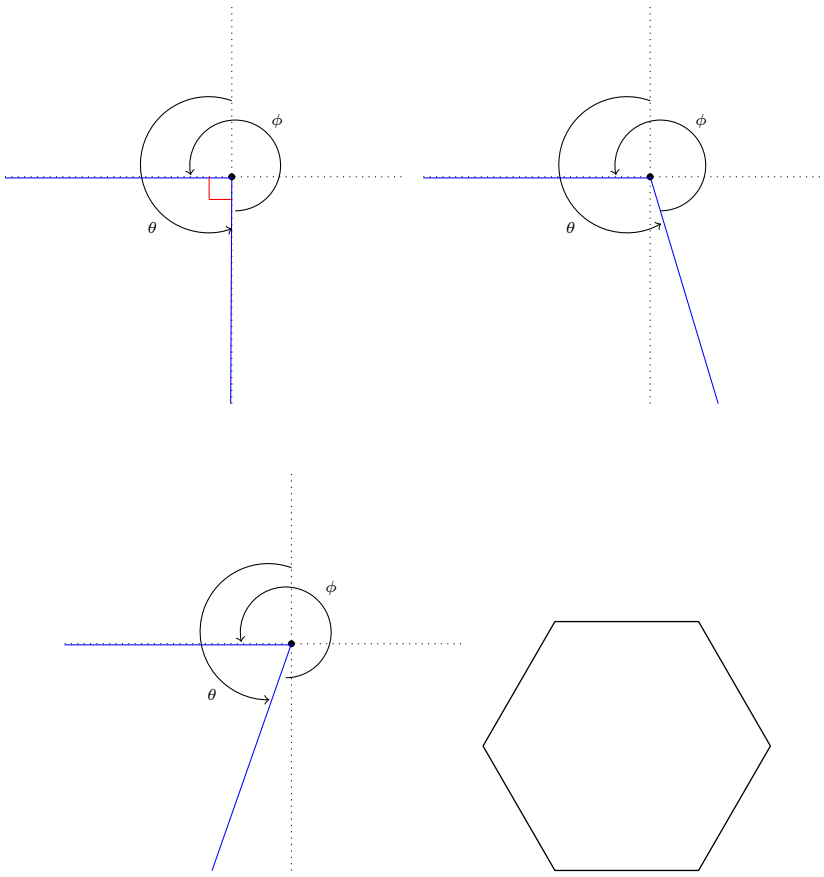

Figure 8.1: Three reflex cones, and a regular polygonal domain.

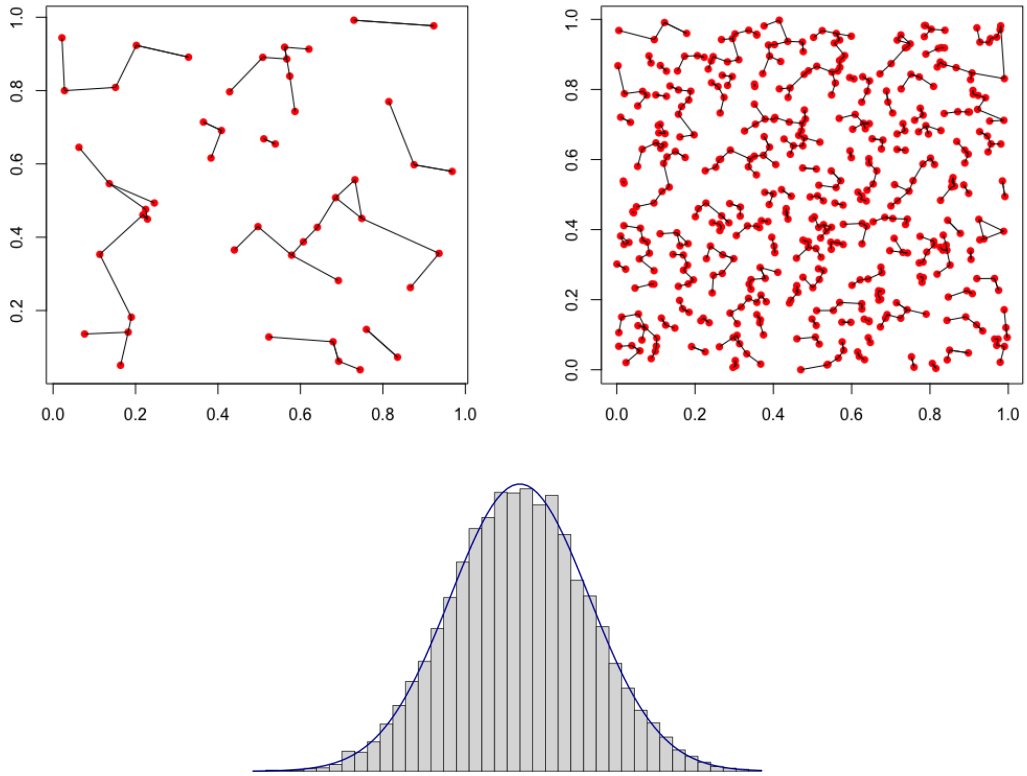

Figure 8.2: Realizations of the MDSF with 50 and 100 random points uniformly generated in the unit square with respect to doubly-aligned reflex cone, as in the first picture in Figure 8.1. Is this a normal limit?

Nomenclature

$\mathbb{R}$ is a set of real numbers, ... page 8

$\|\cdot\|$ is some norm on $\mathbb{R}^d$, ... page 14

$\mathbf{Po}(\lambda)$ is a Poisson distribution with mean λ, ... page 16

$\mathbb{N}$ is a set of natural numbers, ... page 18

$\mathcal{X}_n$ is a point process consisting of n i.i.d random variable on $\mathbb{R}^d$, ... page 18

$\mathcal{P}_\lambda$ is a homogeneous Poisson point process of intensity λ, ... page 18

$\mathbf{E}$ notation of the expectation, ... page 19

$a.s.$ converges almost surly, ... page 19

p^{th} converges in p^{th} moments, ... page 19

$\mathbf{Var}$ notation of the variance, ... page 20

$\mathbb{Z}$ is a set of integer numbers, ... page 25

$\overset{\theta,\phi}{\preccurlyeq}$ is a general cone, ... page 25

$\mathcal{D}_{\theta,\phi}(\boldsymbol{x};\mathcal{X})$ is the distance from point $\boldsymbol{x}$ to its nearest-neighbour in $\mathcal{X}$, ... page 26

$C_{\theta,\phi}(\boldsymbol{x})$ is a closed-half cone associated with both singly-aligned and unaligned cones in $[0,1]^2$, ... page 26

$\mathcal{L}(\mathcal{X})$ a length of the minimal directed spanning forest, ... page 30

$\mathcal{X}$ is locally finite set of point in $[0,1]^2$, ... page 30

$\tilde{\mathcal{L}}_\lambda$ is centred total length in $[0,1]^2$, ... page 30

$T(p)$ is a tile in the $[0,1]^2$, ... page 37

$\mathcal{S}_{p,R}$ is the ball containing all little squares with radius R of the square p, page 37

$\mathbb{T}_S$ is the set of all tiles in $[0,1]^2$, ... page 47

$\mathcal{L}_\lambda^i$ for $i = 1, 2, 3$,is the total edge length for the bulk, intermediate, and boundary of $[0,1]^2$, ... page 54

$\mathcal{L}_\lambda^1$ the contribution to the total edge length coming from the bulk of the unit square, ... page 57

$\mathcal{G} = (\mathcal{V}, \mathcal{E})$ is a dependency graph for $\{Z_p\}_{p\in\mathcal{V}}$, where Z_p is a collection of random variables, ... page 59

$\mathcal{B}_\lambda$ is the event such that for each little square there is a point of Poisson process, page 60

μ is the expected number of points falling in each square $\mu \sim c \log \lambda$, . page 60

$\mathcal{B}_\lambda^{\complement}$ is the complement of the event $\mathcal{B}_\lambda$, ... page 66

$\xi(\boldsymbol{x}; \mathcal{X})$ the distance from point $\boldsymbol{x}$ to its nearest neighbour in $\mathcal{X} \cap C_{\theta,\phi}(\boldsymbol{x})$, page 73

$B_r(\boldsymbol{x})$ is the Euclidean ball centered at $\boldsymbol{x}$ with radius r, ... page 74

$R_\lambda(\boldsymbol{x})$ is the random variable in $[0,1]^2$, ... page 75

$\nu_{\theta,\phi}(\boldsymbol{x})$ is the longest Euclidean distance in $[0,1]^2$, ... page 75

$A_{\theta,\phi}(\boldsymbol{x}, s)$ is the region in $[0,1]^2$ associated with general cone, ... page 79

$\mathcal{L}_\lambda^3$ the contributions coming from bottom boundary of $[0,1]^2$, ... page 94

$\mathcal{L}_\lambda^2$ is the contribution which is coming from the intermediate region of $[0,1]^2$, page 118

Γ_i are cells such that Γ_i portioning $\mathcal{R}_\lambda^2$ from left to right for $(i = 1, \ldots, \ell_\lambda)$, page 118

β_i are cells such that β_i portioning $\mathcal{R}_\lambda^3$ from left to right for $(i = 1, \ldots, \ell_\lambda)$, page 118

ℓ_λ denotes the number of cells, i.e., $\ell_\lambda := \left\lfloor \frac{\lambda^{1-\sigma}}{c \log^2 \lambda} \right\rfloor$, ... page 118

Appendix A

The Dirichlet and Poisson-Dirichlet distribution

In this chapter, we will discuss the concept of the Dirichlet and Poisson-Dirichlet distributions, along with exploring certain distributions, properties obtained as limits according to the Theorem 6.1.1 in Chapter 6.

The Dirichlet distribution will have significance in the later portions of the theory, particularly in the context of spacings and one-dimensional nearest-neighbour graphs, as discussed in Chapter 6. Currently, it forms the fundamental basis for the Poisson-Dirichlet distribution, which plays a central role in this chapter. In this section, we recall what is the Dirichlet distribution and the Poisson-Dirichlet distribution see for example [11] for more details.

Let $\Delta_n \subset \mathbb{R}^n$ denote the n-dimensional simplex, that is

$$\Delta_n := \{(x_1, \ldots, x_n) \in \mathbb{R}^n : x_i \geq 0, 1 \leq i \leq n; \sum_{i=1}^{n} x_i \leq 1\}.$$

Definition A.0.1.

(1) We call a random vector $(X_1, \ldots, X_n)$ a Dirichlet distribution with parameters $\alpha_1, \ldots, \alpha_n$ if $X_n = 1 - \sum_{i=1}^{n-1} X_i$ and $(X_1, \ldots, X_{n-1})$ is distributed on the simplex

Δ_{n-1} with density

$$\frac{\Gamma(\alpha_1 + \dots \alpha_n)}{\Gamma(\alpha_1) \dots \Gamma(\alpha_n)} x_1^{\alpha_1 - 1} \dots x_{n-1}^{\alpha_{n-1} - 1} (1 - x_1 - \dots - x_{n-1})^{\alpha_n - 1}.$$

(2) We further call $(X_1, \dots, X_n)$ a symmetric Dirichlet distribution (with parameter α) if $\alpha_i = \alpha$ for all i.

Let $(X_1, \dots, X_n)$ be a symmetric Dirichlet distribution with parameter $\alpha = \frac{\lambda}{n}$ for some $\lambda > 0$. For some fixed k $(k < n)$, let $(X_{(1)}, \dots, X_{(k)})$ be the vector of the first k order statistics of $(X_1, \dots, X_n)$, where $X_{(1)} \geq X_{(2)} \geq \dots \geq X_{(n)}$. By (Kingman [21]), when $n \to \infty$, for each k we have

$$(X_{(1)}, \dots, X_{(k)}) \xrightarrow{d} (Z_1, Z_2, \dots, Z_k),$$

where the infinite sequence $(Z_1, Z_2, \dots)$ satisfies

$$Z_1 \geq Z_2 \geq \dots, \qquad \sum_{j=1}^{\infty} Z_j = 1.$$

Definition A.0.2. We call above distribution $(Z_1, Z_2, \dots)$ a Poisson-Dirichlet distribution with parameter λ.

Appendix B

Cone classification

In this chapter, we will demonstrate the cone configurations for all type of general cones in the unit square. As mentioned in the discussion there are five new cases we study in this thesis. The first case which is called the doubly-aligned cone where both θ & $\theta+\phi$ are in $\frac{\pi}{2}\mathbb{Z}$, (see Figure B.1 below) limit distribution for doubly-aligned cone obtained by Penrose & Wade. The second case of the general cone is called a singly-aligned if exactly one of θ and $\theta+\phi$ belongs to $\frac{\pi}{2}\mathbb{Z}$ as indicated below. Finally, the general cone is called unaligned if neither θ nor $\theta+\phi$ belongs to $\frac{\pi}{2}\mathbb{Z}$ as shown below.

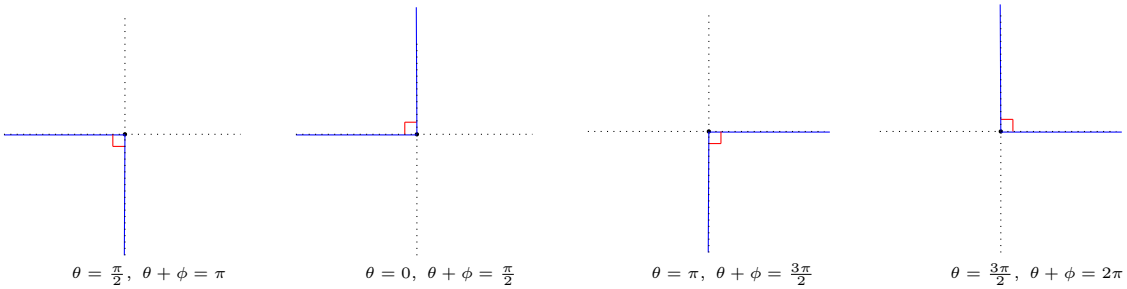

Figure B.1: Doubly-aligned cones in the unit square.

Here we have both singly-aligned cones (obtuse and acute angles) with parameter θ.

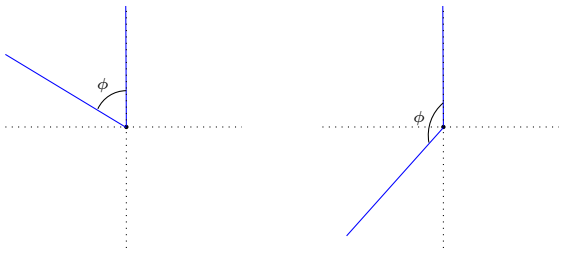

Figure B.2: Singly-aligned cones in the unit square with parameter $\theta = 0$.

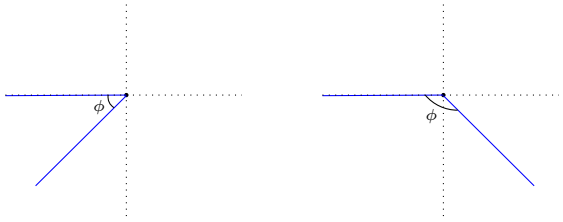

Figure B.3: Singly-aligned cones in the unit square with parameter $\theta = \frac{\pi}{2}$.

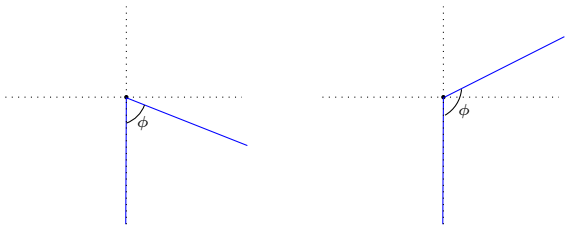

Figure B.4: Singly-aligned cones in the unit square with parameter $\theta = \pi$.

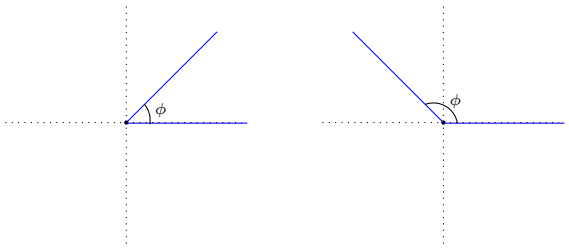

Figure B.5: Singly-aligned cones in the unit square with parameter $\theta = \frac{3\pi}{2}$.

Here we have the singly-aligned cone with respect to the sum of parameters θ and ϕ in $[0, 1]^2$.

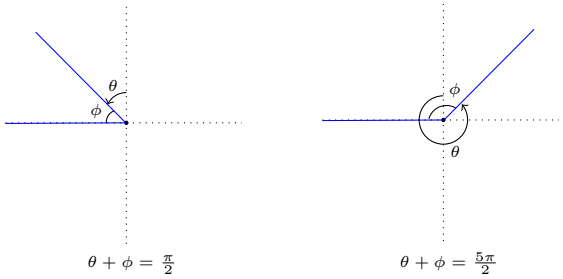

Figure B.6: Singly-aligned cones in the unit square.

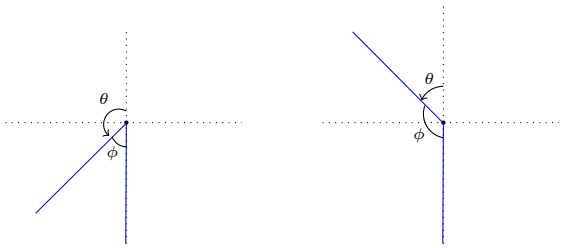

Figure B.7: Singly-aligned cones in the unit square with parameters $\theta + \phi = \pi$.

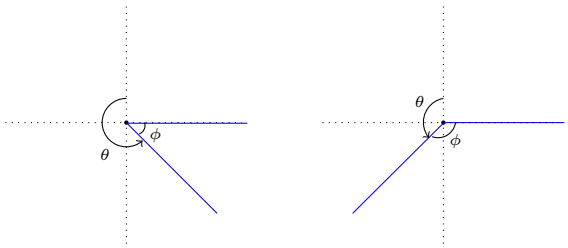

Figure B.8: Singly-aligned cones in the unit square with parameters $\theta + \phi = \frac{3\pi}{2}$.

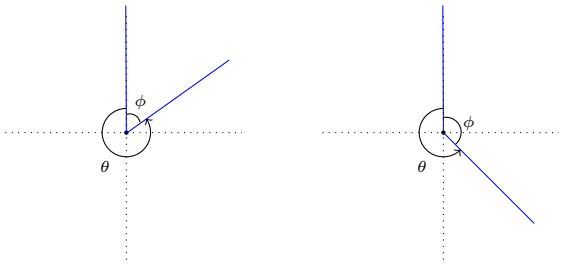

Figure B.9: Singly-aligned cones in the unit square with parameters $\theta + \phi = 2\pi$.

We are now shifting our focus to the unaligned cone within the square. The unaligned cone exhibits various cone shapes, as shown in the following diagrams. In

this discussion, we are examining the scenario of an unaligned cone that contains no axes.

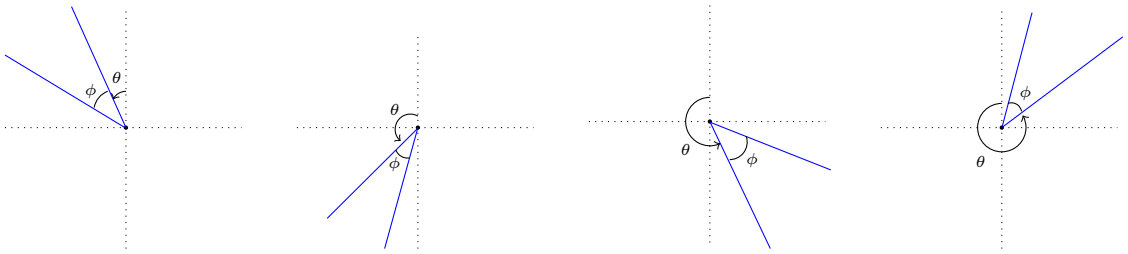

Figure B.10: Unaligned cone in the unit square.

Here we consider the unaligned cone, and it contains one axes.

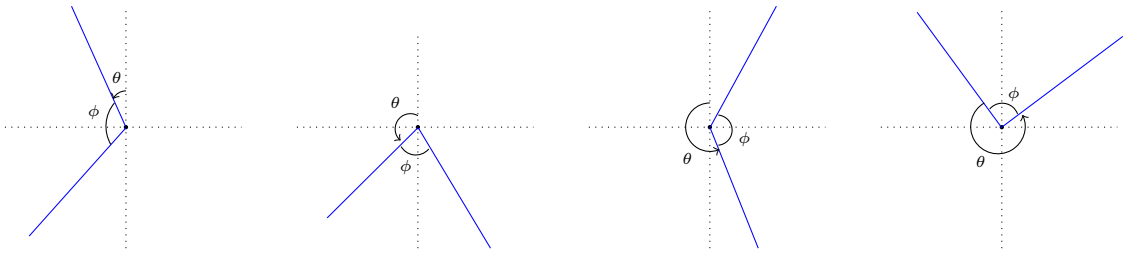

Figure B.11: Unaligned cone in the unit square.

Finally, we consider the unaligned cone, and it contains two axes.

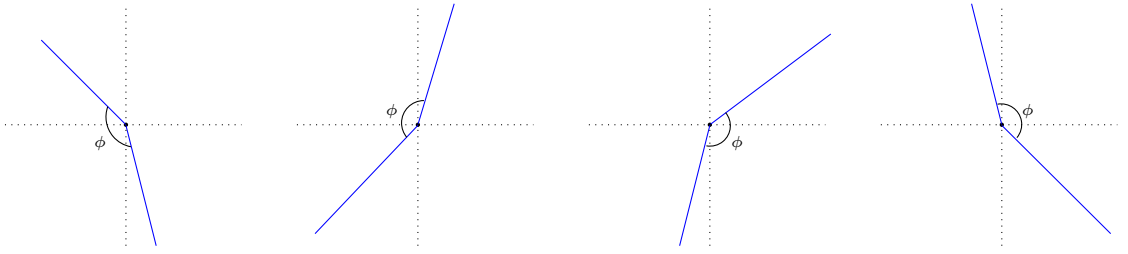

Figure B.12: Unaligned cone in the unit square.

Bibliography

[1] M. Abramowitz, ed. *Handbook of mathematical functions, with formulas, graphs, and mathematical tables*. National Bureau of Standards Applied Mathematics Series, No. 55. Superintendent of Documents. U. S. Government Printing Office, Washington, D.C., 1965, pp. xiv+1046.

[2] M. A. Akinkunmi. *Business Statistics with Solutions in R*. Walter de Gruyter GmbH & Co KG, 2019.

[3] F. Avram, D. Bertsimas. "On central limit theorems in geometrical probability". *Ann. Appl. Probab.* 3.4 (1993), pp. 1033–1046.

[4] P. Baldi, Y. Rinott. "On normal approximations of distributions in terms of dependency graphs". *Ann. Probab.* 17.4 (1989), pp. 1646–1650.

[5] J. Beardwood, J. H. Halton, J. M. Hammersley. "The shortest path through many points". *Proc. Cambridge Philos. Soc.* 55 (1959), pp. 299–327.

[6] N. Berger et al. "Degree distribution of the FKP network model". *Automata, languages and programming*. Vol. 2719. Lecture Notes in Comput. Sci. Springer, Berlin, 2003, pp. 725–738.

[7] J. Bertoin, A. V. Gnedin. "Asymptotic laws for nonconservative self-similar fragmentations". *Electron. J. Probab.* 9 (2004), no. 19, 575–593.

[8] A. G. Bhatt, R. Roy. "On a random directed spanning tree". *Adv. in Appl. Probab.* 36.1 (2004), pp. 19–42.

[9] C. Bhattacharjee. "Gaussian approximation for rooted edges in a random minimal directed spanning tree". *Random Structures Algorithms* 61.3 (2022), pp. 462–492.

[10] P. J. Bickel, L. Breiman. "Sums of functions of nearest neighbor distances, moment bounds, limit theorems and a goodness of fit test". *Ann. Probab.* 11.1 (1983), pp. 185–214.

[11] P. Billingsley. *Convergence of probability measures*. Second. Wiley Series in Probability and Statistics: Probability and Statistics. A Wiley-Interscience Publication. John Wiley & Sons, Inc., New York, 1999, pp. x+277.

[12] J. K. Blitzstein, J. Hwang. *Introduction to probability*. Second. Texts in Statistical Science Series. CRC Press, Boca Raton, FL, 2019, pp. xv+619.

[13] B. Bollobás. "The Erdős-Rényi theory of random graphs". *Paul Erdős and his mathematics, II (Budapest, 1999)*. Vol. 11. Bolyai Soc. Math. Stud. János Bolyai Math. Soc., Budapest, 2002, pp. 79–134.

[14] B. Bollobás. *Graph theory*. Vol. 63. Graduate Texts in Mathematics. An introductory course. Springer-Verlag, New York-Berlin, 1979, pp. x+180.

[15] M. R. Brito, A. J. Quiroz, J. E. Yukich. "Graph-theoretic procedures for dimension identification". *J. Multivariate Anal.* 81.1 (2002), pp. 67–84.

[16] F. Dai, S. J. Ma, X. Q. Wang. "A note on the unified expression of ruin probabilities in the classical risk theory". *J. Nanjing Norm. Univ. Nat. Sci. Ed.* 33.1 (2010), pp. 28–31.

[17] D. Evans, A. J. Jones. "A proof of the gamma test". *R. Soc. Lond. Proc. Ser. A Math. Phys. Eng. Sci.* 458.2027 (2002), pp. 2759–2799.

[18] J. H. Friedman, L. C. Rafsky. "Graph-theoretic measures of multivariate association and prediction". *Ann. Statist.* 11.2 (1983), pp. 377–391.

[19] P. M. Gruber. *Convex and discrete geometry*. Vol. 336. Grundlehren der mathematischen Wissenschaften [Fundamental Principles of Mathematical Sciences]. Springer, Berlin, 2007, pp. xiv+578.

[20] A. Gut. *Probability: a graduate course*. Springer Texts in Statistics. Springer, New York, 2005, pp. xxiv+603.

[21] J. F. C. Kingman. *Poisson processes*. Vol. 3. Oxford Studies in Probability. Oxford Science Publications. The Clarendon Press, Oxford University Press, New York, 1993, pp. viii+104.

[22] A. N. Kolmogorov, S. V. Fomién. *Introductory real analysis*. Translated from the second Russian edition and edited by Richard A. Silverman, Corrected reprinting. Dover Publications, Inc., New York, 1975, pp. xii+403.

[23] S. Manna, G. Mukherjee, P. Sen. "Scale-free network on a vertical plane". *Physical Review E* 69.1 (2004), p. 017102.

[24] M. Mitzenmacher, E. Upfal. *Probability and computing*. Randomized algorithms and probabilistic analysis. Cambridge University Press, Cambridge, 2005, pp. xvi+352.

[25] R. Motwani, P. Raghavan. *Randomized algorithms*. Cambridge University Press, Cambridge, 1995, pp. xiv+476.

[26] M. Penrose. *Random geometric graphs*. Vol. 5. Oxford Studies in Probability. Oxford University Press, Oxford, 2003, pp. xiv+330.

[27] M. D. Penrose. "A central limit theorem with applications to percolation, epidemics and Boolean models". *Ann. Probab.* 29.4 (2001), pp. 1515–1546.

[28] M. D. Penrose. *Convergence of random measures in geometric probability.* 2005. arXiv: math/0508464 [math.PR].

[29] M. D. Penrose. "Gaussian limits for random geometric measures". *Electron. J. Probab.* 12 (2007), pp. 989–1035.

[30] M. D. Penrose. "Multivariate spatial central limit theorems with applications to percolation and spatial graphs". *Ann. Probab.* 33.5 (2005), pp. 1945–1991.

[31] M. D. Penrose, A. R. Wade. "On the total length of the random minimal directed spanning tree". *Adv. in Appl. Probab.* 38.2 (2006), pp. 336–372.

[32] M. D. Penrose, A. R. Wade. "Random minimal directed spanning trees and Dickman-type distributions". *Adv. in Appl. Probab.* 36.3 (2004), pp. 691–714.

[33] M. D. Penrose, J. E. Yukich. "Central limit theorems for some graphs in computational geometry". *Ann. Appl. Probab.* 11.4 (2001), pp. 1005–1041.

[34] M. D. Penrose, J. E. Yukich. "Limit theory for random sequential packing and deposition". *Ann. Appl. Probab.* 12.1 (2002), pp. 272–301.

[35] M. D. Penrose, J. E. Yukich. "Normal approximation in geometric probability". *Stein's method and applications.* Vol. 5. Lect. Notes Ser. Inst. Math. Sci. Natl. Univ. Singap. Singapore Univ. Press, Singapore, 2005, pp. 37–58.

[36] M. D. Penrose, J. E. Yukich. "Weak laws of large numbers in geometric probability". *Ann. Appl. Probab.* 13.1 (2003), pp. 277–303.

[37] D. B. Ramey. *A NON-PARAMETRIC TEST OF BIMODALITY WITH APPLICATIONS TO CLUSTER ANALYSIS.* Thesis (Ph.D.)–Yale University. ProQuest LLC, Ann Arbor, MI, 1982, p. 90.

[38] L. Razdolsky. "Probability based structural fire load". *Structures Congress 2013: Bridging Your Passion with Your Profession.* 2013, pp. 2566–2577.

[39] I. Rodriguez-Iturbe, A. Rinaldo. *Fractal river basins: chance and self-organization.* Cambridge University Press, 1997.

[40] U. Rösler. "A fixed point theorem for distributions". *Stochastic Process. Appl.* 42.2 (1992), pp. 195–214.

[41] W. D. Smith. *Studies in computational geometry motivated by mesh generation.* Thesis (Ph.D.)–Princeton University. ProQuest LLC, Ann Arbor, MI, 1989, p. 488.

[42] S. M. Stigler. "Poisson on the Poisson distribution". *Statist. Probab. Lett.* 1.1 (1982–1983), pp. 33–35.

[43] T. Trauthwein. "Quantitative CLTs on the Poisson space via Skorohod estimates and p-Poincar\'e inequalities". *arXiv preprint arXiv:2212.03782* (2022).

[44] A. R. Wade. "Limiting behaviour of random spatial graphs and asymptotically homogeneous RWRE". PhD thesis. Durham University, 2005.

[45] A. R. Wade. "Explicit laws of large numbers for random nearest-neighbour-type graphs". *Adv. in Appl. Probab.* 39.2 (2007), pp. 326–342.